Reversible Addition Fragmentation Chain Transfer (RAFT) Mediated Polymerization of *N*-vinylpyrrolidone

Dissertation presented in partial fulfillment of the requirements for the degree of

PhD of Polymer Science

by

Gwenaelle Pound

Supervisor: Prof Bert Klumperman

Department of Chemistry and Polymer Science

Faculty of Science

March 2008

Declaration

I, the undersigned, hereby declare that the work contained in this thesis is my own original work and that I have not previously in its entirety or in part submitted it at any university for a degree.

Gwenaelle POUND   *February 2008*

Abstract

Xanthate-mediated polymerization was investigated as a tool for the preparation of well-defined poly(*N*-vinylpyrrolidone) and copolymers of *N*-vinylpyrrolidone. Some results regarding the monomer vinyl acetate are included, mostly for comparison purposes. The structure of the leaving/reinitiating group of the xanthate mediating agent was tuned to match the monomer reactivity. This was achieved by studying the initialization behaviour of monomer-xanthate systems via *in situ* ^{1}H-NMR spectroscopy. Additionally, the latter technique was valuable to identify side reactions affecting the monomer, xanthate and/or polymeric species. Subsequently, experimental conditions were defined, and used to optimize the level of control achieved during polymerization.

Block copolymers were prepared from a xanthate end-functional poly(ethylene glycol) with both vinyl acetate and *N*-vinylpyrrolidone. Finally, the preparation of poly(*N*-vinylpyrrolidone) with a range of well-defined end groups was achieved via post-polymerization treatment of the xanthate end-functional polymerization product. 3 different routes were investigated, which lead to poly(*N*-vinylpyrrolidone) with 1) aldehyde or alcohol, 2) thiol or 3) unsaturated ω-chain-end functionality, in high yield, while the α-chain-end functionality is defined by the structure of the xanthate leaving group. The ω-aldehyde end-functional poly(*N*-vinylpyrrolidone) was successfully conjugated to the lysine residues of the model protein lysozyme via reductive amination.

Particular attention was drawn to characterizing the polymerization products. NMR spectroscopy, liquid chromatographic and mass-spectroscopic techniques were used. The major achievements emerging from polymer analysis carried out in this study included the following:
- a library of NMR chemical shifts for *N*-vinylpyrrolidone derivatives;
- an estimation of the critical conditions for poly(*N*-vinylpyrrolidone) relevant for separation according to the polymer chain-ends;
- conditions for the separation of block-copolymers comprising a poly(ethylene glycol) segment and a poly(*N*-vinylpyrrolidone) or poly(vinyl acetate) segment via liquid chromatography;

- valuable results on matrix-assisted laser ionization-desorption time-of-flight mass spectroscopy (MALDI-ToF-MS) of poly(N-vinylpyrrolidone).

Opsomming

Xantaatgebeheerde- (Eng. xanthate-mediated) polimerisasie is ondersoek vir die bereiding van goedgedefineerde poli(*N*-pirolidoon) en kopolimere daarvan. Verskeie resultate aangaande die monomeer vinielasetaat is ingesluit, meestal vir vergelykingsdoeleiendes. Die struktuur van die verlatende-/herinisiëringsgroep van die xantaatbeheeragent (Eng: xanthate mediating agent) is aangepas om aan te sluit by die reaktiviteit van die monomeer. Dit is verkry deur die inisialisegedrag van monomeriese xantaatsisteme met behulp van *in situ* ¹H-NMR spektroskopie te bestudeer. Verder was laasgenoemde tegniek van waarde om newereaksies wat die momomeer, xantaat en/of polimeerspesies affekteer, te identifiseer. Daarna is geskikte eksperimentele kondisies vasgestel en gebruik vir die optimisering van die mate van beheer wat behaal is gedurende polimerisasie.

Blokkopolimere met beide vinielasetaat en *N*-vinielpirolidoon is vanaf poliëtileenglikol met 'n xantaatendfunksie berei. Daarna is poli(*N*-vinielpirolidoon) met goed gedefineerde endgroepe verkry deur middel van na-polimerisasie behandeling van die xantaatendfunksionele polimerisasieproduk.

Drie verskillende roetes is ondersoek vir die bereiding van poli(*N*-vinielpirolidoon) met die volgende funksionaliteite: 1) aldehied of alkohol 2) tiol of 3) onversadigde ω-kettingend-funksionaliteit in hoë opbrengs, terwyl die α-kettingend-funksionaliteit bepaal is deur die struktuur van die xantaat verlatende groep. The ω-aldehiedendfunksionele poli(*N*-vinielpirolidoon) is suksesvol gekonjugeerd met die lisien residue van die model protein lisosiem deur middel van reduserende aminasie (Eng: via reductive amination).

Spesiale aandag is gegee aan die karakterisering van die polimerisasie produkte. Hiervoor is KMR spektroskopie, vloeistofchromatografie en massaspektrometrie gebruik. Die volgende is dus behaal:

- 'n biblioteek van KMR chemiese verskuiwings vir derivate van poli(*N*-vinielpirolidoon);
- 'n skatting van die kritiese kondisies vir poli(*N*-vinielpirolidoon) toepaslik vir skeiding op grond van polimeerendgroepe;

- kondisies vir die skeiding van blokkopolimere bestaande uit 'n poliëtileenglikol-segment en 'n poli(*N*-vinielpirolidoon)- of polivinielasetaatsegment deur middel van vloeistofchromatografie;

- waardevolle resultate insake "matrix-assisted laser ionization-desorption time-of-flight mass spectroscopy (MALDI-ToF-MS)" van poli(N-vinielpirolidoon).

Table of contents

List of symbols

|	
α	conversion or yield
$[A]_t$	molar concentration of compound A at time t
C_T	chain transfer constant to compound T
DP_n	average degree of polymerization
f	initiator efficiency
k_d	rate constant of initiator decomposition
k_i	rate constant of initiation
k_p	rate constant of propagation
k_t	rate constant of termination
k_{tr}	rate constant of transfer
M_n	average molar mass
r_1, r_2	copolymerization reactivity ratios
R_p	rate of polymerization

List of acronyms

ABDH	2,2'-azobis[2-(2-imidazolin-2-yl)propane dihydrochloride
ACPA	4,4'-azobis-4-cyanopentanoic acid
AIBN	2,2'-azo bis(isobutyronitrile)
ATRP	atom-transfer radical polymerization
b	block
BHT	butylated hydroxytoluene
CHCA	α-cyano hydroxyl cinnamic acid
COSY	correlated spectroscopy
CPAE	α-chlorophenyl acetic acid, ethyl ester
(macro)CTA	(macromolecular) chain-transfer agent
DMAc	*N,N*-dimethylacetamide
DMF	*N,N*-dimethylformamide
(d_6-)DMSO	(deuterated) dimethyl sulfoxide
DRI	differential refractive-index detector
ELSD	evaporative light scattering detector
ESR	electron spin resonance
GPEC	gradient polymer elution chromatography
HFIP	1,1,1,3,3,3-hexafluoro-2-propanol
HMBC	heteronuclear multiple bond correlation
HPLC(-CC)	high performance liquid chromatography (-at critical conditions)
HSQC	heteronuclear single quantum coherence
LC	adsorption liquid chromatography
LRP	living radical polymerization
LS	light scattering
MADIX	macromolecular design via the interchange of xanthate
MALDI-ToF-MS	matrix assisted laser desorption ionization time of flight mass spectroscopy
MAn	methacrylonitrile

MHKS	Mark-Houwink-Kuhn-Sakurada
MM	*trans*-2-[3-(4-*tert*-Butylphenyl)-2-methyl-2-propenylidene]-malononitrile
MMA	methyl methacrylate
MWCO	molecular weight cut-off
NMP	nitroxide-mediated polymerization
NMR	nuclear magnetic resonance
NOESY	nuclear overhauser effect spectroscopy
NVP	*N*-vinylpyrrolidone
NVP-O-NVP	hydrated dimer of *N*-vinylpyrrolidone
PCN	2-cyano-2-propyl
PCR	polymerase chain reaction
PDI	polydispersity index
PEG	poly(ethylene glycol)
PMMA	poly(methyl methacrylate)
PRE	persistent radical effect
PS	poly(styrene)
PTFE	poly(tetrafluoroethylene)
PVAc	poly(vinyl acetate)
PVP	poly(*N*-vinylpyrrolidone)
RAFT	reversible addition-fragmentation transfer
RI	refractive index
SDS-PAGE	sodium dodecyl sulfate polyacrylamide gel electrophoresis
SEC	size-exclusion chromatography
SFRP	stable free-radical polymerization
Sty	styrene
T	transfer agent
TERP	organotellurium-mediated ccontrolled radical polymerization
THF	tetrahydrofuran
TMSN	tetramethyl succinonitrile
TNF	tumor necrosis factor

VAc	vinyl acetate
X	xanthate
X-EP	xanthate elimination product

Chemical structures of xanthates

For clarity, the xanthates discussed throughout this thesis are summarized below. The numbering was attributed arbitrarily.

X3

X4

X5

X6

X7

X9

X10

X12

X13

X14
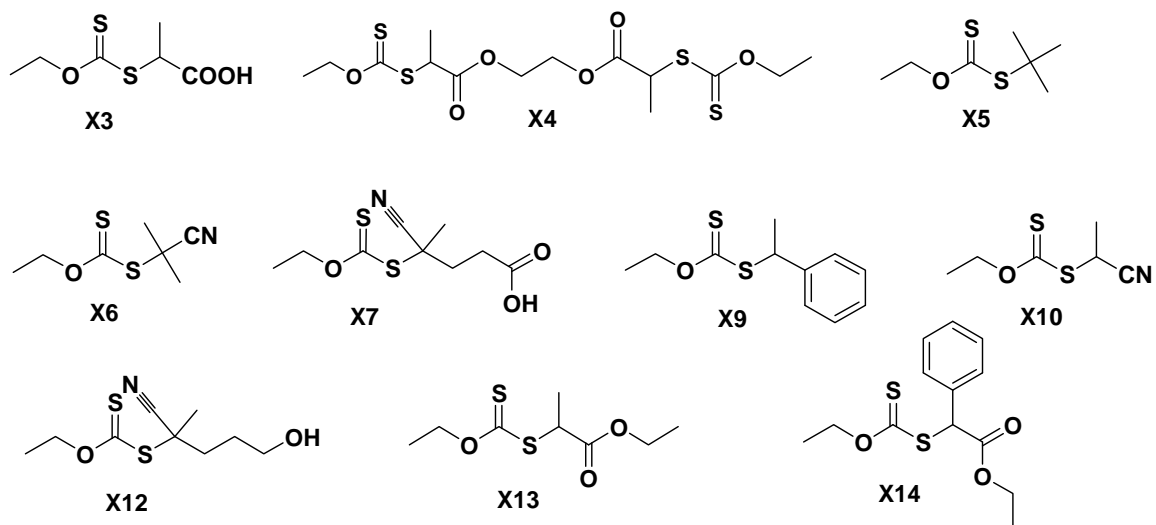
Chapter 1: Introduction

The general public commonly refers to polymers as plastics. From the polymer science perspective, plastics constitute only a subset of the products based on polymers. Polymers are merely large molecules obtained via the formation of linkages between small molecules called monomers. In academia a distinction is made between polymer science, the science of large molecules and organic chemistry, the science of small molecules. Although the rules governing the fabrication of polymeric material are the rules of organic chemistry, the distinction between the two fields arises mostly from the differences in properties of the products. A straightforward observable property is that monomers are generally liquid or low melting point solids, whereas upon polymerization, the product becomes viscous and eventually solid. This and other mechanical characteristics are responsible for the broad use of polymers where hard or tough materials are required. However the scope of applications of polymers is much broader. Poly(vinyl pyrrolidone) (PVP) is a good example of a polymer used for its properties in solution. These properties include solubility in water and polar organic solvents and even in blood plasma. Hence, PVP has applications in the pharmaceutical and cosmetic fields. PVP may be used to tune the viscosity and isotonicity of aqueous solutions (*e.g.* use as plasma expander during the Second World War[1]) or solubilize small molecules via interactions with the polymer (*e.g.* the commercially available PVP-iodine topical disinfectant). Unlike the building block *N*-vinylpyrrolidone, the polymer PVP is non toxic. The properties of the polymer can be tuned for a particular application via copolymerization. Incorporation of vinyl acetate comonomer in PVP results in poly(vinyl acetate – *co* – *N*-vinyl pyrrolidone) copolymer with reduced hygroscopy (industrialized under the name copovidone by BASF), used in the dry state as an excipient for therapeutic tablets. Copolymerization, where the chemical composition of the polymer is modified, is one of the possible ways to tune the properties of polymers. Another way relies on the molar mass and molar mass distribution dependence of the polymer properties. As indicated earlier, there is a strong variation in the properties between a monomer solution and its polymerization product. There are also strong variations of the

properties depending on the length of the polymer chains (characterized via the average degree of polymerization (DP_n): the average number of monomer units per chain), as well as the distribution in chain-lengths (characterized by the polydispersity index (PDI)). Thus the properties of a polymer can be fine-tuned by controlling the molar mass and molar mass distribution of the polymers. Hence tuning the properties of the polymer may be achieved by controlling the polymerization process. Finally, the polymer can present particular architectural features, such as functional end-groups to enable conjugation to other molecules or surfaces. The three-dimensional arrangement of the chains can be modified by creating topological variations such as the formation of a network or introduction of branches or grafts on a linear chain.

This thesis focuses on living free-radical polymerization of NVP as a tool to gain control over the molecular weight characteristics of the polymer and over the end-groups and thus enable novel macromolecular architectures. In chapter 2, the current scientific background is presented with respect to NVP polymerization. The choice of xanthate-mediated polymerization among other living polymerization techniques is discussed, as well as its challenges in the specific case of a poorly stabilized and reactive monomer such as NVP. Experimental conditions for the preparation of xanthate chain-transfer agents, polymerizations and characterization techniques are discussed in chapter 3. The use of *in situ* NMR spectroscopy to identify a suitable xanthate for the mediation of NVP polymerization is presented in chapter 4. Chapter 5 is dedicated to the study of side-reactions affecting the monomer NVP and polymeric species. The preparation and thorough characterization of novel block copolymers with poly(ethylene glycol) are presented in chapter 6. Finally the ability of xanthate-mediated polymerization to yield PVP with functional end-groups and the preparation of PVP-protein bioconjugates are presented in chapter 7. Although the focus of this research was on NVP, a number of experiments with vinyl acetate (VAc) are presented. The main reason for this is that kinetic and mechanistic data are already available in the literature for VAc and it is the well-documented monomer which reactivity is the closest to NVP. Therefore, the data already published for VAc is valuable to circumvent the scarceness of data for NVP.

(1)   Weese, H.; Hecht, G.; Reppe, W. DE Pat. 738994, **1943**.

Chapter 2: Historical and theory

Polymers of NVP

The chemical structures of the monomer *N*-vinylpyrrolidone (NVP) and its homopolymer poly(*N*-vinylpyrrolidone) (PVP) are presented in Figure 2.1:
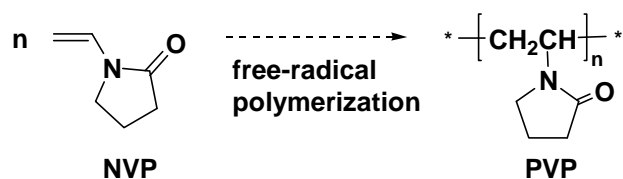

Figure 2.1: Chemical structures of the monomer *N*-vinylpyrrolidone (NVP) and its homopolymer poly(*N*-vinylpyrrolidone) (PVP).

The repeating unit of PVP displays a highly polar cyclic amide group capable of forming hydrogen bonds, whereas the apolar methylene and methine groups of the backbone have a non-polar character. As a result the polymer is soluble in water and in a range of organic liquids.[1] Hence, PVP can be used for its amphiphilic properties as a surfactant for the stabilization of heterogeneous systems.[2]

PVP is a stable (non-biodegradable) biocompatible[3] polymer. Due to its reduced protein and bacterial adhesion,[4] anti-thrombopoietic activity[5,6] and ability to stimulate the growth of endothelial cells[7-9] PVP has proven a good candidate for other blood-contacting applications. These include surface modification of intravenous polyurethane catheters,[4,5] bioprosthetic heart valves,[10] urological implants[11], hemodialysis membranes,[12] microfiltration membranes,[13] eye implants,[14] wound-dressing hydrogels[15] and fluorescence marker for cancer diagnosis.[16] Various therapeutic systems are currently under investigation based on NVP and its copolymers. These range from polymer-drug conjugates[17-19] to polymeric micelles for the solubilization of hydrophobic drugs,[20-23] microspheres,[24] capsules,[25] liposomes,[26] magnetic nanospheres,[27] hydrogel scaffolds for tissue engineering,[28] membranes for transdermal administration of drugs[29] or matrix for extended release pharmaceutical formulations.[30,31] Particular attention has been given to the use of PVP and NVP copolymers as polymeric carriers for tumor targeted protein

therapy and diagnosis.[16,20,32-37] The incorporation of NVP comonomer was found to improve the dispersion of organic components in dental cements.[38] In fact homo- and copolymers of NVP can be used for a broad range of applications, *e.g.* stabilization of beer,[39] separation of metals (selective chelating agent),[40,41] phase-transfer catalyst,[42] asymmetric membranes for gas separation,[43] fuel cell membranes,[44,45] as PCR-amplification enhancer,[46,47] diet supplement,[48] cosmetic excipient and many more under patent protection.

Preparation of PVP

The synthesis of PVP was reported by Fikentscher and Herrle in the 1940's.[49] The polymerization was initially carried out in aqueous solution with the use of hydrogen peroxide and ammonia and traces of heavy metal ions involved in the initiation of the polymerization. The polymerization occurs via a free-radical mechanism. Although it is theoretically conceivable, attempts to polymerize NVP under a cationic mechanism were unsuccessful.[50] They resulted in the formation of a dimeric species and other side-reactions but no polymer was obtained.

Conventional free-radical polymerization

Free-radical polymerization is the most widespread method for the industrial preparation of polymers from vinyl monomers. The technique has a number of advantages including its tolerance to impurities and its applicability to a broad range of monomers and experimental conditions. It can generally be carried out at atmospheric pressure and moderate temperatures, typically in the range 20 – 150 ºC, and polymers with high molar masses can be obtained within short reaction times. The high rates of polymerization are a consequence of the high reactivity of the radical species, which is also responsible for the drawbacks of the technique. Instead of participating in the chain growth process by addition of monomer, the radical species can undergo side-reactions leading to chain transfer or chain termination. The consequences are broad molecular weight distributions and lack of control over the chain-ends.

Kinetics of the conventional free-radical polymerization of NVP

General considerations

NVP is a polar monomer and is capable of hydrogen bonding[51] due to the amide functionality in the pyrrolidone ring. The reactivity of NVP can be influenced by the solvent, resulting in changes in the rate of polymerization (R_p).[51-53] Senogles et al. correlated the heat generated when NVP is mixed with water at different concentrations with the formation of hydrogen bonding between NVP and water molecules.[51] Both the viscosity curve and R_p as a function of concentration followed the same trend as the heat of mixing. They increase with concentration until a maximum is reached at 70 % by volume and then decrease. These results indicate that the occurrence of hydrogen bonding is most likely responsible for concentration and solvent dependence of NVP kinetic constants.

Values reported in the literature for kinetic constants (rates and rate constants) in NVP radical polymerization are often not consistent and must be used with care. Poor reproducibility of kinetic experiments with NVP may be attributed to the difficulty to purify the monomer[54] and the sensitivity of NVP polymerization to the presence of oxygen.[55] In addition to impurities present at the beginning of the polymerization, some may form via degradative side-reactions. They lead to a decrease in the actual monomer concentration and/or to the formation of products which interfere with radical processes. These are discussed later.

Non-ideal kinetic behavior of NVP polymerizations

The ideal kinetic model for free-radical polymerizations represents the case where the only radical source is the initiator, the monomer reacts only by addition to propagating species and termination occurs via combination or disproportionation between two radicals. The mathematical expression of the rate of polymerization is then:

$$R_p = -\frac{d[M]}{dt} = \frac{k_p}{k_t^{0.5}}[M](fk_d[I])^{0.5} \qquad \text{(eq. 2.1)}$$

where k_p, k_t and k_d are the rate constants of propagation, bimolecular termination and initiator decomposition, respectively; f is the initiator efficiency; [M] and [I] are the monomer and initiator concentrations, respectively. It is common in kinetic studies with azo initiators to find that the value for f is arbitrarily taken equal to 0.7. However Ganachaud et *al.*[56] determined f for a number of functional azo initiators with NVP and found values significantly lower than 0.7.

A non-ideal kinetic behavior, *i.e.* cases where R_p is not directly proportional to the monomer concentration, is often reported in NVP polymerizations.[54,57] Cizravi et *al.* studied the dependence of R_p and determined orders of reaction with respect to the concentrations in NVP and the initiator.[57] The study was carried out in aqueous buffered solution with 3 different azoinitiators: 4,4'-azobis-4-cyanopentanoic acid (ACPA), 2,2'-azobisisobutyronitrile (AIBN) and 2,2'-azobis[2-(2-imidazolin-2-yl)propane dihydrochloride (ABDH). They found the following proportionalities: $R_p \propto [NVP][ACPA]^{1.2}$; $R_p \propto [NVP][AIBN]^{1.1}$ and $R_p \propto [NVP]^{2.2}[ABDH]^{1.1}$. There are a number of possible causes for deviations from the ideal kinetic model. Some of the parameters that may cause a deviation in the orders of reaction are:

(i) k_p, k_t and/or f are concentration-dependent, *e.g.* the reactivity of the monomer is solvent-dependent;

(ii) k_p and k_t and are chain-length dependent ;

(iii) bimolecular termination does not occur, *e.g.* high viscosity or highly reactive radicals which transfer but do not terminate;

(iv) termination occurs with non-radical species, *e.g.* inhibitors;

(v) the monomer is consumed by a mechanism other than radical addition, *e.g.* non-radical degradation;

Evidence for pronounced chain-length dependence (point ii) of propagation and termination rate constants have already been reported in many polymerization systems[58-60] and it is likely that the situation also applies to NVP.

The relevance of points iii and iv to the case of NVP would require the determination of transfer and termination rate constants (k_{tr} and k_t). There is little information in the literature regarding kinetic rate constants for NVP polymerizations. It is therefore difficult to decipher the non-ideality reported in the kinetics of NVP radical polymerization. In the following paragraphs we will present and discuss the data already available in the literature and assemble quantitative and qualitative information with regards to the reactivity of NVP towards the main processes in free-radical polymerization which are initiation, propagation, transfer and termination. Initiation and propagation are discussed together as initiation can be seen as a single crosspropagation step between the initiator primary radical and the monomer.

Initiation (crosspropagation) and propagation

The electron donating substituent *N*-pyrrolidonyl has a poor radical stabilizing effect. As a consequence the reactivity of NVP radicals towards monomer addition is high. This is illustrated by a high k_p in the order of 10^3 L·mol^{-1}·s^{-1} in bulk at 20 °C.[61] One way to compare the reactivity of monomer-derived radicals is via experimental determination of reactivity ratios in copolymerization experiments. The reactivity ratios in a system comprising monomer 1 and monomer 2 are defined as the ratio of the homopropagation rate constants (k_{11} and k_{22}) to the crosspropagation rate constants (k_{12} and k_{21}):

$$r_1 = \frac{k_{11}}{k_{12}} ; \; r_2 = \frac{k_{22}}{k_{21}} \qquad \text{(eq. 2.2)}$$

Values of *r* less than 1 indicate a tendency of the radicals to crosspropagate rather than homopolymerize. The reactivity ratios r_{NVP} measured in the copolymerization of NVP with monomers bearing a radical stabilizing group (*e.g.* methacrylic and styrenic monomers) are less than 1 whereas r_2 is above 1 (see Table 2.1).

Table 2.1 : Reactivity ratios of NVP with various comonomers.

Comonomer	reactivity ratios
styrene[62]	$r_{NVP} = 0.04$, $r_{Sty} = 14.6$
4-vinylpyridine[63]	$r_{NVP} = 0.01$, $r_{4\text{-}Vp} = 9.8$
methyl methacrylate	$r_{NVP} = 0.01\text{-}0.07$, $r_{MMA} = 2\text{-}6$
methacrylonitrile[64]	$r_{NVP} = 0.04$, $r_{MAN} = 1.56$
methyl acrylate[65]	$r_{NVP} = 0.09$, $r_{MA} = 0.44$
acrylonitrile[66,a]	$r_{NVP} = 2.28$, $r_{AN} = 0.44$
vinyl acetate[67]	$r_{NVP} = 3.0$, $r_{VAc} = 0.06$

[a] in water, which was found to significantly increase r_{NVP} in other copolymerization systems, *e.g* with *n*-butyl acrylate.[68]

The values in Table 2.1 indicate that NVP radicals have a tendency to crosspropagate with styrene, 4-vinylpyridine, methacrylonitrile and methyl methacrylate rather than homopolymerize whereas crosspropagation of these monomers with NVP is unfavorable. The situation is however different with vinyl acetate and acrylonitrile, which substituents have an even lesser stabilizing effect than the *N*-pyrrolidonyl group.

The tendency of radicals to crosspropagate is a significant parameter in the initiation step. For initiation to take place the initiator derived radicals, also called primary radicals, must add to the monomer. Thus the initiation step can be described as the crosspropagation between the initiator derived radicals and the monomer. A review by Fischer and Radom lists a number of absolute rate constants for the addition of some radicals to alkenes determined experimentally.[69] Unfortunately no value is available for NVP. Theis et *al.* proposed the following method to estimate rate constants of initiation (k_i) based on copolymerization reactivity ratios.[70] Let us consider a comonomer system where monomer 2 bears the same substituents on the radical forming carbon as the initiating radical for which we want to estimate k_i. For instance, the monomer methacrylonitrile produces a radical comparable to 2-cyano-2-propyl, the primary radical produced by decomposition of AIBN. Theis et *al.* postulated that the reactivities of monomer 2 and the initiating radicals would be comparable. Thus k_i would be in the same range as the rate of crosspropagation of monomer 2 with monomer 1 (k_{21}). Eq 2 gives:

$k_{21} = \dfrac{k_{22}}{r_2}$. The value of k_{22} can be replaced by the rate constant of propagation of

monomer 2 (k_{p2}). Thus in the case of NVP initiated with 2-cyano-2-propyl (PCN):

$k_{PCN-NVP} = \dfrac{k_{pMAn}}{r_{MAn}}$, where r_{MAn} is the reactivity ratio r_2 in the polymerization of NVP with

methacrylonitrile.

Before we validate the method, let us consider a few systems for which k_i for the addition of PCN to monomer 2 are available and compare with crosspropagation rate constants with methacrylonitrile (Table 2.2).

Table 2.2: comparison of rates of initiation estimated with the method by Theis et *al.*[70] and absolute rate constants of addition to alkenes measured in solution at 315 K by Fischer and Radom[69] for the radical 2-cyano-2-propyl.

Monomer 2	r_2[61]	$k_{MAn\text{-}2}$ [a] $(\text{L·mol}^{-1}\text{·s}^{-1})$	k_i[69] $(\text{L·mol}^{-1}\text{·s}^{-1})$
vinyl acetate	12	2	41
vinylidene chloride	2.4	10	603
acrylonitrile	1.67	14.4	2020
NVP	1.56	15.3	*not found*
1,1-diphenylethylene	0.48	50	7010
styrene	0.21	114	2410

[a] at 315 K. k_{pMAn}= 23.9 $\text{L·mol}^{-1}\text{·s}^{-1}$ for was calculated from $k_p = 10^{6.43} e^{(-\frac{29700}{RT})}$ in ref.[61]

The estimations based on reactivity ratios are 20 to 180 times smaller than the experimental values for k_i. Fisher and Radom had already mentioned in their review that the values for k_p in homopolymerizations were 10 to 80 times smaller than the rates of addition of model radicals to the monomers considered. They suggested that this would be the cause of the larger steric effect of polymeric species compared to the model radicals. Other influences may include the penultimate effect in copolymerization and chain-length dependence of rate constants. Our comparison presented in table 2 indicates that k_i for PCN radicals will be significantly underestimated with the method by Theis et *al.* Nonetheless this method was able to predict that the rate of initiation of VAc with

PCN is low. The value of r_2 in the copolymerization of NVP with MAn is not sufficiently high for us to extrapolate that the same would apply for NVP.

Head to head versus head to tail addition

Propagation generally occurs via head to tail monomer addition, *i.e.* addition of radicals to the least substituted vinyl carbon center. A low portion of head to head additions may take place. The proportion of head to head addition in NVP polymerization was determined very recently via ^{2}H-NMR.[71] The polymer was prepared via organostibine-mediated polymerization at 60 ºC. The polymerization product endcapped with the organostibine agent was reduced with tributyltin deuteride to yield deuterated chain-ends. The resulting deuterated end-groups on the head to head products CH$_2$D, which ^{2}H-NMR signals was in the methyl region (0.8 - 1.2 ppm), could easily be discriminated from the CHD signal in the region 2.0 - 4.5 ppm. Assuming that the head to head product does not propagate, the probability for head to head addition was 0.02 - 0.08 %. As remarked by the authors, this value is significantly lower than in the case of VAc where 1 - 2 % of head to head additions were measured.[72,73] The higher stability of NVP radicals may be one of the reasons for a higher selectivity of the propagation step.

Transfer

An estimation of the ability of propagating NVP radicals to abstract protons from some substrates can be obtained from chain-transfer coefficients C_T, *e.g.* from solvents. Some C_T values were determined experimentally during the polymerization of NVP in the presence of irreversible chain-transfer agents (T). The reaction considered is the deactivation of a growing radical via proton abstraction:

$$P_n \bullet + T \rightarrow P_n H + T \bullet$$
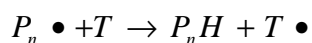
The reaction proceeds without loss in radical species as long as the radical $T \bullet$ can reinitiate polymerization. The chain-growth is stopped, resulting in a decrease in the degree of polymerization compared to polymerizations in the absence of T. C_T is defined as the ratio of the rate coefficient for chain transfer to T and the rate coefficient for propagation ($C_T = k_{tr-T}/k_p$). The higher the value of C_T the higher the reactivity of a

chain transfer agent for a given monomer. The effect of transfer reactions on DP_n is given by the Mayo equation:[74]

$$\frac{1}{DP_n} = \frac{(1 + \lambda)\langle k_t \rangle [R\bullet]}{k_p [M]} + C_M + C_T \frac{[T]}{[M]} \qquad \text{(eq. 2.3)}$$

where λ is the fraction of termination by disproportionation, $\langle k_t \rangle$ the average termination rate coefficient $[R\bullet]$ the overall radical concentration and C_M the chain transfer constant for chain transfer to monomer. Mayo presented a method for the experimental determination of C_T based on the determination of the average degree of polymerization (DP_n) for different concentration ratios of transfer agent to monomer. The plot of the reciprocal of the degree of polymerization (DP_n^{-1}) versus $[T]/[M]$ gives access to C_T.

Table 2.3: Chain transfer coefficients of some irreversible chain transfer agents (T) used as solvents in the polymerization of NVP and comparison with VAc and Styrene.[61]

T	C_T with NVP[a]	C_T with VAc[c]	C_T with Sty[d]
N,N-dimethylformamide[56]	7.91×10^{-5}	5.0×10^{-5}	1.08×10^{-4}
propionic acid methyl ester[75]	5.54×10^{-4}	2.3×10^{-3}	
isopropoxy ethanol[76]	$3.29 \times 10^{-4, b}$		
malonic acid dimethyl ester		1.7×10^{-3}	4.2×10^{-5}
malonic acid diethyl ester[75]	1.22×10^{-3}		4.7×10^{-5}
isobutyric acid methyl ester[77]	1.65×10^{-3}	8.6×10^{-3}	
lactic acid methyl ester		6.40×10^{-2}	
lactic acid ethyl ester[78]	1.03×10^{-2}	7.00×10^{-2}	
2-methylmalonate diethyl ester[75]	1.07×10^{-2}		
2-ethylmalonate diethyl ester			7.2×10^{-5}

[a] at 70 ºC   [b] at 80 ºC   [c] at 60 ºC   [d] at 100 ºC

The values reported in the literature (Table 2.3) are unfortunately not obtained at the same temperature. Nonetheless C_T increases with temperature and the values obtained for VAc determined at the lowest temperature are already higher than those for NVP, which are in turn higher than those for Sty obtained at the highest polymerization temperature. In other words, performing all reactions at the same temperature would only

amplify the trend. Therefore these values are still of qualitative relevance for comparison between monomers. Moreover, a change in temperature of 10 ºC between 60 ºC and 70 ºC has little effect on C_T. Finally the order of reactivity of the transfer agents is consistent between the 3 monomers. Transfer agents are sorted in the order of increasing C_T values.

The order of reactivity of the propagating radicals towards proton abstraction is: *PVAc• > PVP• >> PSty •* , following the reverse order of radical stability, as expected. The C_T values with NVP are 4 to 7 times smaller than with VAc. In comparison with Sty they are 2 to 3 orders of magnitude greater. Therefore NVP should be regarded as a radical with a strong tendency for proton abstraction, although not as strong as VAc.

In the absence of added chain transfer agents, chain transfer to the monomer and to the polymer may also occur. The chain-transfer constant for chain transfer to the monomer NVP at 20 ºC is $C_M = 4.0 \times 10^{-4}$.[61] Let us note that C_M is close to C_T values for many of the molecules presented in table 3. The use of T with C_T almost equal to C_M to provide endfunctional polymers requires that [M] be low compared to [T]. Otherwise a significant amount of chains will transfer to and possibly be initiated by the monomer.

Chain-branching

Chain-branching occurs when transfer to the polymer results in the formation of a mid-chain radical capable of reinitiating polymerization. Proton abstraction from the polymer is relatively high with non-stabilized monomers, such as ethylene, or monomers capable of backbiting, such as *n*-butyl acrylate.[79] Britton et *al.* determined the level of branching in PVAc prepared in bulk at 60 ºC via conventional free-radical polymerization with AIBN using ^{13}C-NMR spectroscopy.[80] The final levels of branching were 0.13 - 0.23 mol %. The major source of proton abstraction was from the acetate methyl group but they also found evidence for proton abstraction from the methylene backbone. The level of branching is expected to be lower in the case of NVP which does not possess a methyl group.

Termination

Termination of active species can occur via deactivation with non-radical species or by second order radical reactions, namely disproportionation or combination. The former includes transfer discussed in the previous paragraph and addition to inhibitors. Some of the known inhibitors are oxygen and substituted phenols often used as stabilizers.[81] Radical-radical termination may take place between two propagating radicals or a propagating radical and a primary radical (primary radical termination[81]). The result is chain termination and loss of two radicals. Bimolecular termination is diffusion controlled.[82,83] Kaplan et *al.*[55] studied termination in the AIBN-initiated polymerization of NVP using the rotating sector technique. This technique gives access to the ratio k_p/k_t by performing measurements of the free-radical lifetime under non-steady state conditions. Among others,[84] pulsed laser polymerization (PLP) is a more recent and preferred technique, which gives direct access to k_p. Unfortunately it has not been reported yet for NVP. Kaplan et al. found $k_p/k_t = 5 \times 10^{-3}$. They included experiments for the determination of R_p under steady-state conditions (constant radical concentration), which give access to k_p^2/k_t and thus determined $k_t = 2.73 \times 10^7$ mol$^{-1} \cdot$L$\cdot$s^{-1} (at 30 ℃). They also demonstrated that the polymerization was retarded in the presence of oxygen. The radicals produced by addition of oxygen did not propagate nor terminate.

The products of combination with initiator-derived radicals have been evidenced via MALDI-ToF-MS.[85] The experiment was carried out in 3-methylbutan-2-one, which served as a solvent and transfer agent. In spite of the low concentration of monomer and radicals compared to 3-methylbutan-2-one, this experiment indicates that radical combination competes with hydrogen abstraction.

The termination processes determine the molecular weight characteristics of the polymer. In the light of the kinetic constants reported here and evaluation of the reactivity of NVP in terms of transfer and propagation, it can be proposed that the main mechanism leading to the cessation of chain-growth is chain-transfer via proton abstraction. This of course is only true if the concentration of radicals is low.

Non-radical reactions

Breitenbach et *al.* first reported the degradation of NVP in the presence of acids in 1956.[86] A summary of the side-products identified thus far is presented in Scheme 2.1. Such reactions proceed via protonation of the double-bond as is the case for many substituted alkenes.[87] The cationic intermediate can add water thus releasing the catalytic proton. The resulting product of hydration *N*-(1-hydroxyethyl)pyrrolidone (I, R=H) was identified via ^{1}H-NMR.[88] It is stable at low temperature (0 ºC) but at higher temperatures it decomposes to acetaldehyde and pyrrolidone (III). Pyrrolidone adds to NVP to yield 1,1-bis(pyrrolidin-2-on-1-yl) ethane (IV). In the absence of water the unsaturated dimeric compound 1,3-bis(pyrrolidin-2-on-1-yl)but-1-ene (II) is obtained.[86] The dimerization is quantitative at room temperature within 24 h in the presence of trifluoroacetic acid.[86,89] There is evidence for the reversibility in water of all reactions presented in Scheme 2.1 except for NVP dimerization (reaction II).[88]
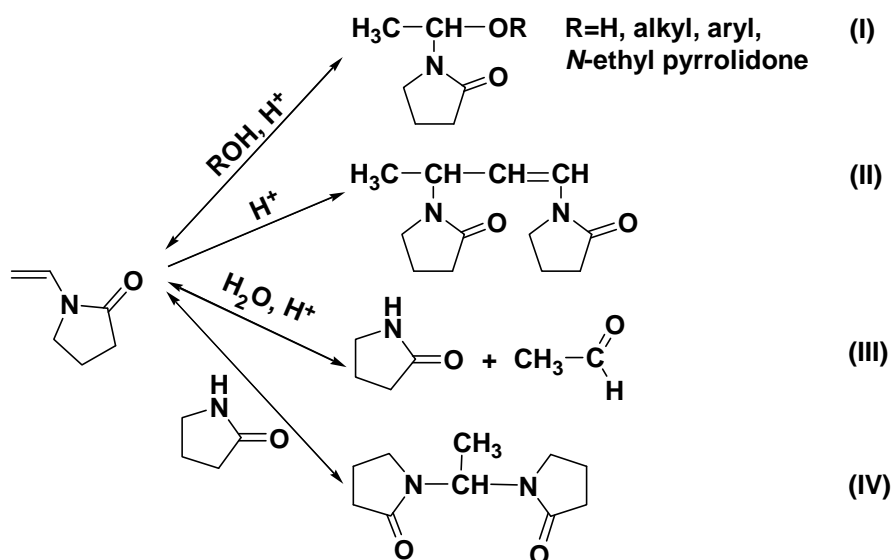
Scheme 2.1 : Side-reactions leading to degradation of NVP.

This reaction scheme was compiled from *Encyclopedia of Polymer Science and Engineering*; 2nd ed.; John Wiley and Sons, Inc., 1989; Vol. 17, p 200-202 and publications by Senogles et *al.*[88] and Breitenbach et *al.*[86]

It is important to keep in mind that these reactions can occur, because they influence polymerization rates. The apparent rate of polymerization decreases if the monomer is consumed via non-radical reactions. Some species may also participate in chain-transfer reactions and influence the molecular weight distribution of the product.

Living radical polymerization

Living radical polymerization (LRP) techniques have been developed in order to overcome the shortcomings of conventional free-radical polymerization. The general concept behind LRPs relies on limiting the effects of transfer and termination reactions, which we will refer to as chain-breaking events. The objectives include control over the molar mass distributions, predictable molar masses and chains endcapped with a reactive moiety. The latter characteristic, also referred to as the "living"[90] character enables chain-extension and the synthesis of block copolymers. The living character may be met in spite of a poor level of control over the molar mass distribution. A debate has animated the scientific community regarding the definition of "living" in the field of free-radical polymerization.[91] The main concern was that radical species have a limited lifetime and therefore transfer and termination are not suppressed in LRPs. Were the reader not convinced yet by the scientific arguments, the terminology living may be supported by lyrical considerations:

> "This helpful and lasting term [*living polymerization]* carries a memory of the romantic period, having freed polymer chemists from many earlier restrictions of their fantasy. Finally, we can draw a purely illustrative analogy to human life. Really, why should we deprive a man of the attribute *living,* even being aware of his mortality?"

Professor Konstantin S. Kazanskii, in comments to *Living Polymerization: Rationale for Uniform Terminology.*[91]

Kinetic basis of LRPs

The kinetic fundamentals of conventional free-radical polymerization apply in LRP. The propensity for radicals to undergo propagation, transfer or termination is reflected and quantified by the rate constants of propagation, transfer and termination. These rate constants are an intrinsic characteristic of the species present in the polymerization medium. Rate constants are a function of temperature and pressure but apart from these parameters the polymer chemist has only limited means to affect the chemoselectivity of the polymerization.

The rate constants are inherent to a given polymerization system, however the probabilities (rates and not rate constants) for radicals to undergo propagation, transfer and termination reactions are a function of the concentration in active species. The rate of radical-radical termination (R_t) is proportional to the square of the radical concentration ($R_t \propto [P_n\bullet]^2$) whereas the rate of propagation is directly proportional to the radical concentration ($R_p \propto [P_n\bullet]$). Therefore a way to avoid termination is by decreasing the concentration in radicals. It is this kinetic "trick" that has been exploited so far for the development of most LRP techniques. For this purpose a controlling agent is introduced in the polymerization medium, which reversibly deactivates the chains. An equilibrium establishes between active and dormant chains. The chains can be reactivated and undergo propagation between two activation deactivation steps. The ratio of active to dormant species is typically lower than $1:10^3$.

Another fundamental requirement for obtaining narrowly distributed polymers is that all chains be initiated at the same time. Living ionic polymerization which was the first example of living polymerization[90,92] is often used as a reference. To illustrate the necessity for all chains to be initiated at the beginning of the polymerization we can cite the case of the anionic living polymerization of butadiene with *n*-butyl lithium. Depending on the solvent initiation is slow and as a result PDIs are high in spite of all chains being living.

The different types of LRPs

A distinction can be made between two classes of LRP techniques with regards to the mechanism involved in the activation-deactivation equilibrium. The distinction is between systems based on the persistent radical effect (PRE)[93-95] and systems based on degenerative transfer. The generic name stable free-radical polymerization (SFRP) was coined for the systems based on the PRE. SFRPs include nitroxide-mediated polymerization (NMP),[96,97] and cobalt-mediated polymerization.[98,99] Certain nitroxides and cobalt porphyrin complexes provide radicals capable of reversibly trapping carbon-centered radicals and unable to crosspropagate with the monomer. Atom-transfer radical polymerization (ATRP)[100-102] is also based on the PRE but it is a catalytic process. In the

dormant form the chains are endcapped with an atom or group (generally a halogen atom) which is removed by transfer from a transition metal catalyst under a redox mechanism. Iron, cobalt, nickel, ruthenium and other transition-metal catalysts can be used but the most studied are copper catalysts.[103] The systems based on degenerative transfer are iodine-transfer,[104] reversible addition fragmentation transfer (RAFT),[105,106] organotellurium (TERP)[107,108] and organostibine-mediated polymerization.[109] Activation occurs via a bimolecular radical transfer between a dormant and an active species. Polymer formation occurs by an overall incorporation of monomer units in the chain-transfer agent (CTA). The molar mass of the CTA increases between two activation/deactivation steps. Apart from the number of monomer units the initial CTA and dormant chains have the chemical same structure, hence the term "degenerative". RAFT mediated polymerization is the focus of this thesis and will now be discussed in more detail.

RAFT-mediated polymerization

RAFT-mediated polymerization is defined as a degenerative process where the CTA is a thiocarbonylthio species of general structure Z-C(S)S-R. In the first publications on RAFT-mediated polymerization,[105,106] the CSIRO group proposed various structures for thiocarbonylthio compounds. They reported that dithioesters (Z = alkyl or aryl) were efficient CTAs to control the molar mass distributions of Sty, acrylates and methacrylates and predicted that dithiocarbamates (Z = dialkylamino) and xanthates (Z = alkoxy) would be relatively inefficient.[105] Simultaneously the Rhodia research group patented the Macromolecular Design via the Interchange of Xanthate (MADIX) process,[110,111] where xanthates are used as CTAs to control the polymerization of VAc under a mechanism identical to the RAFT process. They later proposed dithiocarbamates as universal CTAs[112] (*i.e.* efficient with all monomers). A deeper understanding of the RAFT mechanism gives the tools to estimate the efficiency of the CTAs for a given monomer.

The RAFT mechanism

The generally accepted mechanism of RAFT-mediated polymerization as proposed by the CSIRO group[113] is presented in scheme 2.

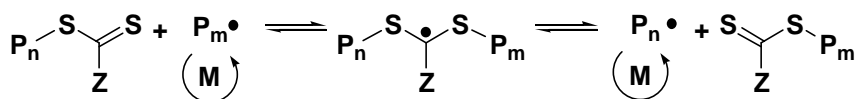**Initiation: by initiator-derived primary radicals**

$I\bullet + M \longrightarrow IM\bullet \longrightarrow \longrightarrow P_n\bullet$
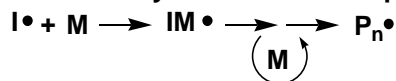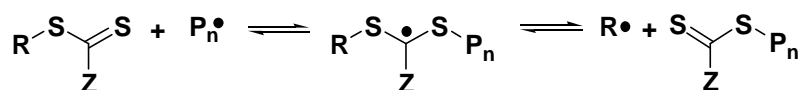
Pre-equilibrium

Reinitiation: by the CTA-derived radicals

$R\bullet + M \longrightarrow RM\bullet \longrightarrow \longrightarrow P_n\bullet$
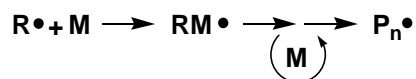
Main RAFT equilibrium

Scheme 2.2: RAFT mechanism.

The polymerization is initiated by a free-radical source, generally produced via thermal decomposition azo initiator such as AIBN but γ radiation[114] or UV radiation may also be applied.[115] After one or more monomer additions the propagating radicals add to the CTA thus producing an intermediate radical. Fragmentation of the intermediate radical follows to release either the leaving group radical R•, which can reinitiate polymerization, or the incoming propagating radical. The main equilibrium is between dormant species end-capped with the CTA and active species which can undergo propagation.
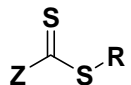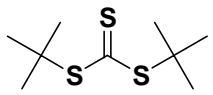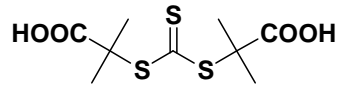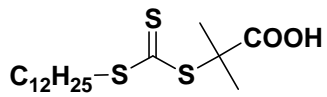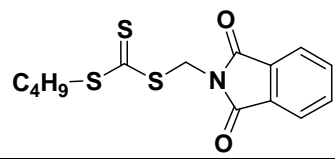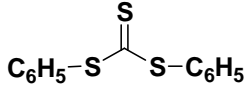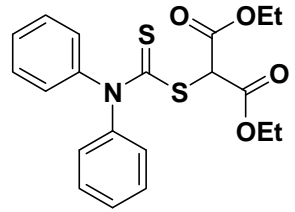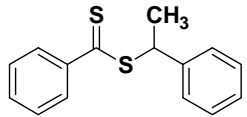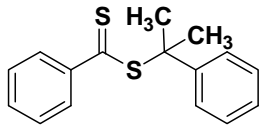
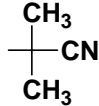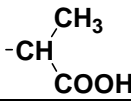## Living radical polymerization of NVP
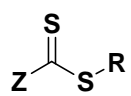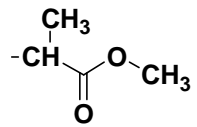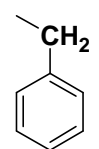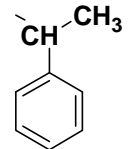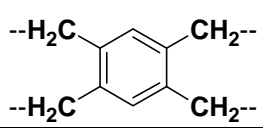
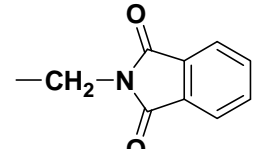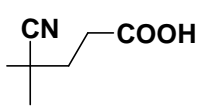In the last four years numerous research groups were actively searching for methods to obtain PVP via living radical polymerization. Pioneering work by Shi et *al.* provided preliminary indication that RAFT polymerization was a plausible option to control the polymerization of vinyl amides.[116] They obtained block copolymers with *N*-vinylformamide from a xanthate endfunctional poly(ethylene glycol) (PEG). Although

the PDI of the product was high, their experiments suggested that xanthates were tolerant to amide functionalities and did not inhibit the polymerization of amide-containing monomers. A literature review of the CTAs investigated so far with NVP is summarized in Table 2.4. The first attempts to control the polymerization of NVP via RAFT-mediated polymerization were published by Chernikova and co-workers.[117,118] They used the symmetrical CTA di-*tert*-butyl trithiocarbonate. An increase in the viscous-average molecular weight with conversion was measured but they did not examine the PDIs. They observed strong rate retardation, which increased with CTA concentration and an apparent inhibition period. With the use of electron spin resonance (ESR) spectroscopy they identified the intermediate radical species corresponding to the pre-equilibrium step but not those from the main equilibrium. Altogether these results suggested that optimization of the structure of the CTA was required, *i.e.* design of a CTA with a less stabilizing Z group to limit retardation and a better leaving/reinitiating R group to eliminate apparent inhibition.[119] Bindu et *al.* used the CTA *S*-(diethylmalonate) *N*-diphenyl dithiocarbamate.[120] They reported the preparation of narrowly distributed PVP (Table 2.4). The polymer was used as a macroCTA to prepare block copolymers with styrene and methyl methacrylate. The efficiency of block copolymer formation was low as indicated by a high ratio of homopolymer in the final product. Devasia et *al.* obtained narrowly distributed PVP ($M_{n,NMR}$ = 8000 – 53 000 g·mol^{-1}, 1.3 < PDI < 1.7) via xanthate-mediated polymerization with *S*-(2-propionic acid methyl ester)-*O*-ethyl xanthate.[121] They used the living polymer thus prepared to synthesize block copolymers with *n*-butyl acrylate and *N*-vinyl caprolactam.[121,122] In a review, Moad et *al.* mentioned the preparation of PVP with M_n = 17 000 g·mol^{-1}, PDI = 1.35 in the presence of *O*-ethyl *S*-(cyanomethyl) xanthate in methanol at 60 ºC.[123] Wan et *al.* reported simultaneous control over the molecular weight distribution and enhancement of the syndiotacticity of PVP by performing the xanthate-mediated polymerization of NVP in fluoroalcohols.[124] They found phenethyl dithiobenzoate to inhibit the polymerization of NVP whereas *O*-ethyl xanthates were efficient CTAs. A strong dependence of the level of control on the nature of the CTA leaving group (phenethyl was less efficient than benzyl) and on the polymerization temperature was reported (60 ºC gave the lowest PDIs and linear increase of M_n with conversion whereas 20 ºC and 120 ºC lead to irregularities in M_n vs.

conversion and higher PDIs. Although low PDIs were obtained with selected xanthates in bulk and in some fluoroalcohols with low M_n (*e.g.* $M_{n,SEC}$ = 10 900 g·mol^{-1}, PDI = 1.14), the PDIs were above 3 when high M_n polymers were prepared (M_n = 92 000 – 164 000 g·mol^{-1}). Bilalis et *al.* used trithiocarbonates and produced PVPs in bulk and in THF with relatively high PDIs (M_n = 7 000 - 97 000 g·mol^{-1}, PDI = 1.5 - 2.3).[125] Although the level of control seemed poor they prepared block copolymers with 2-vinylpyridine. Nguyen et *al.* prepared block copolymers PVP-*block*-PVAc and 4-arm star PVP using a monofunctional or a tetrafunctional xanthate, respectively.[2] They reported a hybrid behavior[126] when the benzyl leaving group was used, as indicated by higher M_n values at the beginning of the polymerization than expected from the stoichiometry. We published a comparative study on NVP polymerization mediated by *O*-ethyl xanthates with 3 different leaving groups.[127] We correlated the ability of the leaving group to give fast and selective initialization with higher level of control over the molecular weights. This work will be discussed and additional results presented in Chapter 4. Postma et *al.* used *O*-ethyl *S*-(phthalimidylmethyl) xanthate to introduce a latent primary amine chain-end.[128] They incriminated their SEC conditions (*N,N*-dimethylacetamide (DMAc) containing 0.045 % w/v LiBr at 80 °C; polystyrene calibration) for inconsistencies between molecular weight data obtained and those expected from the apparent rate of utilization of the CTA. Hu and Zhang prepared well-defined gradient terpolymers of NVP with styrene and maleic anhydride under γ-ray irradiation in the presence of *S,S'*-dibenzyl trithiocarbonate.[129] They attributed the ability of a trithiocarbonate CTA to control the terpolymerization of NVP (whereas it is inefficient in NVP homopolymerization) to the formation of a charge-transfer complex between NVP and maleic anhydride.

Table 2.4: CTAs reported so far for RAFT-mediated polymerization of NVP.

CTA	*Ref.*	M_n (PDI)	SEC conditions: solvent, [Temperature]; calibration std.	Observations
Trithiocarbonates				
	117	NS	NA	ESR identification of preequilibrium intermediate radical; retardation, inhibition
	125	6300 – 14700 (1.9 – 2.1)	DMF [40], PS	in bulk, DMF, water, 80 ºC
	125	8000 (2.3) 90000 (1.5)	DMF [40], PS	in bulk, THF, 80 ºC PDI>2 in H$_2$O PVP-*block*-P(2VP)
	128	22600 (1.48) 26700 (1.61)	DMAc (0.03% w/v LiBr,) [80], PSty	
	129	4200 (1.47) 15700 (1.17)	THF, PSty	terpolymerization with sty and maleic anhydride in THF
Dithiocarbamate				
	120	4200-45800^a (1.3-1.5)	H$_2$O/CH$_3$OH (80/20) containing 0.1 M NaNO$_3$, PEO	in dioxane, 80 ºC, long reaction time (>23h) PVP-*block*-PSty PVP-*block*-PMMA
Dithiobenzoates				
	124	NA	NA	no polymer
	125	135000 (1.6) 65000 (1.9)	DMF [40], PS	very high M_n even at low conversion

Xanthates: Z = -OEt, R =	*Ref.*	M_n (PDI)	SEC conditions: solvent, [Temperature]; calibration std.	Observations
CH₃ / -CH / O-CH₃ / O (methyl 2-substituted ester)	121,122	8000[a] (1.3) / 53000[a] (1.7)	methanol:water 20:80 v/v (NaNO₃ 0.1 M); PVP	in dioxane, 80 ºC / PVP-*block*-P*n*BA / PVCl-*block*-PVP
-CH₂-CN	123	17000 (1.35)	NS	methanol, 60 ºC
benzyl (CH₂-phenyl)	124	12400 (1.47)	DMF (LiCl 0.1 M) [40], PMMA	in bulk or fluoroalcohols
	2	11000 (1.38)	DMAc (0.03% w/v LiBr, 0.05% BHT) [50], PSty	hybrid behavior PVP-*block*-PVAc
CH-CH₃ (1-phenylethyl)	124	10900 (1.14)	DMF (LiCl 0.1 M) [40], PMMA	in bulk or fluoroalcohols
	2	16000 (1.19)	DMAc (0.03% w/v LiBr, 0.05% BHT) [50], PSty	$M_{n,SEC}$ lower (half) than expected PVP-*block*-PVAc
-H₂C / CH₂- / -H₂C / CH₂- (tetra-substituted benzene)	2	35000 (1.2)	DMAc (0.03% w/v LiBr, 0.05% BHT) [50], PSty	4-arm star
CH₃ / -C-CN / CH₃	127	14400 (1.32)	HFIP [40], PMMA	short apparent inhibition
CH₃ / -CH / COOH	127	15500 (1.34)	HFIP [40], PMMA	
-C(CH₃)₃	127	31900 (1.74)	HFIP [40], PMMA	poor leaving group
O / -CH₂-N (phthalimide) / O	128	4400 (1.16) / 18500 (1.54)	DMAc (0.03% w/v LiBr,) [80], PSty	in toluene, 60 ºC
CN / -COOH	130	2000 – 7000 (1.15 -1.21)	DMF (LiCl 0.01 M) [40], PMMA	

[a] M_n determined via ¹H-NMR; *Abbreviations*: NS: not specified, NA: not applicable; DMF: *N,N*-dimethylformamide, DMAc: *N,N*-dimethylacetamide, *n*BA : *n*-butyl acrylate, VCl : *N*-vinylcaprolactam, sty: styrene, 2VP: *2*-vinylpyridine, MMA: methyl methacrylate.

The above-mentioned reports on RAFT polymerization of NVP reveal the influence on the level of control of the Z and R groups of the CTA, the solvent and the temperature. They also point at the necessity to examine the mechanism and kinetics of the xanthate-mediated polymerization of NVP to be able to predict the efficiency of a given CTA. The aim is to limit the apparent inhibition, retardation and hybrid behavior reported in many of these publications. Finally the SEC conditions seem to affect the apparent molecular weight distribution data significantly. They are different in every laboratory and thus make it difficult to compare between studies.

Other LRP techniques were attempted on NVP. Cobalt-mediated polymerization was poorly efficient with PVP but the PDIs could be reduced by incorporation of the comonomer VAc.[131] NMP was inefficient so far,[125] most likely due to the difficulty to control the nitroxide-NVP bond homolysis, as is the case with VAc.[132] NVP was polymerized in the presence of a PMMA macro(azo)initiator prepared via ATRP[131] and very recently ATRP provided PVP with controlled molecular weights.[133] The most conclusive results regarding the LRP of NVP were obtained via organostibine-mediated polymerization[71,109] and TERP.[134] Yusa et *al.* directly compared xanthate-mediated polymerization and TERP of NVP.[134] They found both processes successful but obtained a higher level of control via TERP (PDI = 1.0 – 1.1) than via xanthate-mediated polymerization (PDI = 1.1 – 1.2) under similar conditions.

Characterization of RAFT polymers

Efficient molecular weight control is indicated by M_n increasing linearly with conversion and by a low PDI. M_n can be predicted from the initial stoichiometry. Provided that all of the CTA is consumed at the beginning of the polymerization, that one chain is produced per CTA and that the number of chains initiated by the primary radical source is negligible, $M_{n,theo}$ is given as a function of monomer conversion (α) by:

$$M_{n,theo,\alpha} = \frac{monomer\ consumed}{number\ of\ chains} \times M_M + M_{endgroups} = \frac{[M]_i}{[CTA]_i} \times \alpha \times M_M + M_{CTA}$$

$$(Eq.2.3)$$

where M_M and M_{CTA} are the molar mass of the monomer and the CTA, respectively and $[M]_i$ and $[CTA]_i$ are the initial concentrations in monomer and CTA, respectively. Size-exclusion chromatography (SEC) is the only technique accepted so far to quantitatively measure the molecular weight distributions of polymers. In the RAFT literature $M_{n,theo}$ is often reported and compared to SEC results.

The living character of RAFT-mediated polymerizations is evaluated in terms of the possibility to reactivate the chains. For this purpose the RAFT polymer is isolated and a second monomer can be added (as well as a radical source) for the formation of block copolymers. Alternatively the same monomer is added for chain-extension. M_n must increase upon either process. Block copolymer formation may result in changes in physical properties (*e.g.* mechanical, optical or solution properties), depending on the copolymer system. However changes in properties may also be obtained in a simple blend of two homopolymers. Thus changes in properties are not a guarantee of the success of block copolymer formation. The techniques used to characterize the block copolymers must include their separation from homopolymers, *e.g.* liquid chromatographic techniques.[135] A prerequisite for chain reactivation is that the chains be endfunctional. NMR spectroscopy can be used to detect the presence of the CTA at the chain-end of relatively low M_n polymers (for quantitative analysis typically $M_n < 10\,000$ g·mol^{-1}). The specific UV absorption of thiocarbonylthio compounds is often exploited.[136] Matrix assisted laser desorption ionization time of flight mass spectroscopy (MALDI-ToF-MS) provides the exact mass of the chains. As such it can help identify the nature of the end-groups. Hyphenation of the above-mentioned techniques with SEC is of particular interest as information on the end-groups as well as their repartition over the polymer distribution may be obtained. The characterization techniques with most significance to the work presented in this thesis are exposed below. The relevance of SEC analyses for the characterization of molecular weights and molecular weight distributions and possible alternative techniques are discussed.

Molecular weight and molecular weight distribution

SEC is the most widely used technique for the characterization of molecular weights and molecular weight distributions of polymers. The polymer in solution is

eluted through a column without enthalpic interactions with the packing material. Separation occurs according to the volume of the polymer chains. Chains with a smaller hydrodynamic volume penetrate more pores. Thus the smaller the hydrodynamic volume the higher the eluent volume required to elute the polymer from the column. The hydrodynamic volume of macromolecules increases with molecular weight. While it is difficult to get a grasp on the hydrodynamic volume, Grubisic and Benoit showed that SEC separates according to the product $[\eta] \times M$ where $[\eta]$ is the intrinsic viscosity.[137,138] The proportionality is given by the Mark-Houwink-Kuhn-Sakurada (MHKS) relationship $[\eta] = K \times M^a$, where M is the true molecular weight and K and a are the MHKS parameters. They depend on the polymer-solvent system and the temperature. The relationship does not apply to low molecular weights and MHKS parameters are not always available for the polymer-solvent system considered. True molecular weights can be obtained via SEC using an online viscometer.

Most polymers can be detected using a refractive index (RI) detector. The signal is then proportional to the concentration of polymer eluting. A calibration curve is established with polymer standards of low polydispersity and known molecular weights. Thus the values obtained for the analyte are not true but apparent or relative molecular weights with regards to the standard polymer. The correlation between molecular weight and hydrodynamic volume depends on the quality of the solvent. In good solvents the interactions between the polymer and the solvent are increased. The polymer chain expands and exhibits large dimensions. In poor solvents intramolecular interactions are favored. Chains tend to collapse and display smaller dimensions. The intermediate situation is the theta (θ) solvent for a given polymer (or θ conditions) where polymer-solvent interactions counterbalance polymer-polymer interactions.

Narrowly distributed standards are not always available. For instance PVP standards are not available. The calibration curve is then obtained with a different polymer from the analyte. In such cases two polymer-solvent couples have to be considered. The difference in solvent quality between the analyte and the standard can lead to huge errors in the determination of the molecular weights and PDIs.[139] Such discrepancies can lead to erroneous conclusions on the degree of control achieved in the

polymerization.[140] High PDIs may indicate that the polymerization was not controlled but can also be the result of the eluent being in a better solvent for the analyte than for the standard. Conversely low PDIs can be measured even though control over the polymerization was inefficient in cases where the analyte is in a poorer solvent than the standard. The quality of the solvent for the analyte and the standards can be compared based on MHKS parameters or the second virial coefficient or solubility parameters. In this thesis all SEC results presented were obtained using 1,1,1,3,3,3-hexafluoro-2-propanol (HFIP) as the eluent and calibration with PMMA standards. Neither the parameters characterizing the interactions between HFIP and the polymers nor the solubility parameters of HFIP were found in the literature. Nonetheless let us remark that the Hildebrand solubility parameters for PVP ($\delta = 25.6$ MPa$^{1/2}$) are significantly different from that of PMMA ($\delta = 18.4$ - 19.5 MPa$^{1/2}$).[61] Therefore molecular weight and PDI values for PVP will be presented as PMMA-equivalent values and must not be the only criteria for the evaluation of the living process.

Matrix assisted laser desorption ionization time of flight mass spectroscopy (MALDI-ToF-MS)

MALDI-ToF-MS is an absolute method for the determination of molar masses. It utilizes a soft ionization technique (ultraviolet of infrared laser pulse) to transfer a substrate premixed with a matrix into the gas phase. The energy from the laser is mostly absorbed by the matrix therefore the structure of synthetic polymers may remain intact. The polymer chains are separated according to the ratio of absolute mass over charge (m/z). In general only singly charged polymers are detected. MALDI-ToF-MS is particularly useful for the determination of polymer end-groups. In this case the "reflector" mode is used for optimal resolution. The technique has already been applied to PVP and discrimination between various end-groups was possible.[71,75,85,141,142] However MALDI-ToF-MS often does not quantitatively represent the chemical composition distribution. One of the causes may be fragmentation of the chain(end)s[143] or selective desorption/ionization depending on the end-group. The difficulty in obtaining quantitative results on the polymer end-group distribution will be illustrated for PVP in chapter 6.

Another limitation of MALDI-ToF-MS is molar mass discrimination. This phenomenon is evidenced by comparing the molar mass distribution data obtained via MALDI-ToF-MS with those obtained via SEC. In some cases, particularly for narrowly distributed polymers, a good agreement is obtained between both analyses.[144] For polydisperse samples molar mass discrimination was found to often underestimate[145] but sometimes overestimate the high molar mass fractions.[146] An alternative to bypass mass discrimination is to couple SEC with MALDI-ToF-MS. Narrowly distributed fractions can be collected upon separation via SEC and the fractions analyzed separately with MALDI-ToF-MS to yield true molecular weight values.[144,147,148] Factors influencing mass discrimination include sample preparation (polymer, matrix, couter-ion and their concentration ratio[149] and solvent[150]), instrument parameters[151] and laser intensity.[143] Data processing may also be the cause of inadequate interpretation of MALDI-ToF-MS spectra.[152] Interestingly polydisperse PVP samples (PDI = 1.8 – 2.2) were found to give a good agreement between both techniques under particular conditions, although the authors did not specify the SEC conditions they used.[153] The authors attributed this exceptional behavior to the ability of the matrix to co-crystallize with the polymer. Under other conditions and even after SEC separation low molecular weight contaminants prevented the detection of the main high molecular weight species.[154]

Other characterization techniques

Diffusion ordered NMR spectroscopy (DOSY) has been proposed as a separation technique to evaluate the molecular weight characteristics of uncharged water-soluble polymers including PVP.[155] The technique has not been used yet to determine PDIs and further investigation is required before it is used for molecular weight determination.

Traditional organic chemistry techniques are useful to determine average characteristics of the polymers. Nuclear magnetic resonance (NMR) spectroscopy and UV-Vis spectroscopy will be presented in this thesis mostly for the determination of end-group functionality. ^{1}H-NMR spectroscopy is particularly useful to determine the chemical structure of molecules but is only quantitative at relatively high concentrations. Concentration is limited by the solubility of the polymer in the deuterated solvent. Poor solubility of the polymer or decreased solubility of some segments compared to others

may lead to the disappearance (decrease) of the associated signals. This phenomenon is evidenced when phase-separation or micellization occurs.[156] It may lead to erroneous end-group quantification when solubility factors affect the polymer end-groups differently from the polymer backbone and sidegroups.

Adsorption liquid chromatography (LC) is a method for the separation of molecules with respect to their chemical composition. Separation occurs on the basis of enthalpic interactions between the polymer and the column packing material and their modulation due to interactions with the eluent. However polymers having the same chemical structure (repeating unit and end-groups) elute at different elution volumes depending on chain-length. LC at critical conditions or close to critical conditions (LC-CC) refers to the unique situation where the polymer elutes regardless of the molecular weight.[157] LC-CC is particularly useful for the determination of the chemical composition distribution of homopolymers (end-group functionality) or block copolymers (comonomer distribution). Critical conditions for a given polymer composition refer to a type of column packing material, mobile phase composition, temperature and flow-rate. Separation is extremely sensitive to small variations in these parameters. Gradient polymer elution chromatography (GPEC)[158] is an attractive alternative because it is tolerant to small experimental variations and shortens the length of each analysis. The polymer is injected in a weak solvent causing it to precipitate on the column. The eluent strength is gradually increased thus causing polymer elution. Although separation is a function of both the molecular weight and chemical composition of the macromolecules it is often successfully applied for the separation of block copolymers.[159]

Identification of the causes of non-ideality in living radical polymerization systems

Publications in the filed of living radical polymerization have a common objective, which is to demonstrate or invalidate the success of a given living process in controlling molecular weight distributions and controlling macromolecular architectures. In the present chapter the mechanisms and kinetics of conventional and living radical

polymerizations were presented. Methods for characterization of the resulting polymers were discussed. While characterization methods enable us to identify deviations from an ideal living polymerization system, understanding the mechanism and kinetics of the processes enable us to identify causes of failure. Ultimately, experimental conditions may be improved and the degree of livingness enhanced. To summarize, deviations from ideality in RAFT mediated polymerizations may be due to:

(i) Inappropriate mediating agent. Successful control requires optimization of the CTA structure to enable high rates of addition and fragmentation and ability of the reinitiating group to add to the monomer. Poor transfer efficiency,[160] slow rate of fragmentation[119] and slow rate of reinitiation[161] have been proposed as 3 of the main causes of lack of control in RAFT mediated polymerizations.

(ii) Radical chain-termination. The radical concentration decreases over time indicating that, although reduced in LRP systems, bimolecular radical termination is not suppressed. Monteiro and co-workers demonstrated that the molecular weight distribution of polystyrene prepared in the presence of a difunctional CTA can be tailored by adjusting the initiator concentration.[162] PDIs ranging from 1 to 2 were thus obtained with the same CTA. The loss of end-group functionality (chain-end functional polymers ranging from telechelic to semi-telechelic were obtained) provided evidence that primary radical termination was critical in controlling the molecular weight distribution. Termination may also affect CTA-derived intermediate radicals causing rate retardation[163,164] and influencing the molecular weight distribution, including the fact that three-arm stars may be formed.[165,166]

(iii) Irreversible transfer. Transfer via proton abstraction, which occurs in conventional free-radical polymerization is not suppressed in RAFT mediated polymerization. In the solution RAFT mediated polymerization of acrylic acid the leveling off of M_n at high conversions and increase in PDI was attributed to transfer to the solvent.[167] Favier et al. suggested that

sulfides may form as by-products during RAFT-mediated polymerizations and demonstrating their effect on broadening the molecular weight distribution.[168] The effects of transfer reactions were investigated indirectly in terms of branching in the RAFT mediated polymerization of VAc.{Pinto, 2008 #1124} The authors matched empirical calculations with experimental results and proposed that branching is reduced compared to conventional radical polymerization not only because the molecular weights are lower but also because intramolecular transfer to the polymer is reduced. Nonetheless polymerization rates and molecular weight distributions are not affected.

(iv) Chain deactivation. Particularly relevant to poorly stabilized monomer is the case where head to head monomer addition occurs, which leads to decreased reactivity of the chain-ends. Head to head addition has been identified as the origin for high polydispersity of PVAc prepared via alkyl iodine mediated polymerization[72] and TERP.[170] It is important to note that even though the proportion of head to head addition is low, it may have a significant effect on the level of control at high conversions. In the aforementioned examples, the products of head to head addition linked to the controlling agent do not undergo fragmentation and therefore do not propagate but instead accumulate in the system. As a result polymerization is retarded and PDIs are high. Okamoto and co-workers demonstrated that decreasing the proportion of head to head additions (by performing the polymerization in fluoroalcohols) increased the level of control over the molecular weight distribution.[73] Yamago and co-workers demonstrated that the proportion of non-propagating head to head adducts in the organostibine mediated polymerization of NVP increases with an increase in the initial ratio of monomer to controlling agent.[71] This is because when high M_ns are targeted (*i.e.* when the ratio of monomer to CTA is high) a larger number of propagation steps are required to reach the same monomer conversion, whereas the probability for head to head addition remains the same. They identified the formation of head to head adducts

as the main cause of loss of controllability in NVP polymerization; they did not, however, investigate other causes.

(v) Non-radical chain deactivation. For instance, hydrolysis of RAFT agents in water-based polymerization systems and subsequent broadening of the molecular weight distributions is well documented.[171-173] More generally, side-reactions affecting the living chain-end of the polymer lead to dead chains, thus affecting the molecular weight distribution.

Kinetic and mechanistic investigations of the RAFT mediated polymerization of NVP can help identify causes of non-ideality and define experimental conditions to optimize the level of control over the molecular weight distribution and over the end-groups.

Reference list

(1)   Kirsh, Y.E. *Water Soluble Poly-N-Vinylamides: Synthesis and Physicochemical Properties*; Wiley, Chichester, UK **1998**.

(2)   Nguyen, T.L.U.; Eagles, K.; Davis, T.P.; Barner-Kowollik, C.; Stenzel, M.H. *J. Polym. Sci. Part A: Polym. Chem.* **2006**, *44*, 4372–4383.

(3)   Bindu, N. *Int. J. Tox.* **1998**, *17*, 95-130.

(4)   Kristinsson, K.G. *J. Med. Microbiol.* **1989**, *28*, 249–257.

(5)   Francois, P.; Vaudaux, P.; Nurdin, N.; Mathieu, H.J.; Descouts, P.; Lew, D.P. *Biomaterials* **1996**, *17*, 667-676.

(6)   Abraham, G.A.; de Queiroz, A.A.A.; Roman, J.S. *Biomaterials* **2001**, *22*, 1971-1985.

(7)   Kallrot, M.; Edlund, U.; Albertsson, A.-C. *Biomaterials* **2006**, *27*, 1788-1796.

(8)   Smith, L.E.; Rimmer, S.; MacNeil, S. *Biomaterials* **2006**, *27*, 2806-2812.

(9)   Sanborn, S.L.; Murugesan, G.; Marchant, R.E.; Kottke-Marchant, K. *Biomaterials* **2002**, *23*, 1-8.

(10)   Krasovskaya, S.M.; Uzhinova, L.D.; Andrianova, M.Y.; Prischenko, A.A.; Livantsov, M.V. *Biomaterials* **1991**, *12*, 817–820.

(11)   Tunney, M.M.; Gorman, S.P. *Biomaterials* **2002**, *23*, 4601-4608.

(12)   Higuchi, A.; Shirano, K.; Harashima, M.; Yoon, B.O.; Hara, M.; Hattori, M.; Imamura, K. *Biomaterials* **2002**, *23*, 2659-2666.

(13)   Peng, Q.; Lu, S.; Chen, D.; Wu, X.; Fan, P.; Zhong, R.; Xu, Y. *Macromol. Biosci.* **2007**, *7*, 1149-1159.

(14)   Hong, Y.; Chirila, T.V.; Vijayasekaran, S.; Dalton, P.D.; Tahija, S.G.; Cuypers, M.J.H.; Constable, I.J. *J. Biomed. Mater. Res.* **1996**, *30*, 441-448.

(15)   Lugão, A.B.; Rogero, S.O.; Malmonge, S.M. *Rad. Phys. Chem.* **2002**, *63*, 543-546.

(16)   Chin, W.W.L.; Lau, W.K.O.; Bhuvaneswari, R.; Heng, P.W.S.; Olivo, M. *Cancer Lett.* **2007**, *245*, 127-133.

(17)   Jatzkewitz, H. *Zeit. Phys. Chem.* **1954**, *297*, 149-156.

(18)   Veron, L.; Revol, M.; Mandrand, B.; Delair, T. *J. Appl. Polym. Sci.* **2001**, *81*, 3327-3337.

(19)   D'Souza, A.J.M.; Schowen, R.L.; Topp, E.M. *J. Control. Rel.* **2004**, *94*, 91-100.

(20)   Kamada, H.; Tsutsumi, Y.; Yamamoto, Y.; Kihira, T.; Kaneda, Y.; Mu, Y.; Kodaira, H.; Tsunoda, S.-i.; Nakagawa, S.; Mayumi, T. *Cancer Res.* **2000**, *60*, 6416-6420.

(21)   Le Garrec, D.; Gori, S.; Luo, L.; Lessard, D.; Smith, D.C.; Yessine, M.-A.; Ranger, M.; Leroux, J.-C. *J. Control. Rel.* **2004**, *99*, 83-101.

(22)   Benahmed, A.; Ranger, M.; Leroux, J.-C. *Pharm. Res.* **2001**, *18*, 323-328.

(23)   Kuskov, A.N.; Villemson, A.L.; Shtilman, M.I.; Larionova, N.I.; Tsatsakis, A.M.; Tsikalas, I.; Rizos, A.K. *J. Phys. Condensed Matt.* **2007**, *19*, 205139/205131-205139/205111.

(24)   Sairam, M.; Ramesh Babu, V.; Krishna Rao, K.S.V.; Aminabhavi, T.M. *J. Appl. Polym. Sci.* **2007**, *104*, 1860-1865.

(25)   Zelikin, A.N.; Quinn, J.F.; Caruso, F. *Biomacromolecules* **2006**, *7*, 27-30.

(26)   Torchilin, V.P.; Levchenko, T.S.; Whiteman, K.R.; Yaroslavov, A.A.; Tsatsakis, A.M.; Rizos, A.K.; Michailova, E.V.; Shtilman, M.I. *Biomaterials* **2001**, *22*, 3035-3044.

(27)   Guowei, D.; Adriane, K.; Chen, X.; Jie, C.; Yinfeng, L. *Int. J. Pharm.* **2007**, *328*, 78-85.

(28)   Patel, A.; Mequanint, K. *Macrom. Biosci.* **2007**, *7*, 727-737.

(29)   Sanli, O.; Orhan, E.; Asman, G. *J. Appl. Polym. Sci.* **2006**, *102*, 1244-1253.

(30)   Riis, T.; Bauer-Brandl, A.; Wagner, T.; Kranz, H. *Eur. J. Pharm. Biopharm.* **2007**, *65*, 78-84.

(31)   Lai, M.C.; Hageman, M.J.; Schowen, R.L.; Borchardt, R.T.; Topp, E.M. *J. Pharm. Sci.* **1999**, *88*, 1073-1080.

(32)   Kishida, A. *Trends Pharm. Sci.* **2003**, *24*, 611-613.

(33)   Kamada, H.; Tsutsumi, Y.; Sato-Kamada, K.; Yamamoto, Y.; Yoshioka, Y.; Okamoto, T.; Nakagawa, S.; Nagata, S.; Mayumi, T. *Nature Biotech.* **2003**, *21*, 399-404.

(34)   Yoshioka, Y.; Tsutsumi, Y.; Mukai, Y.; Shibata, H.; Okamoto, T.; Kaneda, Y.; Tsunoda, S.-i.; Kamada, H.; Koizumi, K.; Yamamoto, Y.; Mu, Y.; Kodaira, H.; Sato-Kamada, K.; Nakagawa, S.; Mayumi, T. *J. Biomed. Mat. Res. A* **2004**, *70A*, 219-223.

(35)   Rabin, O.; Perez, J.M.; Grimm, J.; Wojtkiewicz, G.; Weissleder, R. *Nature Mat.* **2006**, *5*, 118-122.

(36)   Tsunoda, S.; Kamada, H.; Yamamoto, Y.; Ishikawa, T.; Matsui, J.; Koizumi, K.; Kaneda, Y.; Tsutsumi, Y.; Ohsugi, Y.; Hirano, T.; Mayumi, T. *J. Control. Rel.* **2000**, *68*, 335-341.

(37)   Chin, W.W.L.; Heng, P.W.S.; Bhuvaneswari, R.; Lau, W.K.O.; Olivo, M. *Photochem. Photobiol. Sci.* **2006**, *5*, 1031-1067.

(38)   Culbertson, B.M. *Prog. Polym. Sci.* **2001**, *26*, 577-604.

(39)   McMurrough, I. *Cerevesia* **1998**, *23*, 27-34.

(40)   Lahiri, S.; Sarkar, S. *Appl. Rad. Isotopes* **2007**, *65*, 387-391.

(41)   del C. Pizarro, G.; Marambio, O.G.; Jeria O, M.; Huerta, M.; Rivas, B.L. *J. Appl. Polym. Sci.* **2006**, *100*, 178-185.

(42)   Kondo, S.; Ozeki, M.; Nakashima, N.; Suzuki, K.; Tsuda, K. *Angew. Makromol. Chem.* **1988**, *163*, 139-147.

(43)   Joo, S.H.; Kim, J.H.; Kang, S.W.; Jang, J.; Kang, Y.S. *J. Polym. Sci., Part B: Polym. Phys.* **2007**, *45*, 2263-2269.

(44)   Smitha, B.; Sridhar, S.; Khan, A.A. *J. Power Sources* **2006**, *159*, 846-854.

(45)   Qiao, J.; Hamaya, T.; Okada, T. *Polymer* **2005**, *46*, 10809-10816.

(46)   Zhang, L.; Liang, Y.; Meng, L.; Lu, X.; Liu, Y. *Chem. Biodiv.* **2007**, *4*, 163-174.

(47)   Koonjul, P.; Brandt, W.; Farrant, J.; Lindsey, G. *Nucl. Acids Res.* **1999**, *27*, 915-916.

(48)   Czechowska-Biskup, R.; Ulanski, P.; Olejnik, A.K.; Nowicka, G.; Panczenko-Kresowska, B.; M. Rosiak, J. *J. Appl. Polym. Sci.* **2007**, *105*, 169-176.

(49)   Fikentscher, H.; Herrle, K. *Modern Plastics* **1943**, *23*, 157-163.

(50)   Madl, A.; Spange, S. *Macromolecules* **2000**, *33*, 5325-5335.

(51)   Senogles, E.; Thomas, R.A. *J. Polym. Sci., Pol. Lett. Ed.* **1978**, *16*, 555-562.

(52)   Czerwinski, W.K. *Makromol. Chem.* **1992**, *193*, 359-368.

(53)   Czerwinski, W.K. *Makromol. Chem.* **1991**, *192*, 1297-1305.
(54)   Bamford, C.H.; Schofield, E.; Michael, D.J. *Polymer* **1985**, *26*, 945-950.
(55)   Kaplan, R.H.; Rodriquez, F. *Appl. Pol. Symp.* **1975**, *26*, 181-195.
(56)   Ganachaud, F.; Theretz, A.; Erout, M.N.; Llauro, M.F.; Pichot, C. *J. Appl. Polym. Sci.* **1995**, *58*, 1811-1824.
(57)   Cizravi, J.C.; Tay, T.Y.; Pon, E.C. *J. Appl. Polym. Sci.* **2000**, *75*, 239-246.
(58)   Vana, P.; Davis, T.P.; Barner-Kowollik, C. *Macromol. Rapid Commun.* **2002**, *23*, 952-956.
(59)   Russell, G.T.; Gilbert, R.G.; Napper, D.H. *Macromolecules* **1992**, *25*, 2459-2469.
(60)   Olaj, O.F.; Zoder, M.; Vana, P.; Kornherr, A.; Schnoll-Bitai, I.; Zifferer, G. *Macromolecules* **2005**, *38*, 1944-1948.
(61)   Brandrup, J.; Immergut, E.H.; Grulke, E.A. *Polymer Handbook*; John Wiley and Sons, Inc, **1999**.
(62)   Huglin, M.B.; Khairou, K.S. *Eur. Polym. J.* **1988**, *24*, 239-243.
(63)   Nicolas, G.; Ligia, G.; Deodato, R. *Polym. Int.* **1998**, *45*, 285.
(64)   Brar, A.S.; Kumar, R.; Kaur, M. *J. Mol. Str.* **2003**, *650*, 85-92.
(65)   Brar, A.S.; Kumar, R. *J. Polym. Sci. Part A: Polym. Chem.* **2002**, *40*, 2225-2236.
(66)   Hou, C.; Wang, C.-G.; Cai, H.-S.; Zhang, W.-X. *J. Appl. Polym. Sci.* **2003**, *89*, 422–425.
(67)   Brar, A.S.; Kumar, R. *Polym. Int.* **2002**, *51*, 519-529.
(68)   Huglin, M.B.; Rehab, M.M. *Eur. Polym. J.* **1987**, *23*, 825-828.
(69)   Fischer, H.; Radom, L. *Angew. Chem. Int. Ed.* **2001**, *40*, 1340-1371.
(70)   Theis, A.; Davis, T.P.; Stenzel, M.H.; Barner-Kowollik, C. *Polymer* **2006**, *47*, 999-1010.
(71)   Ray, B.; Kotani, M.; Yamago, S. *Macromolecules* **2006**, *39*, 5259-5265.
(72)   Iovu, M.C.; Matyjaszewski, K. *Macromolecules* **2003**, *36*, 9346-9354.
(73)   Koumura, K.; Satoh, K.; Kamigaito, M.; Okamoto, Y. *Macromolecules* **2006**, *39*, 4054-4061.
(74)   Mayo, F.R. *J. Am. Chem. Soc.* **1943**, *65*, 2324.
(75)   Ranucci, E.; Ferruti, P.; Annunziata, R.; Gerges, I.; Spinelli, G. *Macromol. Biosci.* **2006**, *6*, 216-227.
(76)   Ranucci, E.; Spagnoli, G.; Sartore, L.; Bignotti, F.; Ferruti, P. *Macromol. Chem. Phys.* **1995**, *196*, 763-774.
(77)   Ranucci, E.; Tarabic, M.; Gilberti, M.; Albertsson, A.-C. *Macromol. Chem. Phys.* **2000**, *201*, 1219–1225.
(78)   Ranucci, E.; Macchi, L.; Annunziata, R.; Ferruti, P.; Chiellini, F. *Macromol. Biosci.* **2004**, *4*, 706-713.
(79)   Ahmad, N.M.; Heatley, F.; Lovell, P.A. *Macromolecules* **1998**, *31*, 2822.
(80)   Britton, D.; Heatley, F.; Lovell, P.A. *Macromolecules* **1998**, *31*, 2828-2837.
(81)   Frank, R.L.; Adams, C.E. *J. Am. Chem. Soc.* **1946**, *68*, 908-908.
(82)   Benson, S.W.; North, A.M. *J. Am. Chem. Soc.* **1961**, *84*, 935-940.
(83)   Buback, M.; Egorovc, M.; Gilbert, R.G.; Kaminsky, V.; Olaj, O.F.; Russell, G.T.; Vana, P. *Macromol. Chem. Phys.* **2002**, *203*, 2570-2582.
(84)   Smith, G.B.; Russell, G.T. *Macromol. Symp.* **2007**, *248*, 1-11.
(85)   Liu, Z.; Rimmer, S. *Macromolecules* **2002**, *35*, 1200-1207.

(86) Breitenbach, J.W.; Galinovsky, F.; Nesvadba, H.; Wolf, E. *Monatsh. Chemie* **1956**, *87*, 580-592.

(87) Nowlan, V.J.; Tidwell, T.T. *Accounts Chem. Res.* **1977**, *10*, 252-258.

(88) Senogles, E.; Thomas, R.A. *J.C.S. Perkin II* **1980**, 825-828.

(89) Zhuo, J.-C. *Molecules [Electronic Publication]* **1999**, *4*, M117.

(90) Szwarc, M.; Levy, M.; Milkovich, R. *J. Am. Chem. Soc.* **1956**, *78*, 2656-2657.

(91) Darling, T.R.; Davis, T.P.; Fryd, M.; Gridnev, A.A.; Haddleton, D.M.; Ittel, S.D.; Matheson, R.R.J.; Moad, G.; Rizzardo, E. *J. Polym. Sci. Part A: Polym. Chem.* **2000**, *38*, 1706-1708.

(92) Szwarc, M. *Nature* **1956**, *176*, 1168-1169.

(93) Fischer, H. *Chem. Rev.* **2001**, *101*, 3581-3610.

(94) Fischer, H. *Macromolecules* **1997**, *30*, 5666-5672.

(95) Fischer, H. *J. Polym. Sci. Part A: Polym. Chem.* **1999**, *37*, 1885-1901.

(96) Connolly, T.J.; Scaiano, J.C. *Tetr. Lett.* **1997**, *38*, 1133-1136.

(97) Moad, G.; Rizzardo, E.; Solomon, D.H. *Macromolecules* **1982**, *15*, 909-914.

(98) Wayland, B.B.; Poszmik, G.; Mukerjee, S.L.; Fryd, M. *J. Am. Chem. Soc.* **1994**, *116*, 7943-7944.

(99) Milani, B.; Stabon, E.; Zangrando, E.; Mestroni, G.; Sommazzi, A.; Zonnoni, C. *Inorg. Chim. Act.* **2003**, *349*, 209-216.

(100) Kato, M.; Kamigaito, M.; Sawamoto, M.; Higashimura, T. *Macromolecules* **1995**, *28*, 1721-1723.

(101) Wang, J.-S.; Matyjaszewski, K. *J. Am. Chem. Soc.* **1995**, *117*, 5614-5615.

(102) Percec, V.; Barboiu, B. *Macromolecules* **1995**, *28*, 7970-7972.

(103) Patten, T.E.; Matyjaszewski, K. *Accounts Chem. Res.* **1999**, *32*, 895-903.

(104) Matyjaszewski, K.; Gaynor, S.; Wang, J.-S. *Macromolecules* **1995**, *28*, 2093-2095.

(105) Chiefari, J.; Chong, Y.K.B.; Ercole, F.; Krstina, J.; Jeffery, J.; Le, T.P.T.; Mayadunne, R.T.A.; Meijs, G.F.; Moad, C.L.; Moad, G.; Rizzardo, E.; Thang, S.H. *Macromolecules* **1998**, *31*, 5559-5562.

(106) Le, T.P.; Moad, G.; Rizzardo, E.; Thang, S.H.; PCT Int. Appl. WO 98/01478, **1998**.

(107) Yamago, S.; Iida, K.; Yoshida, J.-i. *J. Am. Chem. Soc.* **2002**, *124*, 2874-2875.

(108) Yamago, S.; Iida, K.; Yoshida, J.-i. *J. Am. Chem. Soc.* **2002**, *124*, 13666-13667.

(109) Yamago, S.; Ray, B.; Iida, K.; Yoshida, J.-i.; Tada, T.; Yoshizawa, K.; Kwak, Y.; Goto, A.; Fukuda, T. *J. Am. Chem. Soc.* **2004**, *126*, 13908-13909.

(110) Rhodia Chimie: Corpart, P.; Charmot, D.; Biadatti, T.; Zard, S.Z.; Michelet, D.; PCT Int. Appl. WO. 9858974, **1998**.

(111) Charmot, D.; Corpart, P.; Adam, H.; Zard, S.Z.; Biadatti, B.G. *Macromol. Symp.* **2000**, *150*, 23-32.

(112) Destarac, M.; Charmot, D.; Franck, X.; Zard, S.Z. *Macromol. Rapid Commun.* **2000**, *21*, 1035-1039.

(113) Chong, B.Y.K.; Le, T.P.T.; Moad, G.; Rizzardo, E.; Thang, S.H. *Macromolecules* **1999**, *32*, 2071-2074.

(114) Quinn , J.F.; Barner, L.; Rizzardo, E.; Davis, T.P. *J. Polym. Sci. Part A: Polym. Chem.* **2001**, *40*, 19-25.

(115)   Muthukrishnan, S.; Pan, E.H.; Stenzel, M.H.; Barner-Kowollik, C.; Davis, T.P.; Lewis, D.; Barner, L. *Macromolecules* **2007**, *40*, 2978-2980.
(116)   Shi, L.; Chapman, T.M.; Beckman, E.J. *Macromolecules* **2003**, *36*, 2563-2567.
(117)   Leonova, E.; Chernikova, E.; Okhlopkov, A.; Golubev, V. *in Proceedings of 40 International Symposium on Macromolecules, Paris,* **2004**, *Sect. 2.1, Subsect. 2.1.6.*
(118)   Golubev, V.B.; Chernikova, E.V.; Leonova, E.A.; Morozov, A.V. *Polym. Sci., Ser. A* **2005**, *47*, 678-685.
(119)   Vana, P.; Davis, T.P.; Barner-Kowollik, C. *Macromol. Theory Simul.* **2002**, *11*, 823-835.
(120)   Devasia, R.; Bindu, R.L.; Borsali, R.; Mougin, N.; Gnanou, Y. *Macromol. Symp.* **2005**, *229*, 8-17.
(121)   Devasia, R.; L Bindu, R.; Mougin, N.; Gnanou, Y. *Polym. Prepr. (Am. Chem. Soc., Div. Polym. Chem.)* **2005**, *46*, 195-196.
(122)   Devasia, R.; Borsali, R.; Lecommandoux, S.; Bindu, R.L.; Mougin, N.; Gnanou, Y. *Polym. Prepr. (Am. Chem. Soc., Div. Polym. Chem.)* **2005**, *46*, 448-449.
(123)   Moad, G.; Rizzardo, E.; Thang, S.H. *Aust. J. Chem.* **2005**, *58*, 379-410.
(124)   Wan, D.; Satoh, K.; Kamigaito, M.; Okamoto, Y. *Macromolecules* **2005**, *38*, 10397-10405.
(125)   Bilalis, P.; Pitsikalis, M.; Hadjichristidis, N. *J. Polym. Sci. Part A: Polym. Chem.* **2006**, *44*, 659-665.
(126)   Barner-Kowollik, C.; Quinn, J.F.; Nguyen, T.L.U.; Heuts, J.P.A.; Davis, T.P. *Macromolecules* **2001**, *34*, 7849-7857.
(127)   Pound, G.; McLeary, J.B.; McKenzie, J.M.; Lange, R.F.M.; Klumperman, B. *Macromolecules* **2006**, *39*, 7796 - 7797.
(128)   Postma, A.; Davis, T.P.; Li, G.; Moad, G.; O'Shea, M.S. *Macromolecules* **2006**, *39*, 5307-5318.
(129)   Hu, Z.Q.; Zhang, Z.C. *Macromolecules* **2006**, *39*, 1384-1390.
(130)   Goto, A.; Kwak, Y.; Fukuda, T.; Yamago, S.; Iida, K.; Nakajima, M.; Yoshida, J.-i. *J. Am. Chem. Soc.* **2003**, *125*, 8720-8721.
(131)   Kaneyoshi, H.; Matyjaszewski, K. *Macromolecules* **2006**, *39*, 2757-2763.
(132)   Lutz, J.-F.; Lacroix-Desmazes, P.; Boutevin, B.; Le Mercier, C.; Gigmes, D.; Bertin, D.; Tordo, P. *Polym. Prepr. (Am. Chem. Soc., Div. Polym. Chem.)* **2002**, *43*, 287-288.
(133)   Lu, X.; Gong, S.; Meng, L.; Li, C.; Yang, S.; Zhang, L. *Polymer* **2007**, *48*, 2835-2842.
(134)   Yusa, S.-i.; Yamago, S.; Sugahara, M.; Morikawa, S.; Yamamoto, T.; Morishima, Y. *Macromolecules* **2007**, Published on Web 07/10/2007.
(135)   Chang, T. In *Adv Polym Sci*, **2003**; Vol. 163, p 1–60.
(136)   Qiu, X.-P.; Winnik, F.M. *Macromol. Rapid Commun.* **2006**, *27*, 1348-1653.
(137)   Grubisic, Z.; Rempp, P.; Benoit, H. *Journal of Polymer Science Part B: Polymer Letters* **1967**, *5*, 753.
(138)   Benoit, H.C. *J. Polym. Sci., Part B: Polym. Phys.* **1996**, *34*, 1703-1704.
(139)   Netopilik, M.; Kratochvil, P. *Polymer* **2003**, *44*, 3431-3436.
(140)   Guillaneuf, Y.; Castignolles, P. *J. Polym. Sci. Part A: Polym. Chem.* **2008**, *46*, 897-911.

(141) Raith, K.; Kühn, A.V.; Rosche, F.; Wolf, R.; Neubert, R.H.H. *Pharm. Res.* **2002**, *19*, 556-560.

(142) Luo, L.; Ranger, M.; Lessard, D.G.; Le Garrec, D.; Gori, S.; Leroux, J.-C.; Rimmer, S.; Smith, D. *Macromolecules* **2004**, *37*, 4008-4013.

(143) Wetzel, S.J.; Guttman, C.M.; Girard, J.E. *Int. J. Mass Spectrom.* **2004**, *238*, 215-225.

(144) Mourey, T.H.; Hoteling, A.J.; Balke, S.T.; Owens, K.G. *J. Appl. Polym. Sci.* **2005**, *97*, 627-639.

(145) Favier, A.; Ladavière, C.; Charreyre, M.-T.; Pichot, C. *Macromolecules* **2004**, *37*, 2026-2034.

(146) Shimada, K.; Lusenkova, M.A.; Sato, K.; Saito, T.; Matsuyama, S.; Nakahara, H.; Kinugasa, S. *Rapid Commun. Mass Spectrom.* **2001**, *15*, 277-282.

(147) Lou, X.; van Dongen, J.L.J.; Meijer, E.W. *J. Chromatogr. A* **2000**, *896*, 19-30.

(148) Staal, B.B.P. *Characterization of (co)polymers by MALDI-TOF-MS; Chapter 4: The relationship between the MMD from MALDI and from SEC*; Technische Universiteit Eindhoven, **2004**.

(149) Schriemer, D.C.; Li, L. *Anal. Chem.* **1997**, *69*, 4169-4175.

(150) Yalcin, T.; Dai, Y.; Li, L. *J. Am. Soc. Mass Spectrom.* **1998**, *9*, 1303-1310.

(151) Schriemer, D.C.; Li, L. *Anal. Chem.* **1997**, *69*, 4176-4183.

(152) Schnöll-Bitai, I.; Hrebicek, T.; Rizzi, A. *Macromol. Chem. Phys.* **2007**, *208*, 485-495.

(153) Malvagna, P.; Impallomeni, G.; Cozzolino, R.; Spina, E.; Garozzo, D. *Rapid. Commun. Mass Spectrom.* **2002**, *16*, 1599-1603.

(154) Trimpin, S.; Eichhorn, P.; Räder, H.J.; Müllen, K.; Knepper, T.P. *J. Chromatogr. A* **2001**, *938*, 67-77.

(155) Viel, S.; Capitani, D.; Mannina, L.; Segre, A. *Biomacromolecules* **2003**, *4*.

(156) Larsson, A.; Kuckling, D.; Schonhoff, M. *Colloids Surf. A: Physicochem. Eng. Aspects* **2001**, *190*, 185-192.

(157) Macko, T.; Hunkeler, D. *Adv Polym Sci* **2003**, *163*, 61–136.

(158) Staal, W.J.; Cools, P.; Van Herk, A.M.; German, A.L. *J. Liq. Chrom.* **1994**, *17*, 3190-3199.

(159) Philipsen, H.J.A. *J. Chromatogr. A* **2004**, *1037*, 329-350.

(160) Destarac, M.; Brochon, C.; Catala, J.-M.; Wilczewska, A.; Zard, S.Z. *Macromol. Chem. Phys.* **2002**, *203*, 2281-2289.

(161) McLeary, J.B.; McKenzie, J.M.; Tonge, M.P.; Sanderson, R.D.; Klumperman, B. *Chem. Commun.* **2004**, 1950-1951.

(162) Goh, Y.-K.; Monteiro, M.J. *Macromolecules* **2006**, *39*, 4966-4974.

(163) Monteiro, M.J.; de Brouwer, H. *Macromolecules* **2001**, *34*, 349-352.

(164) Kwak, Y.; Goto, A.; Tsujii, Y.; Murata, Y.; Komatsu, K.; Fukuda, T. *Macromolecules* **2002**, *35*, 3026-3029.

(165) Bathfield, M.; D'Agosto, F.; Spitz, R.; Ladavière, C.; Charreyre, M.-T.; Delair, T. *Macromol. Rapid Commun.* **2007**, *28*, 856-862.

(166) Geelen, P.; Klumperman, B. *Macromolecules* **2007**, *40*, 3914-3920.

(167) Loiseau, J.; Doerr, N.; Suau, J.M.; Egraz, J.B.; Llauro, M.F.; Ladaviere, C.; Claverie, J. *Macromolecules* **2003**, *36*, 3066-3077.

(168) Favier, A.; Charreyre, M.-T.; Chaumont, P.; Pichot, C. *Macromolecules* **2002**, *35*, 8271-8280.

(169) Pinto, M.A.; Li, R.; Immanuel, C.D.; Lovell, P.A.; Schork, F.J. *Ind. Eng. Chem. Res.* **2007**, *ASAP article Published on the Web 06/26/2007 DOI:10.1021/ie0609923*.

(170) Kwak, Y.; Goto, A.; Fukuda, T.; Kobayashi, Y.; Yamago, S. *Macromolecules* **2006**, *39*, 4671-4679.

(171) Thomas, D.B.; Convertine, A.J.; Hester, R.D.; Lowe, A.B.; McCormick, C.L. *Macromolecules* **2004**, *37*, 1735-1741.

(172) McCormick, C.L.; Lowe, A.B. *Acc. Chem. Res.* **2004**, *37*, 312-325.

(173) Baussard, J.-F.; Habib-Jiwan, J.-L.; Laschewsky, A.; Mertoglu, M.; Storsberg, J. *Polymer* **2004**, *45*, 3615-3626.

Chapter 3: Experiments and methods

In this chapter the experimental conditions for the synthesis of the xanthate chain-transfer agents used in the course of this study and for polymerizations are described. The choice of some parameters is discussed such as reaction temperature or the use of solvents. The details of experimental procedures for the characterization of the polymers are given.

Introduction

One of the aims of this chapter is to avoid redundant description of synthetic procedures for the preparation of chain-transfer agents (CTAs) and for polymerizations used throughout this thesis. Another aim is to provide arguments for the choice of some experimental parameters which may otherwise seem arbitrary. Poly(*N*-vinylpyrrolidone) (PVP) is not a common polymer in most laboratories, as opposed to polystyrene (PSty), poly(methyl methacrylate) (PMMA) for instance or to a lesser extent poly(vinyl acetate) (PVAc). As a result the procedures for its preparation and isolation (from low molecular weight components) vary from one laboratory to the other. These may affect the final properties of the polymer.

In the course of this study challenges were faced regarding characterization of PVP. Determination of molecular weight distribution data is an issue, due to the absence of narrowly distributed PVP standards for size exclusion chromatography (SEC). Determination of conversion was not straightforward either. The latter difficulty was mostly related to the challenge in extracting the polymer from unreacted monomer. Unlike MMA, Sty and VAc, the vapor pressure of the monomer NVP is too low for it to be efficiently removed by evaporation from the polymerization mixture. Hydrogen bonding between monomer and polymer most likely reduces the efficiency of extraction of the monomer via precipitation from a non-solvent. Additionally, PVP is very hygroscopic. Unless it is handled in an inert atmosphere the pure polymer adsorbs water, which changes the actual mass of polymer in the samples examined as well as its

solubility in organic solvents. Finally, as characterization via MALDI-ToF-MS was investigated evidence was found for fragmentation of some of the end-groups during the analysis. Meticulous experimental details and practical considerations are presented in this chapter to help the reader identify possible bias in comparison with results reported in the literature. Methods for isolation of the polymer and determination of conversion are discussed as well as characterization via SEC and MALDI-Tof-MS.

Synthesis of xanthate chain-transfer agents

Xanthates (also called dithiocarbonates) are thiocarbonyl thio compounds of general formula Z-C(S)S-R where Z is an alkoxy group and R is a variable group connected to the sulfur atom via a central carbon, which has 1, 2 or 3 substituents composed of C, H and possibly N and/or O.

Figure 3.1: Chemical structure of a xanthate chain-transfer agent.

The chemistry of xanthates is ancient and well documented by Zard and co-workers[1] with particular insight into the preparation of xanthates for radical reactions with vinyl monomers.[2] Xanthates are often prepared in high yields and high level of purity. The precursor for all the xanthates used in the present study, potassium *O*-ethyl xanthate, is commercially available. From a synthetic point of view a distinction can be made between 2 classes of xanthate CTAs. The one class is xanthates with a primary or secondary R group. The other is xanthates with a tertiary R group. The former are prepared via nucleophilic substitution of a halogen compound. The latter require other synthetic pathways. Two possible routes were employed which are (i) R group displacement via trans-esterification promoted by phase-separation (ii) addition of tertiary radicals from diazo compounds to xanthic disulfide.

Synthesis of xanthates with a secondary R group

The precursor potassium *O*-ethyl xanthate acts as a nucleophile for substitution reactions with alkyl halides. The synthetic scheme is presented in . The xanthates prepared via this method in the course of this PhD work are presented in Figure 3.2.
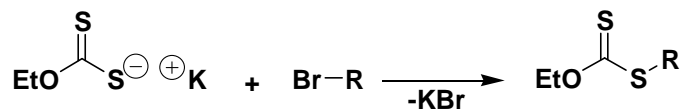
Scheme 3.1: Synthesis of a xanthate CTA via nucleophilic substitution of an alkyl bromide.
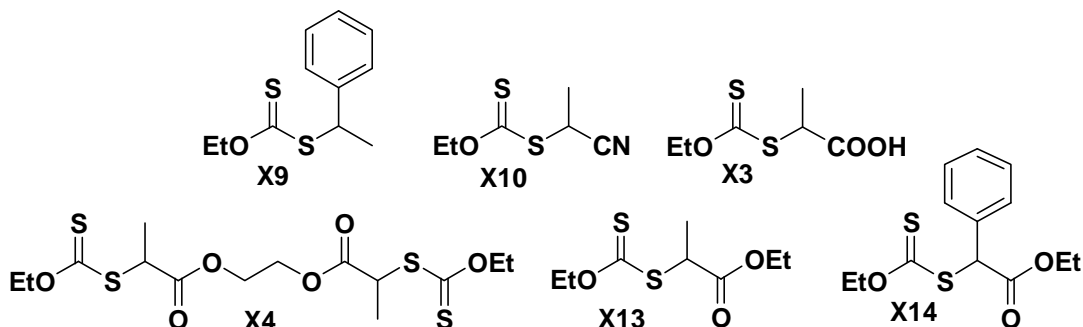
Figure 3.2: Chemical structure of xanthates with a secondary R group synthesized for the present study. The xanthates are ranked from left to right and first to second line in the order of decreasing electron withdrawing character of the R group, as determined by ^{1}H-NMR spectroscopy.

Bromine has better leaving group ability than chlorine. Brominated reagents are therefore more reactive than their chlorinated counterpart. Brominated reagents were commercially available for X3, X4, X10 and X13 only, which enabled quantitative yields to be obtained at room temperature in less than 16 h. Higher temperatures and longer reaction times were necessary for the preparation of X9 and X14 for which only the chlorinated precursors were available. It is interesting to note that the synthesis of X3 was quantitative in aqueous solution in the presence of two equivalents of potassium hydroxide (KOH). The addition of KOH was required to neutralize the weakly acidic brominated precursor *2*-bromopropionic acid and prevent protonation of the xanthic salt, which would otherwise decrease its nucleophilic character. The initial mixture thus contained 3 nucleophiles, *i.e.* HO⁻, -COO⁻ and CSS⁻. Fortunately the nucleophilicity of negatively charged nucleophiles increases in the progression down the period table, insuring faster reaction of the xanthate anion than the oxygenated compounds. Compounds X4 and X14 were prepared from haloalcaloyl halides. The latter was first

esterified with ethylene glycol for the preparation of X4 and the intermediate was isolated prior to reaction with the xanthic salt, whereas the reaction was simply carried out in ethanol for the preparation of X14 in one step. Alternatively a hydroxyl endfunctional polymer can be modified under this synthetic pathway to form a macromolecular xanthate CTA (macoCTA). Chain-end modification of poly(ethylene glycol) monomethyl ether (PEG-OH) was achieved as presented in Scheme 3.2. A telechelic dihydroxyl precursor was modified under the same procedure as X4. The macroCTAs were investigated for their ability to produce block copolymers with NVP and VAc. The experimental details and results are presented in chapter 6.
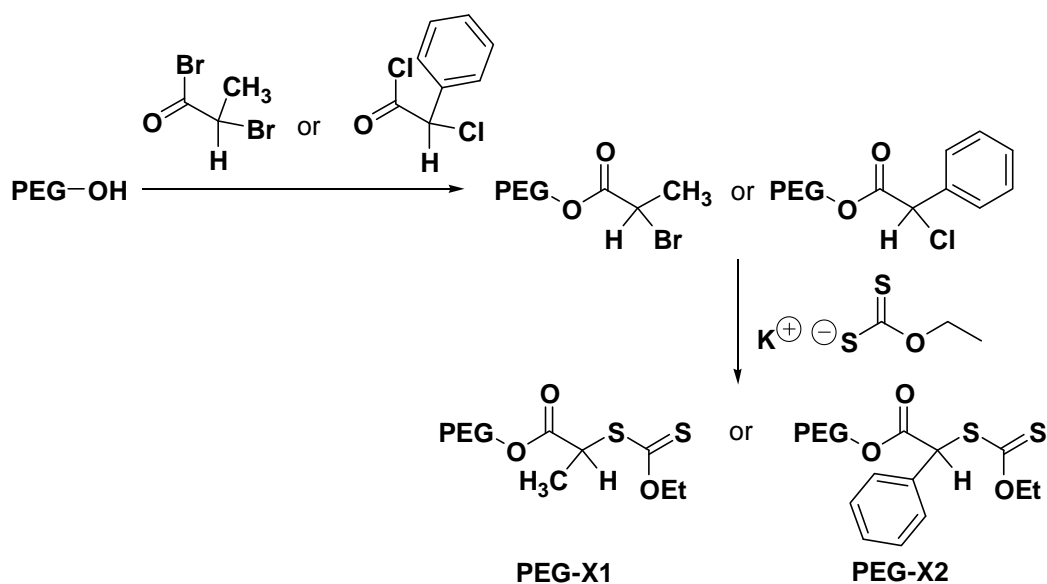
Scheme 3.2: Synthesis of macromolecular chain-transfer agents from hydroxyl endfunctional poly(ethylene glycol).

Synthesis of xanthates with a tertiary R group

Trans-esterification

The procedure was inspired from procedures available in the literature for the preparation of other CTAs.[3] Addition of a mercaptan (R'SH) in a solution containing a xanthate (ZC(S)SR) results in equilibrium between two xanthate species ZC(S)SR' and ZC(S)SR. In order to produce ZC(S)SR' quantitatively it is necessary to apply a driving force that shifts this equilibrium. This can be achieved by performing the reaction in a biphasic hydrophobic / hydrophilic system. When the starting xanthate X3 is used, it

partitions preferably in the aqueous phase at a pH higher than its pK_a (which is in the range 4-5), whereas its oily product of trans-esterification with *tert*-butyl mercaptan (X5) separates from the aqueous phase.
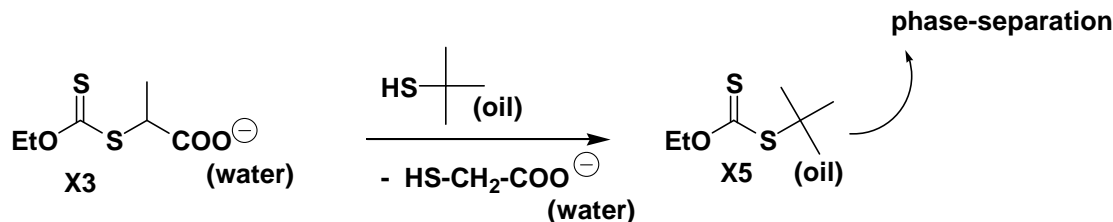
Scheme 3.3: Structure and synthesis of *S*-(*tert*-butyl) *O*-ethyl xanthate (X5) via trans-esterification promoted by phase-separation.

The compound X5 was easily purified from unreacted thiol and other contaminants by Kugelrohr distillation.

Radical reaction with diazo compounds

Tertiary radicals produced by thermal decomposition of diazo compounds react with dithio dissulfides via radical addition and subsequent fragmentation, as presented in Scheme 3.4.[2,4]
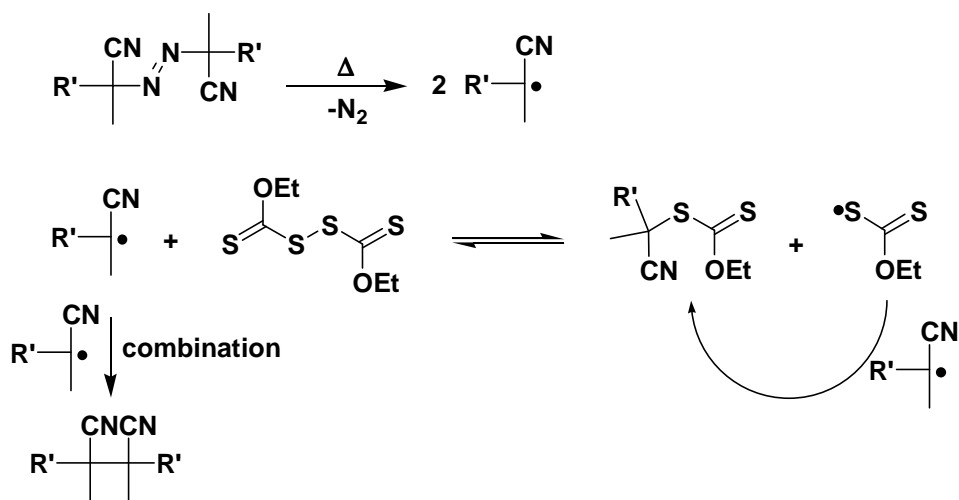
Scheme 3.4: Synthesis of a xanthate CTA via radical reaction with diazo compounds.

Side reactions include recombination of the tertiary radicals from the diazo compounds and therefore an excess of diazo compound must be used. In the case of 2,2'-azo bis(isobutyronitrile) (AIBN) used for the preparation of X6 (see Figure 3.3), the

recombination product tetramethyl succinonitrile (TMSN) is easily removed by sublimation under reduced pressure.
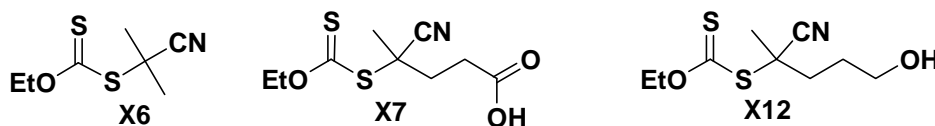
Figure 3.3: Chemical structure of xanthates with a tertiary R group synthesized for the present study via radical reaction with diazo compounds.

Polymerizations

Temperature - Reaction time - Viscosity - Solvents

The parameters solvent, temperature, reaction time and viscosity are interconnected. The polymerization temperature has to be chosen with respect to the reactivity of a given monomer to provide polymer within a decent reaction time. Increasing the polymerization temperature may provide the energy necessary to overcome the activation-energy barriers for side-reactions. Therefore a good balance must be found between reducing reaction time and preventing side-reactions. RAFT-mediated polymerizations are slower than conventional free-radical polymerizations. Thus when NVP was polymerized in bulk at 60 ℃ with the same initial concentration in initiator AIBN ($[AIBN]_0$ = 3 mM), quantitative conversion was reached within 3 h in the absence of CTA, whereas a maximum of 76 % conversion was reached in 6 h in the presence of a CTA (the case reported here is where X13 was used, which was found to be an efficient CTA with no inhibition period). The temperatures 60 ℃ for NVP and 54 ℃ for VAc were chosen as they enable similar conversions for both monomers within the same reaction time (Table 3.1, compare experiments e and f with h). Some VAc polymerizations were carried out at 60 ℃ for direct comparison with NVP. In this case the reaction was stopped at 3.5 h to produce similar yields to polymerizations at 54 ℃ carried out for 6 h (Table 3.1, compare experiments h with i). Monomer conversion at 6 h in NVP polymerizations at 60 ℃ were in the range 20-50 % with most suitable CTAs, which enabled samples to be taken even at low conversion.

Table 3.1: Effect of temperature, solvent and reaction time on monomer conversion and molecular weight distribution data of PVP and PVAc prepared via xanthate-mediated polymerization.

Ref.	Monomer	T (ºC)	CTA	Solvent	time (h)	α (%)	$M_{n,target,\alpha}$ (g·mol^{-1})	$M_{n,SEC}$[a] (g·mol^{-1})	PDI[a]
a	NVP	60	X6	THF	6.0	35	17800	13000	1.56
b		60	X6	ethanol	6.0	25	12800	12000	1.57
c		60	X6	dioxane	6.0	40	20400	11800	1.81
d		60	X3[b]	water	3.3	78	25000	179500	1.80
e		60	X6	bulk	6.0	40	20400	23200	1.31
f		60	X3	bulk	6.0	26	13300	15500	1.34
g		70	X6	bulk	2.6	75	36700	33200	1.52
h	VAc	54	X3[c]	bulk	6.0	36	18200	17200	1.18
i		60	X3[c]	bulk	3.5	34	17600	16000	1.34
j		70	X3	bulk	1.0	99	37900	73000	1.65

[a] Experimental molar masses obtained by Size Exclusion Chromatography (using RI detection) in THF with PS calibration for poly(vinyl acetate) (PVAc) and in HFIP with PMMA calibration for poly(*N*-vinylpyrrolidone) (PVP); [Monomer]$_0$/[Xanthate]$_0$ = 450 (*i.e.* $M_{n,target,100\%}$ [g·mol^{-1}] = 50000 for PVP, 38000 for PVAc) except for experiments indicated with [b] where [Monomer]$_0$/[Xanthate]$_0$ = 270 (*i.e.* $M_{n,target,100\%}$ [g·mol^{-1}] = 30000) and [c] where [Monomer]$_0$/[Xanthate]$_0$ = 580 (*i.e.* $M_{n,target,100\%}$ [g·mol^{-1}] = 50000); [Xanthate]$_0$/[AIBN]$_0$ = 10.

NVP polymerizations carried out in bulk undergo viscosity increase to a critical point at about 60 % conversion, where magnetic stirring is impaired. Polymerizations carried out beyond this point often showed heterogeneity similar to phase separation, *i.e.* the polymer formed a highly viscous nodule in the center of the reaction flask bathing in a less viscous liquid. Bimolecular processes, which are essential in the RAFT mechanism to activate-deactivate chains, are diffusion-controlled processes. The same holds for termination reactions. Such processes are less likely to occur because diffusion coefficients increase upon viscosity increase. They both affect the molecular weight distribution of the polymers. It is predicted that at high viscosity bimolecular radical termination will be reduced (which has a positive effect on reducing PDIs), whereas reduction of the rates of activation / deactivation will lead to broadening of the molecular weight distribution.

It is often observed in RAFT systems that PDI values decrease to a minimum value at moderate conversions and increase at high conversions. As derived from eq. 2.3, the RAFT process gives us 2 main controllable parameters for preparing polymers with a given M_n, namely the initial ratio of monomer to CTA ([NVP]$_0$/[CTA]$_0$) and the

conversion (α). The chromatograms in Figure 3.4. illustrate the ability to produce PVPs with similar M_n by varying both α and the stoichiometry. A noticeable difference in PDIs is observed however, as the polymer at lower α and higher $[NVP]_0/[CTA]_0$ has a significantly lower PDI (1.25) than the one at higher α and lower $[NVP]_0/[CTA]_0$.
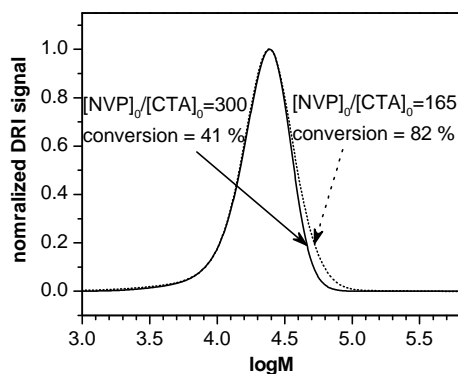

Figure 3.4: Molecular weight distribution (SEC traces) of poly(*N*-vinylpyrrolidone) samples with similar $M_{n,theo,\alpha}$ obtained at different initial monomer to CTA ratios by varying the conversion (α). The polymers were obtained via *S*-(2-cyano-2-propyl) *O*-ethyl xanthate (X6)-mediated polymerization of NVP in bulk at 60 ºC; $[X6]_0/[AIBN]_0 = 8$. Black line: $[NVP]_0/[X6]_0 = 300$, $\alpha = 41$ % ($M_{n,theo,41\%}$ [g·mol^{-1}] = 13800), $M_{n,SEC}$ [g·mol^{-1}] = 15700, PDI = 1.25; Dotted line: $[NVP]_0/[X6]_0 = 165$, $\alpha = 82$ % ($M_{n,theo,82\%}$ [g·mol^{-1}] = 15200), $M_{n,SEC}$ [g·mol^{-1}] = 14700, PDI = 1.44.

Consequently it is preferable to select a higher $[NVP]_0/[CTA]_0$ and limit the conversion in order to reach a given M_n with a minimum PDI value.

Solvents may be added to the polymerization mixture to reduce viscosity at high conversions. Table 3.1 lists some experiments where NVP was polymerized in the presence of X6 in bulk and in solution (50 wt %) in THF, ethanol and 1,4-dioxane (experiments a-c). Experiment d was carried out in water (buffered with phosphate buffer at pH = 7.9). In this case X3 was used to ensure solubility. These experiments were compared with bulk polymerizations (e, f). As indicated by the molecular weight data, control was significantly enhanced when polymerizations were carried out in bulk compared to solutions in THF, ethanol and 1,4-dioxane. Experiment d revealed the absence of control when polymerization was carried out in water as indicated by very high M_n polymer being obtained. RAFT polymerizations are recognized for their tolerance to a broad range of solvents including water.[5-7] In particular xanthates have been used successfully in aqueous systems.[8] The hydrolytic stability of the CTA at the chain-end is crucial for the polymerization to be controlled.[9-11] It is likely that the failure

of experiment d was related to the structure and reactivity of the monomer NVP and its derivatives. Details are presented in chapters 5 and 7, which give evidence for degradative side-reactions affecting xanthate end-groups from PVP.

In conclusion to these comparative studies, it was decided that xanthate-mediated polymerizations of NVP should be carried out in bulk at 60 ºC and conversion should be kept below 60 % to ensure lowest PDIs. These conditions were defined so as to enable optimization of a CTA for NVP. For practical purposes however the use of solvents may be required, for instance where higher conversions should be reached. THF was chosen for copolymerizations of NVP with VAc and block copolymer formation with PEG because it solubilizes the various monomers and corresponding polymers, it is easily removed under vacuum, it did not seem to significantly slow down NVP polymerization and it provided better PDIs than other solvents tested.

Polymer isolation and determination of conversion

Methods applied for polymer isolation were (i) precipitation from a non-solvent; (ii) dialysis followed by freeze-drying. Precipitation from a non-solvent was performed using either *n*-hexane or diethyl ether. A solvent such as dichloromethane (alternatively THF or ethanol) was used to dilute the samples at conversions above 30 %, insuring a fine suspension of polymer in the non-solvent mixture to be obtained. The polymer was obtained in the form of a white to pale yellow powder, relatively sticky at low M_n and brittle at higher M_n (typically $M_n > 10000$ g·mol^{-1}). Shortcomings of this method are that sample mass is lost upon each precipitation step. It is not suitable for very low amounts of samples to be recovered. Also, low M_n chains may dissolve preferentially and be lost upon repeated precipitation steps. Finally, conversion may be underestimated (when product is lost) or overestimated (when contaminants are not successfully removed). After one precipitation step unreacted monomer was still present as indicated by ^{1}H-NMR spectroscopy (see spectrum a), accounting for 5 to 20 % of the powder mass. The amount of remaining unreacted monomer was determined via ^{1}H-NMR spectroscopy and accounted for in the determination of conversion via gravimetry on precipitated samples. SEC and MALDI-ToF-MS analyses were carried out on samples precipitated only once (or even on raw polymerization mixtures) to ensure that the molecular weight data be as

true as possible a reflection of the efficiency of the RAFT mechanism. For other purposes, such as end-group modification, it is necessary that the monomer be removed efficiently. The polymer was therefore redissolved in dichloromethane and precipitation repeated up to 4 times in total to ensure complete removal of the monomer. One advantage of this method is that the polymer is at no stage in contact with water and therefore remains soluble in organic solvents such as THF, dichloromethane, chloroform or 1,4-dioxane.

Dialysis consists of placing the polymer in a porous tube with a molecular weight cut-off (MWCO = 3500 g·mol^{-1} dextran equivalents) enables diffusion of low molecular weight contaminants out of the tube while water enters the tube to compensate for the high osmotic pressure caused by the polymer. Polymerization samples were generally precipitated prior to being placed in solution in distilled water at neutral pH and dialyzed for 16 to 24 h. Water was removed from the purified polymer by freeze-drying. The main concern was that low M_n material would be lost. However, it appeared that even low M_n PVP did not diffuse through the pores. For example similar SEC traces were obtained for the same PVP sample whether it was isolated via precipitation ($M_{n,SEC,}$ = 2180 g·mol^{-1}, PDI = 1.28) or dialysis-freeze-drying ($M_{n,SEC,}$ = 2200 g·mol^{-1}, PDI = 1.27) (Figure 3.6). ^{1}H-NMR spectroscopy indicated that in most cases 16 h of dialysis were sufficient to quantitatively remove the monomer (Figure 3.5, spectrum b). However a disadvantage of this method is that the polymer then contains water which can be present in the polymer sample as hydration water and free water molecules. Hydration water interacts with the polymer amide bonds via hydrogen bonding and is very difficult to remove.[12] Azeotropic distillation was attempted after dissolution of the polymer in toluene but only removed a fraction of the free water (Figure 3.5, spectrum c). The polymer recovered by this method was not soluble in organic solvents unless M_n was low (<5000 g·mol^{-1}). The water content should be taken into account when determining conversion from dialyzed samples. Another disadvantage is that chain-end hydrolysis occurred as will be detailed in chapter 7.
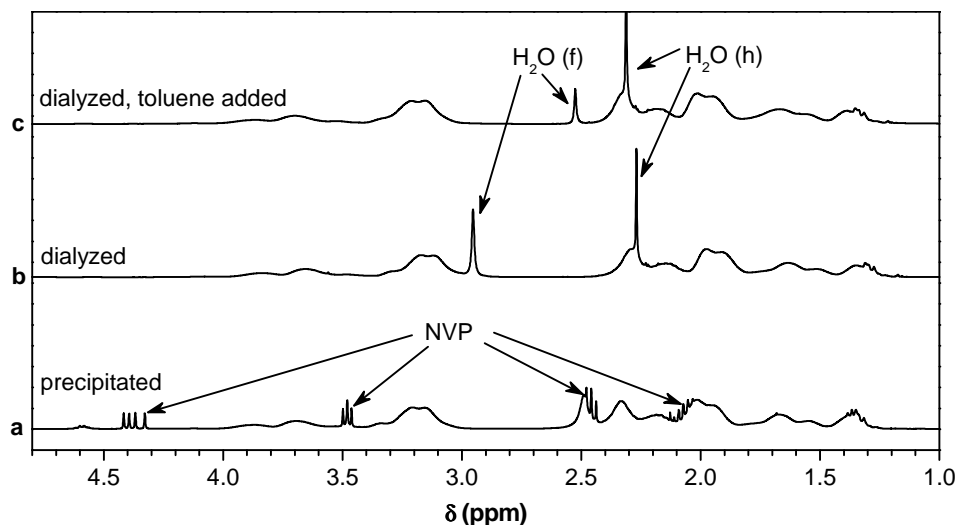
Figure 3.5: Three ^{1}H-NMR spectra a poly(*N*-vinylpyrrolidone) sample after different isolation procedures. The polymer was obtained via *S*-(2-cyano-2-propyl) *O*-ethyl xanthate (X6)-mediated polymerization of NVP in bulk at 60 °C. $[NVP]_0/[X6]_0 = 45$; $\alpha = 52$ %; $M_{n,theo,52 \%}$ [g·mol^{-1}] = 2700. The polymer was precipitated from diethyl ether (a) then dialyzed against distilled water for 16 h and freeze-dried (b) then dissolved at 50 °C in toluene and solvents were evaporated under reduced pressure (c). Peak pointed out with arrows correspond to unreacted monomer (NVP) and water of hydration (H_2O (h)) and free water molecules (H_2O (f)).
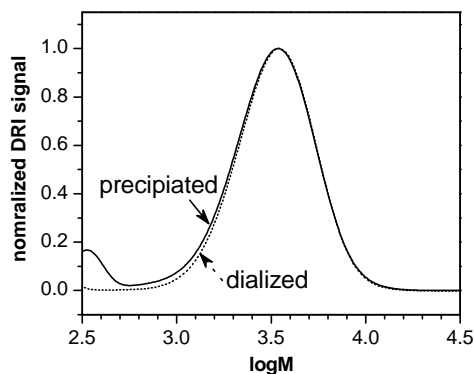
Figure 3.6: Molecular weight distribution (SEC traces) of a poly(*N*-vinylpyrrolidone) sample after different isolation procedures. The polymer was obtained via *S*-(2-cyano-2-propyl) *O*-ethyl xanthate (X6)-mediated polymerization of NVP in bulk at 60 °C. $[NVP]_0/[X6]_0 = 45$; $\alpha = 52$ %; $M_{n,theo,52 \%}$ [g·mol^{-1}] = 2700. The polymer was precipitated from diethyl ether (solid line) then dialyzed against distilled water for 16 h and freeze-dried (dotted line).

^{1}H-NMR spectroscopy was examined as an alternative for determining monomer conversion without the need to isolate the polymer from its unreacted monomer. *In situ* NMR spectroscopy was performed where the polymerization is carried out in an NMR tube placed into the magnet. A sealed glass insert containing formic acid in C_6D_6 was placed in the tube to provide an integration reference. Very little scattering was obtained for conversion values with this method and a large number of data points could be obtained (*e.g.* 1 spectrum every minute). The disadvantage is that samples for SEC,

required to correlate conversion with molecular weight data, are not obtainable. Kinetic studies were carried out by taking samples at various time intervals from the polymerization mixture heated up in an oil bath and closed with a septum. The raw samples were analyzed via SEC for molecular weight data and via NMR spectroscopy for conversion. The sample for NMR spectroscopy and integration reference (trioxane) were weighed and diluted in CDCl$_3$. The conversions obtained by this method compared well with those obtained gravimetrically from precipitated samples.

Reproducibility of NVP polymerization

It was often observed that NVP polymerizations were not reproducible in terms of conversion. To illustrate this point, the following experiment is reported. A polymerization mixture containing NVP, X6 and AIBN ([NVP]:[X6]:[AIBN] = 90:1:0.1) was prepared. Upon dissolution of all components, the mixture was homogenized under magnetic stirring and split into two polymerization reactors. The solutions were degassed via 4 freeze-pump-thaw cycles performed in parallel using the same Schlenk line. The flasks were sealed with a glass stopper and immersed in an oil bath at 60 ºC. After 5 h it was already observed that in one of the two flasks viscosity was too high to enable magnetic stirring whereas the other flask contained a less viscous solution. After 6 h the reactors were cooled in an ice bath and the polymer precipitated. Conversion was 50 % in one and 65 % in the other flask. The SEC chromatograms of the 2 samples indicated that the PDIs were identical whereas M_n was higher in the higher conversion sample (Figure 3.7). Therefore it seems that whatever the cause of retardation / inhibition was, it did not affect significantly the level of control and thus by implication it did not affect significantly the RAFT process.
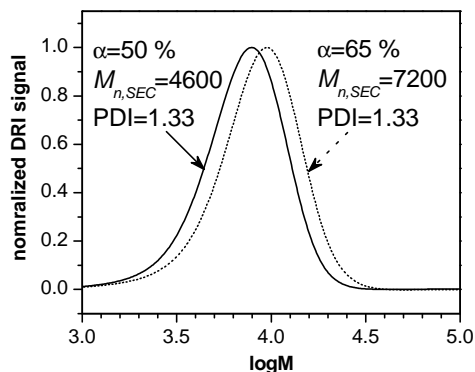
Figure 3.7: Molecular weight distribution (SEC traces) of a poly(*N*-vinylpyrrolidone) sample obtained with different conversions in spite of all user-defined experimental parameters kept equal. NVP was polymerization at 60 ºC in bulk for 6 h in the presence of X6. The molar ratios [NVP]:[X6]:[AIBN] were 90:1:0.1.

The differences in conversions between the two reactors were difficult to rationalize. The cleanliness of the glassware may be incriminated although great care was taken in the cleaning process. The presence of trace amounts of oxygen may also be suspected. Introduction of oxygen due to sampling by perforation through a septum for kinetic studies was often believed to be the cause of non-reproducibility. However for the moment the causes of such differences in conversion in the present experiment were not identified. The author believes that it is important to report on the lack of reproducibility of NVP polymerization with respect to monomer conversion because conversion values are often presented as part of the evaluation of the RAFT process. For instance conversion versus time plots are necessary to compare polymerization rates and thus evaluate the occurrence of inhibition and/or retardation due to the choice of the CTA. The present experiment demonstrates that such comparisons in RAFT-mediated polymerizations of NVP have to be taken with great caution.

Characterization of the polymers

Size-exclusion chromatography

PVP was characterized via SEC in 1,1,1,3,3,3-hexafluoro-2-propanol (HFIP). It would have been more convenient for us to use THF as an eluent because THF is cheaper and because the SEC setup with THF was available in our labs. Unfortunately analyses performed with THF showed tailing at high elution volumes indicating that the polymer

most likely adsorbed to the column. THF was therefore abandoned and HFIP was chosen instead. HFIP dissolved PVP and its copolymers regardless of the molecular weight or post-polymerization treatment. The chromatograms for PVP showed fairly symmetrical peaks (for example, see Figure 3.6). Molecular weight distribution data were calculated on the basis of calibration with narrowly distributed PMMA standards. Therefore the values of M_n and PDI reported are not true values but instead correspond to PMMA equivalents. Although the suitability of PMMA calibration to characterize PVP was not established the author believes that the results are reliable for comparison purposes.

MALDI-ToF-MS

MALDI-ToF-MS mass spectra of PVP prepared via xanthate-mediated polymerization display more than one type of end-groups and fragmentation patterns (Figure 3.8). Fragmentation is identified by the presence of signals resembling a bump rather than well-resolved peaks. The wavelength of the laser used to ionize the samples is 337 nm, which is very close to the absorption wavelength of the C=S bond of the xanthate moiety (peak maximum was measured in HFIP at 341 nm). Therefore it is most likely that the chain ends were cleaved upon ionization. This hypothesis is supported by experiments where the laser intensity was varied (results not shown). The spectra obtained with low laser intensity showed a higher fraction of xanthate-endfunctional chains than the one with the highest laser intensity. To avoid fragmentation of the chain-ends the laser intensity was kept as low as possible. As observed in Figure 3.8, at low laser intensity the main distribution corresponded to xanthate-endfunctional chains, however fragmentation was still present to a significant level. The experimental mass distributions were compared with isotopic patterns calculated for PVP with the end-groups expected from xanthate-mediated polymerization (+39 a.m.u., as K^+ was added to the polymer during sample preparation). In all samples where the polymer was isolated by precipitation the end-groups identified were the R group at one chain-end and either the xanthate group at the other chain-end (signal corresponding to the isotopic pattern (b)) or one monomer unit minus 1 a.m.u. (a). The relative intensity of the peaks corresponding to these 2 end-group distributions was highly dependant on the choice of the matrix. As presented in Figure 3.9, (b) was the main distribution when the matrix

trans-2-[3-(4-*tert*-butylphenyl)-2-methyl-2-propenylidene]-malononitrile (MM) was used whereas (b) was not observed when α-cyano hydroxyl cinnamic acid (CHCA) was used as the matrix. Conversely the intensity of peaks corresponding to (a) was very low with the matrix MM whereas (a) appeared as the main distribution with CHCA. Identification of the xanthate-endfunctional chains with the matrix MM as well as via ^{1}H-NMR spectroscopy confirmed that this structure was actually present in the samples. These results therefore indicate that CHCA is not a suitable matrix for the quantification of PVP end-groups, in contradiction with previous findings with ester-endfunctional PVPs.[13] Other matrices were tested, including 2,5-dihydroxybenzoic acid, trans,trans-1,4-diphenyl-1,3-butadiene, 2-(4'-hydroxyphenylazo) benzoic acid, 1,8,9-trihydroxyanthracene and sinapinic acid. MM was chosen as it gave the lowest level of fragmentation. Such observations however call for extreme caution for the interpretation of MALDI-ToF-MS results with PVP in terms of end-group characterization. It seems that the xanthate end-groups are particularly labile when attached to NVP monomer. On the contrary fragmentation was not observed in PVAc MALDI-ToF-MS mass spectra (results not shown).

The molecular weight distribution data obtained via MALDI-ToF-MS differed significantly depending on the matrix and post-polymerization treatment (Table 3.2). It is not impossible that the history of the polymer sample affects the ability of PVP to co-crystallize with the matrix (*i.e.* the presence of water may favor or prevent co-crystallization) and thus affect MALDI-ToF-MS analysis.[14] However the differences observed in the mass spectra with respect to post-polymerization treatment may also be due to an effect of the chain-ends. With the matrix MM, PDIs were lower than those measured via SEC. M_n values were higher for low M_n samples (Table 3.2, entries k-n). On the contrary M_n values were lower via MALDI-ToF-MS than SEC for higher M_n samples. The latter can be explained due to preferential ionization of low M_n species often observed in MALDI-ToF-MS experiments with polydisperse samples. It was concluded that molecular weight distribution characterization via MALDI-ToF-MS was not accurate under our experimental conditions. Therefore in this thesis only molecular weight data obtained via SEC are reported. MALDI-ToF-MS results are presented regarding end-group characterization on PVP samples for qualitative interpretations. The

general approach was as such: if a certain species is identified, it was present in the sample (whether produced during the analysis or not), however absence of the signal for an expected species was not taken as evidence for its absence from the sample.
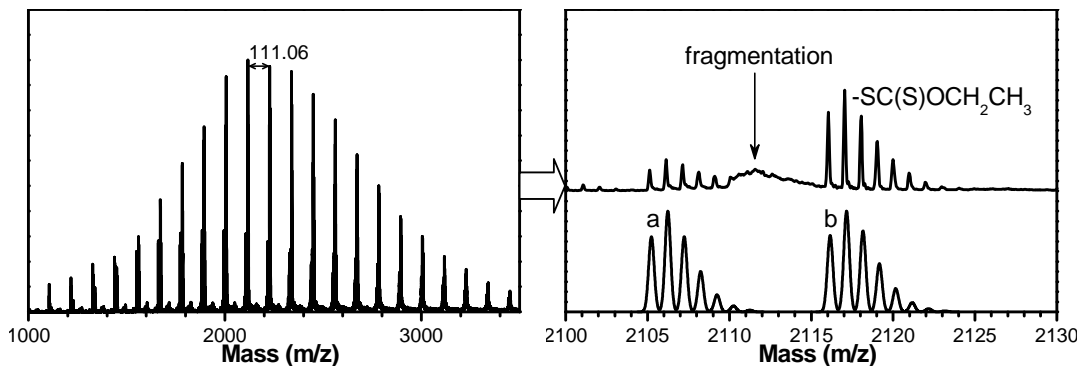

Figure 3.8: MALDI-ToF-MS mass spectrum of poly(N-vinylpyrrolidone) with xanthate end-groups (X6). Right: enlargement of the spectrum in the mass range 2100 – 2130 a.m.u. (top) and simulated isotopic pattern for $C_4H_6N(C_6H_9NO)_{17}C_6H_8NO + K^+$ (a) and $C_4H_6N(C_6H_9NO)_{17}S_2C_3H_5O+ K^+$ (b).
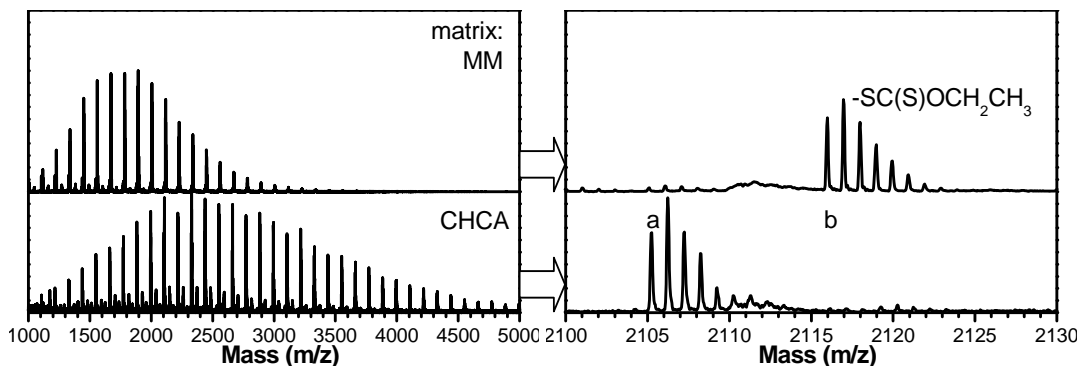
Figure 3.9: Effect of the matrix on MALDI-ToF-MS mass spectra of poly(N-vinylpyrrolidone) with xanthate end-groups. Comparison between *trans*-2-[3-(4-*tert*-Butylphenyl)-2-methyl-2-propenylidene]-malononitrile (MM) (top) and α-cyano hydroxyl cinnamic acid (CHCA) (bottom). Right: enlargement of the spectra in the mass range 2100 – 2130 a.m.u.

Table 3.2: Effect of matrix, method for polymer isolation and molecular weight on the molecular weight data obtained by MALDI-ToF-MS and comparison with data obtained via SEC.

Ref.	postpolymerization treatment	Matrix	$M_{n,MALDI}$ (g·mol⁻¹)	PDI_{MALDI}	$M_{n,SEC}$ (g·mol⁻¹)	PDI_{SEC}
k	precipitation	MM	2482	1.10	2180	1.28
l	dialysis	MM	2507	1.18	2200	1.27
m	precipitation	MM	2090	1.10	2040	1.27
n	precipitation	CHCA	3196	1.29	2040	1.27
o	precipitation	MM	4717	1.20	9600	1.47

Experimental

Materials

N-vinylpyrrolidone (Aldrich, 99 %) was dried over anhydrous magnesium sulfate and purified by distillation under reduced pressure. Vinyl acetate (Protea Chemicals, 99 %), was distilled under reduced pressure, collected in a flask, and cooled down in an ice bath. Tetrahydrofuran (KIMIX) was distilled over lithium aluminum hydride. Toluene, hexane, ethyl acetate and 1,4-dioxane (Merck) were distilled under reduced pressure. Dichloromethane (KIMIX, CP-grade, 99.5 %) and ethanol (SASOL, absolute, 99.5 %) were stored over molecular sieves 3 Å. 2,2'-Azobis(isobutyronitrile) (AIBN) (Riedel de Haen) was recrystallized twice from methanol. Potassium *O*-ethyl dithiocarbonate (95 %, Merck), 2-bromopropionyl bromide (97 %, Fluka), ethyl *2*-bromo propionate (98 %, Fluka), α-chlorophenylacetylchloride (90 %, Aldrich), 1-bromoethyl benzene (Aldrich, 97 %), 2-bromopropionitrile (Aldrich, 97 %), pyridine (Merck, CP-grade, 99.5 %), *tert*-butyl mercaptan (Aldrich, grade), ethylene glycol (Aldrich, 99+ %), sodium hydroxide, potassium hydroxide, hydrochloric acid and the deuterated solvent C_6D_6 (99.6 %, Aldrich) were used without further purification. For column chromatography, silica gel (Fluka, particle size 0.063 – 0.2 mm, Brockmann 2-3) was used.

Synthesis of xanthate chain-transfer agents

Synthesis of *S*-(2-propionic acid), *O*-ethyl xanthate (X3)

Many procedures were tested to determine whether 2-bromopropionic acid should be neutralized prior to addition to the xanthic salt or rather added to an alkaline solution containing the xanthic salt. The procedure which gave the highest yield and highest purity is as follows: Potassium *O*-ethyl xanthate (10.08 g, $6.25 \cdot 10^{-2}$ mol) was dissolved in distilled water (30 g). 3.3 M NaOH (15 mL) was added under stirring. The mixture was cooled with an ice bath. Then *2*-bromopropionic acid (4.50 mL, 7.6 g, $5.0 \cdot 10^{-2}$ mol) was added dropwise. The reaction was left to proceed for 16 h at room temperature. The pH of the solution (pH = 7 at the end of the reaction) was adjusted with 2 M HCl to pH = 1. The product was extracted with diethyl ether (2×200 mL), then from the ethereal phase with sodium carbonate (25 g in 250 mL water, 2×50 mL). The pH was readjusted to pH =

3 with 1 M HCl. The product was extracted with diethyl ether (200 mL), the ethereal phase was dried over anhydrous magnesium sulfate and the solvent was evaporated under reduced pressure. The product, a pale yellow solid (9.22 g, $4.75 \cdot 10^{-2}$ mol) crystallized during solvent evaporation (it could otherwise be recrystallized from hexane). The yield was 76 %, purity > 97 % by NMR. ^{1}H-NMR (300 MHz, CDCl$_3$): δ[ppm] = 11.10, 1H, broad, (COOH), 4.64, 2H, 2×q, ^{3}J$_A$=7.3 Hz, ^{3}J$_B$=7.1 Hz (CH$_2$, diastereotopic group), 4.41, 1H, q, ^{3}J=7.3 Hz (CH), 1.60, 3H, d, ^{3}J=7.3, (CH_3CH), 1.41, 3H, t, ^{3}J$_A$=7.3 Hz, ^{3}J$_B$=7.1 Hz (CH_3CH$_2$).

Synthesis of X4

The difunctional xanthate X4 was prepared according to a procedure published by Taton et al.[15] Ethylene glycol (2.43 g, $3.9 \cdot 10^{-2}$ mol), pyridine (6.0 mL, 5.9 g, $7.4 \cdot 10^{-2}$ mol) and dichloromethane (40 mL) were placed in a 3-neck round bottom flask fitted with a condenser. 2-bromopropionyl bromide (19.5 g, $9.0 \cdot 10^{-2}$ mol) was added slowly. A white precipitate separated from the light yellow solution. After 16 h the precipitate was filtered off. The solution was concentrated under vacuum. Diethyl ether (200 mL) was added. The solution was washed with 1 M HCl (2×50 mL) then saturated NaCl (50 mL) and distilled water (50 mL). The ethereal phase was dried over anhydrous magnesium sulfate. The solvent was evaporated under vacuum. 12.2 g of the dibrominated compound were recovered (Yield = 46 %, purity > 90 % by NMR), which were dissolved in acetonitrile (40 mL). Potassium O-ethyl xanthate (8.6 g, $5.4 \cdot 10^{-2}$ mol) were added portionwise. A white precipitate rapidly separated. The reaction was left under magnetic stirring for 16 h. Solvents were evaporated under vacuum. Diethyl ether (200 mL) was added. The solution was washed with distilled water (4×50 mL). The ethereal phase was dried over anhydrous magnesium sulfate. The solvent was evaporated under vacuum. The product was purified by column chromatography using hexane : diethyl ether 75:25 (v/v) as the eluent. Yield = 65 %, Purity > 95 % by NMR. ^{1}H-NMR (400 MHz, CDCl$_3$): δ[ppm] = 4.62, 4H, q, ^{3}J=7.2 Hz (CH$_3$CH_2), 4.40, 2H, q, ^{3}J=7.3 Hz, (CH), 4.36, s, 4H (CH_2CH$_2$), 1.57, 6H, d, ^{3}J=7.3 (CH_3CH), 1.41, 6H, t, ^{3}J=7.2 (CH_3CH$_2$).

Synthesis of *S*-(*tert*-butyl) *O*-ethyl xanthate (X5)

S-(2-propionic acid) *O*-ethyl xanthate (X3) (8.0 g, $4.1 \cdot 10^{-2}$ mol) was dissolved in dilute alkaline solution containing 4 equivalents of sodium hydroxide (300 mL). Then *tert*-butyl mercaptan (1.53 g, $1.7 \cdot 10^{-2}$ mol) was added under stirring at room temperature. The mixture became turbid, then milky after a few minutes, and was stirred for 20 h. *tert*-Butyl xanthate separated out as a yellow viscous oil. It was extracted with diethyl ether (2×200 mL). The ethereal phase was washed with dilute NaOH (0.1 M, 3×50 mL), with distilled water (50 mL), dried over anhydrous magnesium sulfate and the solvent was evaporated under reduce pressure. The product was purified by Kugelrohr distillation (3 mbar, thermostat at 70 °C) to yield 4.08 g ($2.30 \cdot 10^{-2}$ mol, Yd = 55 %) of yellow oil (purity > 96 % by NMR). ^{1}H-NMR (300 MHz, CDCl$_3$): δ[ppm] = 4.68, 2H, q, ^{3}J=7.3 Hz, (CH_2), 1.49, 9H, s, C(CH_3)$_3$, 1.46, 3H, t, ^{3}J=7.3 Hz, (CH_3-CH$_2$).

Synthesis of *S*-(2-cyano-2-propyl) *O*-ethyl xanthate (X6)

1. Synthesis of *O,O*-diethyl bisxanthate. *O,O*-diethyl bisxanthate was prepared by a method derived from that of Shi et al.[16] Potassium O-ethyl xanthate (10.80 g, $6.7 \cdot 10^{-2}$ mol) was dissolved in distilled water (50 mL). A solution of iodine (3.3 g) and potassium iodide (1.7 g) in distilled water (50 mL) was added dropwise. The mixture was left under magnetic stirring for 48 h. A yellow / orange oil separated, which was extracted with diethyl ether (4×50 mL). The combined ethereal fractions were extracted with distilled water (5×50 mL), dried over anhydrous magnesium sulfate and the solvents were evaporated under vacuum. 6.80 g of yellow oil was obtained (Yd = 82 %), purity > 97 % by NMR. ^{1}H-NMR (400 MHz, CDCl$_3$): δ[ppm] = 4.69, 4H, q, ^{3}J=7.1 Hz, (CH_2), 1.42, 6H, t, ^{3}J=7.1 Hz, (CH_3).

2. Synthesis of *S*-(2-cyano-2-propyl) *O*-ethyl xanthate. *O,O*-diethyl bisxanthate (6.76 g, $2.8 \cdot 10^{-2}$ mol) and AIBN (5.40 g, $3.3 \cdot 10^{-2}$ mol) were dissolved in toluene (40 mL). The solution was degassed with argon for 30 min then placed in an oil bath at 80 °C. After 2 h an additional portion of AIBN (3.6 g, $2.2 \cdot 10^{-2}$ mol) was added. The reaction was stopped after 7.5 h. Solvents were evaporated under vacuum. The product was purified by column chromatography using hexane : ethyl acetate 95:5 (v/v) as the eluent.

Yield = 63 %, Purity > 97 % by NMR. ^{1}H-NMR (400 MHz, CDCl$_3$): δ[ppm] = 4.74, 2H, q, ^{3}J=7.2 Hz (CH_2), 1.75, 6H, s, (C(CH$_3$)$_2$), 1.52, 3H, t, ^{3}J=7.2 Hz (CH$_2$CH_3).

Synthesis of *S*-(2-phenylethyl) *O*-ethyl xanthate (X9)

1-bromoethyl benzene (5 mL, 6.8 g, 3.7·10^{-2} mol) was added dropwise to a solution of potassium *O*-ethyl xanthate (6.46 g, 4.0·10^{-2} mol) in ethanol (40 mL). After 6 h of reaction under magnetic stirring a white precipitate was filtered off. Solvents were evaporated under vacuum. Diethyl ether was added (200 mL). More of the white precipitate was removed by filtration. The filtrate was washed with distilled water (4×50 mL) and was dried with anhydrous magnesium sulfate. The solvents were evaporated under vacuum. The product was recovered with 91 % yield. Purity > 96 % by NMR. ^{1}H-NMR (400 MHz, CDCl$_3$): δ[ppm] = 7.23-7.40, 5H, m (CH_{Ar}), 4.91, 1H, q, ^{3}J=7.1 Hz (CH),4.62, 1H, q, ^{3}J=7.1 Hz (CH_2), 1.72, 3H, d, ^{3}J=7.1 Hz (CH_3CH), 1.39, 3H, t, ^{3}J=7.1 Hz (CH$_2$CH_3).

Synthesis of *S*-(1-cyanoethyl) *O*-ethyl xanthate (X10)

Potassium *O*-ethyl xanthate (2.26 g, 1.4·10^{-2} mol) was dissolved in dry distilled ethanol (30 mL). 2-Bromopropionitrile (1.05 mL, 1.63 g, 1.2·10^{-2} mol) was added dropwise under magnetic stirring. The mixture was stirred at room temperature for 16 h. A white precipitate was filtered off. Diethyl ether (160 mL) was added to the filtrate. The ethereal solution was washed with distilled water (4×50 mL) and was dried with anhydrous magnesium sulfate. The solvents were evaporated under vacuum. The product was purified by column chromatography using hexane : ethyl acetate 95:5 (v/v) as the eluent and recovered with 42 % yield. Purity > 95 % by NMR. ^{1}H-NMR (400 MHz, CDCl$_3$): δ[ppm] = 4.70, 2H, 2×q, ^{3}J$_A$=7.3 Hz, ^{3}J$_B$=7.1 Hz (CH$_2$, diastereotopic group), 4.43, 1H, q, ^{3}J=7.3 Hz (CH), 1.69, 3H, d, ^{3}J=7.3, (CH_3CH), 1.46, 3H, t, ^{3}J$_A$=7.3 Hz, ^{3}J$_B$=7.1 Hz (CH$_2$CH_3).

Synthesis of *S*-(2-ethyl propionate) *O*-ethyl xanthate (X13)

Potassium *O*-ethyl xanthate (9.50 g, 5.8·10^{-2} mol) was dissolved in 30 mL of ethanol with ethyl *2*-bromo propionate (9.48 g, 5.3·10^{-2} mol) for 16 h at room

temperature. A white precipitate was filtered off. The filtrate was diluted with 250 mL diethyl ether, washed with distilled water (4×50 mL), dried over anhydrous magnesium sulfate. The product was purified by column chromatography using hexane : ethyl acetate 95:5 (v/v) as the eluent. 7.0 g of yellow oil was obtained (purity > 99 % by ^{1}H-NMR spectroscopy). ^{1}H-NMR (400 MHz, CDCl$_3$): δ[ppm] = 4.63, 2H, q, ^{3}J=7.2 Hz (C(S)OC*H$_2$*), 4.37, 1H, q, ^{3}J=7.4 Hz (C*H*), 4.20, 2H, q, ^{3}J=7.2 Hz (C(O)OC*H$_2$*), 1.56, 3H, d, ^{3}J=7.4 Hz (C*H$_3$*CH), 1.41, 3H, t, ^{3}J=7.2 Hz (C(S)OCH$_2$C*H$_3$*), 1.28, 3H, t, ^{3}J=7.2 Hz (C(O)OCH$_2$C*H$_3$*).

Synthesis of *S*-(2-ethyl phenylacetate) *O*-ethyl xanthate (X14)

α-chlorophenyl acetylchloride (1.44 g, 7.6·10^{-3} mol) was added to 10.0 mL of absolute ethanol. The solution was stirred for 1h at room temperature. Pyridine (1.85 mL, 2.34·10^{-2} mol) was added dropwise. Potassium *O*-ethyl xanthate (2.44 g, 1.52·10^{-2} mol) was added. The mixture was stirred for 16 h at 50 °C. The solvents were evaporated under vacuum. Diethyl ether was added (160 mL). A white precipitate was removed by filtration. The filtrate was washed with hydrochloric acid (8×40 mL), saturated sodium bicarbonate (4×40 mL) then water (2×30 mL) and was dried over anhydrous magnesium sulfate. The solvents were evaporated under vacuum. The product, which contained 23 % of unreacted α-chlorophenyl acetic acid, ethyl ester was purified by column chromatography using hexane : ethyl acetate 95:5 (v/v) as the eluent. A light yellow oil was recovered (50 %), 93 % pure (by ^{1}H-NMR spectroscopy). ^{1}H-NMR (400 MHz, CDCl$_3$): δ[ppm] = 7.30-7.44, m, 5H (C*H$_{Ar}$*); 5.46, s, 1H (C*H*C$_6$H$_5$); 4.62, q, ^{3}J=7.3 Hz, 2H (SC(S)OC*H$_2$*CH$_3$); 4.25, m, 2H (CH$_3$C*H$_2$*OC(O)); 1.40, t, ^{3}J=7.3 Hz, 3H (SC(S)OCH$_2$C*H$_3$*), 1.25, t, ^{3}J=7.3 Hz, 3H (C*H$_3$*CH$_2$OC(O)). ^{13}C-NMR (100 MHz, CDCl$_3$): δ[ppm] = 211.65 (*C*=S), 169.18 (C=O), 133.37 (C$_{Ar}$), 127.9-129.2 (C*H$_{Ar}$*), 70.18 (C(S)OC*H$_2$*), 62.09 (C(O)OC*H$_2$*), 56.97 (*C*H), 14.00, 13.58.

Polymerization procedures

All polymerizations were carried out in a pear-shaped 50 mL Schlenk flask heated in an oil bath. The polymerization mixture was degassed with a minimum of 3 freeze-pump-thaw cycles followed by the introduction of ultra-high purity argon. The molar

ratio of CTA to initiator was kept constant at approximately 10:1. The molar ratio of monomer to CTA was calculated from equation 2.3, which gives [Monomer]/[CTA]=$(M_{n,\alpha}-MM_{CTA})/(MM_{Monomer}\times\alpha)$ and adjusted on the basis of the required molecular weight at 50 % conversion. For example when PVP with $M_{n,target,\,50\,\%}$ ~ 25000 g·mol^{-1} (*i.e.* DP$_{target,50\,\%}$ ~ 25000/111.1= 225) was required, the ratio [NVP]/[CTA] was 450. A typical polymerization was performed as follows:

Polymerization of *N*-Vinylpyrrolidone with CTA X10 (same procedure as for X3-14)

AIBN (0.004 g, $2\cdot10^{-5}$ mol), the CTA *S*-(1-cyanoethyl) *O*-ethyl xanthate (0.039 g, $2.2\cdot10^{-4}$ mol) and NVP (11.00 g, $9.90\cdot10^{-2}$ mol) were placed in a Schlenk flask and degassed via freeze-pump-thaw. The flask was immersed in an oil bath preheated at 60 ºC. After 6 h of reaction under magnetic stirring poly(*N*-vinylpyrrolidone) was isolated by precipitation in diethyl ether.

Polymerization of Vinyl acetate (VAc)

The same polymerization procedure was applied as for NVP, however the reaction was carried out at 54 ºC (unless indicated otherwise) and the polymer was isolated by evaporation of the solvent and unreacted monomer.

Procedure for kinetic studies (conversion vs. time)

The polymerization mixture was prepared under the same conditions as described above. The Schlenk flask was closed with a rubber septum. Samples were withdrawn from the polymerization mixture using a glass syringe cleaned with argon. A volume of argon equivalent to the volume of the sample withdrawn was injected from the syringe into the polymerization flask to equilibrate the pressure inside the reactor. The sample was placed in a glass vial and a few crystals of hydroquinone were added to quench the radicals. The vials were closed with a plastic lid and cooled down with ice or liquid nitrogen prior to ^{1}H-NMR and SEC analyses.

Procedure for *in situ* NMR spectroscopy experiments (chapters 4 and 5)

In a typical *in situ* NMR spectroscopy polymerization experiment, the desired amount of initiator (AIBN), xanthate CTA, monomer and deuterated solvent C_6D_6 (0.25 g, 50 wt %) were weighed (molar ratio 5:1:0.1). The solutions were transferred to NMR tubes. The tubes were flushed with ultra-high purity argon for 5 minutes. A sealed glass insert containing the integration reference standard (formic acid in C_6D_6) was inserted. *In situ* ^{1}H-NMR experiments were carried out on a 600 MHz Varian [Unity]Inova spectrometer. A 5 mm inverse detection PFG probe was used for the experiments and the probe temperature was calibrated using an ethylene glycol sample in the manner suggested by the manufacturer using the method of Van Geet.[17] [1]H spectra were acquired with a 3 μs (40°) pulse width and a 4 sec acquisition time. For the ^{1}H kinetic experiments, samples were inserted into the magnet at 25 °C and the magnet fully shimmed on the sample. A spectrum was collected at 25 °C to serve as a reference. The sample was then removed from the magnet and the cavity of the magnet was raised to the required temperature (60 °C or 70 °C). Once the magnet cavity had stabilized at the required temperature, the sample was re-inserted (time zero) and allowed to equilibrate for approximately 5 minutes. Additional shimming was then carried out to fully optimize the system and the first spectra were recorded approximately 5 min after the sample was inserted into the magnet. Integration of the spectra was carried out using ACD labs 7.0 1-D ^{1}H-NMR processor[®]. All FID files were processed at once. Phase correction and baseline correction were applied to the Fourier-transformed spectra and peaks were integrated manually. The concentrations were determined relative to the internal reference (formic acid) contained in the glass insert.

^{1}H-NMR and ^{13}C-NMR one-dimensional experiments, ^{13}C-Distorsionless Enhancement by Polarization effect (DEPT), selective TOtal Correlation SpectroscopY (TOCSY) and Nuclear Overhauser Effect SpectroscopY (NOESY) experiments and a series of two-dimensional experiments including homonuclear ^{1}H/^{1}H-COrrelated SpectroscopY (COSY) as well as ^{1}H/^{13}C-Heteronuclear Single Quantum Coherance (HSQC) and ^{1}H/^{13}C-Heteronuclear Multiple-Bond Correlation (HMBC) NMR

spectroscopy experiments on *ex situ* samples enabled the assignment of peaks for the various species involved in the xanthate-mediated polymerizations.

Characterization techniques

NMR spectroscopy

^{1}H-NMR and ^{13}C-NMR spectra were recorded on a Varian-400 or 600 MHz Varian ^{Unity}Inova spectrometer.

UV-Vis spectroscopy

UV-Vis spectra were measured with a Perkin Elmer Lambda 20 photodiode array spectrophotometer.

Size-exclusion chromatography

The SEC set-up consisted of an eluent degasser (Alltech Elite), a gradient pump (Shimadzu, LC-10AD), an injector (Spark Holland, MIDAS), a two-column set (PSS, PFG Linear XL 7 μm, 8 x 300 mm, separation window 10^2 – 10^6 Da), a column oven (Spark Holland, Mistral) at 40 ºC, detectors in series: Dual Wavelength UV Detector (Waters, 2487); Light Scattering (RALS/LALS) and Viscometry (Viscotek, 270) and Differential Refractive-Index Detector (DRI) (Waters, 2414). The injection volume was 50 μL, the flow rate was 0.8 mL·min^{-1}. The eluent HFIP (Biosolve, AR-grade) with 0.02 M KTFA added (potassium trifluoro acetate, 3.0 g·L^{-1}, Fluka 91702) was redistilled after use. A short silica column was placed after the pump to catch free fluoride, possibly present in HFIP. A particle filter 0.2 µm PTFE was placed between columns and UV detector to prevent small particles to enter the LS detector. Data acquisition and processing was performed with Viscotec Omnisec 4.0 (all detectors) and Waters Empower 2.0 (UV and refractive index detectors). The calculated molecular weights were based on a calibration curve for poly(methyl methacrylate) standards (molecular weight range 650 - 1.5·10^4 g.mol^{-1}) of narrow polydispersity (Polymer Laboratories) in HFIP.

Matrix-Assisted Laser-Desorption Ionization-Time-of-Flight-Mass Spectrometry (MALDI-ToF-MS)

MALDI-ToF-MS measurements were performed on a Voyager DE-STR instrument (Applied Biosystems, Framingham, MA) equipped with a 337-nm nitrogen laser. Positive-ion spectra were acquired in the reflector mode. *trans*-2-[3-(4-*tert*-Butylphenyl)-2-methyl-2-propenylidene]-malononitrile was used as the matrix. The matrix was dissolved in THF at a concentration of approximately 40 mg·mL^{-1}. Potassium trifluoroacetate was used as the cationization agent and was added to THF at a concentration of 1 mg·mL^{-1}. The polymer sample was dissolved in THF at a concentration of 2 mg·mL^{-1}. In a typical measurement, the matrix, cationization agent, and sample solutions were premixed in a 10:1:5 ratio. Approximately 0.5 μL of the obtained mixture was hand-spotted on the target plate and left to dry. For each spectrum, 1000 laser shots were accumulated. Data Explorer software (Applied Biosystems) was used for data interpretation.

High Performance Liquid Chromatography (HPLC)

HPLC was performed using a dual pump HPLC set up comprising the following units: Waters 2690 Separations Module (Alliance); Agilent 1100 series variable wavelength UV detector; PL-ELS 1000 detector. Data was recorded and processed using PSS WinGPC unity (Build 2019) software. A C18 grafted silica column was used (Luna RP C18 3 μm 150 × 4.60 mm, Phenomenex) at 30 °C. The mobile phase composition was water (deionized, with 0.1 % formic acid) : acetonitrile at a flow rate of 0.5 mL·min^{-1}. Samples were prepared in the same solvent composition as the mobile phase at the beginning of each elugram, at concentrations of 5 mg·mL^{-1}. The injection volume was 10 μL.

Additional experimental details, which are specific to a particular application, will be given in other chapters, *i.e.* preparation of block copolymers (chapter 6) and chain-end modification of PVP (chapter 7).

Reference List

(1)   Zard, S.Z. *Angew. Chem. Int. Ed. Engl.* **1997**, *36*, 672-685.

(2)   Bouhadir, G.; Legrand, N.; Quiclet-Sire, B.; Zard, S.Z. *Tetr. Lett.* **1999**, *40*, 277-280.

(3)   Ladaviere, C.; Dörr, N.; Claverie, J. *Macromolecules* **2001**, *34*, 5370-5372.

(4)   Thang, S.H.; Chong, Y.K.B.; Mayadunne, R.T.A.; Moad, G.; Rizzardo, E. *Tetr. Lett.* **1999**, *40*, 2435-2438.

(5)   Chiefari, J.; Chong, Y.K.B.; Ercole, F.; Krstina, J.; Jeffery, J.; Le, T.P.T.; Mayadunne, R.T.A.; Meijs, G.F.; Moad, C.L.; Moad, G.; Rizzardo, E.; Thang, S.H. *Macromolecules* **1998**, *31*, 5559-5562.

(6)   Mitsukami, Y.; Donovan, m.S.; Lowe, A.B.; McCormick, C.L. *Macromolecules* **2001**, *34*, 2248-2256.

(7)   Sumerlin, B.S.; Donovan, m.S.; Mitsukami, Y.; Lowe, A.B.; McCormick, C.L. *Macromolecules* **2001**, *34*, 6561-6564.

(8)   Smulders, W. *Macromolecular architecture in aqueous dispersions: 'living' free-radical polymerization in emulsion*; Technical University of Eindhoven: Eindhoven, **2002**.

(9)   Thomas, D.B.; Convertine, A.J.; Hester, R.D.; Lowe, A.B.; McCormick, C.L. *Macromolecules* **2004**, *37*, 1735-1741.

(10)   Baussard, J.-F.; Habib-Jiwan, J.-L.; Laschewsky, A.; Mertoglu, M.; Storsberg, J. *Polymer* **2004**, *45*, 3615-3626.

(11)   McCormick, C.L.; Lowe, A.B. *Acc. Chem. Res.* **2004**, *37*, 312-325.

(12)   Kirsh, Y.E. *Water Soluble Poly-N-Vinylamides: Synthesis and Physicochemical Properties*; Wiley, Chichester, UK, **1998**.

(13)   Ranucci, E.; Ferruti, P.; Annunziata, R.; Gerges, I.; Spinelli, G. *Macromol. Biosci.* **2006**, *6*, 216-227.

(14)   Malvagna, P.; Impallomeni, G.; Cozzolino, R.; Spina, E.; Garozzo, D. *Rapid. Commun. Mass Spectrom.* **2002**, *16*, 1599-1603.

(15)   Taton, D.; Wilczewska, A.; Destarac, M. *Macromol. Rapid Commun.* **2001**, *22*, 1497-1503.

(16)   Shi, L.; Chapman, T.M.; Beckman, E.J. *Macromolecules* **2003**, *36*, 2563-2567.

(17)   Van Geet, A.L. *Anal. Chem.* **1968**, *40*, 2227-2229.

Chapter 4: Mechanistic and kinetic aspects[a]

In this chapter the first experimental evidence of selective initialization of poorly stabilized monomers in Reversible Addition Fragmentation chain Transfer (RAFT) mediated living radical polymerization is presented. Xanthate chain transfer agents (CTAs) of the general formula EtO-C(=S)-SR were used to mediate the polymerization of NVP and VAc. *In situ* ^{1}H-NMR spectroscopy was performed to follow the concentrations of xanthate and monomer and to identify the non-radical species involved in the RAFT mechanism. Various xanthate CTAs were screened, which vary only by the nature of their leaving group. Fast and selective initialization was found to guarantee a high degree of control over the molar mass distribution of the polymer. Consequently, the study of the initialization via *in situ* NMR spectroscopy can help devise a suitable CTA for a given monomer.

Introduction

The influence of the structure of the CTA on the level of control has been perceived since the discovery of the RAFT process. The stabilizing effect of the Z group[1] and the ability of the R group to fragment from the CTA and reinitiate polymerization[2] were acknowledged as critical. The range of Z and R groups designed is wide[3] and theoretically any vinyl monomer can be matched with a suitable CTA, provided the monomer does not contain a functional group capable of degradation of the thiocarbonylthio functionality (*e.g.* unprotected primary or secondary amine). The CTA is efficient if it provides a fast equilibrium between active and dormant species, *i.e.* fast radical addition and fast fragmentation of adduct radicals (see Scheme 4.1). This requires a subtle adjustment between the rates of addition (k_{add} and $k_{-\beta}$) and fragmentation (k_β and k_{-add}) with respect to the rates of reinitiation (k_i) and propagation (k_p). Experimentally, rate constants are not available separately due to the interconnection between several

[a] This chapter in an extension of the work presented in the publication: Pound, G.; McLeary, J.B.; McKenzie, J.M.; Lange, R.F.M.; Klumperman, B. *Macromolecules* **2006**, *39*, 7796 - 7797.

competing reactions where the product of one reaction becomes the reagent of another one.

$$R-S-\overset{S}{\underset{Z}{\|}}\!\!-S \;+\; RM_n^\bullet \quad \underset{k_p(M)}{\overset{k_{add}}{\underset{k_{-add}}{\rightleftharpoons}}} \quad R-S-\overset{\bullet}{\underset{Z}{C}}-S-M_nR \quad \overset{k_\beta}{\underset{k_{-\beta}}{\rightleftharpoons}} \quad R^\bullet \;+\; S=\overset{S}{\underset{Z}{C}}-S-M_nR$$
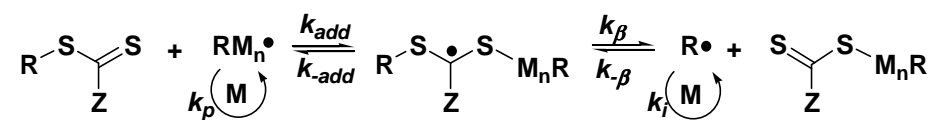
Scheme 4.1: RAFT pre-equilibrium and rate constants of radical reactions.

Coote and Radom have implemented computational studies to specifically study the RAFT mechanism.[4-12] Based on the calculation of geometries, energies and frequencies of all relevant species, they afford kinetic and mechanistic information on the rates of the individual reactions. However *ab initio* studies suffer from various shortcomings even at a high level of theory. The calculations are based on the gas phase whereas polymerizations are carried out in bulk or solvents; the methodology is not suitable for diffusion-controlled processes (*e.g.* bimolecular termination) and as pointed out by the authors the chain-length dependence of rate constants results in an impractical number of variables (they identified a minimum of 100 adjustable parameters if chain-length dependence is considered only up to the stage of the dimer).[11] The authors provide valuable guidelines for the preselection of potential CTAs for a given monomer[8] nonetheless identification of a suitable CTA for a new monomer still relies on experimental screening. The efficiency of the CTA is estimated experimentally on the basis of molecular weight distribution characteristics, which as we discussed in the introduction are subject to substantial errors depending on experimental conditions. Alternatively, kinetic and mechanistic approaches provide information on the causes of success or failure of a CTA-monomer system. Our objectives were to develop a technique to estimate the efficiency of CTAs with poorly stabilized vinyl monomers and identify the factors influencing molecular weight control. The focus of these experiments was mainly investigation of the pre-equilibrium or initialization step. McLeary et al. defined initialization as "the process by which the starting RAFT agent (CTA) is consumed".[13] In this chapter we present the use of *in situ* ^{1}H-NMR spectroscopy to follow the concentration of the non-radical species involved in the RAFT mechanism, namely the monomer, the CTA and their derivatives. Then polymers were prepared and analyzed via

SEC to correlate the initialization behavior with molecular weight distribution data. The main focus was on NVP but some experiments are presented with VAc for comparison.

Selectivity of the initialization step

The 7 xanthates presented in Figure 4.1 were prepared and tested as CTAs for the control of NVP polymerization. In a typical experiment 1 equivalent of xanthate, 5 equivalents of NVP and 0.1 equivalent of initiator 2,2-azobis(isobutyronitrile) (AIBN) were dissolved in an equal mass of deuterated solvent C_6D_6. The solution was placed in an NMR tube and degassed with argon. A sealed insert with formic acid was placed in the tube to serve as a reference for peak integrations. The tube was inserted in the NMR spectrometer where the temperature was 70 °C and one ^{1}H NMR spectrum was recorded every minute or every two minutes.
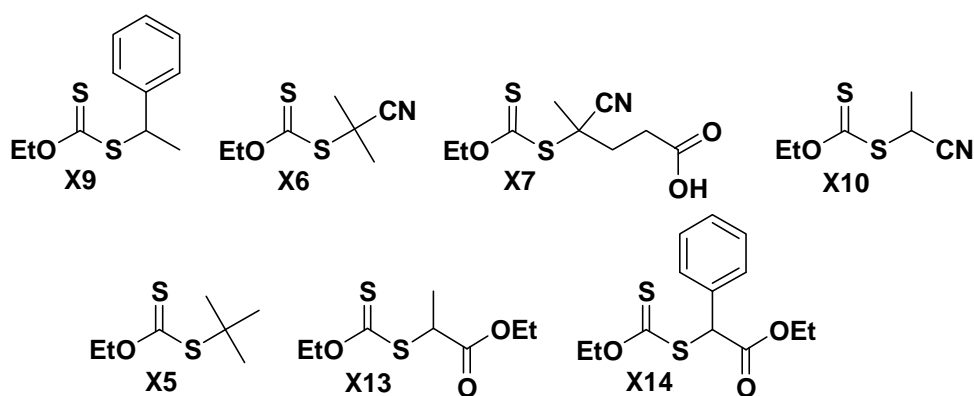
Figure 4.1: Xanthate chain transfer agents. The xanthates are ranked from left to right and first to second line in the order of decreasing electron withdrawing character of the R group, as determined by ^{1}H NMR spectroscopy.
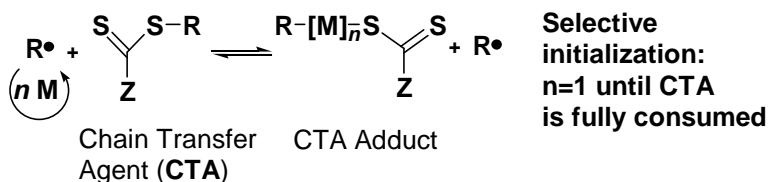
Figure 4.2: Mechanism of fragmentation of the initial chain-transfer agent.

The selectivity of the initialization step is illustrated with the example of 2-cyano-2-propyl xanthate (X6). From the concentration profiles of the xanthate, monomer (NVP), and the single monomer adduct of X6 shown in Figure 4.3, we observe that during the first 275 minutes, the reaction is highly selective. It consists of the overall

incorporation of one monomer unit in the initial CTA (Figure 4.2). There is no significant further polymerization until the xanthate is completely converted into the single monomer adduct. Thus the concentration profile of the monomer follows that of the initial CTA, decreasing in equimolar amount. At the end of the initialization process, a slight but sudden change in the rate of monomer consumption occurs. This change corresponds to the change in the structure of the thiocarbonylthio species present in the reaction mixture. During the initialization period two types of CTAs are present, *i.e.* the initial CTA and the single monomer adduct. Beyond initialization only one type of CTA is present which produces NVP-derived radicals.
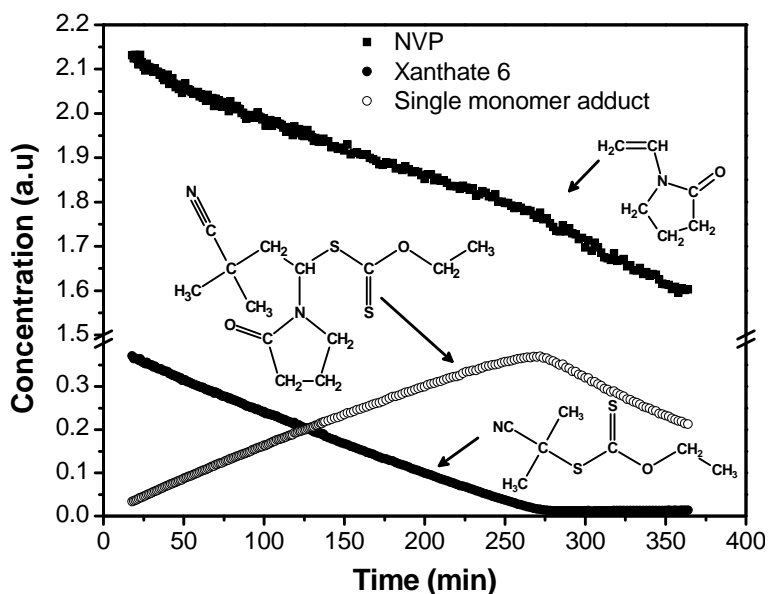
Figure 4.3: Concentration profiles of the species involved in initialization in the xanthate (X6)-mediated polymerization of NVP at 70 ºC in C_6D_6, [Monomer]$_0$/[Xanthate]$_0$ = 5, probed by *in situ* ^{1}H-NMR spectroscopy (R$_6$ = 2-cyano-2-propyl).

A selection of four ^{1}H NMR spectra at different reaction times is shown in Figure 4.4. This figure qualitatively confirms the selectivity during the first monomer addition. Similar behavior was earlier observed for dithiobenzoate-mediated polymerization of styrene.[14] However, for a poorly stabilized monomer such as NVP or VAc, it is quite unexpected to see such high selectivity.
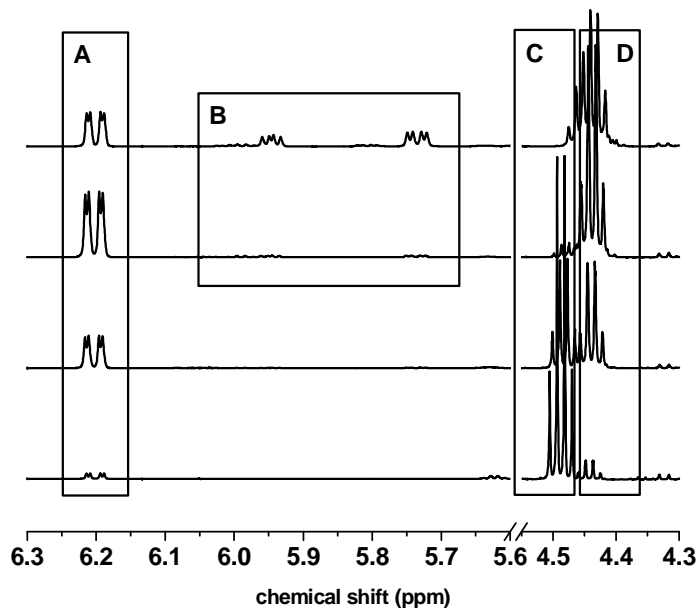
Figure 4.4 : Four ^{1}H NMR spectra at different reaction times. From bottom to top: t (min) = 17; 137; 257; 377. A: single monomer adduct (<u>CH</u>-S); B: oligomer adducts (<u>CH</u>-S); C: initial xanthate (O-<u>CH₂</u>-CH₃); D: single monomer adduct and oligomer adducts (O-<u>CH₂</u>-CH₃).

The nature of the leaving group radical (R•) was identified as the determining factor in the initialization process. The efficiency of initialization and length of the initialization period for a given monomer depend on the rate constants of addition to the CTA, of fragmentation of the CTA radical adduct, of reinitiation (k_i) and how they compare with k_p. We have to keep in mind that during initialization there are two types of CTAs, *i.e.* two k_{add}s and two k_{β}s for the addition and fragmentation of monomer-derived radicals to CTAs. Coote et al. showed that the R group has little influence on the stability of the CTA adduct radical.[4] Thus R is expected to have little effect on k_{add}s. The fact that the rate of monomer consumption increases suddenly once initialization is over indicates one of two things. Either the rate of fragmentation is higher in the main equilibrium than during initialization or the rate constant of addition of the leaving group radical to the monomer (k_i) is small in comparison with k_p. The radical 2-cyano-2-propyl is significantly more stable than NVP-derived radicals due to the presence of the electron withdrawing cyano group and steric stabilization from the bulky methyl substituents. Consequently fragmentation should be favored for the release of the R group, i.e the overall k_{β} is higher during the initialization period. Therefore it can be concluded that k_i is small and that reinitiation is the rate-determining step. This is also supported by the fact

that the CTA concentration follows an almost linear decay indicating pseudo-zero order dependence of the rate of this reaction on the CTA concentration.

Until it was directly observed via *in situ* ^{1}H-NMR spectroscopy monitored polymerizations, slow selective initialization due to a low k_i (slow reinitiation) was often mistaken for inhibition.[13] The slow formation of the single monomer adduct and the abnormally high concentration of the 2-cyano-2-propyl combination product (tetramethyl succinonitrile (TMSN)) gave evidence of the slow rate of addition of 2-cyano-2-propyl radicals to VAc (VAc-X6) and its effect on the rate of CTA conversion. As illustrated in Figure 4.5, the rate of consumption of X6 is slow. The monomer is consumed in equimolar ratio with X6 to produce the single monomer adduct VAc-X6. After 15 h of reaction initialization was almost complete (more than 95 % of the initial xanthate had been converted to its single monomer adduct). At that point the ratio of single monomer adduct to TMSN was 8:1, indicating that at least one in four 2-cyano-2-propyl radicals had been involved in bimolecular combination instead of reinitiation via addition to VAc.
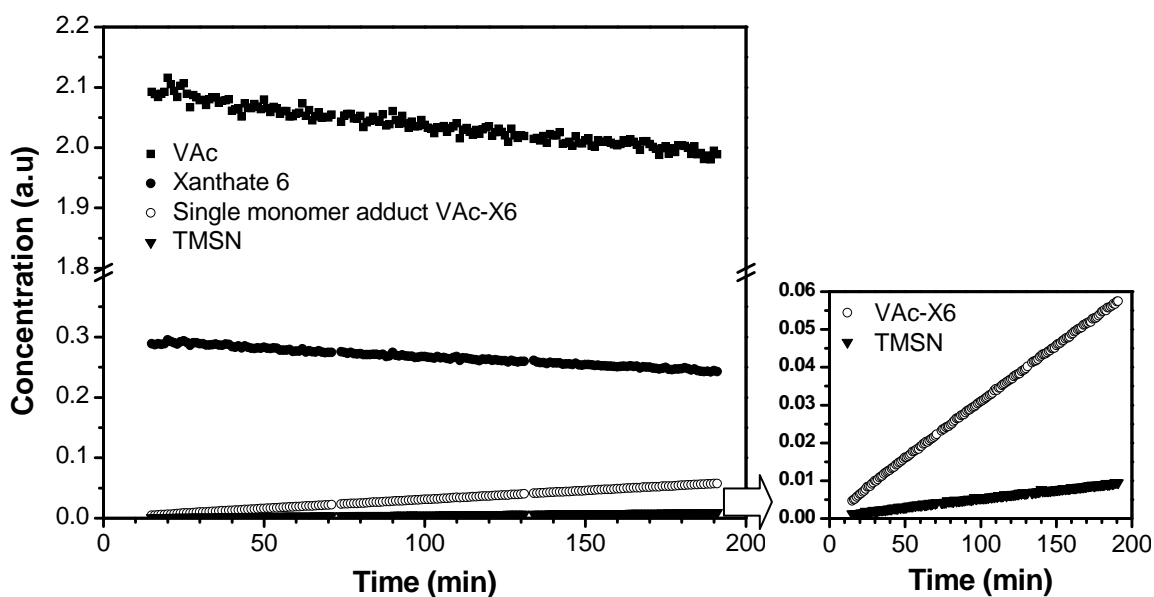
Figure 4.5 : Concentration profiles in the *S*-(2-cyano-2-propyl) *O*-ethyl xanthate (X6)-mediated polymerization of vinyl acetate in C_6D_6 at 70 ºC. X6 consumption determined with δ = 1.33 ppm (t, 3H, -OCH$_2$-*CH$_3$*). The concentration in tetramethyl succinonitrile (TMSN) is abnormally high. Right: enlargement of the single monomer adduct and TMSN signals in the concentration range 0-0.06 a.u.

Slow reinitiation with NVP was observed with xanthate X9, where the R group is 2-phenylethyl. The R group is different from the 2-cyano-2-propyl primary radical

produced by AIBN decomposition. The slow rate of reinitiation of NVP with 2-phenylethyl results in slow selective decomposition of the CTA to produce the single monomer adduct NVP-X9 and a second single monomer adduct species NVP-2-cyano-2-propyl, identical to NVP-X6 (Figure 4.6).
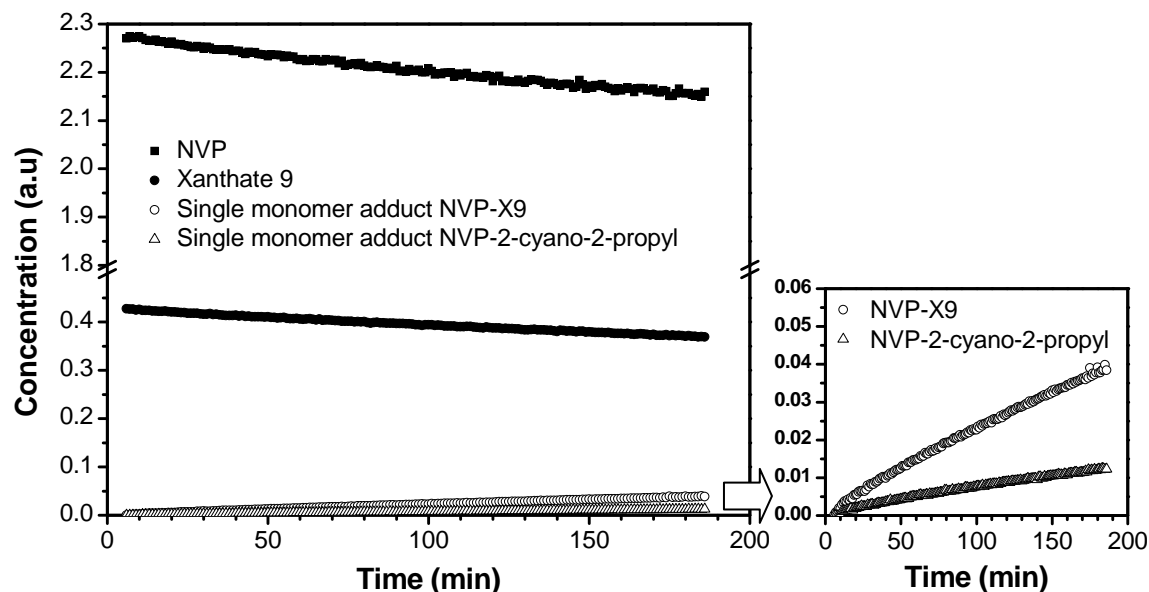
Figure 4.6 : Concentration profiles in the *S*-(2-phenylethyl) *O*-ethyl xanthate (X9)-mediated polymerization of NVP in C_6D_6 at 70 °C. Right: enlargement of the concentration profiles of the two single monomer adduct species (NVP-X9 and NVP-2-cyano-2-propyl due to (re)initiation from the initiator-derived radicals) in the concentration range 0-0.06 a.u.

There are two possible pathways for the formation of NVP-X6 in this experiment. Upon AIBN decomposition 2-cyano-2-propyl radicals are formed which can either add to the monomer or to the CTA. The radical 2-phenylethyl is more stable than 2-cyano-2-propyl due to the mesomeric radical stabilization effect of the phenyl substituent. Consequently an overall exchange of the R group is likely to occur if 2-cyano-2-propyl adds to the CTA. Peaks which could correspond to X6 were observed in the NMR spectra but the compound could not be quantified due to peak overlap and the very low concentration of the species. Apparent inhibition was reported in the X9-mediated polymerization of NVP.[15,16] The present experiment confirms that its origin is the low rate of addition of 2-phenylethyl radicals to NVP. So far X9 was reported as the CTA giving the best results for NVP (in terms of linear increase of M_n with conversion and PDI).[15,16] The *in situ* NMR spectroscopy experiments suggest that X6 would be a better CTA for NVP as it maintains the selectivity of the initialization step while reducing its length.

Non-selective initialization

We showed that the use of X9 and X6 with NVP and VAc provide selective initialization. By contrast, the use of xanthate X5 ($R_3 = $ *tert*-butyl) led to the simultaneous formation of oligomeric adducts (n=1,2 and higher). This was attributed to the monomer-derived radicals having better leaving group ability than the *tert*-butyl R group (probably because the bulky R group stabilizes the thiocarbonylthio compound thus favoring fragmentation of adduct radicals on the side of the monomer). From the concentration profiles presented in Figure 4.7 it is clear that more than one molar equivalent of monomer units was consumed before complete conversion of the initial CTA, indicating that propagation had already occurred to a significant extent. In such a so-called "hybrid" system,[17] higher molar mass material is obtained from the beginning of the reaction and new xanthate endcapped chains are formed late in the polymerization leading to broad molar mass distribution of the resulting polymer.

Another possible cause of hybrid behavior is when the rate of addition to the CTA is smaller than the rate of propagation. In this case radicals can undergo multiple monomer addition prior to addition to the CTA. The present experiment on its own does not enable us to identify the cause of the hybrid behavior. However we can assume once again that the rate of addition of monomer-derived radicals to the CTA is not significantly influenced by the nature of the R group. Considering that initialization was selective with other *O*-ethyl xanthate (*e.g.* X6 and X9) leads us to the conclusion that the rate of addition to the CTA is higher than the rate of propagation. Therefore it is likely that even in the system NVP-X5 addition to X5 did occur prior to propagation but fragmentation occurred to release the incoming propagating radical species instead of the R group.
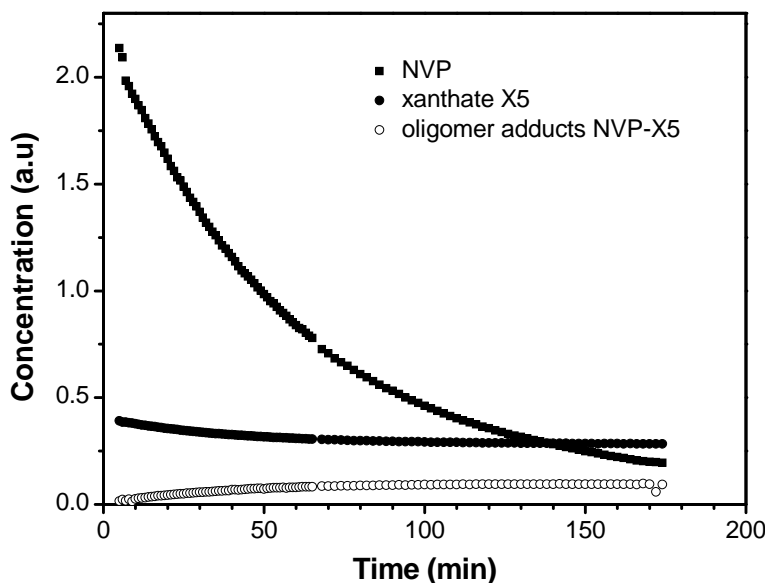
Figure 4.7 : Example of non-selective initialization. Concentration profiles in the *tert*-butyl *O*-ethyl xanthate (X5)-mediated polymerization of NVP in C_6D_6 at 70ºC. The single monomer adduct was not identified but instead oligomer adducts formed.

NMR spectroscopy for probing the efficiency of CTAs

For the evaluation of a CTA via *in situ* ^{1}H NMR spectroscopy the parameters to take into account are the selectivity of the initialization step and its length. The latter will indicate the likelihood of apparent inhibition to take place due to slow initialization. When "real" polymerizations are carried out, *i.e.* when the ratio of monomer to CTA concentration is high, the rate of reinitiation increases due to the increase in monomer concentration. This would be in favor of shortening the inhibition period. However in the case of X9 with NVP for instance, initialization remained so slow that no monomer conversion was detected in the first 6 h at 60 ºC whereas with the use of another xanthate (with R = benzyl) 70 % conversion had been reached.[16] Initialization studies can be performed to differentiate between real inhibition and apparent inhibition due to a slow rate of reinitiation. In order to shorten the initialization period a CTA with a less stabilized R group (*i.e.* 2-cyano-2-propyl instead of phenyl ethyl) must be used. Initialization studies must then be repeated in order to verify that initialization remains selective.

The lack of selectivity of the initialization step will indicate a hybrid system. It needs to be stressed that the possible causes of hybrid behavior can be: (1) choice of the Z-group (modulates k_{add});[1] (2) ability of the R-group to fragment from the intermediate radical (relative to the oligomer / polymer chain); (3) ability of the R-group radical to reinitiate with the monomer. The variation of R and Z groups of RAFT agents and their study via *in situ* ^{1}H-NMR spectroscopy will quickly pinpoint the origin of poor selectivity in initialization.

Optimization of the R group structure

The system VAc-X13 showed fast and selective initialization (the CTA was consumed within 25 min) whereas NVP with X13 underwent hybrid behaviour (Figure 4.8). The concentration in X13 in the experiment with NVP was halved after only 10 minutes. X13 was converted to single NVP adduct which concentration reached a plateau in approximately 40 min and higher adducts were formed simultaneously from the beginning of the reaction.

It is important to note that in spite of the poor selectivity of the initialization step in this system less than 10 % of the initial xanthate was present after 90 min while less than 2 equivalents of NPV had been consumed relative to the amount of xanthate. In this respect X13 behaves noticeably differently from X5. It is likely that 2-propionic acid, ethyl ester (R_{13}) and NVP-derived radicals have similar reactivities. Consequently fragmentation occurs statistically on either side of CTA adduct radicals. The number of propagation steps prior to release of the R group will affect the polydispersity. This number remains low in the system NVP-X13 and therefore the PDI is probably not going to be much higher than in the system NVP-X6 where initialization is completely selective.

It may be advantageous to use X13 with NVP or a xanthate which has an R group with similar reactivity because of the fast consumption of the CTA. Fast initialization ensures that an optimized fraction of the chains are initiated with the R group instead of the primary radical source. On the contrary, long initialization may increase the reaction

time to such an extent that significant side reactions will take place leading to significant radical loss and/or transfer.
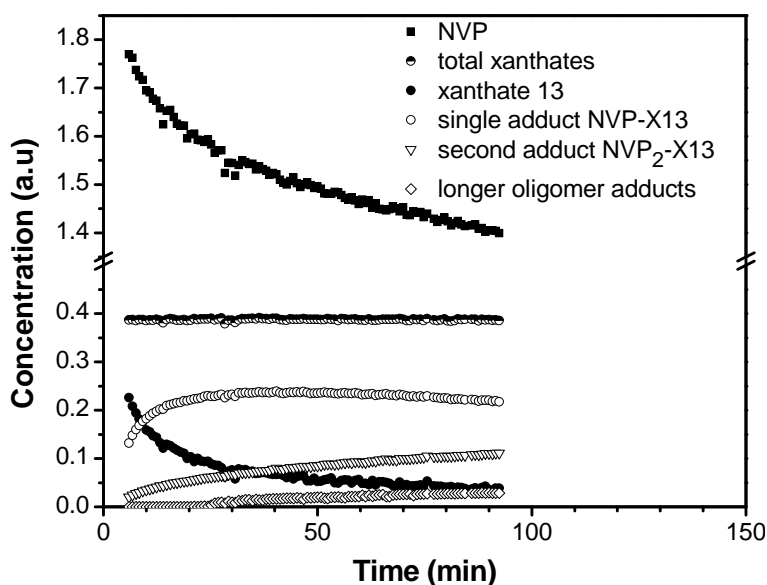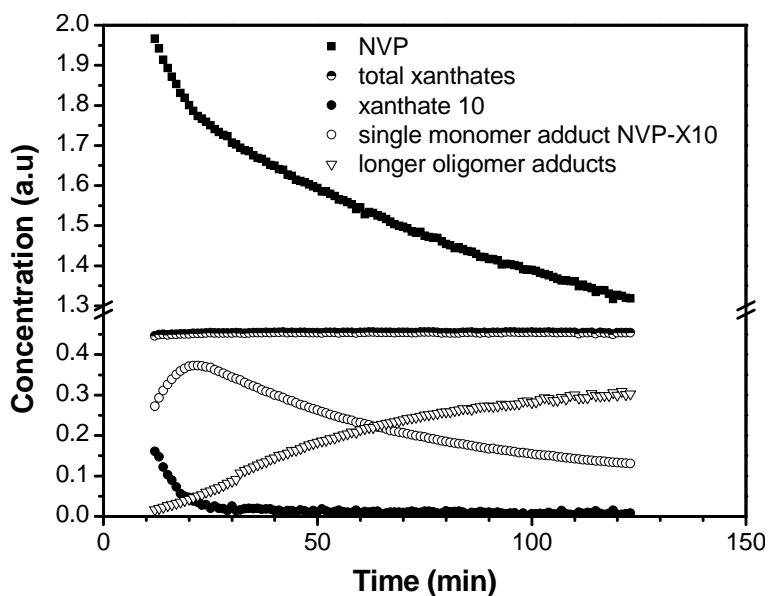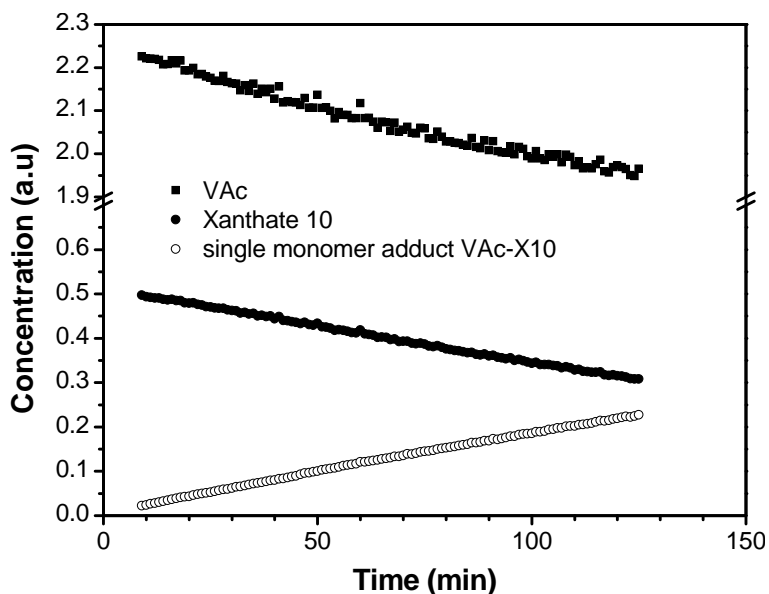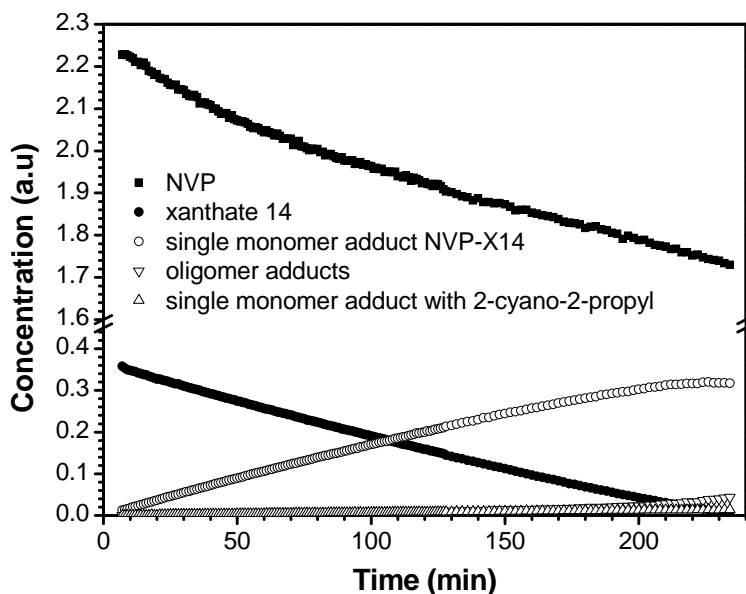

Figure 4.8 : Concentration profiles in the *S*-(2-ethylpropionate) *O*-ethyl xanthate (X13)-mediated polymerization of NVP in C_6D_6 at 70ºC.

The experiments reported so far indicate that, in order to achieve fast and selective initialization with NVP, the R group should have better leaving group ability than 2-propionic acid, ethyl ester (R_{13}) and be able to reinitiate polymerization faster than 2-cyano-2-propyl (R_6). For this purpose the CTAs X10 (R_{10} = 1-cyanoethyl) and X14 (R_{14} = 2-ethyl phenylacetate) were prepared and tested. Prediction of the relative stability of radicals between R groups where only one substituent is modified is generally accurate. The phenyl substituent in X14 is expected to increase the radical stability of the leaving group compared to the equivalent with a methyl substituent. Thus R_{14} should be a better leaving group than R_{13}. Removal of one of the methyl substituents of R_6 corresponding to the structure R_{10} should decrease the leaving group ability and enhance the rate of reinitiation. Therefore it can be predicted that initialization will be faster with X10 than X6 and slower with X14 than X13. Estimation of the relative leaving group / reinitiating ability of R_{14} with R_6 and R_{10} with R_{13} and how they compare with NVP and VAc polymerization rates is not straightforward because more than one of the R group substituents are being varied. For this purpose initialization experiments were carried out.

Initialization with X10 and NVP was not fully but reasonably selective with a ratio of single to second monomer adduct of approximately 7:1 at the end of the initialization time. The initialization time was short (X10 was consumed within 25 min). The rate of monomer conversion changed (decreased) suddenly beyond initialization. It is not possible in this case to identify the origin of this change, which may be either better fragmentation ability of R_{10} than NVP-derived radicals or a higher rate of crosspropagation between the 2-cyanoethyl radical and NVP than the rate of propagation or a combination of both. The fast consumption of the CTA and decrease in the rate of monomer consumption beyond initialization indicate that R_{10} is a good leaving group and reinitiating group with respect to NVP.
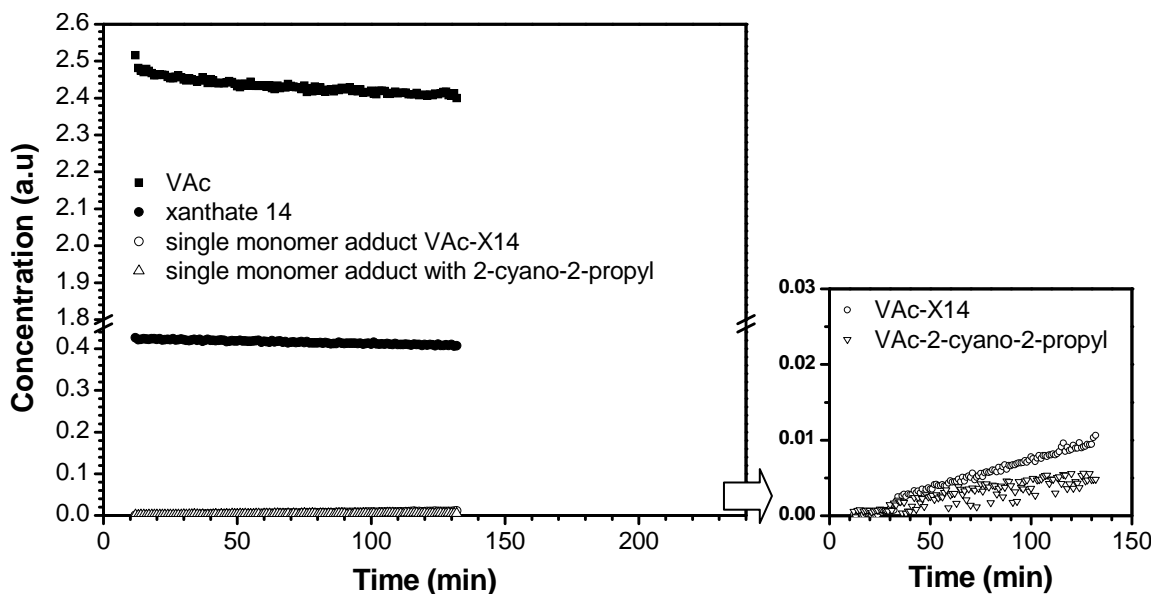

Figure 4.9: Concentration profiles in the *S*-(1-cyanoethyl) *O*-ethyl xanthate (X10)-mediated polymerization of NVP in C_6D_6 at 70ºC.

The experiment was repeated with VAc (Figure 4.10). As expected, initialization was selective and slower than NVP with the same CTA. The rate of X10 conversion with VAc was faster than X6 indicating that 1-cyanoethyl is a better reinitiating group for VAc than 2-cyano-2-propyl. Adversely the reaction was significantly slower than with X13. Experiments with a higher ratio of monomer to CTA would be required to estimate the length of the initialization period under the concentrations commonly used for polymerization. Should initialization be long with respect to polymerization time, then X13, which gives fast and selective initialization, would be a better choice to optimize control over the polymerization of VAc.

Another essential consideration for the choice of a CTA is the ease and cost of the CTA synthesis. The syntheses of both X10 and X13 are straightforward and quantitative. However 1-bromo-2-cyanoethane, the precursor for X10, is costly compared to 2-bromo-2-propionic acid ethyl ester, the precursor for X13. The synthesis of X6 is more challenging than X10 or X13 and the isolated yield is lower. These elements may be in favor of the use of X10 with NVP rather than X6, whereas X13 is preferred to X10 for VAc.

Figure 4.10: Concentration profiles in the *S*-(1-cyanoethyl) *O*-ethyl xanthate (X10)-mediated polymerization of VAc in C_6D_6 at 70ºC.

The initialization behavior of NVP with X14 is very similar to that with X6. When X14 was used with NVP, initialization was selective until more than 90% of the initial CTA was consumed, then higher adducts started forming (see Figure 4.11). Complete conversion of X14 was achieved within 230 min.

Figure 4.11: Concentration profiles in the *S*-(2-ethyl phenylacetate) *O*-ethyl xanthate (X14)-mediated polymerization of NVP in C_6D_6 at 70ºC.

The use of X14 with VAc led to selective but very slow initialization. The *in situ* ^{1}H NMR experiment was pursued in an oil bath at 70 ºC for an additional 16 h in the lab. It was thus possible to increase the concentration in the products. At the end of the experiment the monomer was evaporated under vacuum prior to analysis and the resulting oil dissolved in $CDCl_3$ instead of C_6D_6 for a better separation of peaks otherwise overlapping in C_6D_6. Relevant signals are indicated with a letter on the NMR spectrum in Figure 4.13 and the corresponding structures are reproduced above the spectrum. The reaction mixture was composed of four main xanthate species. They were identified as the initial xanthate X14 (68 mol %) and its single monomer adduct (19 mol %); the 2-cyano-2-propyl derived single monomer adduct (9 mol %) and the CTA *S*-(2-cyano-2-propyl) *O*-ethyl xanthate (5 mol %) resulting from the exchange of R groups via addition of AIBN-derived 2-cyano-2-propyl radicals onto X14 and subsequent fragmentation of R_{14}. Characteristic peaks are indicated in the following spectrum and the corresponding structures represented in Figure 4.13.

Figure 4.12 : Concentration profiles in the *S*-(2-ethyl phenylacetate) *O*-ethyl xanthate (X14)-mediated polymerization of VAc in C_6D_6 at 70 ºC. Right: enlargement of the concentration profiles of the two single monomer adduct species (VAc-X14 and VAc-2-cyano-2-propyl due to (re)initiation from the initiator-derived radicals) in the concentration range 0-0.03 a.u.
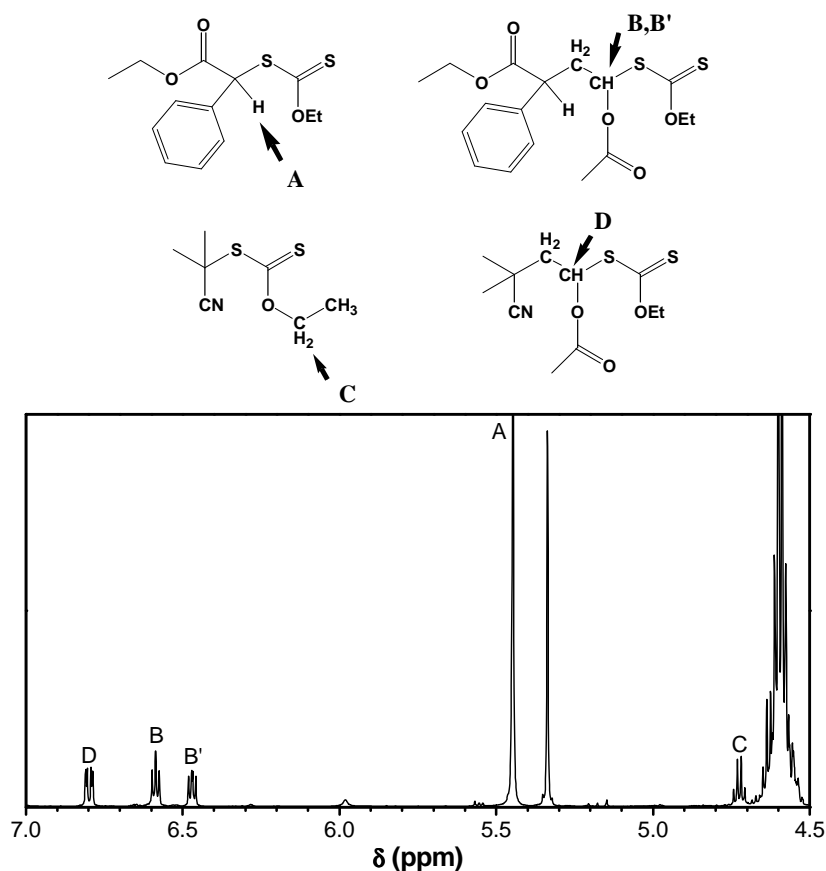
Figure 4.13 : ^{1}H NMR spectrum at time = 18.2 h in the experiment presented in Figure 4.12. A: X14; B,B': VAc-X14 single monomer adduct; C: *S*-(2-cyano-2-propyl) *O*-ethyl xanthate (X6); D: VAc-X6 single monomer adduct.

Elements of comparison between NVP and VAc R group classification

The experiments with X6, X9 and X14 showed that initialization was selective with both monomers and systematically slower with VAc. This is not surprising considering that VAc produces a less stable radical than NVP. As a result fragmentation of the R group from the CTA adduct resulting from the addition of VAc is favored compared to NVP. As a consequence a CTA which yields selective initialization with NVP will also yield selective initialization with VAc. As a corollary, if a CTA does not provide selective initialization with VAc, initialization will not be selective with NVP either. This case was illustrated with X5 where *tert*-butyl is not stable enough a radical for efficient fragmentation of CTA adducts with either monomer. Regarding the length of the initialization period, the differences in radical stabilities imply that reinitiation is faster with NVP than with VAc and therefore the initialization period will be shorter with NVP than with VAc.

The experiments with X13 and X10 give elements for a fine comparison of the relative radical stabilities relative to VAc and NVP. Initialization is selective for VAc with both CTAs but it is significantly slower with X10. For NVP initialization is almost selective with X10 whereas hybrid behavior is observed with X13. Classification of the radicals derived from the monomers and the R groups tested in this study can be proposed based on the selectivity and length of the initialization period. The radicals are reported in the order of decreasing stability in Scheme 4.2 and the relative position of the monomer-derived radicals are indicated with an arrow.

It is noteworthy to mention that this classification does not follow the order of electronegativity of the R group. The latter was estimated by measuring the chemical shifts of the methylene protons in the ethoxy group of the xanthates (reported in Table 4.1). The most stable radicals are produced by the most electron withdrawing R groups (R_9 and R_6) as indicated by high chemical shifts. However for less electron withdrawing R groups the order of radical stability does not match. This is most likely due to competing steric and mesomeric effects, which affect the unpaired electron of the radicals but not necessarily the stability of the thiocarbonylthio compounds. It is unfortunate that

such a straightforward technique for the classification of R groups is not applicable whereas it was used successfully to predict the reactivities of xanthates with variable alkoxy substituents in the polymerization of Vac.[18] The present results however support *ab initio* calculations which predicted complex interactions between electronic and steric effects of the 3 substituents regarding fragmentation of CTA adduct radicals.[8]
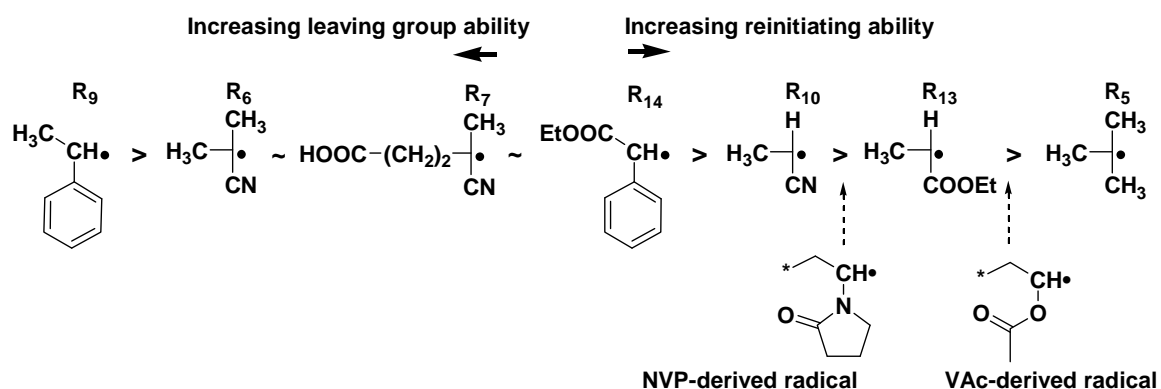
Scheme 4.2: Relative stabilities of R group-derived radicals based on *in situ* ^{1}H NMR spectroscopy initialization studies with respect to the monomers NVP and VAc. The corresponding *O*-ethyl xanthates give selective initialization if the structure of their R group is represented on the left handside from the monomer; the further away from the monomer the longer the initialization time.

Table 4.1 : ^{1}H NMR chemical shifts (in $CDCl_3$) of the xanthate ethoxy methylene protons as a function of the R group structure.

R group	chemical shift (ppm) of -CH_2-O-C(S)S
R_9 = 2-phenylethyl	4.878
R_7 = 4-(4-cyano)propanoic acid	4.790
R_6 = 2-cyano-2-propyl	4.748
R_{13} = 2-cyanoethyl	4.695
R_5 = *tert*-butyl	4.678
R_{13} = 2-ethylpropionate	4.628
R_{14} = 2-ethylphenylacetate	4.622

Selectivity of initialization at higher monomer:CTA ratios

Initialization studies presented so far were carried out with a high initial concentration in CTA, *i.e.* [Monomer]$_0$:[CTA]$_0$ = 5:1. The reason for this is that high concentrations are required to enable the identification and quantification of the species via ^{1}H NMR spectroscopy. It is necessary to increase the ratio [Monomer]$_0$:[CTA]$_0$ to produce polymers. A lower CTA concentration is expected to modify the rates of the

reactions involved in the RAFT equilibria, including initialization. The effect of decreasing the initial CTA concentration on the selectivity of initialization and its length were investigated and the results are presented in Figure 4.14. The experiments consisted of copolymerization of NVP with VAc mediated by X10 at different initial concentration ratios, *i.e.* $[VAc]_0$:$[NVP]_0$:$[X10]_0$ = 220:220:1 and 5:5:1. The use of a comonomer mixture of NVP and VAc did not influence the selectivity of initialization in this system at the ratio 5:5:1, most likely because X10 provided selective initialization with both monomers, as indicated by the homopolymerization experiments (Figures 4.9 and 4.10). Unexpectedly at such a low concentration, the decrease in CTA concentration could be quantified. This was achieved by integrating the signal of the methyl protons of the R group (δ [ppm] = 1.27, d, 3H). The signal corresponds to 3 protons at the initial concentration of $5 \cdot 10^{-4}$ M each, *i.e.* $1.5 \cdot 10^{-3}$ M. Although this value is close to the generally accepted detection limit of 10^{-3} M, the signal whose decay is presented in Figure 4.14 (left) was well-defined with a high signal to noise ratio. A closer look at the very beginning of the experiment indicates a decrease in VAc concentration which was attributed to its evaporation in the NMR tube in the first few minutes where temperature equilibrated. Side-reactions were identified which consumed some NVP at the beginning of the experiment. These are presented in the following chapter.

The concentration profiles (Figure 4.14, left) indicate that the concentration in either monomer appeared to be unchanged during the first 110 min after which they both started being consumed. X10 was consumed within 110 min. This is therefore a typical case where apparent inhibition corresponds to slow initialization. The scatter in the monomer signal is such that small concentration changes (<5 %) would not be quantified. The CTA derivatives were not quantified due to their concentration being too low. It is possible that a limited number of monomer addition steps occurred prior to addition to the CTA, which cannot be evaluated under these concentrations. However, from the apparent inhibition until X10 is fully consumed, it can be concluded that even at high ratio of monomer to CTA initialization was selective to a certain extent.

The comparison in the CTA concentration decay between the copolymerization systems at different initial concentration ratios (Figure 4.14, right) provides valuable information.
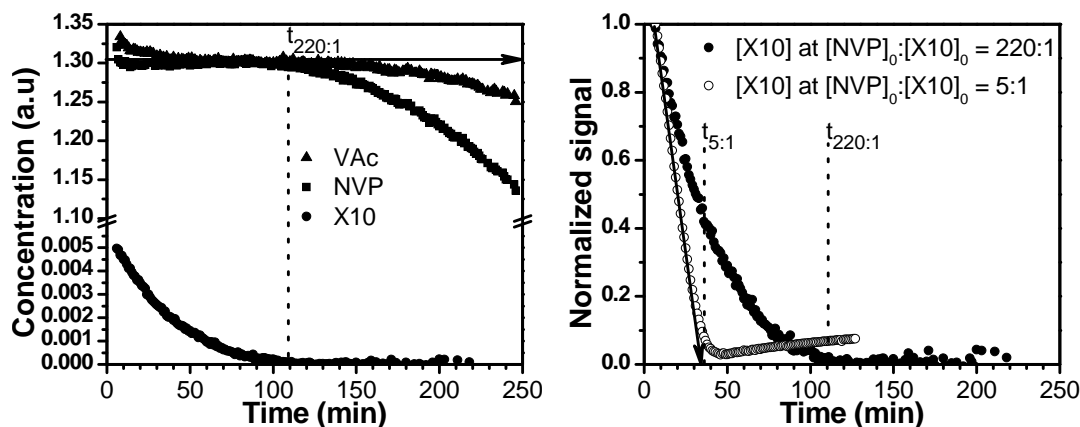
Figure 4.14: Concentration profiles in the *S*-(1-cyanoethyl) *O*-ethyl xanthate (X10)-mediated copolymerization of NVP and VAc in C_6D_6 at 70ºC; $[X10]_0:[AIBN]_0 = 8:1$. Left: VAc, NVP and X10 concentrations for the initial concentrations $[VAc]_0:[NVP]_0:[X10]_0 = 220:220:1$. Right: Normalized signal of the xanthate concentration vs. time with $[VAc]_0:[NVP]_0:[X10]_0 = 220:220:1$ (filled circles), $[VAc]_0:[NVP]_0:[X10]_0 = 5:5:1$ (open circles). Note that the apparent increase in [X10] beyond initialization is an artifact due to a new signal forming at the same chemical shift as that used to follow X10 concentration.

Firstly the initialization time is shorter in the experiment at lower $[Monomer]_0:[CTA]_0$ ratio. This is most probably due to the lower radical flux in the slowest system because of the choice to keep the ratio $[X10]_0:[AIBN]_0 = 8:1$ constant. $[AIBN]_0$ was thus 44 times lower in the slower system, whereas initialization was only 3 times slower. Therefore it can be predicted that at constant $[AIBN]_0$, the initialization period will be shorter with a lower $[CTA]_0$. This observation is consistent with initiation being the rate determining step because a higher ratio $[Monomer]_0:[CTA]_0$ increases the rate of reinitiation and reduces the rate of addition to the CTA. Secondly, from a qualitative point of view it can be mentioned that the decrease in [X10] follows an almost linear trend at high $[X10]_0$ whereas a curvature is observed at lower $[X10]_0$. This indicates a slight loss in selectivity of the reaction at the end of the initialization step as a factor of concentration, as previously observed in other monomer/CTA systems.[14] The selectivity of the reaction at the beginning indicates that propagating radicals show a higher rate of addition to xanthate species than propagation. However as the initial CTA is being consumed, the ratio of concentrations [monomer adduct]:[CTA] increases. As a result, the probability for radicals to add to monomer adducts rather than to the initial CTA increases. Thus the number of addition-fragmentation steps required before the last fractions of CTA are encountered increases. Hence the opportunities for the propagating radical to add to the monomer increase. It is not excluded that at low CTA concentration (*i.e.* high target M_n) the rate constant of addition to the CTA is not high enough to prevent

multiple monomer additions from occurring during initialization or during the main equilibrium.

In conclusion, this *in situ* NMR spectroscopy experiment where a relatively low concentration of CTA was used indicates that initialization can remain selective under common polymerization concentrations. The incorporation of more than one monomer equivalent before complete conversion of the initial CTA is more likely to occur when $[CTA]_0$ is low but when X10 was used in a ratio 1:220 with NVP and VAc no significant monomer conversion was observed until X10 was consumed. These results support the validity of *in situ* NMR spectroscopy initialization experiments at low CTA concentration for the study of polymerization systems. Recently chromatographic techniques were successfully applied to investigate initialization at low CTA concentration in cumyl dithiobenzoate-mediated polymerization of styrene and methyl methacrylate.[19] The authors successively identified the formation of the CTA adducts resulting from incorporation of 1 then 2, and then 3 styrene units, after which the main RAFT equilibrium established, whereas methyl methacrylate polymerized to a significant extent before complete conversion of the CTA.

Initialization behavior and molecular weight distribution data

Bulk polymerizations of NVP and VAc with low concentrations of CTA were performed in order to correlate the characteristics of initialization with the molar mass distribution of the polymers determined via SEC (Table 4.2). It was confirmed that selective initialization leads to more narrowly distributed molar masses, whereas the absence of initialization results in higher polydispersities, while still producing polymer chains endcapped with the xanthate mediating moiety.

Table 4.2. Relationship between initialization and molecular weight distribution.

Monomer	CTA	Conversion (%)	$M_{n,target,\alpha}$ (g·mol^{-1})	$M_{n,SEC}$[a] (g·mol^{-1})	PDI[a]	Selective Initialization (time, min)[b]
VAc	X9	<1	-	-	-	
	X6	<1	-	-	-	Yes (>900)
	X13	28	9900	9700	1.26	Yes (25)
	X5	54	19800	21500	1.43	No
NVP	X9	7	3400	3800	1.67	Yes (>900)
	X6	26	12400	14400	1.32	Yes (225)
	X10	45[c]	22300	23800	1.30	Yes (25)
	X13	76	39200	31500	1.40	No
	X5	48	24100	31900	1.74	No

[a]Experimental molar masses obtained by Size Exclusion Chromatography (using RI detection) in THF with PS calibration for poly(vinyl acetate) (PVAc) and in HFIP with PMMA calibration for poly(*N*-vinylpyrrolidone) (PVP) prepared via xanthate-mediated polymerizations in bulk at 60 ºC for 3.5 h (PVAc) or 6 h (PVP); [Monomer]$_0$/[Xanthate]$_0$ = 450; [Xanthate]$_0$/[AIBN]$_0$ = 10. [b]Initialization refers to selective formation of the single monomer adduct investigated by *in situ* ^{1}H-NMR spectroscopy polymerizations in C$_6$D$_6$ at 70 ºC; [Monomer]$_0$/[Xanthate]$_0$ = 5. [c]polymerization was stopped at 4 h instead of 6 h because the high viscosity of the sample was impairing magnetic stirring.

Samples were withdrawn from the polymerization of NVP mediated by X6 (DP$_{target}$ = 450) to investigate the living character of the polymerization. SEC chromatograms were obtained from the raw polymerization samples. They indicate an almost linear increase of M_n with monomer conversion, which is strong evidence for the livingness of the system (Figure 4.15).
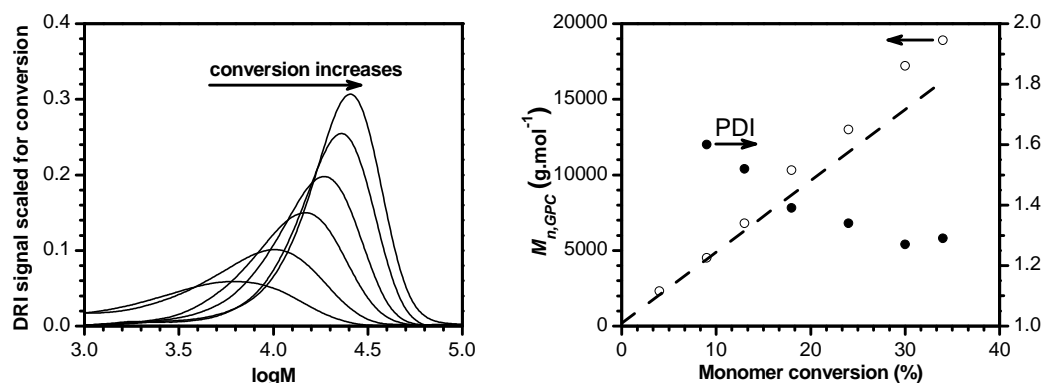
Figure 4.15: Evolution of the molecular weight distribution (SEC traces) in the *S*-(2-cyano-2-propyl) *O*-ethyl xanthate (X6)-mediated bulk polymerization of NVP at 60 ºC. [Monomer]$_0$/[Xanthate]$_0$ = 450; [Xanthate]$_0$/[AIBN]$_0$ = 10. Right: corresponding M_n (open circles) and PDI (black circles) values calculated from PMMA calibration and theoretical M_n calculated from the stoichiometry (dashed line).

The PDI values decreased with conversion to the minimum value of 1.27 at 30 % conversion. For the samples taken at low conversion (<10 %) the monomer peak overlapped with the polymer signal, resulting in poor baseline resolution. Therefore the PDI value was not reported and the M_n value is only an estimation obtained by arbitrarily

truncating the polymer peak at its minimum with the monomer peak. Although this M_n value is not accurate it is important to remark that no high molecular weight species were present at low conversions.

An inhibition period was observed as indicated by the apparent absence of monomer conversion in the first 50 min of the reaction (Figure 4.16). It is likely that initialization took place with a slower rate than the rate of polymerization, as expected from the *in situ* NMR spectroscopy initialization studies. During this process only 1/450 equivalents of monomer is consumed corresponding to less than 1 % of monomer conversion, which is below the detection limit. The initialization time appears to be significantly shorter in this experiment than when the *in situ* experiment was carried out at 70 ºC in 50 wt % in C_6D_6 with a ratio $[NVP]_0/[X6]_0 = 5$. Factors contributing to shortening the initialization time are the higher concentration in monomer due to the higher $[NVP]_0/[X6]_0$ ratio and to the absence of solvent. This concentration effect apparently overruled the effects of a lower temperature and the use of a lower initial concentration in initiator, which decrease the radical concentration in the system as well as the rate constants for radical reactions.
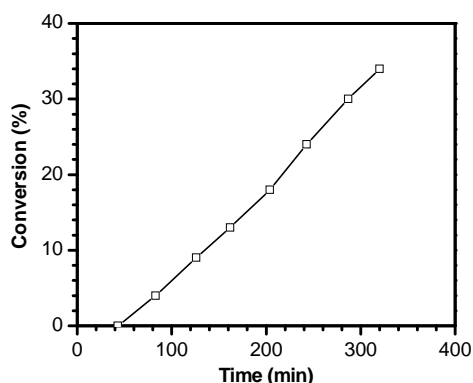
Figure 4.16: Evolution of conversion with time in the *S*-(2-cyano-2-propyl) *O*-ethyl xanthate (X6)-mediated bulk polymerization of NVP at 60 ºC. $[Monomer]_0/[Xanthate]_0 = 450$; $[Xanthate]_0/[AIBN]_0 = 10$.

Other factors may have contributed to this apparent inhibition period, such as radical quenching by contaminants such as oxygen. In this case overestimation of the initialization time would result. Adversely if multiple monomer additions occurred before the end of initialization, monomer conversion would take off before the CTA is fully consumed resulting in underestimation of the initialization time. Consequently it is risky to compare initialization times between the *in situ* NMR spectroscopy experiments,

where the actual concentrations in CTA and its derivatives were measured, with the inhibition period observed by plotting the conversion versus time in polymerization experiments where high M_n is targeted and only the monomer conversion is accessible.

As reported in Table 4.2, polymerization of NVP mediated by X5 yielded a polymer with high PDI and M_n value higher than expected from the initial ratio of monomer to CTA. The polymerization was repeated with $[Monomer]_0/[CTA]_0 = 135$ and samples were withdrawn at different time intervals. The plot of the conversion versus time indicates that there was no inhibition period. The evolution of M_n with conversion corresponds to a poorly controlled system where high molecular weight polymer is produced from the beginning of the polymerization. The slight increase in M_n with conversion, while PDIs decrease, are an indication that all or a portion of chains are living. However PDIs are high (1.70 - 1.79) confirming the prediction obtained via *in situ* NMR spectroscopy that X5 would not be suitable for controlling the polymerization of NVP.
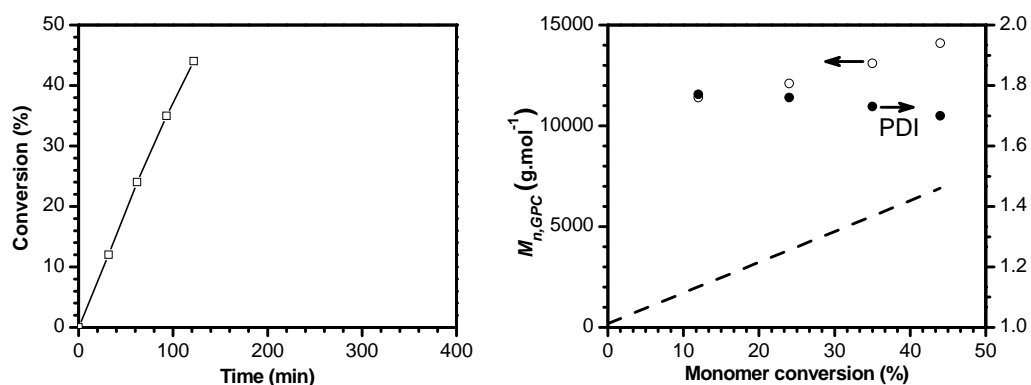
Figure 4.17: Evolution of conversion with time in the *S-(tert*-butyl) *O*-ethyl xanthate (X5)-mediated bulk polymerization of NVP at 60 ºC; $[Monomer]_0/[Xanthate]_0 = 135$; $[Xanthate]_0/[AIBN]_0 = 10$ (left). Evolution of M_n and PDI determined by SEC in HFIP with PMMA calibration (right) and theoretical M_n calculated from the stoichiometry (dashed line).

Conclusions

In conclusion, *in situ* ^{1}H-NMR spectroscopy can quantitatively probe the process of initialization involved in the transformation of a CTA into a dormant oligomeric chain. Conversely, kinetic studies combined with molar mass distribution characterization are not sufficient to pinpoint the origin of either inhibition or high polydispersities in

RAFT/MADIX mediated polymerization. The results presented here show that NMR spectroscopy allows a defined distinction to be made between a "hybrid" RAFT mediated polymerization and an ideal RAFT mediated polymerization for the first time. Moreover, it allows the investigation of the origin of the hybrid behavior. In this specific investigation the leaving and reinitiating abilities of the CTA R group were correlated to the occurrence of selective initialization, which in turn was correlated to well-defined molar mass distribution. This technique can thus be used to directly probe the efficiency of a CTA in controlling the polymerization of a given monomer.

Slow reinitiation was deduced as the origin of slow and selective initialization in systems where the CTA R group was more stable than the monomer-derived radicals. Classification of the relative stabilities of R group radicals and monomer-derived radicals (NVP• and VAc•) was proposed based on the length and selectivity of the initialization step. The radical stabilities decreased in the order: $C_6H_5CH(CH_3)$• > $R'CH_2C(CN)(CH_3)$• ~ $C_6H_5CH(CO_2Et)$• > $CH_3CH(CN)$• > NVP• > $CH_3CH(CO_2Et)$• > VAc• > $C(CH_3)_3$•.

Reference List

(1)   Chiefari, J.; Mayadunne, R.T.A.; Moad, C.L.; Moad, G.; Rizzardo, E.; Postma, A.; Skidmore, M.A.; Thang, S.H. *Macromolecules* **2003**, *36*, 2273-2282.

(2)   Chong, Y.K.B.; Krstina, J.; Le, T.P.T.; Moad, G.; Postma, A.; Rizzardo, E.; Thang, S.H. *Macromolecules* **2003**, *36*, 2256-2272.

(3)   Favier, A.; Charreyre, M.-T. *Macromol. Rapid Commun.* **2006**, *27*, 653-692.

(4)   Coote, M.L.; Wood, G.P.F.; Radom, L. *J. Phys. Chem. A* **2002**, *106*, 12124-12138.

(5)   Barner-Kowollik, C.; Coote, M.L.; Davis, T.P.; Radom, L.; Vana, P. *J. Polym. Sci. Part A: Polym. Chem.* **2003**, *41*, 2828-2832.

(6)   Coote, M.L.; Radom, L. *J. Am. Chem. Soc.* **2003**, *125*, 1490-1491.

(7)   Coote, M.L.; Radom, L. *Macromolecules* **2004**, *37*, 590-596.

(8)   Coote, M.L.; Henry, D.J. *Macromolecules* **2005**, *38*, 1415-1433.

(9)   Feldermann, A.; Coote, M.L.; Stenzel, M.H.; Barner-Kowollik, C. *J. Am. Chem. Soc.* **2004**, *126*, 15915.

(10)   Coote, M.L.; Izgorodina, E.I.; Krenske, E.H.; Busch, M.; Barner-Kowollik, C. *Macromol. Rapid Commun.* **2006**, *27*, 1015-1022.

(11)   Coote, M.L.; Krenske, E.H.; Izgorodina, E.I. *Macromol. Rapid Commun.* **2006**, *27*, 473-497.

(12)   Coote, M.L.; Izgorodina, E.I.; Cavigliasso, G.E.; Roth, M.; Busch, M.; Barner-Kowollik, C. *Macromolecules* **2006**.

(13)   McLeary, J.B.; Calitz, F.M.; McKenzie, J.M.; Tonge, M.P.; Sanderson, R.D.; Klumperman, B. *Macromolecules* **2004**, *37*, 2383-2394.

(14)   McLeary, J.B.; McKenzie, J.M.; Tonge, M.P.; Sanderson, R.D.; Klumperman, B. *Chem. Commun.* **2004**, 1950-1951.

(15)   Nguyen, T.L.U.; Eagles, K.; Davis, T.P.; Barner-Kowollik, C.; Stenzel, M.H. *J. Polym. Sci. Part A: Polym. Chem.* **2006**, *44*, 4372–4383.

(16)   Wan, D.; Satoh, K.; Kamigaito, M.; Okamoto, Y. *Macromolecules* **2005**, *38*, 10397-10405.

(17)   Barner-Kowollik, C.; Quinn, J.F.; Nguyen, T.L.U.; Heuts, J.P.A.; Davis, T.P. *Macromolecules* **2001**, *34*, 7849-7857.

(18)   Stenzel, M.H.; Cummins, L.; Roberts, G.E.; Davis, T.P.; Vana, P.; Barner-Kowollik, C. *Macromol. Chem. Phys.* **2003**, *204*, 1160–1168.

(19)   Han, X.; Fan, J.; He, J.; Xu, J.; Fan, D.; Yang, Y. *Macromolecules* **2007**, *40*, 5618-5624.

Chapter 5: Side-reactions

As presented in Chapter 4, *in situ* NMR spectroscopy can be used to follow the concentration of relevant species during RAFT-mediated polymerizations. Strikingly a large number of species are formed during xanthate-mediated polymerization of NVP, which do correspond to the compounds expected from the RAFT mechanism. In contrast, experiments with VAc proceed as expected with little to no side-products. In this chapter the structures of side-products forming during *in situ* NMR initialization experiments with NVP and various xanthates are presented. The mechanisms for the formation of species which could interfere with control over the molecular weight distribution and chain-end functionality of the polymers are discussed.

Monomer consumption via non-radical reactions

Dimer formation

The unsaturated dimer of NVP (Scheme 5.1) was observed in many polymerization systems. The nature of the xanthate R group was a determining factor for the dimer formation in homopolymerization experiments. Xanthates 3, 7 and 12, which R groups contain carboxylic acid or hydroxyl functionalities, catalyzed the dimer formation whether AIBN was present or not. For example the unsaturated dimer was obtained quantitatively by heating NVP with an equimolar amount of X3 at 70 ºC for 3 h in C_6D_6. NVP was fully consumed, whereas the concentration in X3 was unchanged. The dimer was identified via NMR spectroscopy (^{1}H NMR spectrum in Figure 5.1 (A)) as well as high resolution mass spectroscopy, which also revealed the presence of the trimer ($M_{exp} = 333.04$ a.m.u, $M_{theo} = 333.05$ a.m.u). Significant dimer formation was observed in xanthate-mediated copolymerization experiments with the comonomer maleic anhydride (MAh), regardless of the xanthate R group. Concentration profiles are reported in Figure 5.1 (B-D).

Acid-catalyzed dimerization of NVP was reported in the literature since 1956.[1-4]
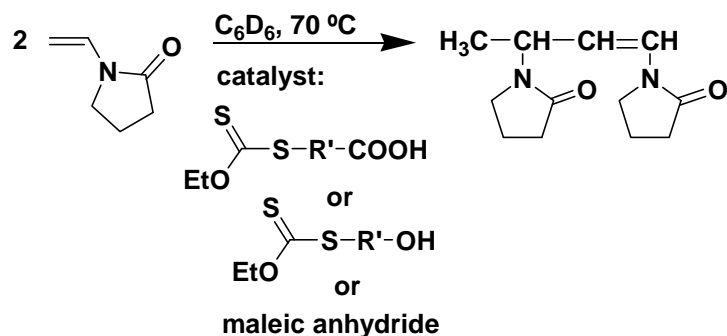
Scheme 5.1: reaction scheme for the formation of NVP unsaturated dimer.
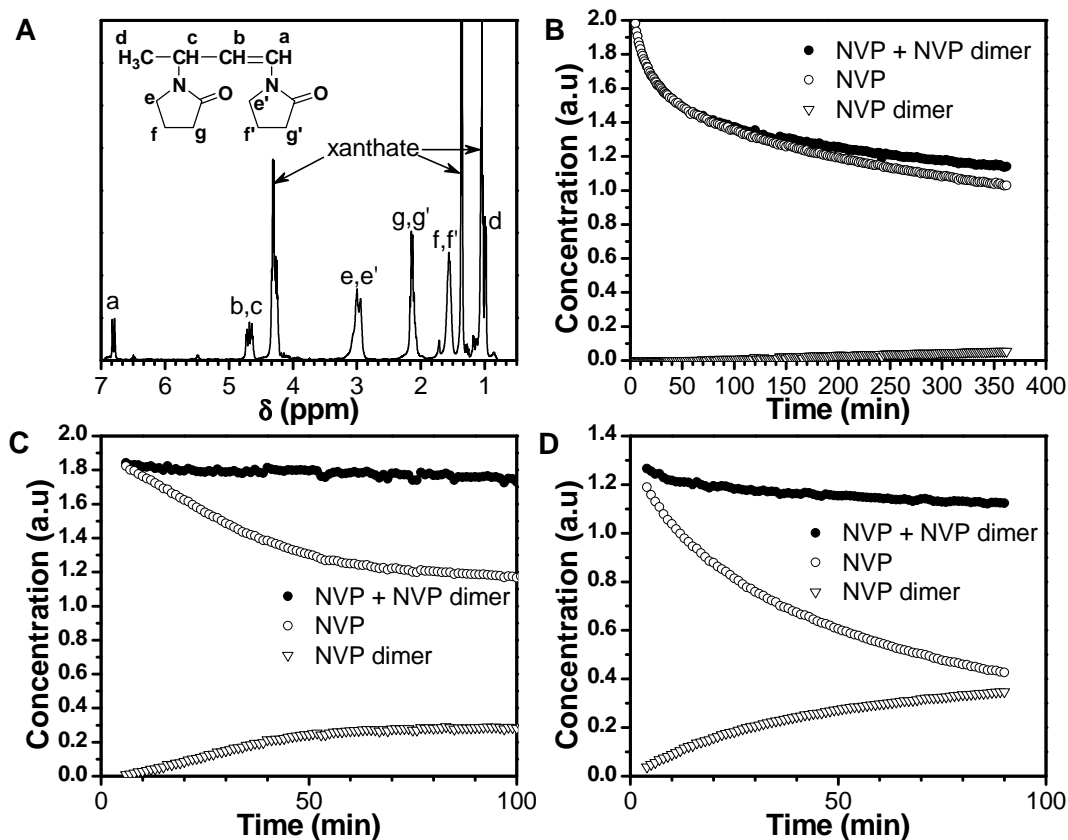
Figure 5.1: NVP unsaturated dimer. ^{1}H NMR spectrum of the reaction mixture after NVP was heated for 3 h at 70 ºC with 1 equivalent of *S*-(2-propionic acid) *O*-ethyl xanthate (X3) in C_6D_6 (A); concentration profiles of NVP and its unsaturated dimer in xanthate-mediated homo and copolymerizations (*in situ* NMR initialization experiments) at 70 ºC in C_6D_6, [NVP]:[CTA]:[AIBN] = 5:1:0.1, homopolymerizations in the presence of X3 (B) and X12 (C); copolymerization with 1 equivalent of maleic anhydride and X10 (D).

The dimer was also reported as a side-product in the electrochemical polymerization of NVP in an aprotic anhydrous medium.[5] The dimer forms via a cationic mechanism initiated by addition of a proton to the monomer double-bond. In the electrochemical system the proton was released upon oxidation of NVP. To the author's knowledge alcohol-catalyzed dimerization has not been reported so far. This reaction

may provide an alternative explanation to the observed retardation of NVP conventional free-radical polymerization in alcohols.[6,7]

As illustrated in particular in figures C and D, consumption of NVP for the formation of its unsaturated dimer is misleading when NVP consumption is studied for kinetic purposes. If exclusively the decrease in NVP concentration is taken into account in the experiment corresponding to figure D, it would appear that NVP conversion was approximately 70 %. However 80 % of the consumed NVP was actually not involved in radical (cross)-propagation.

The kinetics of the dimer formation varied among the different experiments reported here. In the presence of maleic anhydride the dimer concentration followed a logarithmic law, whereas in the presence of the hydroxyl functional xanthate (X12) the trend was close to linear at the beginning and seemed to reach a plateau after 60 min of reaction. It is surprising that the concentration in dimer remained low in the *in situ* initialization experiments where acid functional xanthates were used (X3 and X7), whereas in the absence of initiator and a ratio of monomer to xanthate of 1:1 NVP was fully consumed to form the dimer. This may be due to the consumption of the acidic proton of the xanthate R group for another side-reaction which is described in Scheme 5.2.
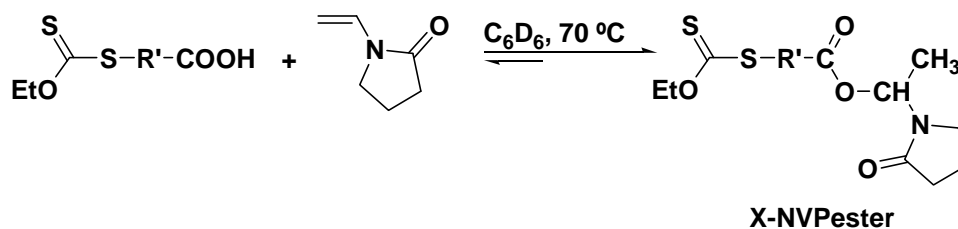
Scheme 5.2: Synthetic scheme for the esterification of the CTA R group carboxylic acid of the generic xanthate X with NVP to form X-NVP xanthate.

All ^{1}H and ^{13}C NMR spectroscopy signals corresponding to the product of esterification of the CTA *S*-(2-propionic acid) *O*-ethyl xanthate (X3-NVP ester, consisting of 2 enantiomers) were unambiguously identified. They are reported in Appendix A. The reaction was very fast. Hence the compound was absent from the reaction mixture at 25 ºC but had reached its maximum concentration (close to 20 % of the total xanthate concentration) before the first spectrum was taken at 70 ºC, *i.e.* less

than 5 min. The implications of this reaction are minor. It is likely that the reactivity of the CTA in terms of radical addition and fragmentation is not significantly influenced whether the carboxylic acid is in its protonated form or esterified. Hence the rates of monomer and CTA conversion, as determined via *in situ* NMR initialization experiments, were similar whether X3 was used or X13, where X13 is the ethyl ester of X3. Considering that acid functional CTAs undergo fast esterification with NVP and may also catalyze the dimerization of NVP, it appears preferable to use the corresponding ester rather than the original CTA in its protonated form. Moreover for initialization experiments, the use of a CTA which can undergo esterification with NVP should be avoided in order to limit the complexity of the NMR spectra. Indeed, with X3 for instance, 3 CTA species are present at the beginning of the experiment, *i.e.* X3 and its NVP ester, which presents two enantiomeric isomers. Upon conversion of the CTAs to their single monomer adduct, each species forms two new enantiomeric forms, *i.e.* 6 species. Also, monomer conversion helps determining the number of monomer additions prior to xanthate conversion. Consumption of more than one monomer equivalent during the initialization period would generally indicate a poorly selective initialization step (or hybrid system), whereas only one NVP equivalent should be consumed in systems where initialization is selective. However, more than one NVP equivalent was consumed in systems where NVP participated in esterification reactions, even though initialization was selective. Such observations were misleading in the case where X7 was used because the ester X7-NVP ester formed. Nonetheless the xanthate derivatives comprised only one monomer unit, indicating that initialization was selective.

It is not clear whether the product would form in the absence of water (present in the form of traces in the deuterated solvent) or not. In the presence of water, hydration of the double bond may occur, which is presented in the following paragraph. The resulting hydroxylated compound may be the intermediate in the esterification reaction with the carboxylic acid R group.

Hydration of the double bond

Hydration of the vinyl bond of NVP was observed upon distillation of NVP, which was carried out under reduced pressure and argon atmosphere. Prior to distillation,

NVP (0.6 L) was dried over magnesium sulfate. The salts were filtered off and NVP placed in a 1 L 3-neck round bottom flask. The distillation set up was attached to a Schlenk line, degassed by bubbling argon through the solution for 20 min. The main product distilled at 81 °C at less than 1 mbar, which is a higher temperature than values generally reported in the literature.[3] The ^{1}H NMR spectrum of a sample taken from the middle fraction just after distillation revealed the presence of side-products in high amounts (Figure 5.2). The same fraction was stored at 4 °C for 24 h, which caused it to crystallize. The NMR analysis was repeated. At this point only NVP was detected. Such results indicate that the hydration of NVP is reversible and takes place at elevated temperature. The dehydration reaction produces water. Therefore it can be concluded that even comparatively high amounts of water do not prevent NVP from crystallizing at 4 °C.
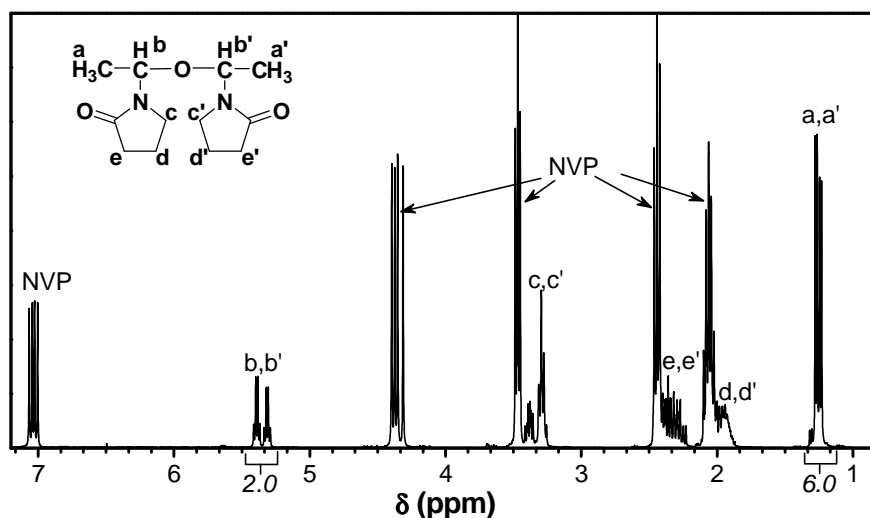
Figure 5.2: ^{1}H NMR spectrum of a mixture of NVP and its hydration products collected upon distillation.

Identification of the structure presented in Figure 5.2 (NVP-O-NVP) was not straightforward. It is not possible to obtain a correlation between the protons and carbons of the substituents on each side of the oxygen atom due to the molecule being symmetrical (the HMBC spectrum indicates a correlation between H_b and C_b, which may not be differentiated from a correlation between $H_{b'}$ and C_b because H_b and $H_{b'}$ are homotopic). The structure could not be strictly confirmed, however it is the most probable structure considering (i) the reversibility of the reaction (ii) the absence of any other compound (in particular no acetaldehyde and no other derivatives containing an *N-*

pyrrolidonyl moiety) and (iii) the presence of 2 chiral centers as indicated by two sets of signals for the methine protons b and b' and the methyl protons a and a'.

The nature of the substituents determines the reactivity of alkene double-bonds towards hydration in particular via electronic effects.[8] Therefore it is not surprising to find major differences between alkenes towards hydration, as is the case here between NVP and VAc. Denisov et al. predicted that copolymerization of NVP with acid-functional monomers such as acrylic acid and crotonic acid would result in degradation of NVP. They confirmed the formation of the product of addition of water to the double-bond (NVP-OH).[9] They also found that, in the absence of water, methanol can add to the double-bond to form NVP-OMe. Formation of the structure reported in Figure 5.2 can therefore be explained as the product of water addition to NVP which undergoes a second addition to another NVP molecule. It cannot be excluded that a concerted mechanism favors the formation of such a compound in one step.

The putative NVP-O-NVP was present in all initialization experiments in C_6D_6 at 70 °C, regardless of the xanthate used. The concentration profiles for this species are presented in Figure 5.3 as a function of the xanthate structure. In the experiment where *S*-(2-cyano-2-propyl) *O*-ethyl xanthate (X6) was used, the concentration of NVP-O-NVP reached a plateau within 150 min, whereas with other xanthates it continued forming all along the experiment. The plateau was reached within 20 min only when the experiment was carried out at 60 °C instead of 70 °C.

The maximum concentration of NVP-O-NVP did not exceed 2 % of the initial monomer. Therefore its influence on decreasing the apparent monomer concentration is hardly detectable. It is very likely that this compound does not have any influence on the RAFT mechanism.
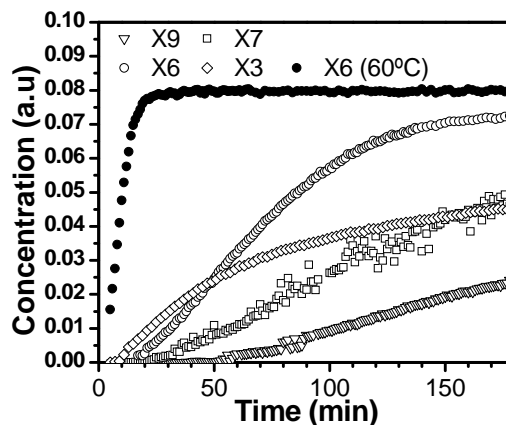
Figure 5.3: concentration profiles of the product of hydration of NVP (NVP-O-NVP) in C_6D_6 as a function of the xanthate structure. All experiments were carried out at 70 ºC unless otherwise indicated.

Hydrolysis

Senogles et al. studied the kinetics and mechanism of NVP hydrolysis in acidic aqueous medium.[3] Further decomposition of NVP-OH was observed in dilute solution producing pyrrolidone and acetaldehyde. Pyrrolidone then reversibly adds to NVP to form 1,1-bis(*N*-pyrrolidonyl)-ethane. The relative concentration of each compound was a function of the reaction temperature and concentration. These findings prompted us to investigate the fate of NVP hydration products under the conditions used for polymerizations and initialization studies. Traces of acetaldehyde and 1,1-bis(*N*-pyrrolidonyl)-ethane were generally present in the in situ NMR spectroscopy reaction mixtures in C_6D_6. However their concentration was low compared to other side-products (*e.g.* dimer or hydration products). It seems that under our experimental conditions, the presence of water induced the formation of the dimeric hydration compound (NVP-O-NVP) predominantly compared to hydrolysis.

Endgroup degradation

Xanthate elimination

The exceptional thermal lability of the *O*-ethyl xanthate moiety adjacent to a *N*-vinylpyrrolidone (NVP) adduct was first reported by Tournier and Zard.[10,11] They obtained the unsaturated product of monomolecular elimination of the xanthate in

quantitative yield by refluxing a single NVP-xanthate adduct in chlorobenzene (131 ºC). Xanthate thermolysis, also referred to as the Chugaev elimination, is mostly documented for *S*-methyl xanthates (R-SC(S)-OR' where R=methyl) as the synthetic pathway is broadly applied to produce olefins from the corresponding alcohol. In this case the olefin obtained is the R' unsaturated derivative and methyl mercaptan and C(O)S are released. However elimination can occur from the *S*-substituent as opposed to the *O*-substituent by changing the nature of R and R' or tuning the experimental conditions. A critical parameter is the proton-donating character of the solvent.[12]

Unsaturated species resulting from xanthate elimination (XEP for "xanthate-elimination product") were identified during *in situ* NMR initialization experiments. In the experiment carried out with xanthate 14 (Scheme 2.3) the unsaturated NVP-derivative was identified, which is likely to originate from xanthate elimination from the single monomer adduct ($X_{14}EP$). Its concentration increased exponentially during the reaction. In some experiments, after 7.5 h the ratio of elimination product to xanthate adducts was 1 : 5.
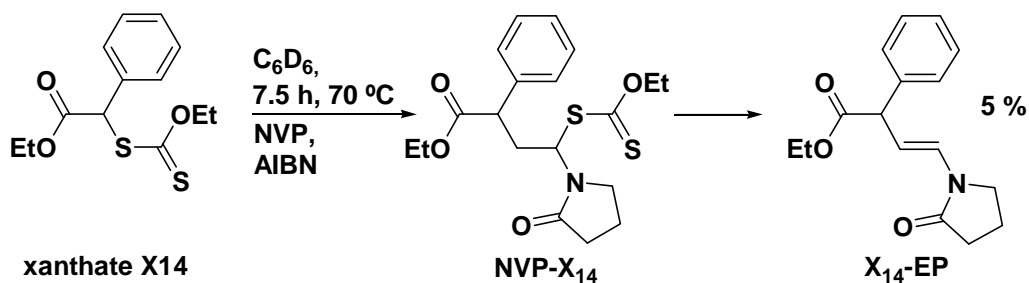
Scheme 5.3: Single monomer adduct of NVP with X_{14} and its unsaturated elimination product.

The same type of unsaturated product (X_6-EP) was identified in the cyanoisopropyl xanthate (X_6)-mediated in situ NMR polymerization of NVP at 60, 70 and 75 ºC. At the end of the initialization time in the experiment at 70 ºC, the ratio of X_6-EP to single adduct NVP-X_6 was 1:20. The rate of formation of X_6-EP decreased abruptly beyond initialization, as the single adduct started being converted to higher adducts. It is likely that xanthate elimination continued with higher adducts (dimer, trimer, etc.). It should be noted that the formation and identification of XEPs comprising one NVP unit is more likely to occur when initialization is slow because the lifetime of the single monomer adduct is longer. X_{14} and X_6 show comparable initialization times towards

NVP, but X_{14}-EP was detected at a significantly higher concentration than X_6-EP. This indicates that the penultimate unit, *i.e.* the CTA leaving group attached to the NVP unit, plays a significant role in this irreversible xanthate-elimination step. The NMR experiments (COSY, hmqc, hsqc, NOESY, DEPT), which are required to unambiguously identify the structures were not performed with all xanthates. Nonetheless the proton spectra display well-defined signals which may correspond to such elimination products forming with xanthate 3 ($R_3 = $ *2*-propionic acid, $\delta = 4.88$ ppm, dd) and xanthate 13 ($R_{13} = $ *2*-propionic acid ethyl ester, $\delta = 4.79$ ppm, dd).

The formation of unsaturated species via xanthate elimination during the polymerization reaction depends mostly on the nature of the solvent, the temperature and initialization time. Polymerizations were generally carried out in bulk at 60 ºC for 6 h and thus we can consider this phenomenon to be minor although a possible cause for the presence of dead chains.

Xanthate hydrolysis

Hydrolysis of xanthate species during polymerization was examined by performing initialization experiments with *S*-(2-cyano-2-propyl) *O*-ethyl xanthate (X6) in a solution containing D_2O. The use of D_2O on its own as the solvent resulted in a biphasic emulsion-like system. Therefore DMSO-*d_6* was added to the reaction mixture to provide a clear solution. The rate of consumption of X6 was significantly higher in DMSO-*d_6* / D_2O compared to C_6D_6 (Figure 5.4). This is not surprising considering that the rate of NVP consumption via free-radical polymerization is higher in aqueous solution than in organic solvents[13,14] and is even higher at approximately 75 % (v/v) in buffered aqueous solution than in bulk.[15] The total xanthate concentration was constant in C_6D_6 whereas it decreased to approximately 80 % of its initial value within 125 min in the mixture DMSO-*d_6* / D_2O. This indicates that the xanthate underwent degradative side-reactions in DMSO-*d_6* / D_2O.
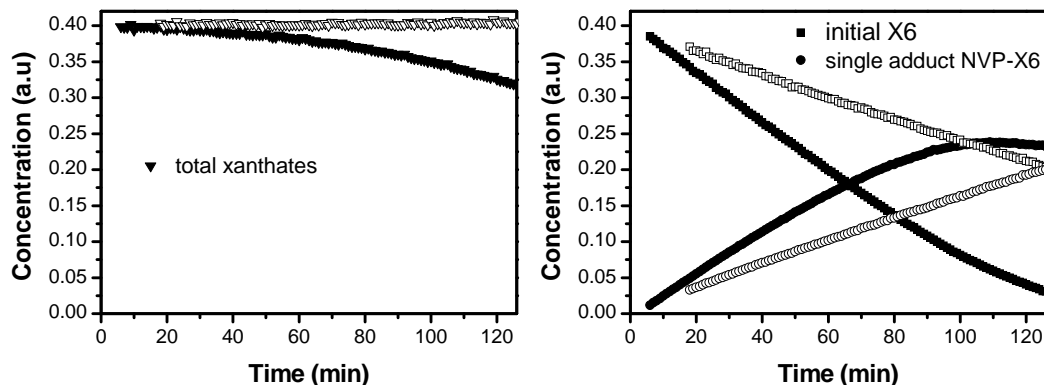
Figure 5.4: Effect of the solvent on the consumption of xanthate species. Initialization experiment with NVP in the presence of *S*-(2-cyano-2-propyl) *O*-ethyl xanthate (X6) in a mixture DMSO-d_6 / D_2O 50 wt% (closed symbols) and in C_6D_6 (open symbols).

Case-study with *S*-(2-ethyl phenylacetate) *O*-ethyl xanthate (X14)

Monomer consumption was generally determined by integrating the vinyl proton signal at 7.0-7.1 ppm. In this experiment the aryl protons overlapped with vinyl signals. The vinyl methylene signals at 4.15 and 4.19 ppm were used instead for monomer conversion. The reaction was carried out for 4 h inside the magnet of the NMR spectrometer at a temperature of 70 ºC and continued in the lab for another 3.5 h. The aim was to increase the concentration in reaction products. As indicated in the spectrum corresponding to a total reaction time of 7.5 h (Figure 5.5), a large number of species were identified. For comparison, a spectrum corresponding to the same experiment with VAc was presented in Figure 4.13. The number of signals in the region 4.5 – 7.0 ppm is significantly higher in the case of NVP, suggesting that the number of new species is higher with NVP. Initialization was slower with VAc than NVP and therefore in the case of VAc the reaction was carried out for 18.2 h in total to enable detection of relevant species. In spite of the longer reaction time, very few side products were present with VAc compared to NVP.
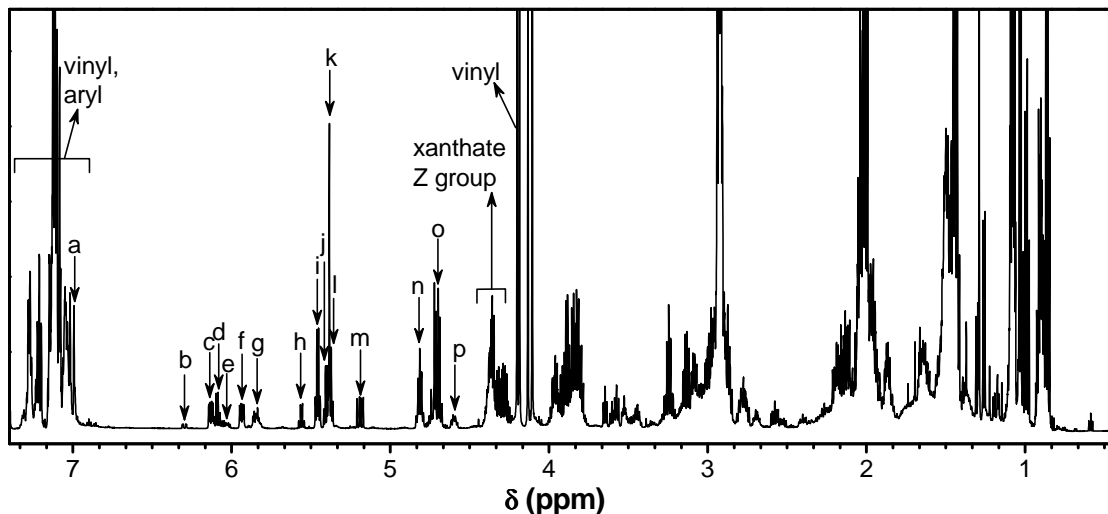
Figure 5.5: ^{1}H NMR spectrum used for the identification of species formed during the initialization experiment with NVP and X14. The reaction was carried out for 7.5 h at 70 ºC in C_6D_6. The arrows and letters indicate the signals for compounds referred to in the text.

The synthesis of the CTA X14 involves nucleophilic addition of potassium *O*-ethylxanthate to α-chlorophenyl acetic acid, ethyl ester (CPAE). It was difficult to remove the unreacted CPAE, whether by achieving quantitative conversion into the desired xanthate or via repeated column chromatography. CPAE was identified with signal k. Integration of k was constant in the experiment with VAc, whereas it appeared to increase with NVP. The increase was due to overlap with the signals of newly formed species (signals j and l). The effect of CPAE in the reaction with NVP was evaluated by comparing two experiments carried out with a mixture of X14 and CPAE at different molar ratios, namely 7:3 and 9:1. The concentration profiles of X14 and its single monomer adduct with NVP are presented in Figure 5.6. Although the reaction appears to be slightly faster when only 10 % of unreacted CPAE is present instead of 30 %, the difference in rate is within experimental error (< 5 %).

The presence of CPAE contaminant does not seem to affect the rate of initialization with NVP to any measurable extent. Its concentration remained constant in the experiment with VAc. In conclusion, it seems that CPAE does not undergo any transformation under the experimental conditions. However these conclusions do not exclude the participation of CPAE as a catalyst in reactions which do not affect the rate of radical processes.
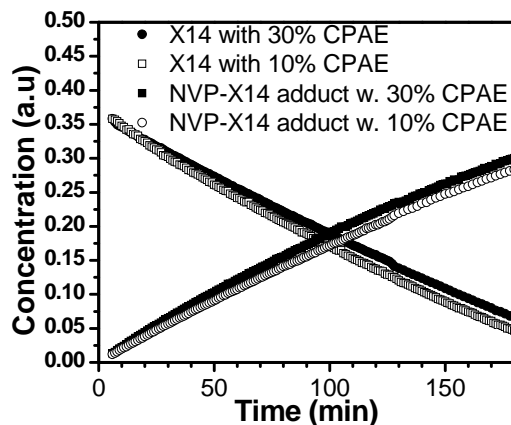
Figure 5.6: Comparison of two *in situ* NMR initialization experiments where the CTA X14 contained 30% of α-chlorophenyl acetic acid, ethyl ester (filled symbols) versus 10% of the same contaminant (open symbols).

Signals b, c, e, f and g correspond to species expected from the RAFT mechanism, *i.e.* single monomer adducts from the R group (c and f), single monomer adducts from the initiator primary radical (b) and oligomer adducts (e and g). The latter were present in low amounts as the reaction was continued beyond the end of initialization. Signals a, d, g-j and k-p do not correspond to species expected from the RAFT mechanism. d, g, h, i, j, l and n are quartets, which couple with methyl protons, as indicated by the ^{1}H/^{1}H-COSY experiment reported in Figure 5.7. In particular d, h, i, j and l clearly do not couple with any other proton. This indicates a CH_3-CH moiety isolated from the rest of the molecule by heteroatoms. Among these species were identified the products of hydration (NVP-O-NVP, signals i and l).
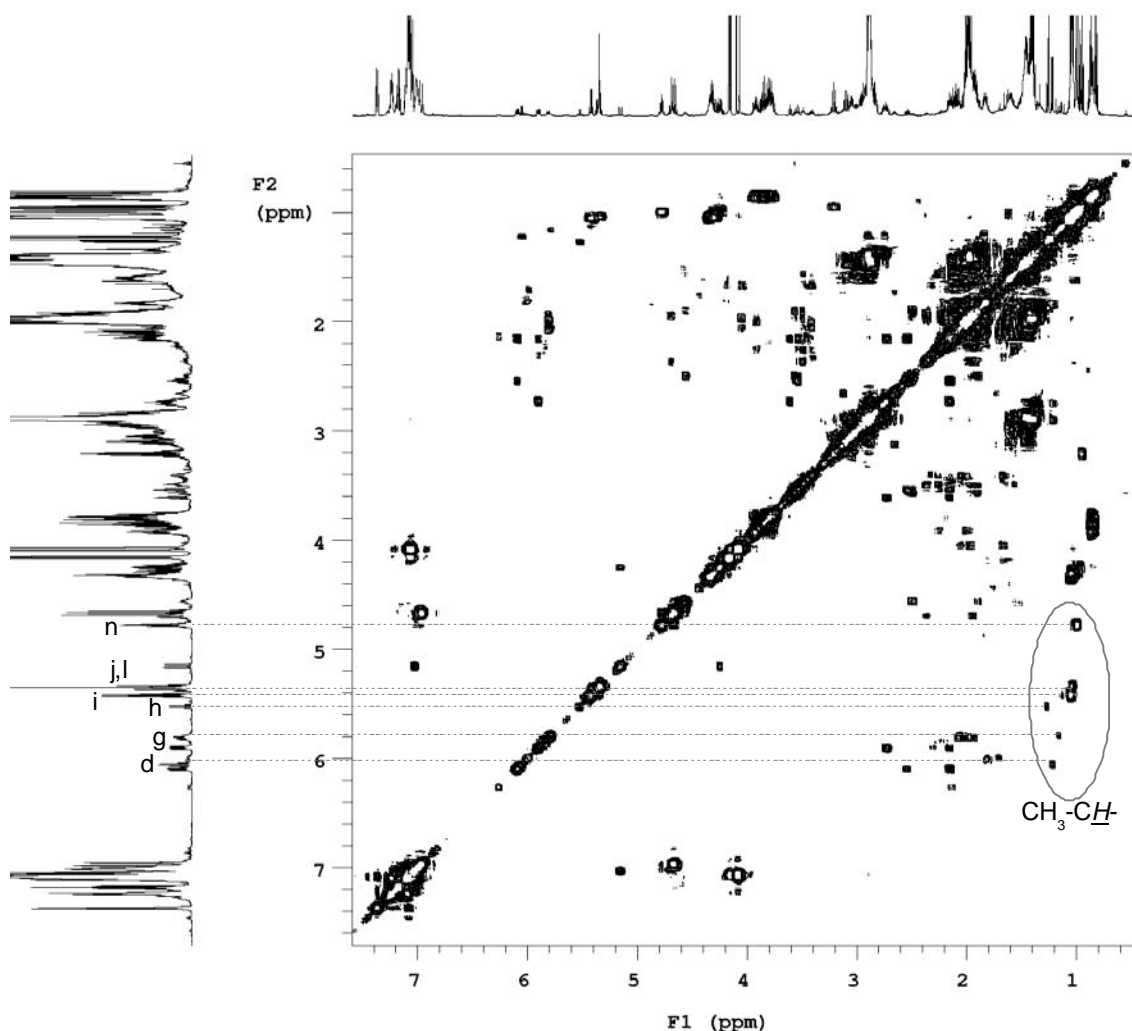
Figure 5.7: Homonuclear ^{1}H/^{1}H-COrrelated SpectroscopY (COSY).

Identification of other species was possible via a combination of interpretations from 2D ^{1}H/^{13}C-heteronuclear experiments. The spectra corresponding to HSQC and HMBC experiments are presented in Figure 5.8 and Figure 5.9, respectively. Peaks o and m were thus assigned to NVP unsaturated dimer and the product of xanthate elimination (X_{14}-EP), respectively. For the assignment of the structure X_{14}-EP, Nuclear Overhauser Effect SpectroscopY (NOESY) was carried out (Figure 5.10), which enabled identification of peaks otherwise overlapping with numerous signals. Figure 5.9 reveals the presence of a new xanthate species and the corresponding adducts identified from peaks d and g, respectively. Long-range correlations with peak d enabled identification of the structure as compound *S*-(1-pyrrolidonylethyl) *O*-ethyl xanthate (NVP-xanthate). A mechanism for the formation of NVP-xanthate is proposed in Scheme 5.4. It involves the

addition of the carbocationic product of proton addition to the NVP double-bond (also proposed for the acid-catalyzed formation of NVP unsaturated dimer and hydration products[1,3]) and addition to xanthic acid. Xanthic acid may form as a result of xanthate elimination from the chain-ends. Addition of dithiobenzoic acid to vinyl and acrylic compounds was reported for the *in situ* preparation of the RAFT agent during polymerization.[16,17] It is important to note that the formation of NVP-xanthate subsequent to xanthate end-group elimination would have an effect on the molecular weight distribution similar to irreversible transfer. The number of chains increases and new chains are formed late in the polymerization, resulting in an increase in the PDI. The radical concentration is not affected and therefore the rate of polymerization would not be influenced by this transfer-like reaction. Provided that the xanthic acid produced by elimination of the xanthate endgroups is quantitatively converted to the new xanthate species NVP-xanthate, the number of xanthate end-functional chains would be constant. Note that the insert with the internal reference was removed from the tube before the end of the reaction (because it was required for other ongoing experiments) and therefore it is not possible to tell whether the total xanthate concentration remained constant or decreased. A decrease would be observed if not all of the eliminated xanthate participated in the formation of NVP-xanthate. Other species may form subsequent to xanthate elimination. Degradation of the xanthic acid may also take place, producing carbon disulfide and ethanol. The multitude of peaks in the regions where ethanol peaks would appear (0.96 and 3.34 ppm in C_6D_6[18]) does not exclude its possible presence.

The structure of the compound corresponding to peak h could be not determined unambiguously. The chemical shift and pattern are similar to that reported for the methine proton of 1,1-bis(*N*-pyrrolidonyl) ethane.[19] Apart from consuming low amounts of monomer, 1,1-bis(*N*-pyrrolidonyl) ethane should not have a significant influence on the polymerization kinetics and mechanism.

A summary of the structures identified via assignment of the peaks in the region 4.5 – 7.0 ppm is presented in Table 5.1. Their abundance is given as a percentage of the total xanthate species, which were identified in the region 5.75 – 6.30 ppm.
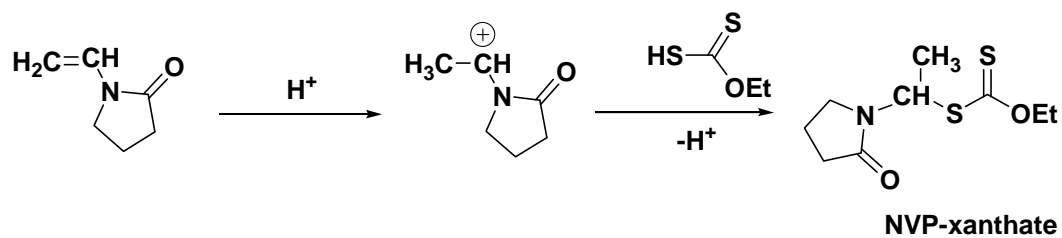
Scheme 5.4: proposed reaction scheme for the acid-catalyzed formation of *S*-(1-pyrrolidonylethyl) *O*-ethyl xanthate (NVP-xanthate).
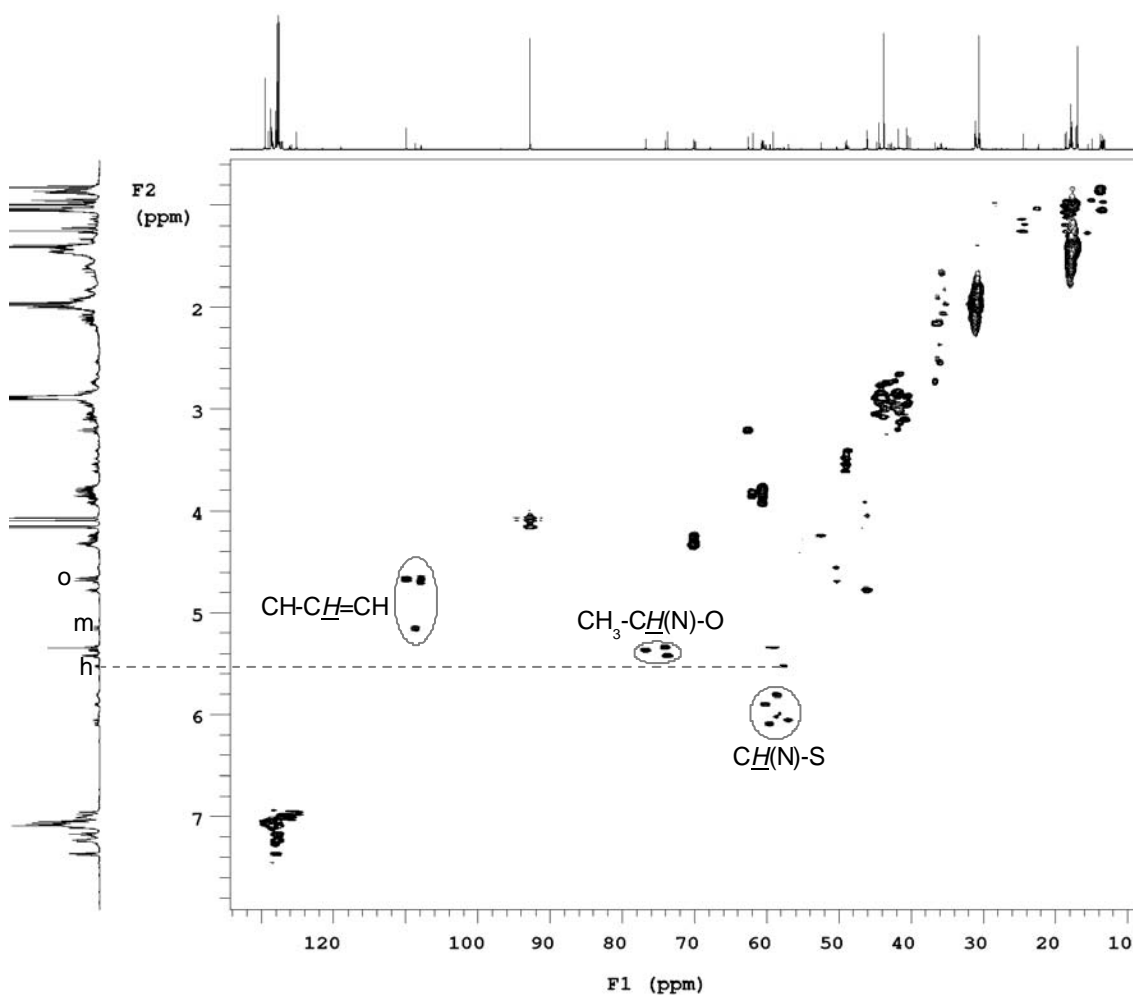
Figure 5.8: ^{1}H/^{13}C-Heteronuclear Single Quantum Coherance (HSQC) spectrum.
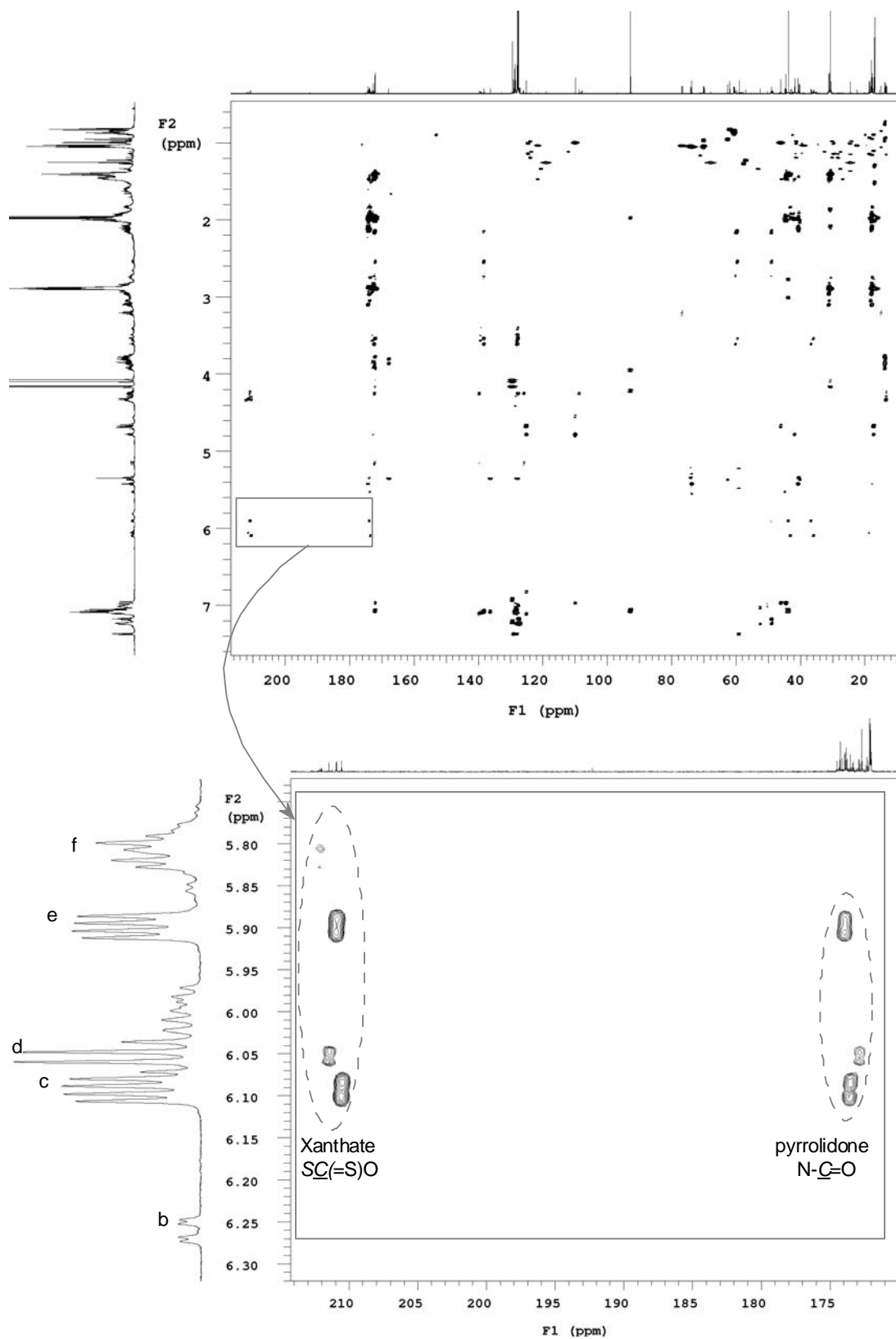
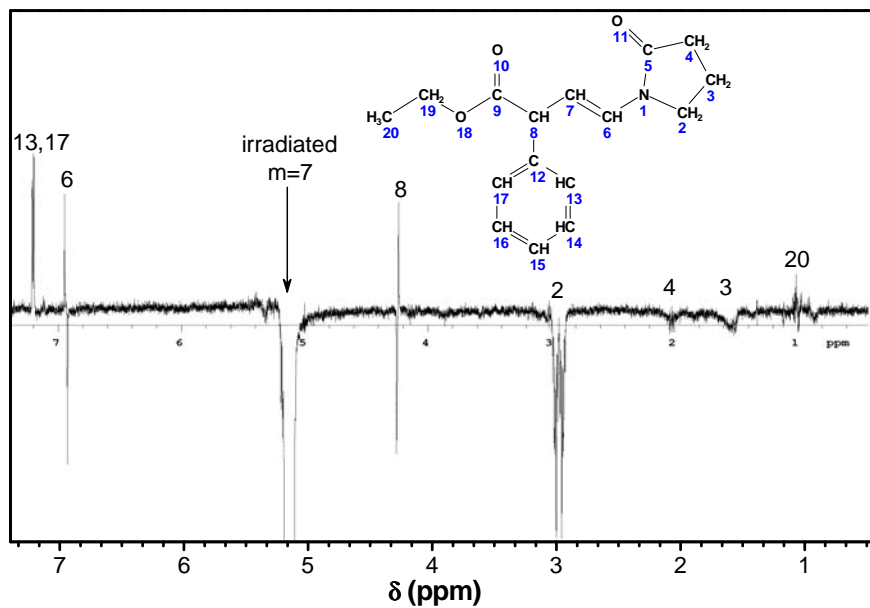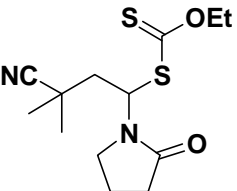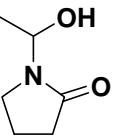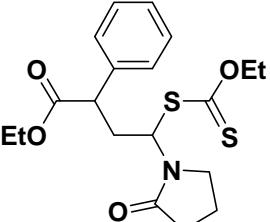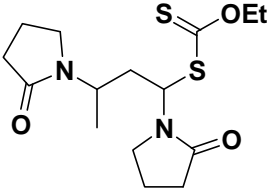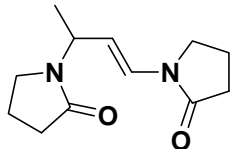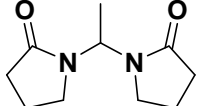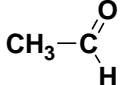Figure 5.9: ^{1}H/^{13}C-Heteronuclear Multiple-Bond Correlation (HMBC) NMR spectrum.
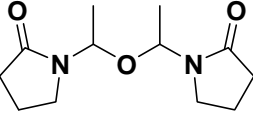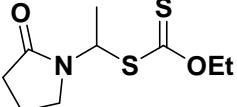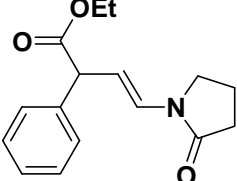
Figure 5.10: Nuclear Overhauser Effect SpectroscopY (NOESY) spectrum for the identification of the unsaturated product of xanthate elimination X14-EP.

Table 5.1: structures identified as products and by-products in the *in situ* NMR spectroscopy initialization experiment with NVP and *S*-(2-ethyl phenylacetate) *O*-ethyl xanthate (X14) at 70 ºC.

Peak	Structure	Integration[a]	Peak	Structure	Integration[a]
b	S, OEt, NC, N, O	2.6	i	OH, N, O	46.2
c,f	phenyl, O, OEt, EtO, S, S, N, O	12.8+18.4	j,l	O, N, O, N, O	19.4+22.6
d	O, N, S, S, OEt	8.5	m,a	OEt, O, phenyl, N, O	14.1
g	S, OEt, N, S, O, N, O + other oligomer adducts	20.2	n,o	N, O, N, O	51.3
h	O, N, N, O	8.5	not shown	$CH_3 - C$, O, H	3.0

[a] an integration value of 100 was assigned to the region 5.75 – 6.30 ppm (where all C*H*-S signals were identified). The integration values in this table are therefore a reflection of the relative abundance (%) of each species relative to the sum of xanthate species at the end of the experiment (7.5 h).

Identification of by-products gives a valuable insight into possible causes for the loss of control over the molar mass distribution when X14 is used to mediate the polymerization of NVP. In particular, elimination of the xanthate moiety from NVP adducts occurred to a significant extent. As a result the unsaturated species corresponding

to peak m was found with a relative abundance of 14 %. The new xanthate (NVP-xanthate) identified with peak d suggests that xanthate elimination does not result in a net loss of xanthate species but instead produces new chains. Xanthate elimination provides an explanation for the presence of unsaturated chain-ends generally accounting for a low fraction of the endgroups (*e.g.* less than 5 % when the polymerization carried out at 60 ºC with *S*-(2-cyano-2-propyl) *O*-ethyl xanthate (X6) and monomer conversion is close to 50 %). A significant fraction of chains may be initiated with 1-pyrrolidonyl ethane, which is not due to transfer to the monomer but to the formation of NVP-xanthate.

Conclusions

A significant number of by-products were identified during initialization experiments. Some are related to the reactivity of NVP and are likely to form independently of the presence of RAFT agent or initiator. They are summarized in Scheme 5.5. The by-products include NVP unsaturated dimer and hydration products. The formation of the dimer was catalyzed by maleic anhydride comonomer or xanthates with a hydroxyl functional R group and to a lesser extent with a carboxylic acid R group. The carboxylic acid esterified in the presence of NVP. Hydration of NVP double-bond may have enabled such an esterification reaction to occur. These compounds were identified in organic medium (C_6D_6), where traces of water were present. The author believes it is important to be aware of by-products related to non-radical reactions affecting the monomer NVP. In particular, consumption of the monomer for side-reactions results in the impossibility to reach quantitative monomer conversion into polymeric species. Also, the by-products possess methyl groups, which are generally more prone to proton abstraction than the methine and methylene protons of the monomer and polymer. Labile protons may participate in transfer reactions, which lead to a loss of control over the chain-ends and molecular weight distribution of the polymer. In order to limit the formation of NVP dimer and hydration products the use of compounds with acid or hydroxyl functionalities should be avoided. Alternatively, it may be interesting to investigate the use of stabilizers, such as mild bases, or the effect of the solvent polarity on side-reactions. The products of NVP degradation are easily identified

via ^{1}H-NMR spectroscopy because their methine protons display a signal in the region 4.6 – 5.6 ppm, where polymer peaks are absent. Therefore a spectrum of the raw mixture at the end of the polymerization will indicate the presence of degradation compounds.

Side-reactions affecting the xanthate species were investigated. Unsaturated products due to elimination of the xanthate from monomer adducts were identified. The xanthate R group was found to affect the concentration of xanthate-elimination products at the end of the initialization period. Elimination of the xanthate from single monomer adducts and from the polymer chain-end further in the polymerization produces dead chains. Therefore it may significantly influence the molecular weight distribution of the polymer. The reaction is different from endgroup hydrolysis or aminolysis, which are so far the most studied degradative side-reactions studied in relation to RAFT-mediated polymerization in aqueous medium.[20] The difference lies in the fact that xanthic acid produced upon xanthate elimination may react with the monomer to produce a new xanthate species, which we identified. As a consequence, the overall reaction is similar to an irreversible transfer reaction where a dead chain is formed (in our case with an unsaturated end-group) and a new chain is initiated (with a 1-pyrrolidonyl ethyl initiating group).

A preliminary study indicated that the presence of water (a mixture of D_2O and DMSO-d_6 was used as the NMR spectroscopy solvent) results in a net loss of xanthate species. The reaction was not studied in details, as water was found to hydrolyze the chain-ends at moderate temperature and pH (details are provided in chapter 7), which prompted us to avoid water as a solvent for the xanthate-mediated polymerization of NVP.
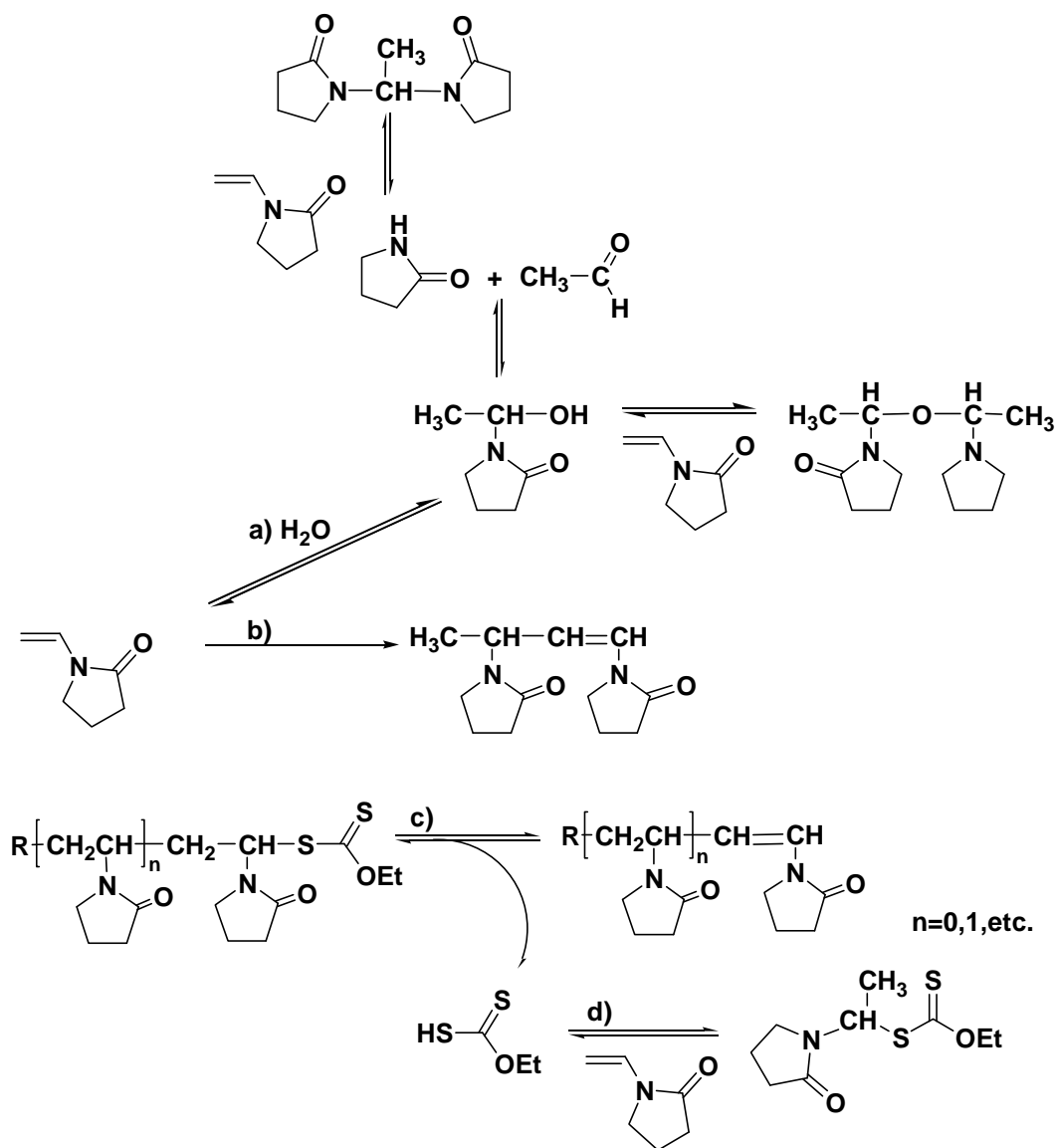
Scheme 5.5 : Summary of the by-products identified during *in situ* NMR spectroscopy initialization experiments with NVP and *O*-ethyl xanthates at 70 ºC in C_6D_6. Special reaction conditions: b) xanthate R-group with a carboxyl acid or hydroxyl functionality or maleic anhydride comonomer.

Reference list

(1)   Breitenbach, J.W.; Galinovsky, F.; Nesvadba, H.; Wolf, E. *Monatsh. Chemie* **1956**, *87*, 580-592.
(2)   Madl, A.; Spange, S. *Macromolecules* **2000**, *33*, 5325-5335.
(3)   Senogles, E.; Thomas, R.A. *J.C.S. Perkin II* **1980**, 825-828.
(4)   Zhuo, J.-C. *Molecules [Electronic Publication]* **1999**, *4*, M117.
(5)   Doneux, C.; Caudano, R. *Langmuir* **1997**, *13*, 4898-4905.
(6)   Gupta, K.C. *J. Appl. Polym. Sci.* **1994**, *53*, 71-78.
(7)   Bamford, C.H.; Schofield, E.; Michael, D.J. *Polymer* **1985**, *26*, 945-950.
(8)   Nowlan, V.J.; Tidwell, T.T. *Accounts Chem. Res.* **1977**, *10*, 252-258.
(9)   Denisov, V.M.; Ushakova, V.N.; Kol'tsov, A.I.; Panarin, E.F. *Inst. Vysokomol. Soedin.* **1989**, *62*, 660-664.
(10)   Gagosz, F.; Zard, S.Z. *Org. Lett.* **2003**, *5*, 2655-2657.
(11)   Tournier, L.; Zard, S.Z. *Tetr. Lett.* **2005**, *46*, 455-459.
(12)   Quiclet-Sire, B.; Zard, S.Z. *Tetr. Lett.* **1998**, *39*, 9435-9438.
(13)   Marten, F.L. In *Encyclopedia of Polymer Science and Engineering*, 2nd ed.; John Wiley and Sons, Inc., **1989**; Vol. 17, p 203.
(14)   Czerwinski, W.K. *Makromol. Chem.* **1992**, *193*, 359-368.
(15)   Senogles, E.; Thomas, R.A. *J. Polym. Sci., Pol. Lett. Ed.* **1978**, *16*, 555-562.
(16)   Bai, R.-K.; You, Y.-Z.; Pan, C.-Y. *Polym. Int.* **2000**, *49*, 898-902.
(17)   Bai, R.-K.; You, Y.-Z.; Zhong, P.; Pan, C.-Y. *Macromol. Chem. Phys.* **2001**, *202*, 1970-1973.
(18)   Gottleib, H.E.; Kotlyar, V.; Nudelman, A. *J. Org. Chem.* **1997**, *62*, 7512-7515.
(19)   Kaupp, G.; Matthies, D. *Chem. Ber.* **1987**, *120*, 1897-1903.
(20)   Thomas, D.B.; Convertine, A.J.; Hester, R.D.; Lowe, A.B.; McCormick, C.L. *Macromolecules* **2004**, *37*, 1735-1741.

Chapter 6: PEG-based block copolymers[b]

Introduction

Poly(ethylene glycol) (PEG) is widely used in the pharmaceutical and biomedical fields. It is a non-ionic polymer, soluble in water and most common organic solvents. The incorporation of a PEG segment in a macromolecule modulates its solution properties. Many synthetic pathways are available for the preparation of block copolymers comprising a PEG block. Each block can be prepared separately and connected by post-polymerization coupling of functional end-groups.[1] Commercially available PEGs prepared via anionic polymerization can be found with one or two hydroxyl end-functionalities, which enable almost unlimited chemical modification[2] and the preparation of di-, tri- or multi-block copolymers. The main prerequisite for this approach is that the second polymeric block must be quantitatively end-functionalized. Thus, this method has been used mostly to prepare biodegradable block copolymers of PEG with a second block obtained via polycondensation or ring opening polymerization.[3,4] Poly(NVP) (PVP) and poly(VAc) (PVAc) are typical examples of widely used industrial polymers that can only be prepared via free-radical polymerization. Conventional free-radical polymerization does not normally provide end-functionality because of transfer and termination reactions. By taking advantage of transfer reactions, however, Ranucci et al. synthesized a variety of low molecular weight PVPs bearing chain-end functionality, which could potentially be used to make block copolymers with PEG.[5-8] The other synthetic approach consists of growing a second block from an end-functional PEG precursor. By selecting a macromolecular precursor bearing a functional group capable of controlling the polymerization of the second comonomer, not only is it possible to obtain block copolymers, but also to control the molecular weight distribution of the blocks. The recent development of living radical polymerization techniques has made it possible to

---

match an appropriate control agent with almost any polymerizable monomer. Modified PEGs have been used as initiators for atom-transfer radical polymerization,[9] nitroxide-mediated polymerization[10] and as macromolecular chain-transfer agents (macroCTAs) for reversible addition-fragmentation transfer (RAFT)-mediated polymerization.[11,12] NVP and VAc present comparable polymerization characteristics; however PVP is water-soluble whereas PVAc is hydrophobic. As a result block copolymers of PEG with NVP are all-hydrophilic while PEG-*b*-PVAc block copolymers are amphiphilic. Finding a common synthetic pathway for materials with dramatically different solution properties is an appealing concept. Successful control of VAc polymerization has only been reported using xanthates as mediating agents under a RAFT mechanism.[13,14] The first examples of block copolymers containing a PVP block prepared via living polymerization were reported recently with the syntheses of polystyrene-*b*-poly(NVP) and poly(methyl methacrylate)-*b*-poly(NVP) via organostibine-mediated polymerization[15,16] and PVP-*b*-PVAc[17] via xanthate-mediated polymerization. While the introduction of organostibine functionality would require complicated chain end modification reactions, modification of a commercially available PEG with a xanthate moiety is relatively straightforward and well-documented.[12] The ability of xanthates to control the polymerization of both monomers led us to investigate the use of xanthate end-functional PEGs to prepare well-defined block copolymers with NVP and VAc. Some studies have been reported on the use of xanthates for the polymerization of NVP. The group of Kamigaito and Okamoto published the first paper on xanthate-mediated polymerization of NVP. They reported a living/controlled character with a phenyl ethyl leaving group in spite of long "inhibition".[18] A few leaving groups producing radicals centered on a primary carbon were investigated, *i.e.* cyanomethyl[19], benzyl[17,18] and phtalimidyl methyl.[20] Coote et al. recommend that the leaving group be chosen with comparable (slightly higher or slightly lower) radical stability with respect to that of the monomer-derived radical.[21] We showed that good control was achieved with a propionic acid leaving group, although initialization was not completely selective[22] (see also chapter 4). On the basis of these results we chose the leaving groups for the present study. We first looked at the efficiency of two PEG-based macroCTAs in reinitiating the polymerization of VAc and NVP and studied the initialization behavior of the polymerization with low molecular

weight xanthate model compounds bearing similar reinitiating groups via ^{1}H-NMR spectroscopy. We then identified a suitable macroCTA and carried out thorough characterization of the block copolymers via size-exclusion chromatography (SEC), high performance liquid chromatography (HPLC) and matrix-assisted laser-desorption ionization time-of-flight-mass spectrometry (MALDI-ToF-MS). In this chapter the notation A_mB_p is used to refer to a block copolymer prepared from the macroCTA A_m via polymerization of B with an average degree of polymerization of p. The value of m was determined via ^{1}H-NMR spectroscopy as the ratio of integration of the polymer end-groups to the polymer backbone. The value of p was calculated based on the value of conversion and the assumption that each copolymer chain comprises a macroCTA block and that all of the starting macroCTA is converted to a block copolymer.

Experimental Section

Chemicals. *N*-vinylpyrrolidone (Aldrich, 99 %) was dried over anhydrous magnesium sulfate and purified by distillation under reduced pressure. Vinyl acetate (Protea Chemicals, 99 %), was distilled under reduced pressure, collected in a flask, and cooled down in an ice bath. THF (KIMIX) was distilled from lithium aluminum hydride. Dichloromethane (KIMIX, CP-grade, 99.5 %) and ethanol (SASOL, absolute, 99.5 %) were stored over molecular sieves 3 Å. AIBN (Riedel de Haen) was recrystallized twice from methanol. Potassium *O*-ethyl dithiocarbonate (95 %, Merck), 2-bromopropionyl bromide (97 %, Fluka), ethyl *2*-bromo propionate (98 %, Fluka), α-chlorophenylacetylchloride (90 %, Aldrich), pyridine (SAARCHEM, CP-grade, 99.5 %) and the deuterated solvent C_6D_6 (99.6 %, Aldrich) were used without further purification. For column chromatography, silica gel (Fluka, particle size 0.063 – 0.2 mm, Brockmann 2-3) was used. Poly(ethylene glycol) mono methyl ether (EG$_{75}$-OH) (Pluriol A3010E, $M_{n,NMR}$=3300 g·mol^{-1}, $M_{n,SEC}$=12100 g·mol^{-1} (PMMA equivalents in HFIP), PDI=1.06) and the telechelic dihydroxyl poly(ethylene glycol) (HO-EG$_{90}$-OH) (Pluriol E4000, $M_{n,NMR}$=4000 g·mol^{-1}, $M_{n,SEC}$=18300 g·mol^{-1} (PMMA equivalents in HFIP), PDI=1.08) were donated by BASF AG and used as received.

Synthesis of macroCTA EG$_{75}$-X1

    1. Synthesis of 2-bromopropionic acid [poly(ethylene glycol) methyl ether] ester (EG$_{75}$-Br). Poly(ethylene glycol) mono methyl ether (EG$_{75}$-OH, 32.0 g, $9.7 \cdot 10^{-3}$ mol) was placed in a 3-neck flask and stirred with pyridine (2.00 mL, $2.60 \cdot 10^{-2}$ mol) in dichloromethane (80 mL). While the mixture was still cold 2-bromopropionyl bromide (2.40 mL, $2.26 \cdot 10^{-2}$ mol) was added slowly. The mixture was stirred for 16 h at room temperature. A white precipitate was filtered off. Dichloromethane (300 mL) was added. The solution was washed with saturated ammonium chloride (4×50 mL) then with saturated sodium hydrogen carbonate (4×50 mL) and water (50 mL) then dried over anhydrous magnesium sulfate. The solvents were evaporated under vacuum. EG$_{75}$-Br was obtained (26.56 g, 83 % recovery, purity > 99 % by ^{1}H-NMR). ^{1}H-NMR (400 MHz, CDCl$_3$): δ[ppm] = 4.36, q, ^{3}J=6.8 Hz, 1H (C*H*); 4.28, m, 2H, (C*H$_2$*OC(O)); 3.61, s, 3.5-3.8, m, (C*H$_2$*C*H$_2$*O- PEG backbone); 3.34, s, 3H, (C*H$_3$*O); 1.79, d, ^{3}J=6.8 Hz, 3H (C*H$_3$*).
2. Synthesis of EG$_{75}$-X1. EG$_{75}$-Br (3.30 g, $1.0 \cdot 10^{-3}$ mol) was dissolved in dichloromethane (15 mL) in a 3-neck flask and stirred with pyridine (4.20 mL, $5.3 \cdot 10^{-2}$ mol). Potassium *O*-ethyl xanthate (0.48 g, $3.0 \cdot 10^{-3}$ mol) was added portion-wise. The mixture was stirred at room temperature for 16 h. Dichloromethane was added (140 mL). The solution was washed with concentrated ammonium chloride (4×40 mL) then saturated sodium bicarbonate (4×50 mL) and water (50 mL) then dried over anhydrous magnesium sulfate. The solvents were evaporated under vacuum and the resulting powder purified via Soxhlet extraction with diethyl ether. 2.80 g of EG$_{75}$-X1 was obtained (85 % recovery). ^{1}H-NMR indicated quantitative conversion of the end-groups. ^{1}H-NMR (600 MHz, CDCl$_3$): δ[ppm] = 4.61, q, ^{3}J=7.2 Hz, 2H (SC(S)OC*H$_2$*CH$_3$); 4.39, q, ^{3}J=7.5 Hz, 1H, (C*H*CH$_3$); 4.28, m, 2H, (C*H$_2$*OC(O)); 3.62, s, 3.5-3.8, m, (-C*H$_2$*C*H$_2$*O- PEG backbone); 3.36, s, 3H, (C*H$_3$*O); 1.79, d, ^{3}J=7.5 Hz, 3H (CHC*H$_3$*); 1.40, t, ^{3}J=7.2 Hz, 3H, (SC(S)OCH$_2$C*H$_3$*). $M_{n,SEC}$=11900 g·mol^{-1} (PMMA equivalents in HFIP), PDI=1.06.

    In another experiment, the second step of the reaction was carried out for 10 h instead of 16 h. A 75 % pure EG$_{75}$-X1, containing approximately 20 % of unreacted EG$_{75}$-Br and less than 5 % EG$_{75}$-OH (determined by ^{1}H-NMR spectroscopy and HPLC)

was obtained. This sample is used in the section dedicated to HPLC analyses in order to identify the various PEG derivatives according to their end-groups. Note that this 75 % pure product was not used for polymerizations.

Synthesis of the difunctional macroCTA X1-EG$_{90}$-X1

The same synthetic procedure as for EG$_{75}$-X1 was applied; however the molar equivalents of reagents were doubled so as to account for the difunctionality of the starting dihydroxyl telechelic PEG HO-EG$_{90}$-OH. X1-EG$_{90}$-X1 was obtained with 78 % yield and purity > 90 % by ^{1}H-NMR spectroscopy. ^{1}H-NMR (400 MHz, CDCl$_3$): δ[ppm] = 4.61, q, ^{3}J=7.3 Hz, 4H (2×SC(S)OCH_2CH$_3$); 4.38, q, ^{3}J=7.5 Hz, 2H, (2×CHCH$_3$); 4.26, m, 4H, (2*CH_2OC(O)); 3.61, s, 3.4-3.8, m, (-CH_2CH_2O- PEG backbone); 1.55, d, ^{3}J=7.5 Hz, 6H (2×CHCH_3); 1.38, t, ^{3}J=7.3 Hz, 6H, (2×SC(S)OCH$_2$CH_3). $M_{n,SEC}$=21900 g·mol^{-1} (PMMA equivalents in HFIP), PDI=1.08.

Synthesis of macroCTA EG$_{75}$-X2

In a first step, chlorophenyl acetic acid [poly(ethylene glycol) methyl ether] ester (EG$_{75}$-Cl) was prepared from EG$_{75}$-OH and α-chlorophenyl acetylchloride according to a procedure reported in the literature.[11] Then EG$_{75}$-Cl (4.40g, 1.3·10^{-3} mol) was dissolved in dichloromethane (40 mL) in a 3-neck flask fitted with a condenser and pyridine (1.70 mL, 2.15·10^{-2} mol) was added. Potassium O-ethyl xanthate (0.64 g, 3.9·10^{-3} mol) was added portion-wise. The mixture was refluxed for 24 h. Dichloromethane was added (140 mL). A white precipitate was filtered off. The solution was washed with saturated ammonium chloride (4×40 mL) then concentrated sodium bicarbonate (4×50 mL) and water (50 mL) then dried over anhydrous magnesium sulfate. The polymer solution was concentrated under vacuum and the polymer was recovered by precipitation from cold diethyl ether. 3.48 g of EG$_{75}$-X2 was obtained (79 % recovery and purity > 95 % by ^{1}H-NMR spectroscopy). ^{1}H-NMR (400 MHz, CDCl$_3$): δ[ppm] = 7.25-7.45, m, 5H, (C$_6$H$_5$); 5.44, s, 1H, (CHC$_6$H$_5$); 4.59, q, ^{3}J=6.8 Hz, 2H (OCH_2CH$_3$); 4.27, m, 2H, (CH_2OC(O)); 3.61, s, 3.5-3.8, m, (-CH_2CH_2O- PEG backbone); 3.34, s, 3H, (CH_3O); 1.37, t, ^{3}J=6.8 Hz, 3H, (OCH$_2$CH_3). $M_{n,SEC}$=11700 g·mol^{-1} (PMMA equivalents in HFIP), PDI=1.06.

The syntheses of S-(2-ethyl propionate)-(O-ethyl xanthate) (X13) and S-(2-ethyl phenylacetate)-(O-ethyl xanthate) (X14) were already described in chapter 3.

Polymerization procedures

All polymerizations were carried out in a pear-shaped 50 mL Schlenk flask heated in an oil bath. The polymerization mixture was degassed with a minimum of 4 freeze-pump-thaw cycles followed by the introduction of ultra-high purity argon. A typical polymerization was performed as follows.

Polymerization of *N*-vinylpyrrolidone for diblock copolymer synthesis

NVP (2.00 g, $1.80 \cdot 10^{-2}$ mol), AIBN (0.100 g of a 0.032 g solution in 1.000 g of benzene, $1 \cdot 10^{-5}$ mol), EG_{75}-X1 (0.140 g, $4.2 \cdot 10^{-5}$ mol) and THF (2.14 g) were placed in a Schlenk flask and degassed via freeze-pump-thaw. The flask was immersed in an oil bath preheated at 60 ºC. After 15 h poly(ethylene glycol)-*b*-poly(*N*-vinylpyrrolidone) (EG_{75}-NVP_{347}) was isolated by precipitation in diethyl ether (monomer conversion = 77 %, $M_{n,SEC}$ = 52300 g·mol^{-1} (PMMA equivalents in HFIP), PDI = 1.35). Several EG_{75}-NVP_n diblock copolymers were prepared with different average degrees of polymerization (*n*) for the PVP block with the same procedure by varying the initial concentration ratios of NVP to EG_{75}-X1 and conversion.

Polymerization of N-vinylpyrrolidone for triblock copolymer synthesis

NVP (2.00 g, $1.80 \cdot 10^{-2}$ mol), AIBN (0.017, $1.0 \cdot 10^{-4}$ mol), X1-EG_{90}-X1 (0.80 g, $2.0 \cdot 10^{-4}$ mol) and THF (2.14 g) were placed in a Schlenk flask and degassed via freeze-pump-thaw. The flask was immersed in an oil bath preheated at 60 ºC. After 15 h poly(*N*-vinylpyrrolidone)-*b*-poly(ethylene glycol)-*b*-poly(*N*-vinylpyrrolidone) (NVP_{38}-EG_{75}-NVP_{38}) was isolated by precipitation in diethyl ether (monomer conversion = 85 %, $M_{n,SEC}$ = 37700 g·mol^{-1} (PMMA equivalents in HFIP), PDI = 1.10).

Polymerization of vinyl acetate for diblock copolymer synthesis

VAc (1.60 g, $1.82 \cdot 10^{-2}$ mol), AIBN (0.008 g $5 \cdot 10^{-5}$ mol), EG_{75}-X1 (0.665 g, $1.90 \cdot 10^{-4}$ mol) and THF (2.3 g) were placed in a Schlenk flask and degassed via freeze-

pump-thaw. The flask was immersed in an oil bath preheated at 54 ºC. After 14 h poly(ethylene glycol)-*block*-poly(vinyl acetate) (EG$_{75}$-VAc$_{88}$) was isolated by evaporation of the solvent and unreacted monomer (monomer conversion = 90 %, $M_{n,NMR}$ = 6600 g·mol^{-1}). Several EG$_{75}$-VAc$_n$ diblock copolymers were prepared with different n for the PVAc block with the same procedure by varying the initial concentration ratios of VAc to EG$_{75}$-X1 and conversion.

X13-mediated polymerization of NVP in the presence of EG$_{75}$-OH

NVP (1.00 g, 9.0·10^{-3} mol), AIBN (0.003 g, 2·10^{-5} mol), X1' (0.023 g, 1.0·10^{-4} mol), EG$_{75}$-OH (0.231 g, 6.6·10^{-5} mol) and THF (1.23 g) were placed in a Schlenk flask and degassed via freeze-pump-thaw. The flask was immersed in an oil bath preheated at 60 ºC. After 17 h a mixture of the starting poly(ethylene glycol) EG$_{75}$-OH and poly(*N*-vinylpyrrolidone) NVP$_{77}$-X1' was isolated by precipitation in diethyl ether (monomer conversion = 86 %, $M_{n,SEC}$ = 9600 g·mol^{-1} (PMMA equivalents in HFIP), PDI = 1.33).

Conventional free-radical polymerization of NVP in the presence of EG$_{75}$-OH

NVP (1.00 g, 9.0·10^{-3} mol), AIBN (0.003 g, 2·10^{-5} mol), EG$_{75}$-OH (0.233 g, 6.7·10^{-5} mol) and THF (1.23 g) were placed in a Schlenk flask and degassed via freeze-pump-thaw. The flask was immersed in an oil bath preheated at 60 ºC. After 17 h a mixture of the starting poly(ethylene glycol) EG$_{75}$-OH and poly(vinylpyrrolidone) (PVP) was isolated by precipitation in diethyl ether (monomer conversion > 99 %, $M_{n,SEC}$ = 30300 g·mol^{-1} (PMMA equivalents in HFIP), PDI = 2.71, bimodal).

Hydrolysis of poly(ethylene glycol)-*b*-poly(N-vinylpyrrolidone) diblock copolymer

0.050 g of diblock copolymer EG$_{75}$-NVP$_{347}$ ($M_{n,SEC}$ = 52300 g·mol^{-1}, PDI = 1.35) was dissolved in 0.01 M potassium hydroxide (3 mL). The solution was stirred at room temperature for 16 h. The pH was adjusted to 7 by addition of hydrochloric acid (0.1 M) and dialyzed against distilled water for 8 h to remove the salts. Water was eliminated by

freeze-drying and the sample analyzed via HPLC and SEC. The same procedure was applied to the diblock copolymer EG$_{75}$-NVP$_{46}$.

Characterization techniques

^{1}H-NMR and ^{13}C-NMR spectra were recorded on a Varian-400 or 600 MHz Varian ^{Unity}Inova spectrometer.

SEC. The SEC set-up consisted of an eluent degasser (Alltech Elite), a gradient pump (Shimadzu, LC-10AD), an injector (Spark Holland, MIDAS), a two-column set (PSS, PFG Linear XL 7 μm, 8 x 300 mm, separation window 10^2 – 10^6 Da), a column oven (Spark Holland, Mistral) at 40 ℃, detectors in series: Dual Wavelength UV Detector (Waters, 2487); Light Scattering (RALS/LALS) and Viscometry (Viscotek, 270) and Differential Refractive-Index Detector (DRI) (Waters, 2414). The injection volume was 50 μL, the flow rate was 0.8 mL·min^{-1}. The eluent HFIP (Biosolve, AR-grade) with 0.02 M KTFA added (potassium trifluoro acetate, 3.0 g·L^{-1}, Fluka 91702) was redistilled after use. A short silica column was placed after the pump to catch free fluoride, possibly present in HFIP. A particle filter 0.2 µm PTFE was placed between columns and UV detector to prevent small particles to enter the LS detector. Data acquisition and processing was performed with Viscotec Omnisec 4.0 (all detectors) and Waters Empower 2.0 (UV and refractive index detectors). The calculated molecular weights were based on a calibration curve for poly(methyl methacrylate) standards (molecular weight range 650 - 1.5·10^4 g·mol^{-1}) of narrow polydispersity (Polymer Laboratories) in HFIP.

HPLC was performed using a dual pump HPLC set up comprising the following units: Waters 2690 Separations Module (Alliance); Agilent 1100 series variable wavelength UV detector; PL-ELS 1000 detector. Data was recorded and processed using PSS WinGPC unity (Build 2019) software. The conditions used for the separation of PEG-*b*-PVP samples were as follows. A C18 grafted silica column was used (Luna RP C18 3 μm 150 × 4.60 mm, Phenomenex) at 30 ℃. The flow rate was 0.5 mL·min^{-1}. In the following part of the discussion, a difference is made between HPLC under isocratic conditions and gradient HPLC. For clarity, the terms HPLC at critical conditions and gradient polymer elution chromatography (GPEC) will be used, which refer to isocratic

and gradient conditions, respectively. The mobile phase composition for HPLC at critical conditions of PEG-OH was water (deionized, with 0.1 % formic acid):acetonitrile 56:44 (v/v). For GPEC analyses the mobile phase was water (deionized, with 0.1 % formic acid):acetonitrile and the composition ranged from 68:32 to 45:55 (v/v). Prior to HPLC and GPEC analyses, NVP-containing polymers were dialyzed for 24 h in distilled water using SnakeSkin® pleated dialysis tubing (Pierce, 3.500 MWCO). Samples were prepared in the same solvent composition as the mobile phase at the beginning of each elugram (68:32 (v/v)), at concentrations of 5 mg·mL^{-1}. The injection volume was 10 μL. A PVP sample (NVP$_{19}$) prepared via xanthate-mediated polymerization was used as a reference to estimate the elution volume limit of PVP homopolymers under the size-exclusion mode ($M_{n,SEC}$ = 2430 g·mol^{-1} (PMMA equivalents in HFIP), PDI = 1.23). For GPEC analysis of PEG-*b*-PVAc copolymers, identical conditions were used except for the eluent composition, which was varied from 45:55 (v/v) (water:acetonitrile) to 100 % acetonitrile.
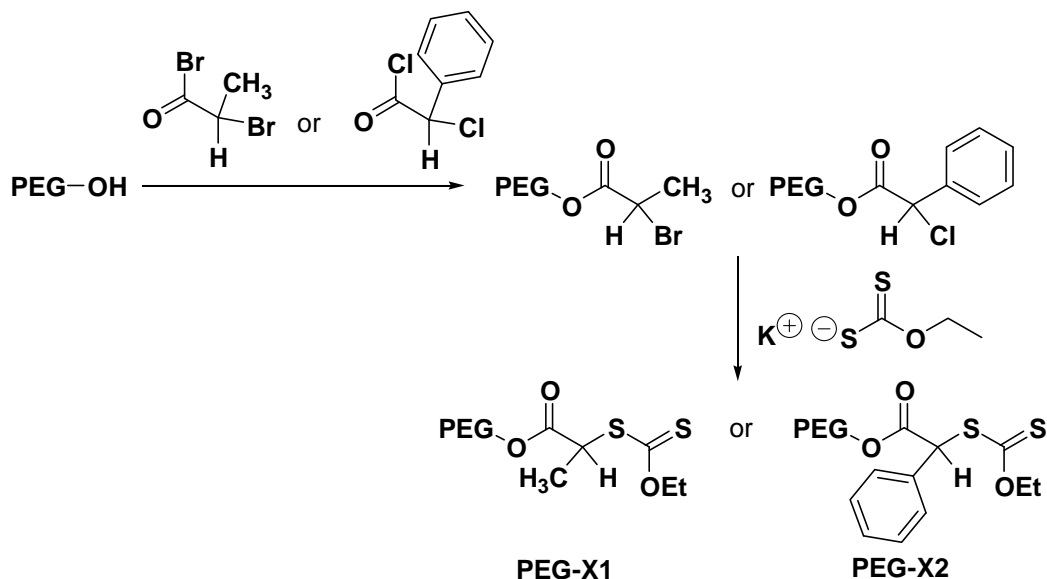
Scheme 6.1 : Synthetic schemes for the modification of hydroxyl end-functional poly(ethylene glycol) monomethyl ether (PEG-OH) into xanthate derivatives PEG-X1 and PEG-X2 for the use as macromolecular chain-transfer agents.

Initiation: by initiator-derived primary radicals

I• + M ⟶ IM•
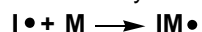
Reinitiation: by the macromolecular chain-transfer agent-derived radicals

PEG⟍R• + M ⟶ PEG⟍RM•

Initialization

$$\text{PEG}\diagdown_{R}\overset{S}{\underset{OEt}{\diagup}}S \;+\; \text{PEG}\diagdown_{RM\bullet} \;\rightleftharpoons\; \text{PEG}\diagdown_{R}\overset{S}{\underset{OEt}{\diagup}}\overset{\bullet}{\diagup}S\diagdown_{MR}\text{PEG} \;\rightleftharpoons\; \text{PEG}\diagdown_{R\bullet} \;+\; S\overset{}{\underset{OEt}{\diagup}}S\diagdown_{MR}\text{PEG}$$

Main RAFT equilibrium

$$\text{PEG}\diagdown_{M_n}\overset{S}{\underset{OEt}{\diagup}}S \;+\; \text{PEG}\diagdown_{M_p\bullet}\,(M) \;\rightleftharpoons\; \text{PEG}\diagdown_{M_n}\overset{S}{\underset{OEt}{\diagup}}\overset{\bullet}{\diagup}S\diagdown_{M_p}\text{PEG} \;\rightleftharpoons\; \text{PEG}\diagdown_{M_n\bullet}\,(M) \;+\; S\overset{}{\underset{OEt}{\diagup}}S\diagdown_{M_p}\text{PEG}$$
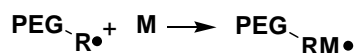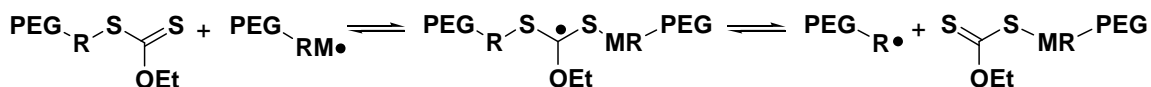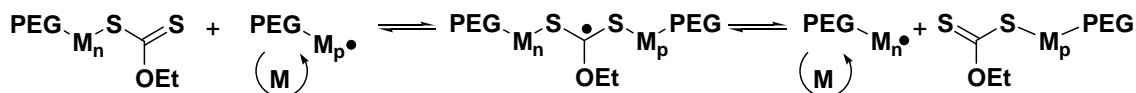
Termination by recombination

PEG-M_n• + •M_p-PEG ⟶ PEG-M_(n+p)-PEG
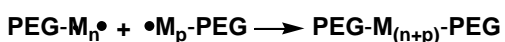
Scheme 6.2 : Reaction scheme for block copolymer synthesis from poly(ethylene glycol) (PEG)-based macromolecular chain-transfer agents via reversible addition-fragmentation transfer (RAFT)-mediated polymerization.

Comparison between the two macroCTAs

Two xanthate-end-functional PEGs were prepared (Scheme 6.1) in order to investigate the effect of the structure of the macromolecular leaving group on the ability to generate copolymers with poorly stabilized vinyl monomers. The two macroCTAs only differ by the nature of one of the substituents on the carbon adjacent to the xanthate, namely a methyl substituent for EG$_{75}$-X1 versus phenyl for EG$_{75}$-X2. The polymerization conditions and conversions are presented in Table 6.1. The macroCTA-mediated polymerization is expected to proceed as shown in Scheme 6.2, in accordance with the generally accepted mechanism of RAFT-mediated polymerization.

Table 6.1: Polymerization conditions, conversions and molecular weight data of the diblock copolymers for the comparison of the two macromolecular chain-transfer agents (macroCTAs) EG_{75}-X1 and EG_{75}-X2.

Ref	Monomer	Molar ratios [monomer]: [xanthate]: [initiator]	macro-CTA	Time (h)	T (ºC)	α (%)	$M_{n,target,a}$ (g·mol^{-1})^a	$M_{n,SEC}$ (g·mol^{-1})^b
1a	VAc	98:1:0.2	EG_{75}-X1	14	54	90^c	7600	6600
1b	VAc	47:1:0.2	EG_{75}-X1	12	54	15^c	600	530
1c	NVP	98:1:0.2	EG_{75}-X1	15	60	98^d	11000	12200
1d	NVP	70:1:0.2	EG_{75}-X1	15	60	65^d	5100	5700
1e	VAc	98:1:0.2	EG_{75}-X2	15	54	<2^c		
1f	VAc	47:1:0.2	EG_{75}-X2	14	54	<2^c		
1g	NVP	70:1:0.2	EG_{75}-X2	15	60	<2^d		
1h	NVP	98:1:0.2	EG_{75}-X2	15	60	<5^d		

^{a} number average molecular weight (M_n) of the poly(vinyl monomer) block based on initial molar ratios of the polymerization mixture and conversion with the assumption that each chain contains one xanthate chain-end and that the initial xanthate was quantitatively converted. ^{b} determined as the ratio of the xanthate signals to monomer backbone signals via ^{1}H-NMR spectroscopy analysis of the polymer after dialysis and freeze-drying. ^{c} determined gravimetrically after evaporation of the solvent and monomer. ^{d} determined gravimetrically after precipitation of the polymer from diethyl ether.

Block copolymers were obtained with the macroCTA EG_{75}-X1 and both NVP and VAc monomers (experiments 1a-d). The incorporation of VAc units into the macroCTA was evidenced by ^{1}H-NMR spectroscopy. Experiment 1b was stopped after 15 % monomer conversion so as to obtain a short PVAc block for end-group characterization (approximately 6 VAc units per chain). The areas of interest in the ^{1}H-NMR spectrum of the starting macroCTA (EG_{75}-X1) and the resulting EG_{75}-VAc$_6$ (Fig.6.1) are indicated with an arrow. The integration value for the xanthate end-group signals (peaks a and g) did not decrease during the polymerization but the peaks became broader due to the introduction of tacticity in the copolymer. The signal for the methine proton of the VAc unit in α-position from the xanthate was identified at 6.6 ppm (j').[22] The reinitiating group signals (b and f) showed increased multiplicity and a shift to lower fields indicating their quantitative conversion to macromolecular species. Experiment 1b confirmed that the macromolecular xanthate was quantitatively converted to oligomeric VAc adducts even at low conversion. NVP cannot easily be removed by evaporation under vacuum as is the case with VAc. The polymer has to be precipitated many times to ensure successful removal of the monomer, whose signals otherwise overlap with some of the macroCTA signals. Another problem is that the characteristic C*H*-S signals are spread between 5.5 and 6.1 ppm in the case of NVP resulting in decreased resolution. As a result the

experiment was not repeated with NVP but instead characterization of the block copolymers presented in the second part of the chapter aimed at detecting the possible presence of unmodified macroCTA.
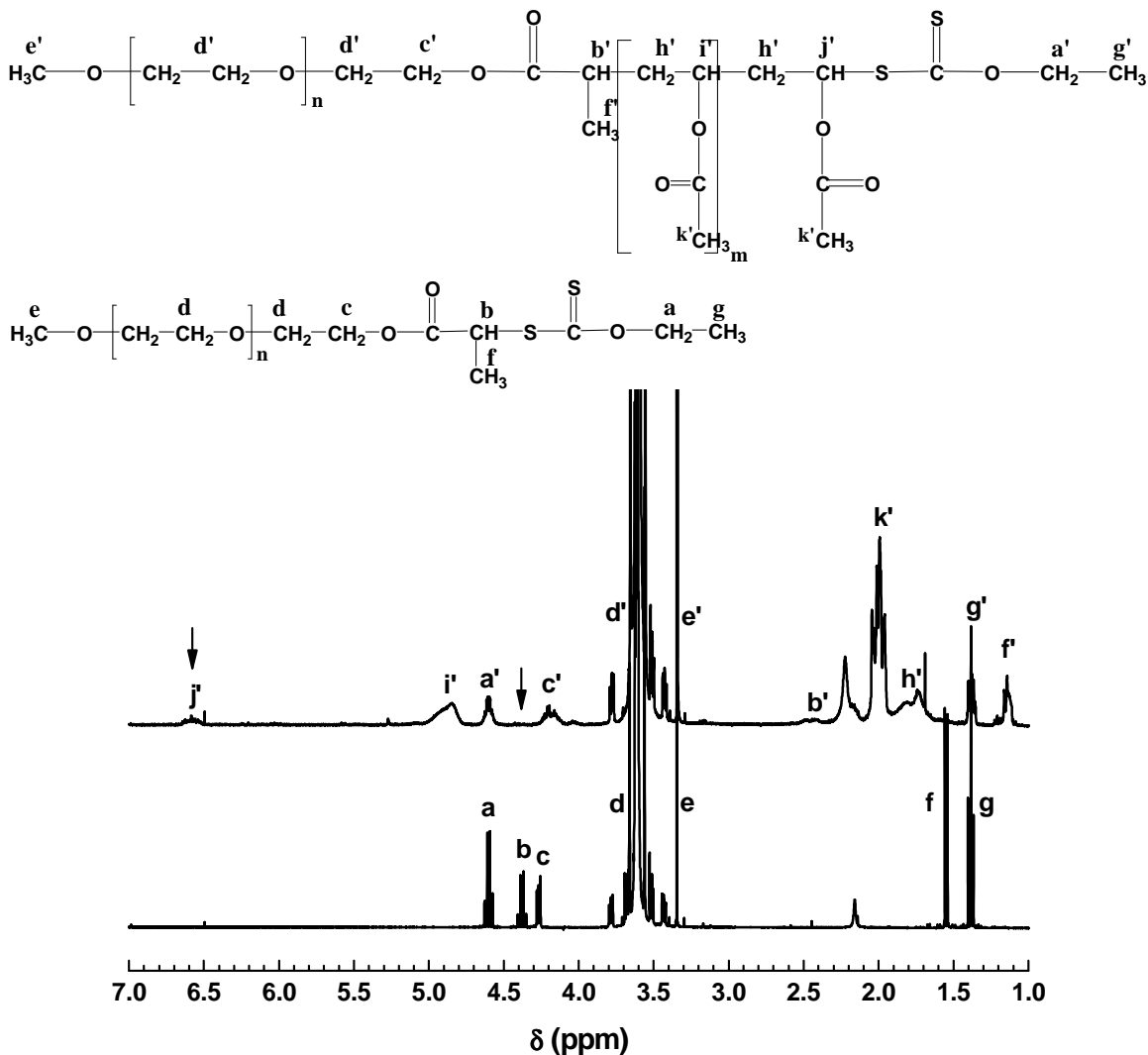

Figure 6.1: 600 MHz ^{1}H-NMR spectra in CDCl$_3$ of the starting macromolecular chain-transfer agent EG$_{75}$-X1 (bottom) and of the copolymer EG$_{75}$-VAc$_6$ (top) and their respective structures.

In Table 6.1, experimental molar masses from NMR are listed instead of those based on SEC. The main reason is that hydrodynamic volumes of PEG strongly deviate from those of PMMA (which was used as calibration standard). SEC results of the block copolymers in this study are therefore likely to be a very poor reflection of the true molar mass. Below it will be shown by HPLC that there was no significant homopolymer in the

reaction mixture. Therefore the values calculated from NMR most likely provide a good estimation of average molar masses.

In the presence of the macroCTA EG_{75}-X2, no copolymer was obtained at all, regardless of whether VAc or NVP was used (experiments 1e-h). At this point it is important to report that the reproducibility of the experiments was poor in terms of conversion. In preliminary work, two xanthate-mediated NVP polymerization experiments were conducted in parallel where the initial polymerization mixture was divided into two flasks. Both flasks were subjected to four freeze-pump-thaw cycles in parallel on the same Schlenk line and were heated in the same oil bath. The final yield was 44 % in one flask and 69 % in the other. Consequently the yield cannot strictly be taken as an indication of the efficiency of the CTA (nor initialization time). Nonetheless, the complete and systematic absence of polymerization when EG_{75}-X2 was used is remarkable. In a blank experiment, PVP was obtained via simple free-radical polymerization in the presence of EG_{75}-OH with quantitative conversion within 3.5 h. In another experiment, PVP was obtained via polymerization in the presence of EG_{75}-OH and the low molecular weight CTA *S*-(2-ethyl propionate)-(*O*-ethyl xanthate), (X13) with 86 % yield in 17 h. These two experiments confirm that EG_{75}-OH does not inhibit the polymerization of NVP in the presence or absence of xanthate species. It was reported in the literature that impurities present in the CTA or traces of oxygen in the polymerization mixture may inhibit the xanthate-mediated polymerization of VAc.[23] In our case it cannot be strictly excluded that impurities were at the origin of the inhibition, however the only end-groups detected in the macroCTAs via 600 MHz ^{1}H-NMR were xanthate end-groups. Moreover the synthetic pathway for both macroCTAs being similar, it is unlikely that impurities able to fully inhibit the polymerization were present in only one of the two macroCTAs.

In order to pinpoint the origin of the inhibition we investigated the polymerization of NVP and VAc with low molecular weight xanthate analogues. We reported earlier that when NVP and VAc were polymerized in the presence of a xanthate the nature of the leaving group played a determining role in the mechanism of initialization and in turn in the level of control achieved[22] (see also chapter 4). A fine balance can be reached where

the R group is good enough a leaving group so that R· radicals are formed preferentially upon fragmentation of CTA adduct radicals and where R· is reactive enough towards the monomer to enable fast reinitiation. This feature is crucial for the synthesis of well-defined block-copolymers. If the macro-R group is not good enough a leaving group, new chains will be initiated late in the polymerization resulting in increased polydispersity. If the macro-R group is not able to efficiently reinitiate polymerization, termination and/or transfer of the macroCTA will occur, leading to heterogeneous homopolymer / copolymer mixtures or no polymerization at all. We extended our initialization studies via *in situ* ^{1}H-NMR spectroscopy to NVP and VAc polymerization with the CTAs *S*-(2-ethyl propionate)-(*O*-ethyl xanthate) (X13) and *S*-(2-ethyl phenylacetate)-(*O*-ethyl xanthate) (X14), which produce radicals with a similar chemical environment as EG_{75}-X1 and EG_{75}-X2, respectively (Fig. 6.2).
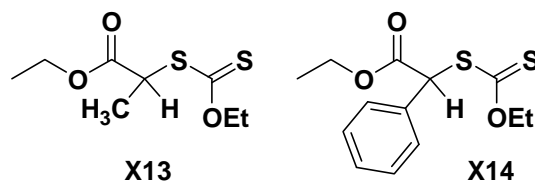
Figure 6.2: structure of the low molecular weight chain transfer agents used in the initialization study via *in situ* ^{1}H-NMR spectroscopy.

We found that with X13, initialization was highly selective and fast with VAc, whereas loss of selectivity was observed with NVP (Figure 4.8 in chapter 4). The concentration in single monomer adduct with NVP started decreasing while peaks corresponding to higher adducts appeared before all of the starting X13 was consumed. The lack of selectivity in the initialization step means that the monomer concentration decreases from the beginning of the reaction to form oligomeric or polymeric species in spite of the presence of the initial CTA. The consequence is that chains are formed later in the polymerization, which leads to an increase in the polydispersity index and could possibly result in the presence of initial CTA in the final polymer. When using a macroCTA, the final mixture may even contain some starting homopolymer. Although initialization was not completely selective with NVP, less than 1.5 equivalents of NVP were necessary for complete conversion of the CTA X13. This is an indication that NVP and 2-ethyl propionate-derived radicals have comparable radical stability. The number of monomer units per chain at the end of initialization will depend on the initial

stoichiometry. The lower the initial concentration in CTA, the higher the number of monomer additions prior to quantitative conversion of the CTA.

On the contrary, initialization was highly selective with X14 for both monomers (Figures 4.11 and 4.12 in Chapter 4). This means that the only reaction taking place was the conversion of one monomer unit with one X14 equivalent to form single monomer adducts. This feature can be very interesting to ensure optimized control of the polymerization. The study on the initialization behavior suggested that X14 could be a better CTA to control the polymerization of NVP than X13. Nonetheless the initialization time should also be taken into consideration. 220 min were necessary for the initial CTA X14 to be fully converted to its single monomer adduct with NVP, whereas the concentration in X13 was halved within 10 min and X13 was fully converted within 90 min. With the monomer VAc, initialization was extremely slow. 68 % of the initial X14 was still present after 18.2 h (Figure 4.13 in chapter 4). The leaving group in X14 is expected to be more stable than that of X13 because of the significantly stronger radical stabilizing effect of the phenyl substituent compared to a methyl substituent. Therefore fragmentation of intermediate radicals towards the release of the R group should be favored in X14 compared to X13. As we observed that the rate of conversion of the CTA is lower in the case of X14 than X13, the rate-limiting step must be the rate of addition of the leaving radicals onto the monomer, *i.e.* the reinitiation step. Although block copolymer synthesis involves higher monomer to CTA ratios, it is likely that initialization remained selective with EG$_{75}$-X2. Thus the apparent inhibition of the polymerization by EG$_{75}$-X2 can be attributed to the poorer efficiency of the macroR group with a phenyl substituent to reinitiate the polymerization, at least in the case of VAc. This is supported by the ^{1}H-NMR spectrum of the PEG recovered from the failed copolymerization with VAc. It indicated that the xanthate moieties were still present while approximately 40 % of the leaving group had been modified. Signals similar to that of the low molecular weight adducts were detected in the region 6.3 – 6.9 ppm (Figure 6.3), which suggest that selective initialization may have occurred with the macroCTA EG$_{75}$-X2 and that the process was not complete when the experiment was stopped. Peak assignment of the PEG end-groups was not achieved due to the high molecular weight of the CTA. However

these results indicate that the absence of polymerization was not due to degradation of the xanthate functionality.
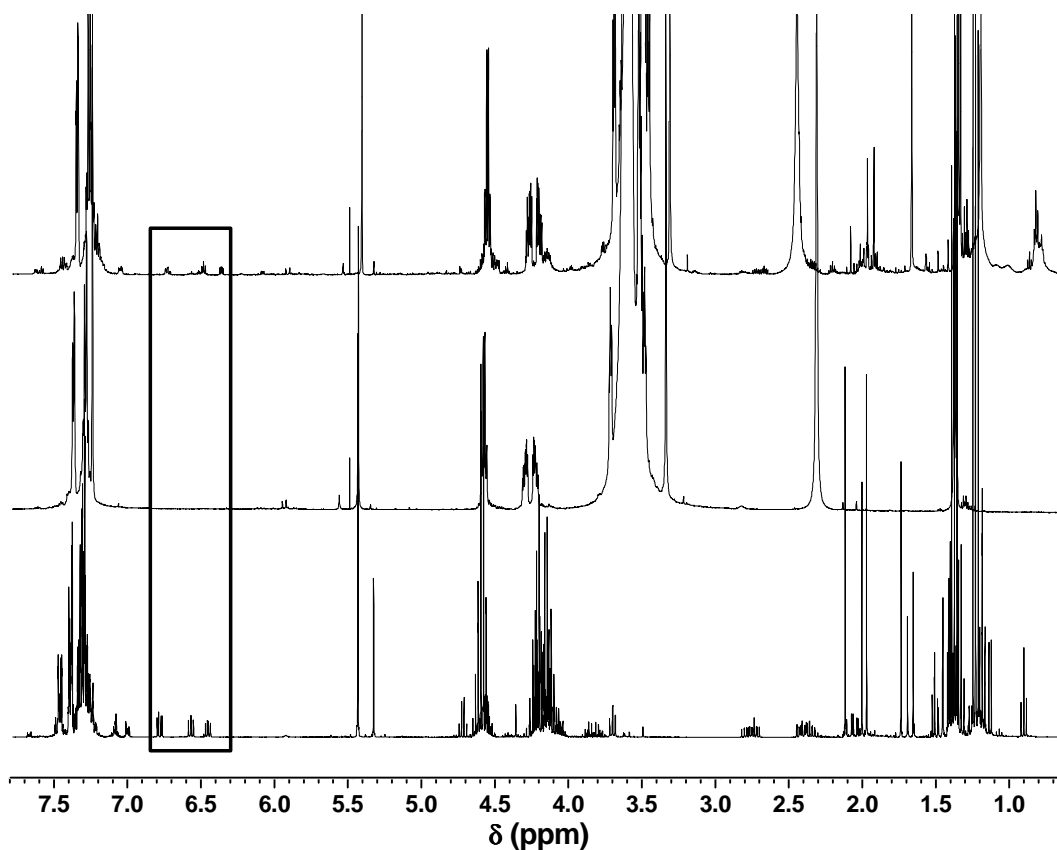
Figure 6.3: ^{1}H-NMR spectrum at time = 18.2 h during the *S*-(2-ethyl phenylacetate)-(*O*-ethyl xanthate) (X14)-mediated polymerization of vinyl acetate in C_6D_6 at 70 ºC (bottom), starting poly(ethylene glycol) macroCTA EG_{75}-X2 (middle) and resulting product after an attempt to polymerize VAc for 15 h at 54 ºC in THF with EG_{75}-X2 (top).

After the attempted polymerization with NVP for 15 h, a large proportion of xanthate end-groups were missing. Heating of the polymerization was pursued for 48 h and polymerization of NVP occurred on the longer time scale. 65 % monomer conversion was achieved but further characterization indicated that the sample was a mixture of homopolymers and possibly a fraction of block copolymer. Initialization is slower with X14 than X13, but it may not be the only cause for the apparent inhibition with NVP in the polymerization mediated by X14. For further comparison, NVP was polymerized in the presence of X14 under the same conditions as for the block copolymer synthesis. 19 % yield was obtained within 15 h. NMR spectroscopic analysis revealed the presence of xanthate end-groups but also a significant amount of other end-groups, mostly unsaturated species in a molar ratio 60:40 (xanthate:unsaturated). The same ratio of end-

groups was obtained when polymerization was carried out in bulk. In conclusion, the case of NVP is unclear and a combination of low reinitiation efficiency and the occurrence of side-reactions affecting the xanthate moieties seem to be responsible for the failure to obtain PEG-PVP block copolymers from EG_{75}-X2.

Characterization of the block copolymers

The macroCTAs EG_{75}-X1 and X1- EG_{90}-X1 were used to mediate another batch of polymerizations of NVP listed in Table 2. The copolymer homogeneity was characterized in terms of molecular weight distribution and copolymer composition. The molecular weight distributions were analyzed using SEC so as to estimate the level of control over chain-length. HPLC was used to investigate the presence of homopolymers.

Size-exclusion chromatography (SEC)

The macroCTAs and copolymers with NVP were analyzed in HFIP. The livingness of NVP polymerization mediated by the macroCTA EG_{75}-X1 is illustrated in Figure 6.4. Two polymerizations were carried out in parallel at 60 ºC with the same initial composition. The polymerizations were stopped at 6 h and 15 h, respectively. The SEC chromatograms indicate a shift of the molecular weight distributions to higher M_n as conversion increased.

Number average molecular weight (M_n) and polydispersity index (PDI) calculations were based on PMMA calibration. While the values for M_n of the homo-PVPs prepared via xanthate-mediated polymerization were generally close to the theoretical ones (see ref. 2f, table 2), the M_n of the PEG-based copolymers were systematically significantly higher. The M_n of the PEG used as a CTA (ref. 2b, table 2) as determined by ^{1}H-NMR was 3300 g·mol^{-1}, whereas the SEC analysis gave a value of 11900 g·mol^{-1}. Such a discrepancy is common in SEC chromatography, which separates the macromolecules according to their hydrodynamic volume and thus depends on the interactions between the polymer and the elution solvent.
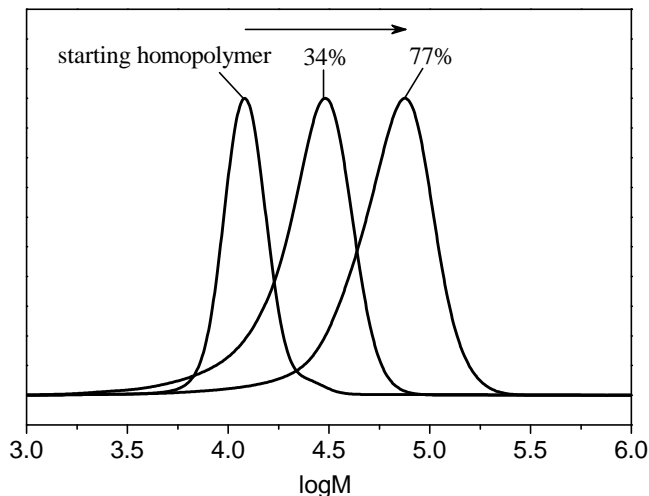
Figure 6.4**:** Evolution of the molecular weight distributions in the macromolecular xanthate EG_{75}-X_1-mediated polymerization of NVP as a function of conversion. From left to right: starting homopolymer EG_{75}-X_1 ($M_{n,SEC}$ = 12000 g·mol^{-1}, PDI = 1.06); diblock copolymer EG_{75}-PVP (reaction time = 6 h, conversion = 34 %, $M_{n,SEC}$ = 19200 g·mol^{-1}, PDI = 1.43); EG_{75}-PVP (reaction time = 15 h, conversion = 77 %, $M_{n,SEC}$ = 52300 g·mol^{-1}, PDI = 1.35). The molar ratios [NVP]:[EG_{75}-X1]:[AIBN] were 450:1:0.2. The reaction was carried out at 60 ºC in a 50 wt% solution in tetrahydrofuran.

The fact that the M_n values obtained for the diblock copolymers (ref. 2c and 2d, table 2) match the sum of the M_n of the starting PEG and the theoretical M_n calculated for the PVP block may be only a coincidence. Nonetheless, the chromatograms presented in Figure 6.5 provide valuable information. The experimental M_n increased with the NVP content in the copolymer. As predicted by the RAFT mechanism, lower CTA concentrations resulted in increased M_n values. The low polydispersity of the PEG macroCTA was retained in the copolymers. These results indicate the ability of the PEG-based macroCTA EG_{75}-X_1 to control the polymerization of NVP. Further qualitative analysis of the chromatograms revealed however that a second low molecular weight distribution accounting for less than 10 % of the total integration was present in most block-copolymer samples. Unfortunately SEC provides little information on the homogeneity of the sample. For instance ref. 2f (table 2), which is a mixture of narrowly distributed PVP and PEG homopolymers (NVP_{77}-X1 + EG_{75}-OH), appears as a monomodal distribution (Fig. 6.5d). The substantially higher elution volume for this sample, compared with the elution volume for the triblock copolymer which has similar NVP content (Fig. 6.5e), is an indication that the structures are different. The difference in elution volumes is consistent with the assumed structure of the polymers (*i.e.*

homopolymer mixture versus triblock copolymer). Nonetheless this example illustrates the need to complement SEC with other separation techniques. In the following section we present the outcome of HPLC analyses, which aimed at determining the chemical homogeneity of the copolymers. Finally, let us remark that the SEC traces of the diblock copolymers do not display any detectable peak at lower retention volume than the main distribution. This observation is relevant for the examination of bimolecular termination products. Recombination between propagating diblock copolymer radicals would result in PEG-*b*-PVP-*b*-PEG triblock copolymers (Scheme 2). The presence of two PEG segments in the recombination product would result in a significantly higher hydrodynamic volume than the diblock-copolymers. The absence of signal corresponding to high hydrodynamic volume indicates that bimolecular termination between propagating diblock copolymer radicals did not occur to a significant extent.

Table 6.2: Molecular weight data for poly(vinylpyrrolidone) (PVP), poly(ethylene glycol) (PEG) and their block copolymers.

Ref	Experiment description	[M]/ [CTA]	α (%)	$M_{n,theo,\alpha}$ (g·mol^{-1})[a]	Theoretical (co)polymer composition	$M_{n,SEC}$[a] (g·mol^{-1})	PDI
2a	starting material	-	-	-	EG$_{75}$-OH	12100	1.06
2b	modified starting material	-	-	-	EG$_{75}$-X1	11900	1.06
2c	EG$_{75}$-X1-mediated diblock copolymerization of NVP	70	65	5100	EG$_{75}$-NVP$_{46}$	17000[b]	1.10
2d	EG$_{75}$-X1-mediated diblock copolymerization of NVP	450	77	38500	EG$_{75}$-NVP$_{347}$	52300[b]	1.35
2e	conventional radical polymerization of NVP with EG$_{75}$-OH	-	>99	-	EG$_{75}$-OH + PVP	30300[c]	2.71
2f	X13-mediated polymerization of NVP with EG$_{75}$-OH	89	86	9900	EG$_{75}$-OH + NVP$_{77}$-X13	9600	1.33
2g	X1-EG$_{90}$-X1-mediated triblock copolymerization of NVP	88	75	4200×2	NVP$_{38}$-EG$_{90}$-NVP$_{38}$	37700[b]	1.10
2h	hydrolysis of the diblock copolymer EG$_{75}$-NVP$_{46}$	-	-	-	EG$_{75}$-OH + NVP$_{46}$	8100[c]	1.42

(Co)polymerizations were carried out at 60 °C in 50 wt% solution in tetrahydrofuran with a ratio [xanthate]:[initiator] of 1:0.2. In experiment 2e, where no chain-transfer agent was used, the initiator concentration was the same as in experiment 2f ([monomer]:[initiator]=445). Polymerizations were carried out for 15 h, except for 2e, which was quantitative at 3.5 h and 2f, which was conducted for 17 h. Hydrolysis was carried out by stirring the diblock copolymer in aqueous potassium hydroxide at pH=12 at room temperature for 16 h. [a] number average molecular weight of the vinyl polymer block based on initial molar ratios of the polymerization mixture and conversion. [b] presence of a low molecular weight peak excluded from the calculations. [c] bimodal distribution resulting from the overlap of PEG and PVP homopolymer distributions..
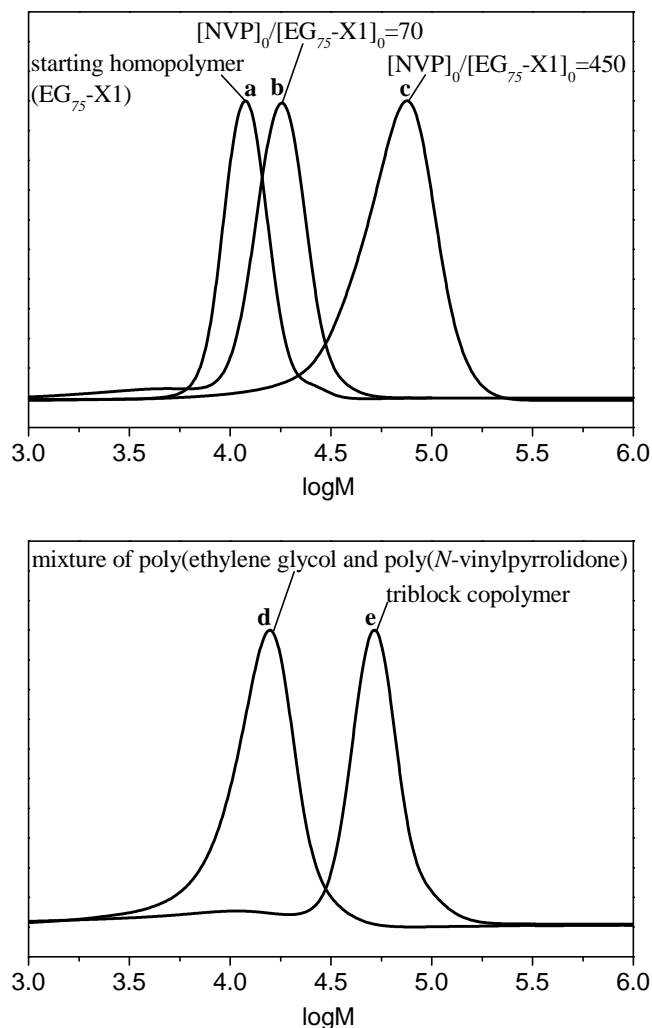
Figure 6.5: Size-exclusion chromatograms measured in HFIP of the macromolecular chain-transfer agent EG$_{75}$-X1 (a); the poly(ethylene glycol)-*b*-poly(NVP) diblock copolymers EG$_{75}$-NVP$_{46}$ (b) and EG$_{75}$-NVP$_{347}$ (c); the mixture of poly(ethylene glycol) (EG$_{75}$-OH) and poly(NVP) (NVP$_{77}$-X13) homopolymers (d) and the poly(NVP)-*b*-poly(ethylene glycol)-*b*-poly(NVP) triblock copolymer NVP$_{38}$-EG$_{90}$-NVP$_{38}$ (e).

EG$_{75}$-NVP$_{46}$ was obtained at 65 % conversion with the initial concentration ratio [NVP]$_0$:[EG$_{75}$-X1]$_0$ = 70:1 and EG$_{75}$-NVP$_{347}$ was obtained at 77 % conversion with the initial concentration ratio [NVP]$_0$:[EG$_{75}$-X1]$_0$ = 450:1.

HPLC analysis of the copolymers

Macko and Hunkeler[24] have compiled a variety of critical conditions reported in the literature, which enable the separation of PEGs according to the nature of the end-groups via reversed-phase HPLC. We chose an eluent mixture composed of water and acetonitrile, which was able to dissolve all homo- and copolymer samples. We used dual

detection, *i.e.* ELSD to identify macromolecular species and UV detection at a specific wavelength for the xanthate functionality (341 nm, results not shown) to help determine the chemical nature of the eluting species. Under these conditions, the chromatogram of the 75 % pure EG_{75}-X1 macroCTA (Fig. 6.6a) revealed the presence of four distinct chemical structures. The main peak at 4.6-5.7 mL showed a strong UV absorption and was attributed to the expected EG_{75}-X1 structure. Comparison with the chromatogram of the starting compound PEG monomethyl ether (EG_{75}-OH) and the absence of UV absorption (results not shown) revealed that the first peak in the PEG-xanthate derivative (1.4-1.7 mL) corresponds to EG_{75}-OH. The second main peak was most likely unreacted EG_{75}-Br (as confirmed by ^{1}H NMR spectroscopy).
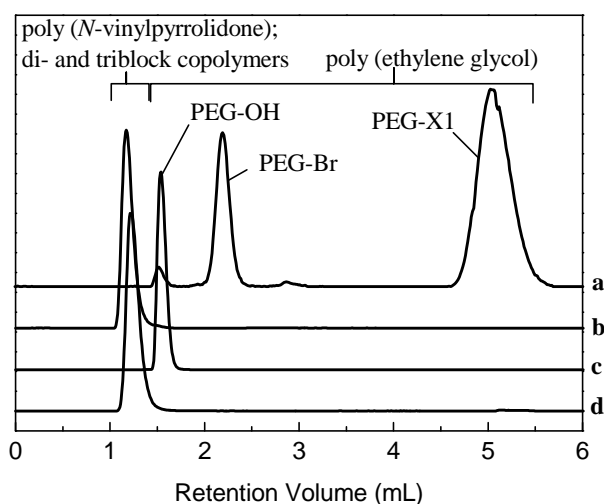
Figure 6.6: HPLC chromatograms at critical conditions for poly(ethylene glycol) monomethyl ether of a 75 % pure EG_{75}-X1 (PEG-X1) (a); poly(ethylene oxide) monomethyl ether EG_{75}-OH (PEG-OH) (b); diblock copolymer EG_{75}-NVP_{46} (c) and reference homopolymer NVP_{19} (d). The experimental details for the preparation of the diblock copolymer are in Table 2.

For the synthesis of the block copolymers, HPLC analysis was used to quantify the purity of the macroCTAs. Only EG_{75}-X1 samples which did not display any other signal than those corresponding to EG_{75}-X1 and EG_{75}-OH in low amounts were used. Both the diblock copolymer EG_{75}-NVP_{46} and the homopolymer NVP_{19}, used as a reference, eluted at very low elution volumes (less than 1.5 mL), before all PEG derivatives. The dead volume of the column was measured at 1.5 mL, which indicates that under these conditions the PVP sample and block copolymers containing a PVP segment elute under the size exclusion mode, whereas PEGs with OH or hydrophobic

end-groups eluted under the adsorption mode. PVPs and PEGs are both water-soluble polymers. This analysis showed that with the selected solvent composition, PVP has a more hydrophilic behavior than PEG. To enable separation of the block copolymers from PVP homopolymer, it is therefore required that the interaction between the PVP segments and the column be increased. The column being grafted with hydrophobic moieties, interactions with PVP are increased by decreasing the hydrophobicity of the eluent, *i.e.* increasing the water content.

In the following part gradient HPLC was applied, also named Gradient Polymer Elution Chromatography (GPEC).[25] The initial composition of the eluent was chosen close to the critical conditions for PVP and the final composition was more hydrophobic than the critical composition for PEGs. This way, separation of both PEG and PVP polymers is expected to occur in the adsorption mode. GPEC was preferred to isocratic HPLC at critical conditions for PVP so as to reduce the eluent volume and thus limit the time required to elute the more hydrophobic PEGs. As illustrated in Figure 6.7d, the PEG chromatogram still displayed efficient separation according to end-groups, with the same number of well-resolved peaks as under PEG critical conditions. The GPEC chromatogram of the diblock copolymer (Fig. 6.7b) unambiguously confirmed the absence of starting EG_{75}-X1 macroCTA. The copolymer peaks present a shoulder at higher elution volumes, which indicates the presence of EG_{75}-OH. No PVP homopolymer was detected. At this point it is particularly interesting to return to the interpretation of the SEC chromatogram of the same polymer (Figure 6.5, b). It displayed a peak of low intensity at a higher elution volume (logM ~ 3.5) compared to the copolymer main peak and starting PEG. GPEC results indicate that the diblock copolymer sample does not contain homopolymers except for unmodified PEG. The signal observed in SEC may therefore be due to the presence of low molecular weight PVP formed upon hydrolysis of the ester linkage between the two blocks. This may have occurred during storage of the compound or during the SEC analysis, possibly via trans-esterification with the eluent HFIP. The GPEC chromatogram of the copolymer NVP_{38}-EG_{90}-NVP_{38}, (Fig 6.7a) confirmed that the main structure was a copolymer, however it did not enable us to discern between di- and triblock copolymer. A small amount of PVP homopolymer was detected (2.0-2.2 mL).

Additional experiments were carried out to test the efficiency of the RAFT process in synthesizing PEG-derived block copolymers and the ability of GPEC to detect the presence of homopolymer contaminants. The diblock copolymer EG_{75}-NVP_{46} was hydrolyzed in basic aqueous solution (pH=12). The chromatogram of the resulting mixture presented two distinct peaks corresponding to homopolymers PVP and EG_{75}-OH (Fig. 6.7c). Quantitative hydrolysis of the ester linkage between the two blocks was assessed by the disappearance of the copolymer peak. This analysis demonstrated the usefulness of GPEC to identify the composition of polymer mixtures which were analyzed via SEC. It gave evidence for the origin of the bimodality of SEC chromatograms when related to the presence of the homopolymers.
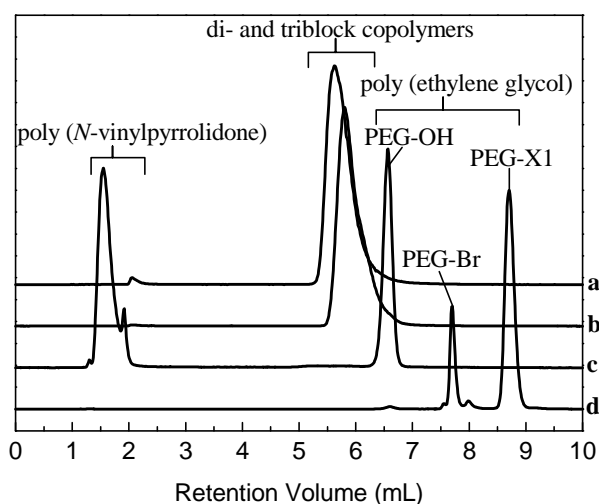
Figure 6.7: gradient polymer elution chromatograms of poly(ethylene glycol) (PEG) and poly(*N*-vinyl pyrrolidone) (PVP) homopolymers and their block copolymers. Triblock copolymer NVP_{38}-EG_{90}-NVP_{38} (a), diblock copolymer EG_{75}-NVP_{46} before (b) and after hydrolysis (c) and comparison with 75 % pure EG_{75}-X1 (d).

Hydrolysis was carried out by stirring the diblock copolymer in aqueous potassium hydroxide at pH=12 at room temperature for 16 h. The 75 % pure EG_{75}-X1 contained 20 % of unreacted EG_{75}-Br and less than 5 % of EG_{75}-OH, as determined by ^{1}H NMR spectroscopy. Experimental details for the block copolymers are given in Table 2.

Upon hydrolysis, the SEC chromatogram displayed a bimodal peak with a shoulder at higher elution volume than the starting EG_{75}-NVP_{46} (results not shown). The hydrolysis experiment was repeated with the diblock copolymer EG_{75}-NVP_{347}. Figure 6.8 shows the SEC traces of the diblock copolymer EG_{75}-NVP_{347} before and after hydrolysis, and the starting macroCTA as a reference. The longer PVP segment enabled a better separation between the distributions via SEC. The results are fully in accordance with the

observation from the GPEC experiments before and after hydrolysis. Let us remark that the hydrolysis was carried out at pH=12. As indicated by GPEC and SEC analyses, basic hydrolysis resulted in cleavage of the ester linkage between the two blocks. It is well know that xanthates, like other CTAs used for RAFT, also undergo degradation under basic conditions. In preliminary work on PVP homopolymers we observed that SEC traces indicated an increase in M_n upon hydrolysis at pH=12. This is most likely due to the formation of thiol end-groups, which can undergo oxidation, resulting in the formation of disulfide bridges between two chains and subsequent doubling of M_n.[26] Most probably this reaction at the chain-ends also occurs in the present case. It may account for the shoulder at high M_n values in the SEC chromatogram in Figure 6.8.
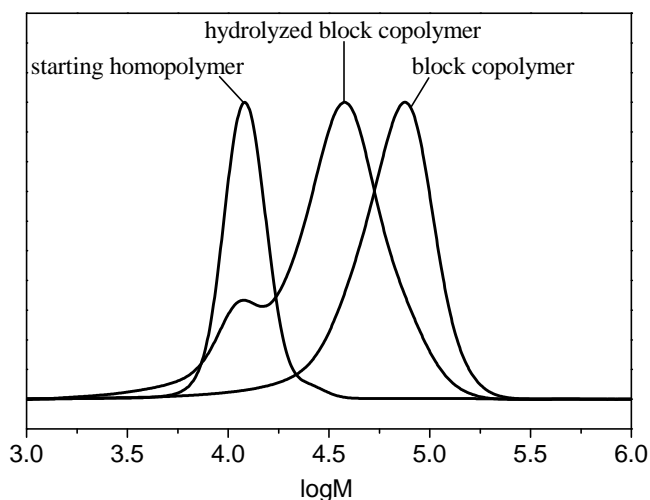
Figure 6.8. SEC traces of the starting homopolymer chain-transfer agent (EG$_{75}$-X1); the poly(ethylene glycol)-*b*-poly(NVP) diblock copolymer (EG$_{75}$-NVP$_{347}$); and its product of basic hydrolysis.

Hydrolysis was carried out by stirring the diblock copolymer in aqueous potassium hydroxide at pH=12 at room temperature for 16 h.

As indicated previously, the only observable impurity in the macroCTAs used for polymerization was unmodified PEG-OH. The following experiments were carried out to investigate the possible influence of PEG-OH on the polymerization of NVP and possible formation of copolymers via a mechanism other than RAFT at the macroCTA chain end. NVP was polymerized in the presence of unmodified EG$_{75}$-OH (ref. 2e, table 2) and in the presence of EG$_{75}$-OH and the low molecular weight xanthate X13 (ref. 2f, table 2). In the absence of RAFT agent, quantitative conversion of the monomer was reached within

3.5 h and high viscosity disabled magnetic stirring, whereas in the other polymerization experiment, where a xanthate RAFT agent was used, conversion did not exceed 86 % in 17 h. The high rate of monomer conversion and increase in viscosity, which could be related to the gel effect, are an indication of the uncontrolled character of the polymerization. The chromatograms of both products reveal the presence of homopolymers PEG-OH and PVP (Figure 6.9).
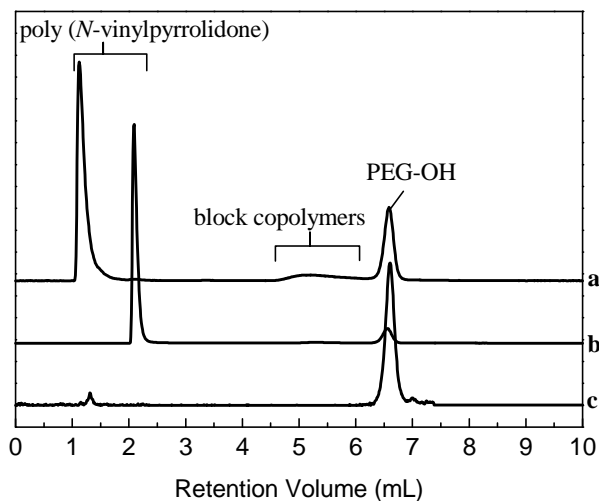
Figure 6.9: gradient polymer elution chromatograms of poly(ethylene glycol) monomethyl ether (PEG-OH) and mixtures with poly(NVP) prepared via conventional free-radical polymerization in the presence of EG_{75}-OH (Table 2, ref. 2e) (a), poly(NVP) (NVP_{77}-X13, Table 2, ref. 2e) prepared via xanthate-mediated polymerization in the presence of EG_{75}-OH and the chain-transfer agent X13 (b) and comparison with EG_{75}-OH (c).

PVPs did not elute at the same elution volume, which may be due to differences in molecular weights and/or end-groups. Traces of copolymer were detected in the sample containing PVP prepared without a CTA in the presence of EG_{75}-OH (Fig 6.9a, peak at elution volume 4.5 – 6.3 mL). A possible cause for copolymer formation is grafting via chain-transfer to PEG and subsequent growth of PVP branches.[27] Chain-branching is less likely to occur to a significant extent in the presence of a CTA.[28] This translates experimentally in the absence of copolymer signal (Figure 6.9b) where X13 was added to the polymerization mixture. These experiments confirmed that EG_{75}-OH mostly remained unmodified but did not inhibit either xanthate-mediated or conventional free-radical polymerization of NVP. They also confirmed that, although transfer to PEG may occur, it is not the origin for the formation of PEG-*b*-PVP copolymers in high yield as obtained with PEG-xanthate-mediated polymerization of NVP.

Separation of the PEG-*b*-PVAc polymers was not as challenging as PEG-*b*-PVP because of the significant difference in hydrophilicity of the two blocks. Gradient HPLC was performed with initial conditions close to the critical conditions for PEG. By increasing the hydrophobicity of the mobile phase the diblock copolymers were eluted followed by the PVAc homopolymers (Figure 6.10).
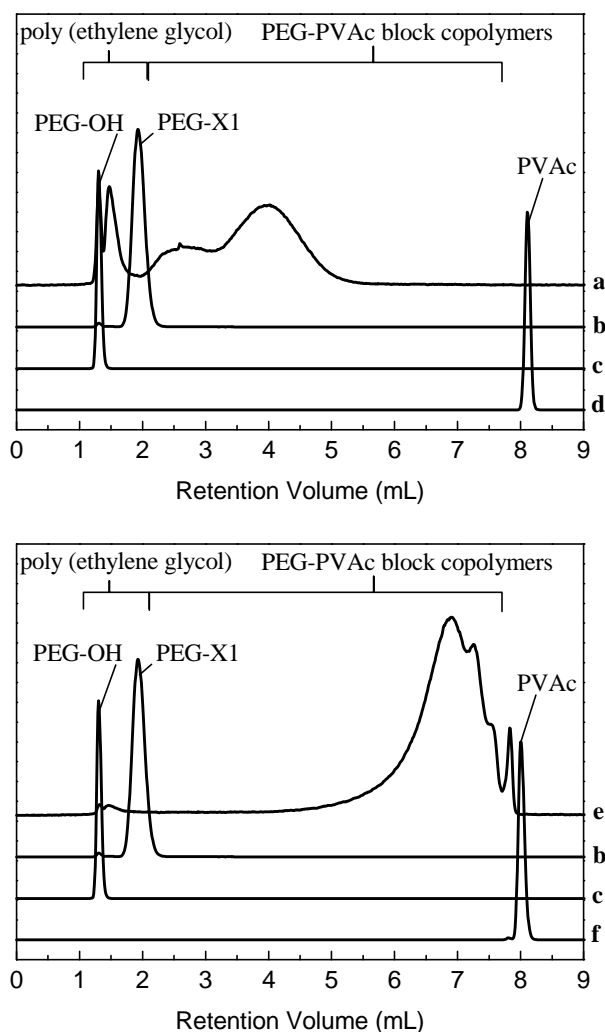
Figure 6.10: gradient polymer elution chromatograms of poly(ethylene glycol) (PEG) (EG$_{75}$-X1 (b) and EG$_{75}$-OH (c)); poly(vinyl acetate) (PVAc) homopolymers (VAc$_{28}$ (d) and VAc$_{73}$ (f)) and block-copolymer EG$_{75}$-VAc$_6$ and EG$_{75}$-VAc$_{88}$. VAc$_{28}$ (d) and VAc$_{73}$ (f) were used as references and were prepared in bulk in the presence of *S*-(2-ethyl propionate)-(*O*-ethyl xanthate) (X13).

As expected, a longer PVAc block resulted in increased retention time. The chromatogram of EG$_{75}$-VAc$_6$ confirmed that even at low conversion the macroCTA was fully converted and that the product was a copolymer of PEG with VAc. The separation revealed the presence of PEG-OH in all samples. As PEG-OH was only present in trace

amounts and since the peak area decreased relative to increased PVAc block length, it was probably due to incomplete conversion of the starting material rather than the blocks being hydrolyzed.

MALDI-ToF mass-spectrometry

The nature of the block copolymer end-groups was investigated via high resolution MALDI-ToF-MS, which was performed on low molecular weight polymers, typically in the range of 1000-8000 g·mol^{-1}. MALDI-ToF-MS spectra of copolymers are complex because a distribution in copolymer composition is superimposed to the distribution in degrees of polymerizations. Consequently, the observed complexity of the spectrum of the copolymer EG$_{75}$-VAc$_6$ compared to that of the homopolymer EG$_{75}$-X1 (Fig. 6.11 a and b) was a first indication that copolymerization was successful. The increase in molecular weights resulting from the growth of a PVAc block from the PEG macroCTA was evidenced by a shift of the distribution to higher m/z values. Willemse et al.[29] have demonstrated the usefulness of high resolution (reflector mode) MALDI-ToF-MS in copolymer analysis by reporting the complete structural analysis of polystyrene-*b*-polyisoprene samples. We applied their method to identify the chemical composition of the end-groups of PEG-*b*-PVAc samples. The type of comonomer sequence was already defined by the chemistry employed (only block copolymers or homopolymers could be obtained as opposed to random/statistical copolymers). Moreover the average composition of the copolymers had been determined as a function of the conversion in VAc and confirmed via ^{1}H-NMR spectroscopy, which greatly contributed to simplifying the calculations. The predictions for the expected structure of the diblock copolymer matched the experimental results (Fig. 6.11 c and d) with a correlation coefficient for the chemical composition of 0.955, confirming the presence of the xanthate end-group and the low degree of polymerization of the PVAc block.

In the case of NVP-containing homo- and copolymers we found significant fragmentation of the xanthate moiety even at low laser intensity and therefore we recommend other techniques, such as UV detection during SEC or HPLC analyses to investigate the presence of the xanthate at the chain-end.
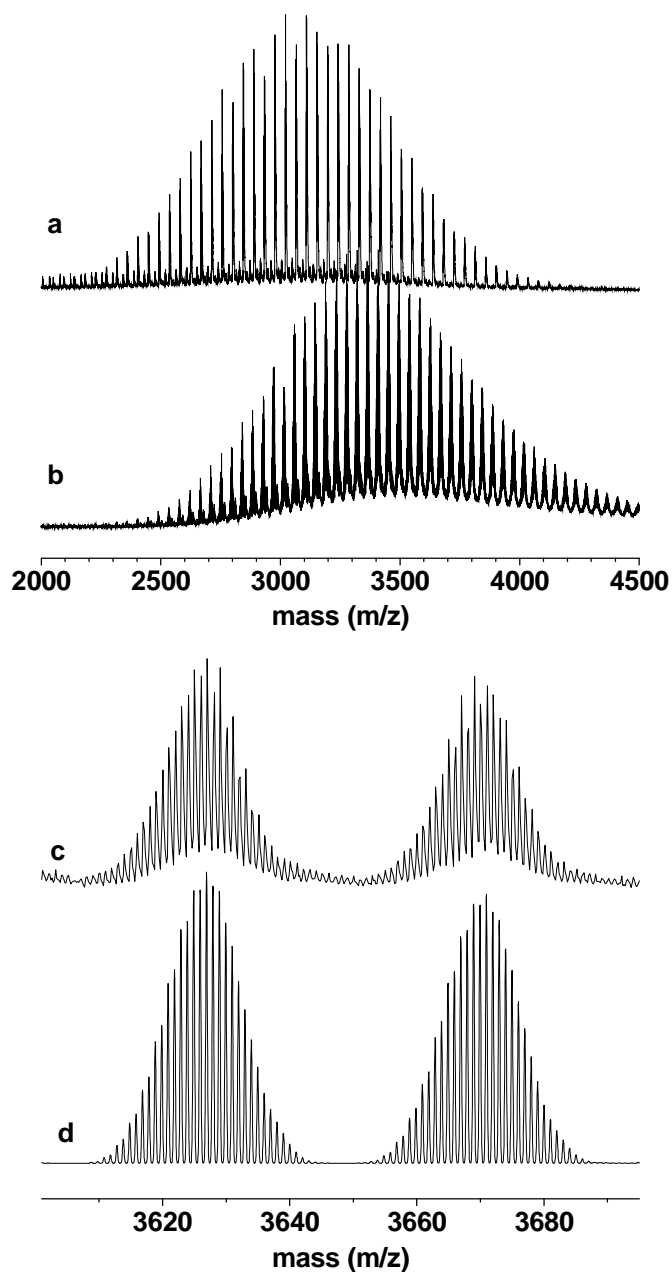
Figure 6.11: MALDI-ToF-MS spectra of the macromolecular chain-transfer agent EG$_{75}$-X1 (a) and the block copolymer EG$_{75}$-VAc$_6$ (b); expansion of the experimental spectrum of EG$_{75}$-VAc$_6$ (c) and predicted isotopic pattern for CH$_3$O-(CH$_2$CH$_2$O)$_n$-C(O)CH(CH$_3$)-(CH$_2$CH(O)COCH$_3$)$_m$-SC(S)OC$_2$H$_5$, K$^+$ (d).

Conclusions

The RAFT methodology was successfully applied to the synthesis of block copolymers of PEG with the poorly stabilized monomers VAc and NVP. Commercial mono or di-hydroxyl end-functional PEGs were modified into macroCTAs by

introduction of a xanthate moiety. Of the two monofunctional macroCTAs prepared, the one which had a leaving group stabilized by a phenyl substituent did not provide block copolymers with the monomers tested. The cause of inhibition was identified as low reinitiation efficiency with VAc, while the case of NVP was more complex and inhibition could be caused by a combination of low reinitiation efficiency and side reactions. The leaving group with a methyl substituent produced copolymers which were further analyzed by a combination of chromatographic and spectroscopic techniques. ^{1}H-NMR spectroscopy confirmed the absence of unmodified macroCTA in the final polymeric samples. MALDI-ToF-MS indicated the presence of the xanthate functionality on PEG-*b*-PVAc copolymers. Under the experimental conditions, only copolymers with a PVAc block could be successfully analyzed by MALDI-ToF-MS for end-group determination because significant fragmentation occurred with PVP-containing polymers. The control over the molecular weight distributions was estimated via SEC. Block copolymers with PEG-*b*-PVP and PVP-*b*-PEG-*b*-PVP where the PVP segments were short (M_n ~ 5000 g·mol^{-1}) were obtained with a very low polydispersity index (PDI~1.1). With a longer PVP segment (M_n ~ 39 000 g·mol^{-1}) an increase in polydispersity was observed (PDI~1.4). The presence of homopolymers was investigated via gradient HPLC. A good separation between PEG and PVP or PEG and PVAc and their block copolymers was achieved. The samples generally contained traces of hydroxyl functional PEG, most likely due to incomplete conversion during the synthesis of the macroCTA. Quantitative hydrolysis of a PEG-*b*-PVP sample was performed under basic conditions. Detection of PVP homopolymer and hydroxyl-functional PEG confirmed the presence and accessibility of the ester linkage between the blocks. The possible degradation of the block copolymers can be profitable for their use as biomaterials. While the molecular weight of the block copolymer can be sufficiently high to enable relatively long circulation time in the body, each of its fragments released upon hydrolysis might be short enough to enable renal clearance. This might be an interesting feature considering that both PEG and PVP have been used as drug carriers to improve the plasma half-life of drugs.[30]

Reference List

(1)   Durmaz, H.; Dag, A.; Altintas, O.; Erdogan, T.; Hizal, G.; Tunca, U. *Macromolecules* **2007**, *40*, 191-198.
(2)   Li, J.; Kao, W.J. *Biomacromolecules* **2003**, *4*, 1055-1067.
(3)   Harada, A.; Kataoka, K. *Macromolecules* **1995**, *28*, 5294-5299.
(4)   Ahn, C.-H.; Chae, S.Y.; Bae, Y.H.; Kim, S.W. *J. Control. Rel.* **2004**, *97*, 567-574.
(5)   Ranucci, E.; Spagnoli, G.; Sartore, L.; Bignotti, F.; Ferruti, P. *Macromol. Chem. Phys.* **1995**, *196*, 763-774.
(6)   Ranucci, E.; Tarabic, M.; Gilberti, M.; Albertsson, A.-C. *Macromol. Chem. Phys.* **2000**, *201*, 1219–1225.
(7)   Ranucci, E.; Macchi, L.; Annunziata, R.; Ferruti, P.; Chiellini, F. *Macromol. Biosci.* **2004**, *4*, 706-713.
(8)   Ranucci, E.; Ferruti, P.; Annunziata, R.; Gerges, I.; Spinelli, G. *Macromol. Biosci.* **2006**, *6*, 216-227.
(9)   Cheng, S.; Xu, Z.; Yuan, J.; Ji, P.; Xu, J.; Ye, M.; Shi, L. *J. Appl. Polym. Sci.* **1999**, *77*, 2882-2888.
(10)   Chen, X.; Gao, B.; Kops, J.; Batsberg, W. *Polymer* **1998**, *39*, 911-915.
(11)   Perrier, S.; Takolpuckdee, P.; Westwood, J.; Lewis, D.M. *Macromolecules* **2004**, *37*, 2709-2717.
(12)   Shi, L.; Chapman, T.M.; Beckman, E.J. *Macromolecules* **2003**, *36*, 2563-2567.
(13)   Destarac, M.; Charmot, D.; Franck, X.; Zard, S.Z. *Macromol. Rapid Commun.* **2000**, *21*, 1035-1039.
(14)   Stenzel, M.H.; Cummins, L.; Roberts, G.E.; Davis, T.P.; Vana, P.; Barner-Kowollik, C. *Macromol. Chem. Phys.* **2003**, *204*, 1160–1168.
(15)   Yamago, S.; Ray, B.; Iida, K.; Yoshida, J.-i.; Tada, T.; Yoshizawa, K.; Kwak, Y.; Goto, A.; Fukuda, T. *J. Am. Chem. Soc.* **2004**, *126*, 13908-13909.
(16)   Ray, B.; Kotani, M.; Yamago, S. *Macromolecules* **2006**, *39*, 5259-5265.
(17)   Nguyen, T.L.U.; Eagles, K.; Davis, T.P.; Barner-Kowollik, C.; Stenzel, M.H. *J. Polym. Sci. Part A: Polym. Chem.* **2006**, *44*, 4372–4383.
(18)   Wan, D.; Satoh, K.; Kamigaito, M.; Okamoto, Y. *Macromolecules* **2005**, *38*, 10397-10405.
(19)   Moad, G.; Rizzardo, E.; Thang, S.H. *Aust. J. Chem.* **2005**, *58*, 379-410.
(20)   Postma, A.; Davis, T.P.; Li, G.; Moad, G.; O'Shea, M.S. *Macromolecules* **2006**, *39*, 5307-5318.
(21)   Coote, M.L.; Krenske, E.H.; Izgorodina, E.I. *Macromol. Rapid Commun.* **2006**, *27*, 473-497.
(22)   Pound, G.; McLeary, J.B.; McKenzie, J.M.; Lange, R.F.M.; Klumperman, B. *Macromolecules* **2006**, *39*, 7796 - 7797.
(23)   Favier, A.; Barner-Kowollik, C.; P. Davis, T. *Macromol. Chem. Phys.* **2004**, *205*, 925-936.
(24)   Macko, T.; Hunkeler, D. *Adv Polym Sci* **2003**, *163*, 61–136.
(25)   Staal, W.J.; Cools, P.; Van Herk, A.M.; German, A.L. *J. Liq. Chrom.* **1994**, *17*, 3190-3199.

(26)   Lima, V.; Jiang, X.; Brokken-Zijp, J.; Schoenmakers, P.J.; Klumperman, B.; Van der Linde, R. *J. Polym. Sci., Part A: Polym. Chem.* **2005**, *43*, 959–973.

(27)   Zhang, Y.; Lam, Y.M. *J. Colloid Interface Sci.* **2005**, *285*, 80-85.

(28)   Pinto, M.A.; Li, R.; Immanuel, C.D.; Lovell, P.A.; Schork, F.J. *Ind. Eng. Chem. Res.* **2008**, *ASAP article Published on the Web 06/26/2007 DOI:10.1021/ie0609923*.

(29)   Willemse, R.X.E.; Staal, B.B.P.; Donkers, E.H.D.; vanHerk, A.M. *Macromolecules* **2004**, *37*, 5717-5723.

(30)   Kaneda, Y.; Tsutsumi, Y.; Yoshioka, Y.; Kamada, H.; Yamamoto, Y.; Kodaira, H.; Tsunoda, S.-i.; Okamoto, T.; Mukai, Y.; Shibata, H.; Nakagawa, S.; Mayumi, T. *Biomaterials* **2004**, *25*, 3259-3266.

Chapter 7: Endfunctional PVP

This chapter is dedicated to the study of the end-groups of poly(*N*-vinylpyrrolidone) (PVP) prepared via xanthate-mediated polymerization and synthesis of chain-end functional PVP. Polymers prepared via RAFT-mediated polymerization are end-capped with a thiocarbonyl thio functional group at the ω-chain-end. Chain-end functionality can be designed to match a particular application. A number of ways are reported in the literature to either convert the ω-end-group into a thiol functional group via aminolysis[1-3] or via reduction with sodium borohydride[4,5] or with lithium aluminum hydride. Alternatively the thiocarbonyl thio functionality can be removed via thermolysis[6], radical coupling[7] or radical reduction.[8-10] As a result, the polymer thermal stability is generally enhanced. It appeared that in the case of PVP prepared via xanthate-mediated polymerization removal of the xanthate end-group occurred under particularly mild conditions. Our first observations regarding the xanthate lability were brought about as the xanthate concentration decreased slightly during polymerization and dramatically upon isolation of the polymer via dialysis and subsequent freeze-drying. Thermolysis was studied as a means to simply remove the xanthate moiety from the chain-ends. Aminolysis and hydrolysis were evaluated for the preparation of PVP with reactive end-groups. Oligomers were prepared (M_n = 1000 – 5000 g·mol^{-1}) to ensure high resolution NMR spectra and MALDI-ToF-MS mass spectra and separation according to the end-groups via liquid chromatographic techniques. Finally the use of PVP with an aldehyde end-group for the preparation of PVP-lysozyme conjugates is reported.

Thermolysis

Xanthate removal from PVP oligomer chain-ends was quantitative when a solution of the oligomers in chlorobenzene was heated at reflux (131 ºC) for 16 h or upon heating the polymer in the dry state for a minimum of 16 h at 120 ºC under vacuum. Elimination of the xanthate moiety from single NVP adducts during initialization experiments at 70 ºC was presented in Chapter 5. When xanthate elimination affects

polymeric xanthate species, unsaturated chain-ends are obtained (Scheme 7.1). Unsaturated end-groups were identified in the NMR spectra of NVP oligomers after thermolysis; whereas the xanthate signal was no longer present (Figure 7.1). For example, NVP oligomers were prepared with *S*-(2-cyano-2-propyl) *O*-ethyl xanthate (X6) in bulk at 60 °C with 49 % yield in 6 h ($M_{n,\,theo,\,49\,\%} = 2640$ g·mol^{-1}). The spectrum of the oligomers isolated by precipitation from diethyl ether confirmed the presence of xanthate moieties and with the assumption that each chain was end-capped with one xanthate moiety we determined $M_{n,\,NMR} = 3000$ g·mol^{-1}. The xanthate end-group was quantitatively removed by heating the polymer at 120 °C for 16 h under vacuum. The resulting end-groups were identified as unsaturated moieties corresponding to more than 90 % of the initial xanthate end-groups.
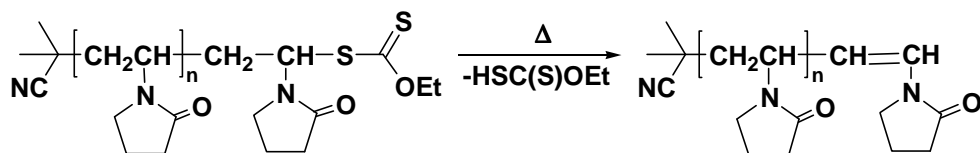
Scheme 7.1: Thermolysis of xanthate end-group from PVP.
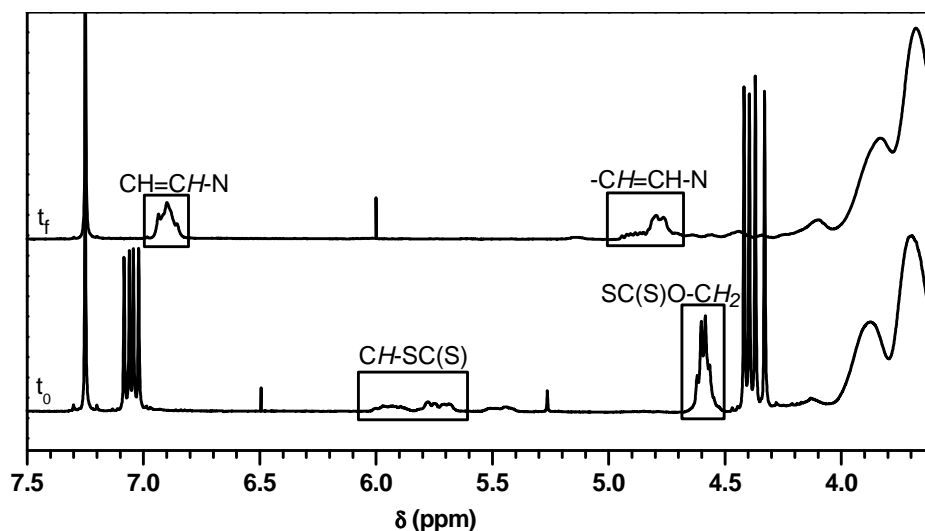
Figure 7.1: ^{1}H-NMR spectrum of thermolyzed PVP-xanthate recorded in CDCl$_3$. PVP was polymerized with *S*-(2-cyano-2-propyl) *O*-ethyl xanthate (X6) (t$_0$, bottom, $M_{n,\,SEC}$ = 2710 g·mol^{-1} (PMMA equivalents in HFIP), PDI = 1.21) and heated at 120 °C for 16 h (t$_f$, top) enlargement in the region relevant for the xanthate and unsaturated end-groups.

A comparative study by Perrier and coworkers on the thermal stability of low molecular weight RAFT agents pointed out the importance of the stabilizing group

structure and of the structure of the moiety adjacent to the thiocarbonyl thio moiety.[11] Xanthates had the lowest decomposition temperature (75 ℃ for *S*-(2-methyl propionate)-*O*-ethyl xanthate) followed by trithiocarbonates and eventually dithiobenzoates. This one and other studies[6,12] generally reported thermolysis at temperatures higher than 180 ℃ except for a conflicting study on poly(methyl methacrylate) oligomers where an onset temperature of 65 ℃ was reported for the loss of dithiobenzoate chain-ends.[13]

Thermolysis in the PVP-xanthate system occurs at relatively low temperature and leads to well-defined end-groups. Postma et al. studied the thermolysis of PVAc prepared with a xanthate CTA at temperatures above 200 ℃.[14] On the ^{1}H-NMR spectrum of the product they observed signals corresponding to methylene protons, which they attributed to a macromonomer forming via a radical backbiting reaction followed by a *β*-scission mechanism similar to what they proposed for poly(butyl acrylate) with loss of a trithiocarbonate end-group. This type of signals was not observed in the present study, suggesting that the unsaturated compound obtained upon thermolysis of xanthate end-groups from PVP chains is not a macromonomer suitable for free-radical polymerization. The SEC traces of the polymer before and after thermal treatment are very similar, indicating that chain-scission did not occur to a significant extent under these conditions, *e.g.* $M_{n,SEC}$ = 2900 g·mol^{-1}, PDI = 1.24 before thermolysis; $M_{n,SEC}$ = 3030 g·mol^{-1}, PDI = 1.22 after thermolysis.

PVP isolated by precipitation from diethyl ether generally displayed mainly xanthate signals and only weak signals (<5 % of xanthate end-groups) corresponding to unsaturated species. The average molar masses determined experimentally by ^{1}H-NMR ($M_{n,\,NMR}$, based on the ratio of integration of the xanthate to monomer peaks) were close to theoretical values ($M_{n,\,theo,\,\alpha}$, based on initial concentrations of xanthate and monomer) although slightly higher. These calculations are based on the hypothesis that one xanthate end-group is present at each chain-end. Deviations may have two origins: either not all of the initial xanthate was consumed to produce chain-ends or a portion of the chain-end underwent degradation. Note that irreversible transfer reactions do not influence the value of $M_{n,\,NMR}$. Discrepancies may therefore be due to:

- the presence of impurities in the initial xanthate (in this case the amount of xanthate introduced in the polymerization mixture is lower than the amount weighed and thus $M_{n, \text{theo}, \alpha}$ is underestimated);

- a "hybrid" behavior of the RAFT agent with the given monomer, where chains grow before all of the initial xanthate is consumed and low molecular weight xanthate species are eliminated from the polymer during post-polymerization treatment;

- degradation of xanthate species during the polymerization, which produces dead chains;

- loss of end-group functionality during post-polymerization treatment.

The hypothesis of hybrid behavior can be discarded in the system NVP-2-cyano-2-propyl *O*-ethyl xanthate (X6) because M_n increases linearly with conversion and initialization is selective, which means that the initial xanthate is consumed from the beginning of the polymerization.[15] The difference between $M_{n, \text{NMR}}$ and $M_{n, \text{theo}, \alpha}$ in the present example accounts for approximately 12 %. It may be explained partly by the loss of xanthate chain-ends due to xanthate elimination (unsaturated end-groups accounted for approximately 5 %) and partly by the presence of impurities in the xanthate (*Note that the main impurity identified in the NMR spectrum of X6 is tetramethyl succinonitrile (<2 mol%), which is not reactive in any way under our experimental conditions. Other impurities are traces of solvent*). Other causes for the loss of xanthate end-groups have not been identified but cannot be excluded.

Xanthate thermolysis: Effect of solvent polarity

The polarity of the solvent was suspected to play a role in the nature of the end-groups obtained via thermolysis. To investigate this point, PVP was heated at 80 ºC in DMSO-d_6 and C_6D_6 for which the Hildebrand solubility parameters are 29.7 and 18.8, respectively.[16] ^{1}H-NMR spectra were taken at different time intervals. In C_6D_6 solvent signals overlap with some relevant polymer end-group signals. C_6D_5H at $\delta = 7.15$ ppm

overlaps with unsaturated species and CH_2Cl_2 used in the dissolution / precipitation steps appears at $\delta = 4.35$ ppm and overlaps with O-CH_2- from the xanthate. Nevertheless it was possible to confirm the change in the structure of the end-groups. The initial spectrum displayed mostly the xanthate signals which decreased with heating time while unsaturated signals ($\delta = 4.5$-5.0 ppm and $\delta = 7.0$-7.4 ppm) appeared (Figure 7.2). The ratio of integrations of polymer to end-group signals in the initial sample did not exactly coincide with those measured for the same polymer in DMSO-d_6, D_2O or $CDCl_3$. This may be due to reduced solubility of PVP in C_6D_6 at 25 ºC and possibly selective solubilization of the end-groups compared to the polymer backbone and thus quantitative analysis was not performed.
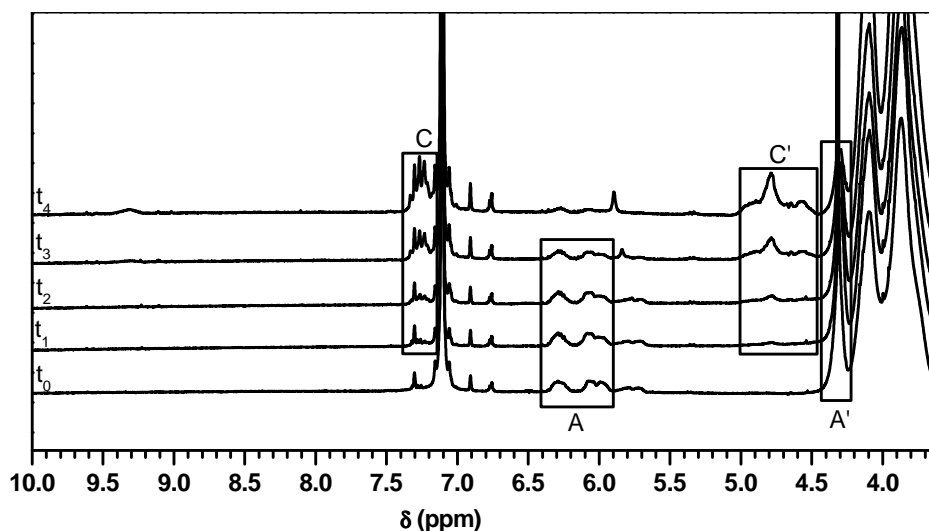
Figure 7.2: ^{1}H-NMR-monitored thermolysis of xanthate end-groups in C_6D_6. The polymer (0.060 g) was dissolved in C_6D_6 (0.8 ml). The solution was transferred to an NMR tube and heated in an oil bath at 80 ºC for 47.6h. During the experiment the tube was withdrawn from the oil bath and ^{1}H-NMR spectra taken at various time intervals: $t_1 = 1.8$; $t_2 = 3.6$; $t_3 = 23.6$ and $t_4 = 47.6$ h.

When heating was carried out on the polymer in solution in DMSO-d_6, the spectra were significantly different from those taken at the same time intervals in C_6D_6 and so were the end-groups in the final sample ($t_4 = 47.6$ h). Firstly, the xanthate signals (A and A' in Figure 7.3) were absent from the first spectrum taken at $t_1 = 1.8$ h, indicating fast transformation of the end-groups. Nonetheless the xanthate species were not directly converted to unsaturated end-groups, as indicated by the absence of signals C and C' in the spectrum at t_1. An intermediate species identified with signals B and B' formed readily. B was consumed as thermal treatment of the solution was pursued. The spectra at

$t_3 = 23.6$ h and $t_4 = 47.6$ h were identical, indicating that the end-groups formed after 23.6 h were thermally stable under these conditions. The end-groups identified in the spectrum at t_4 corresponded to unsaturated end-groups (C and C') and an aldehyde functionality (D), which account for approximately 60 % and 30 % of the initial xanthate end-groups, respectively.
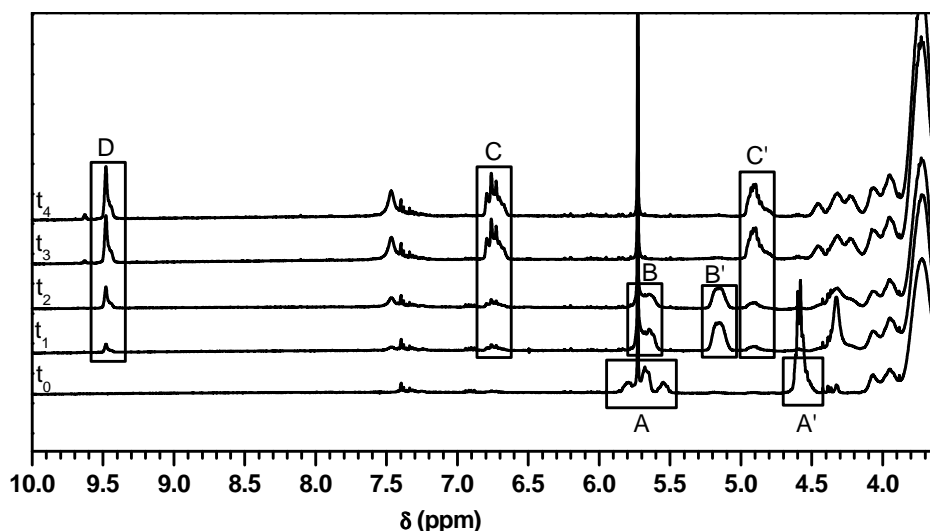
Figure 7.3: ^{1}H-NMR-monitored thermolysis of xanthate end-groups in DMSO-d_6. The polymer (0.060 g) was dissolved in DMSO-d_6 (0.8 ml). The solution was transferred to an NMR tube and heated in an oil bath at 80 ºC for 47.6h. During the experiment the tube was withdrawn from the oil bath and ^{1}H-NMR spectra taken at various time intervals: $t_1 = 1.8$; $t_2 = 3.6$; $t_3 = 23.6$ and $t_4 = 47.6$ h.

Identification of the intermediate structure and final aldehyde end-group are presented in following sections of this report. This comparative experiment gives evidence for two different pathways in the thermal degradation of PVP at moderate temperature (80 ºC) depending on the solvent. In both cases unsaturated chain ends were obtained but in the case of DMSO-d_6 aldehyde end-groups were also present. The presence of water in the thermolysis solution may be critical, as will be discussed in the next section.

Hydrolysis of xanthate end-groups

Hydrolysis of the xanthate at PVP chain-ends was first suspected as unexpected end-groups were obtained upon isolation of the polymer via dialysis followed by freeze-drying. Dialysis was often performed because removal of the monomer was rarely fully

efficient even after 3 dissolution / precipitation steps. The polymer (PVP prepared with *S*-(2-cyano-2-propyl) *O*-ethyl xanthate (X6), $M_{n,NMR}$ = 3400 g·mol^{-1}) was precipitated once from diethyl ether, redissolved in distilled water at a concentration of 25 g·L^{-1} and dialyzed for 24 h at room temperature. The polymer recovered after freeze-drying was analyzed with ^{1}H-NMR. The spectrum after dialysis indicates that monomer and residual solvent removal was efficient but only 40 % of the initial xanthate end-groups were still present (Figure 7.4). Apparent end-group loss could be the result of the loss of low M_n material during the dialysis process, which may have occurred in this experiment where the polymer M_n is close to the molecular weight cut-off of the dialysis tubing (SnakeSkin® pleated dialysis tubing, Pierce, 3.500 MWCO). However a new signal appeared upon dialysis at δ = 5.2 – 5.5 ppm, indicating the conversion of the xanthate to another type of chain-ends.
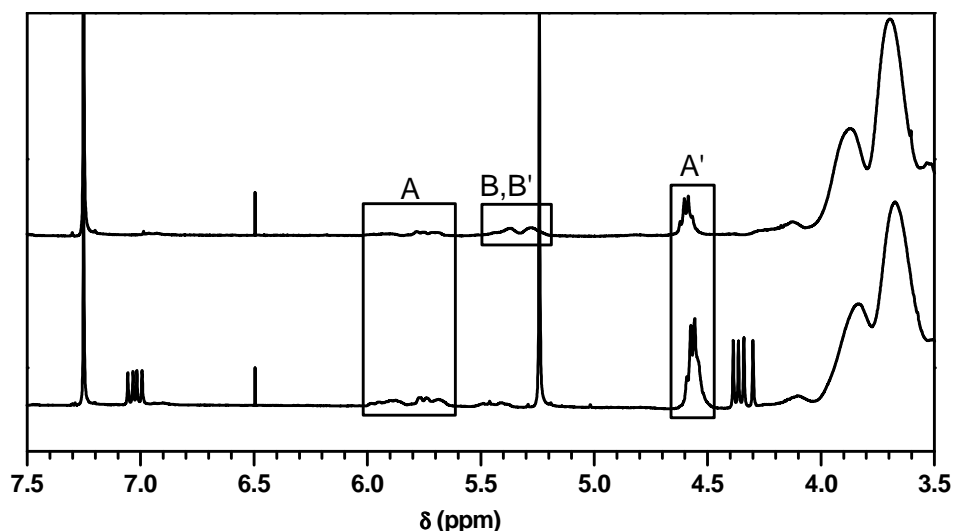
Figure 7.4: ^{1}H-NMR spectra of PVP in CDCl$_3$ before (bottom) and after dialysis at room temperature for 24 h (top).

The conversion of the end-groups was accelerated by preheating the dialysis solution. For this purpose the polymer in aqueous solution was incubated in a water bath at 40 ºC for 16 h. The resulting solution was dialyzed for 16 h at room temperature and freeze-dried. Upon this treatment the xanthate end-groups had been entirely removed (Figure 7.5). The new end-groups displayed signals (B, B') identical to those of PVP heated in DMSO-d_6 at 80 ºC for 1.8 h (Figure 7.3). After hydrolysis of the end-groups the polymer was heated at 120 ºC for 20 h under vacuum in the absence of solvent. The final

end-groups were aldehyde end-groups accounting for more than 90 % of the initial xanthate end-groups as measured in the precipitated sample. Note that the temperature of 120 ℃ was required for quantitative conversion of peaks B and B' to D, however the presence of aldehyde end-groups was detected at lower temperature (*e.g.* 20 % after 5 h at 80 ℃; 40 % after 29 h at 80 ℃; 60 % after an additional 5 h at 100 ℃). The nature of the endgroup was confirmed via ^{13}C NMR spectroscopy. The signal at 201 ppm is characteristic for an aldehyde functionality and displays the multiplicity and poor resolution of a polymeric signal (Figure 7.6).
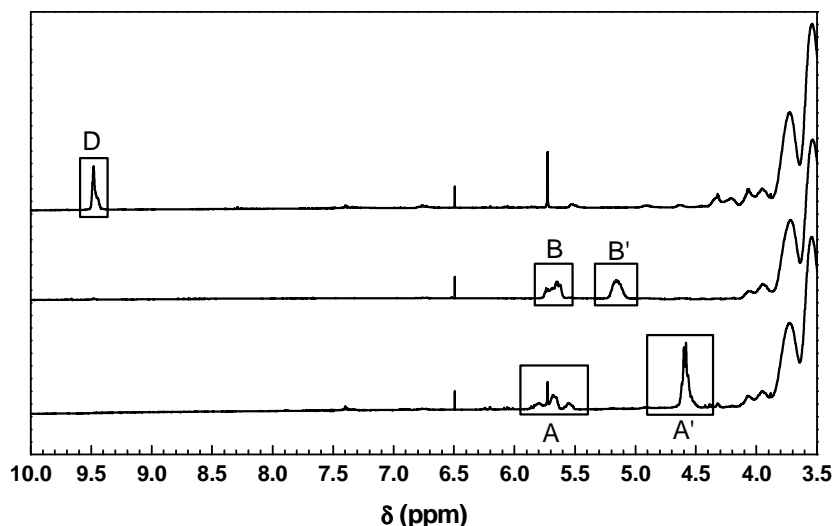
Figure 7.5: ^{1}H-NMR spectra of PVP in DMSO-d_6 precipitated 3 times from diethyl ether (bottom), heated in water at 40 ℃ for 16 h, dialyzed and freeze-dried (middle) and after an extra 20 h at 120 ℃ in the dry state under vacuum (top).

        The same intermediate (peaks B and B') formed when the polymer was heated at 40 ℃ in water as when heating was carried out at 80 ℃ in DMSO-d_6 but not in C_6D_6, which suggests that the presence of water (contained in the solvent as well as in the form of water of hydration bound to the polymer via hydrogen bonding) may be of major relevance. It must be noted that once the polymer is in contact with water, water is very difficult to remove without subjecting the polymer to increased temperature, *i.e.* without the xanthate end-groups also being removed. Therefore it is necessary to use dry solvents all along post-polymerization treatment (and in particular avoid dialysis) where aldehyde end-groups are unwanted.
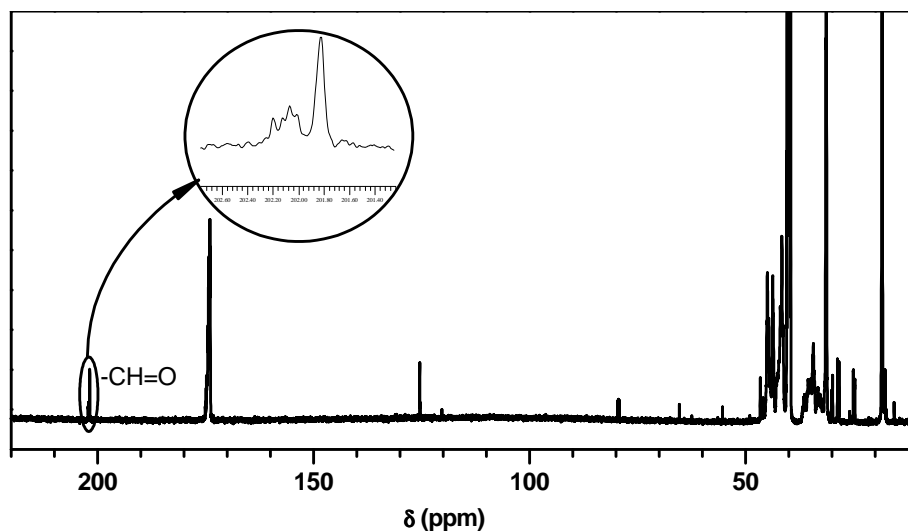
Figure 7.6: ^{13}C-NMR spectrum of PVP with aldehyde end-group in DMSO-d_6. The polymerization product was precipitated in diethyl ether, dissolved in water, heated at 40 ºC for 16h, dialyzed, freeze-dried and heated at 120 ºC under vacuum for 20 h.

The hydrolytic stability of RAFT agents is known to be pH-dependant.[17] The influence of the pH of the polymer solution was tested by varying its value in the range 3-13 via addition of formic acid or sodium hydroxide. The same (hydroxyl) end-groups were obtained where the pH of the solution was in the range 3-10, whereas a significant fraction of thiol end-groups were most likely obtained when the pH was higher than 10.
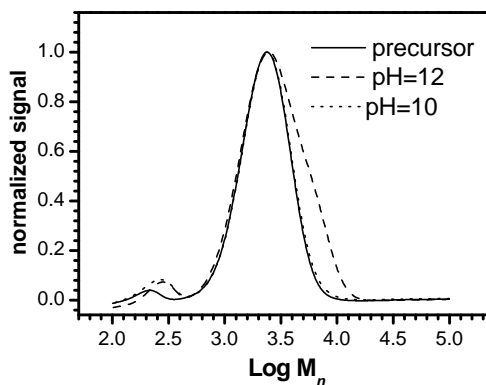
Figure 7.7: SEC chromatogram of PVP before and after hydrolysis at different pH. Hydrolysis was carried out by heating a solution of PVP with xanthate endgroup ($M_{n,SEC}$ = 2900 g·mol^{-1}, PDI = 1.24) in aqueous solution at 40 ºC for 16 h. The pH of the polymer solution was adjusted with KOH.

The presence of thiol end-groups was deduced due to the increase in M_n, as observed via SEC (Figure 7.7), most likely due to the coupling of thiol endfunctional chains. This point will be discussed below in the section dedicated to the preparation of

thiol endfunctional PVP. To avoid the presence of thiol chain-ends hydrolysis was carried out at pH = 4-5.

To the author's knowledge no synthetic pathway has been reported in the literature, which leads to the direct conversion of a xanthate into an aldehyde. Therefore it is likely that the formation of this type of end-groups is related to the presence of the pyrrolidone substituent. It is commonly accepted that formation of unexpected aldehyde end-groups occurs in the aqueous hydrogen peroxide-initiated free-radical polymerization of NVP as a result of termination by combination with a hydroxyl radical and subsequent elimination of the terminal pyrrolidone unit (Scheme 7.2).[18]
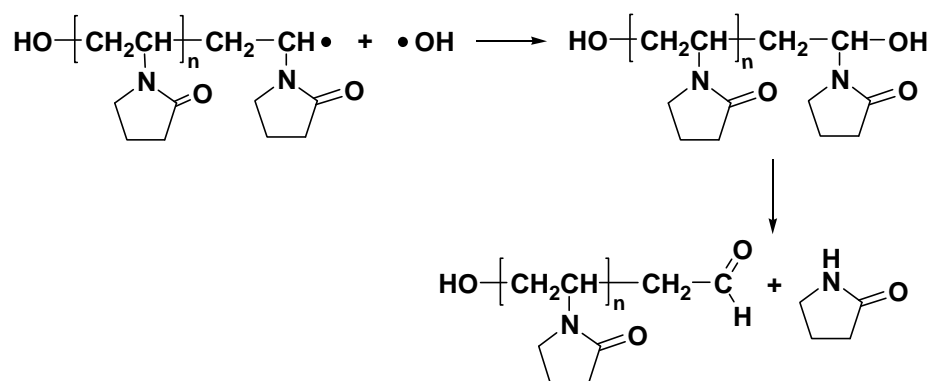
Scheme 7.2: Proposed scheme for the formation of aldehyde ω-chain-ends in the conventional free-radical polymerization of NVP initiated with hydrogen peroxide. Polymeric radicals are terminated by radical combination with hydrogen peroxide-derived hydroxyl radicals. The hydroxyl telechelic polymer undergoes elimination of pyrrolidone which results in α-hydroxyl, ω-aldehyde PVP.

We can then propose the mechanism as depicted in Scheme 7.3 for the formation of an aldehyde end-group upon heating of the dialyzed polymer. This reaction scheme is supported by the presence of peaks in the ^{1}H-NMR spectrum of the dialyzed PVP, which most likely correspond to ω-hydroxyl PVP.
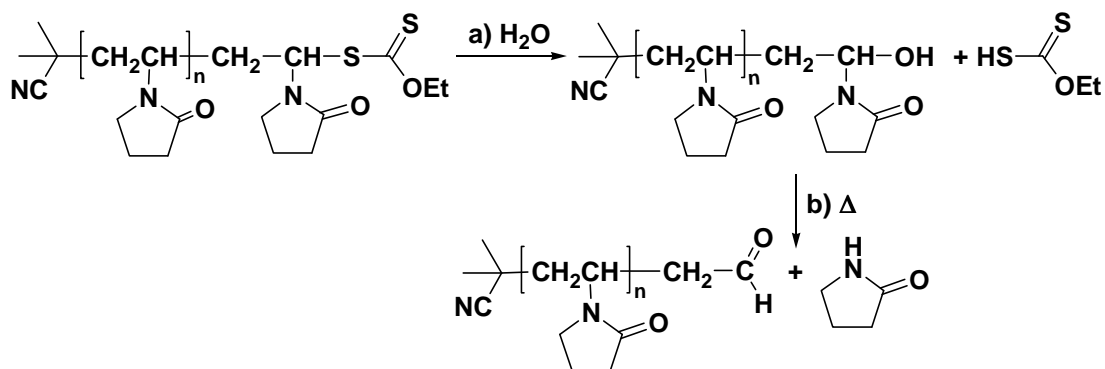
Scheme 7.3: Preparation of PVP with aldehyde end-group from PVP prepared via xanthate-mediated polymerization. Reaction conditions: a) H_2O, pH = 4-10, 40 ºC, 16 h; b) 120 ºC, <1 mbar, 16 h.

MALDI-ToF-MS was performed on the dialyzed sample and on the same polymer after thermal treatment (Figure 7.8). Although the NMR spectrum of the dialyzed polymer did not show any aldehyde end-group, the main distribution in the mass spectrum was very similar to that of the polymer with the aldehyde end-group ($+Na^+$). This could be due to fragmentation of the terminal pyrrolidone ring during the analysis. Another explanation may be that the chains with aldehyde end-groups are ionized and fly more easily than other species. Thus, even a low concentration of chains with aldehyde end-groups would be detected in the MALDI-ToF-MS spectrum. After thermal treatment of the dialyzed polymer, MALDI-ToF-MS confirmed the presence of the aldehyde end-group ($-CH_2CHO$).
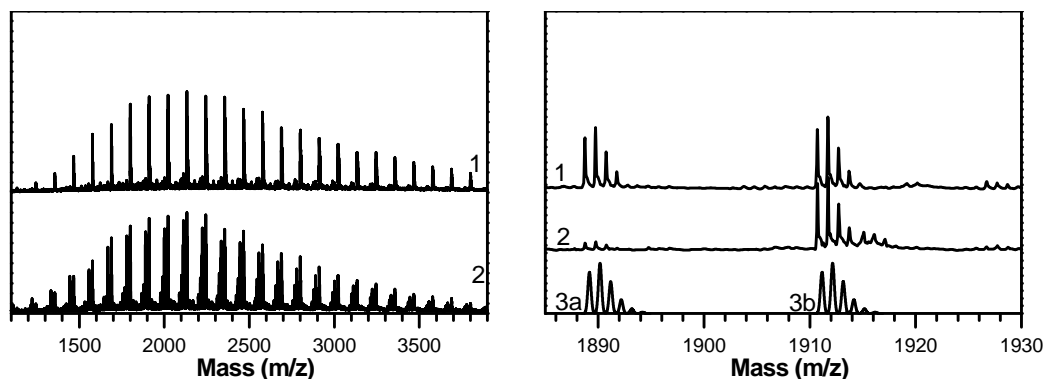
Figure 7.8: MALDI-ToF-MS spectra of hydrolyzed PVPs. Left: PVP heated at 40 ºC in distilled water for 16 h and dialyzed at room temperature (1) and the same dialyzed polymer after heating at 120 ºC for 20 h (2). Right: enlargement of the experimental spectra 1 and 2 and calculated isotopic patterns for $C_4H_6N(C_6H_9NO)_{16}CH_2CH0+H^+$ (3a) and $C_4H_6N(C_6H_9NO)_{16}CH_2CH0+Na^+$ (3b).

In conclusion, the end-groups obtained upon removal of the xanthate via hydrolysis at 40 ºC can be considered as precursors for the aldehyde endfunctional PVP,

which was obtained in high yields upon heating of the hydrolyzed polymer at 120 ºC. The susceptibility of NVP-xanthate derivatives to hydrolysis regardless of the pH and at low temperature provides an explanation to the failure of xanthate to mediate the polymerization of NVP in water, which we observed in preliminary experiments. It is a limitation to industrial applications, where water would have been the solvent of choice in terms of being inexpensive, "green" and a good solvent for high molecular weight PVP. Although it was not studied here the alcoholysis of xanthate end-groups may also be a shortcoming for the use of alcohols as polymerization solvents.

Aminolysis

Thiocarbonyl thio compounds are known to undergo fast and quantitative conversion to thiol via aminolysis with primary or secondary amines.[19] This method has been applied to polymers prepared via RAFT-mediated polymerization to provide thiol semi-telechelic and telechelic styrenic,[12,20,21] acrylic[4,22,23] and methacrylic[2,21] polymers. The reversible oxidative coupling of the thiol endfunctional polymers via disulfide bond formation is generally avoided by adding a reducing agent to the reaction mixture,[24] whereas other side reactions may still take place such as cyclization in the case of poly(methyl methacrylate) to form thionolactone end-groups.[25]

We applied the general aminolysis procedure to xanthate endfunctional PVP, which consists of reacting an excess of cyclohexylamine with the polymer in solution in THF at room temperature. The polymer ($M_{n,\text{NMR}}$ = 2600 g·mol^{-1}) was recovered by precipitation from diethyl ether. The ^{1}H-NMR spectrum of the product in DMSO-d_6 indicated that the xanthate end-groups had successfully been removed after 16 h. Note that the reaction may be faster than 16 h but the kinetic study of aminolysis was not performed. New signals appeared between 4.9 and 5.2 ppm. DMSO is an oxidizing agent and therefore it is likely that the signals correspond to disulfide end-groups rather than thiol.[26] The SEC chromatograms of the product in HFIP (Figure 7.9) was bimodal corresponding to the superposition of 2 distributions, the one being identical to the initial polymer and the second corresponding to double the M_n. The higher M_n structure was

identified in the MALDI-ToF-MS analysis (Figure 7.10, peak distribution 2). Its mass matched the calculated mass for the structure corresponding to 2 chains bound via a disulfide bond.
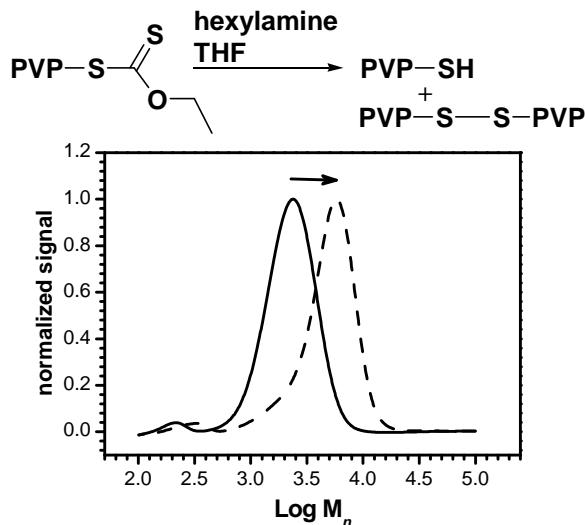
Figure 7.9: Reaction scheme and SEC chromatogram of PVP before and after aminolysis with cyclohexylamine. Aminolysis was performed at room temperature in THF for 16 h in the absence of reducing agent.
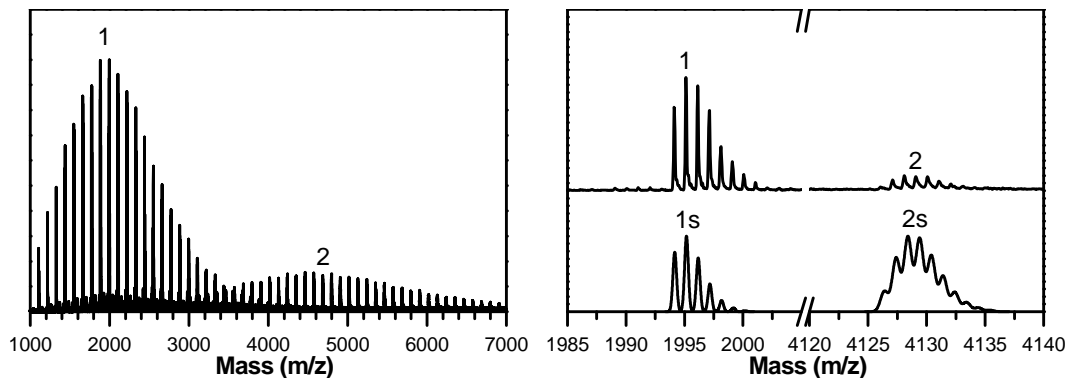
Figure 7.10: MALDI-ToF-MS spectrum of aminolyzed PVP. Left: experimental spectrum of the product of PVP-xanthate aminolysis with cyclohexylamine. Right: enlargement on the experimental spectrum (top) and simulated isotopic patterns (bottom) for $C_4H_6N(C_6H_9NO)_{16}C_6H_8NO+K^+$ (PVP-CH=CH-pyrrolidone, 1s) and $(C_4H_6N)_2(C_6H_9NO)_{35}S_2+K^+$ (PVP-S-S-PVP, 2s)

The low M_n distribution identified in the MALDI-ToF spectrum (peak distribution 1) did not match the calculations for PVP with a thiol end-group but to PVP with unsaturated chain-ends. Peaks corresponding to unsaturated end-groups were absent from the NMR spectrum. Therefore the low M_n distribution in the MALDI-ToF spectrum was

either due to selective identification of trace amounts of polymer with unsaturated chain-end or was formed during the analysis due to fragmentation.

Further characterization regarding the nature of the end-groups was performed using Ellman's method for thiol derivatization.[27] The compound bis(*p*-nitrophenyl disulfide) (Ellman's reagent) produces 1 equivalent of the yellow anion nitrobenzenethiolate upon coupling with thiols at pH = 8.0. The anion concentration is measured via UV-vis spectroscopy (λ_{max} = 412 nm; $\varepsilon_{412\ nm}$ = 13600 L·mol^{-1}·cm^{-1} in phosphate buffer at pH = 8.0). Before aminolysis the precursor polymer in aqueous solution produced a peak at λ_{max} = 280 nm (Figure 7.11), indicating the presence of the xanthate end-group. The absorbance at 280 nm decreased upon treatment with cyclohexylamine. In the presence of an excess of Ellman's reagent, only the solutions containing PVP treated with cyclohexylamine became yellow and showed a strong absorption at 412 nm. The polymer does not absorb at 412 nm, therefore the absorbance is due to the presence of nitrobenzene thiolate, confirming that the polymer bears thiol end-groups.
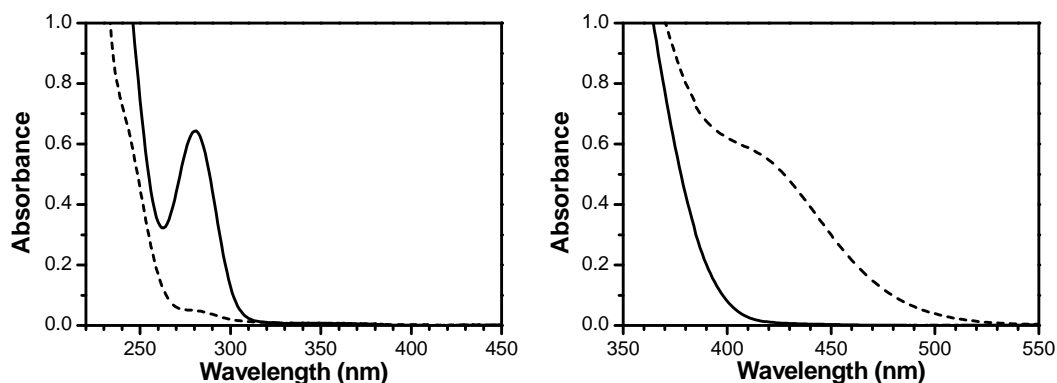
Figure 7.11: UV-vis spectra of the polymer with xanthate end-groups (—) and after treatment with cyclohexylamine in dichloromethane at room temperature for 16 h (---) in the absence (left) and in the presence of Ellman's reagent (right).

These results confirmed that aminolysis leads to successful xanthate end-group removal and is an efficient method for the preparation of thiol endfunctional PVP.

MALDI-ToF-MS

MALDI-ToF-MS was envisaged as a tool to confirm qualitatively the structure of the polymer end-groups. Our aim was to identify the presence of the end-groups expected from the RAFT mechanism and identified via NMR spectroscopy, as well as identify end-groups due to side-reactions, such as transfer and termination. The xanthate *S*-(2-cyano-2-propyl) *O*-ethyl xanthate (X6) was used so as to ensure that the α-end-group be stable. The structures of the ω-end-groups that will be discussed in this paragraph are presented in Scheme 7.4, as well as possible pathways for their formation.

As reported in chapter 3, it was soon observed that xanthate end-groups tend to undergo fragmentation from PVP chain-ends during MALDI-ToF-MS analysis. Chains with xanthate end-groups (Scheme 7.4, species **I**) were directly observed, however, via MALDI-ToF-MS with the use of a matrix with low ionization energy (*trans*-2-[3-(4-*tert*-butylphenyl)-2-methyl-2-propenylidene]-malononitrile (MM)), although fragmentation did occur to a variable extent (Figure 7.12). Even in cases where fragmentation was significant (for example where high laser intensity was used or where the matrix was α-cyano hydroxyl cinnamic acid (CHCA)), the xanthate end-groups could indirectly be inferred, because fragmentation invariably yielded a broad signal corresponding to the mass of the polymer chain with xanthate end-groups minus approximately 5 Da (signal **I'** in Figure 7.12), and a well-resolved signal corresponding exactly to the mass of the polymer with unsaturated chain-end (**III**). Most likely the well-resolved signal originates from the chains that undergo fragmentation in the matrix, *i.e.* before they start flying, whereas the poorly resolved signal is due to the chains that undergo fragmentation during their flight.[28] Unfortunately for our purposes, the structure of the chain-end upon fragmentation of the xanthate (**III**) is identical to that of unsaturated chains produced via termination by disproportionation and very close to the corresponding saturated species from disproportionation or proton abstraction (**II**). Due to signal overlap, little can be deduced from our MALDI-ToF-MS spectra with respect to the mode of termination of the chains. The author does not believe that the absence of a given signal in MALDI-ToF-MS spectra is sufficient evidence to conclude on the absence of the corresponding species in the sample. A list of the species that were not detected is however given to

explain why these species will not be discussed any further and why the pathways required for their formation were not put forward as cause for the loss of end-group functionality. The species that were not detected in any of the samples were species **IV**, **V** and **VII**. The absence of **IV** was expected, due to the low concentration in initiator and relatively low temperature at which the polymerizations were carried out, resulting in a low concentration in radicals. Although the value of the ratio of termination via disproportionation versus combination was not found in the literature for the polymer PVP, it is a general rule that combination is predominant over disproportionation. Therefore it is likely that the fraction of chains that underwent termination (under our experimental conditions) is too low to be detected via MALDI-ToF-MS. The absence of **V** is consistent with the hypothesis discussed in the introduction that the probability for chain-branching in NVP polymerization is lower than in the case of vinyl acetate polymerized via conventional free-radical polymerization, *i.e.* lower than 0.23 mol%. The absence of species **VII** from samples obtained via hydrolysis of **I** is noticeably surprising, considering that it is the main species anticipated from NMR spectroscopy. It is likely that ω-hydroxyl end-groups also undergo fragmentation. This hypothesis is supported by the fact that signals corresponding to unsaturated end-groups (**III**) and aldehyde end-groups (**VIII**) were present in significant amount in the MALDI-ToF-MS spectra although they were not detected via NMR analysis of the same sample.

As discussed in chapter 5, xanthate elimination may occur during the polymerization and the resulting xanthic acid may add to the monomer to produce a new xanthate species, which we called NVP-xanthate. The consequence of the participation of NVP-xanthate in the polymerization is that chains with 1-ethylpyrrolidone α-end-group would be formed (species **VI**). The signal corresponding to **VI** ($+K^+$) was identified in the MALDI-ToF-MS spectra. On the spectrum reported in Figure 7.12 the average molar mass seems to be lower for the distribution of species **VI** than for the main distribution (**I**). This observation would be consistent with the proposed mechanism similar to transfer. However it is very likely that the MALDI-ToF-MS spectrum is not a true reflection of the molar distribution and in particular the end-groups may aggravate inaccuracy related to molar mass discrimination, as already discussed in chapter 3. For

the same reason quantification of the end-groups via MALDI-ToF-MS was not attempted.

To conclude, MALDI-ToF-MS provided us with further evidence that xanthate elimination may occur during polymerization and may lead to the formation of a new xanthate species. The structures corresponding to the products of bimolecular termination and chain-branching were not identified. Fragmentation of ω-chain-ends occurred to a significant extent during MALDI-ToF-MS analyses where the end-groups were xanthate or hydroxyl. MALDI-ToF-MS is not a suitable method to identify species related to proton abstraction (**II**) due to signal overlap with the omnipresent signal for species with unsaturated end-groups, whether formed during polymerization or as a result of fragmentation during MALDI-ToF-MS analysis.
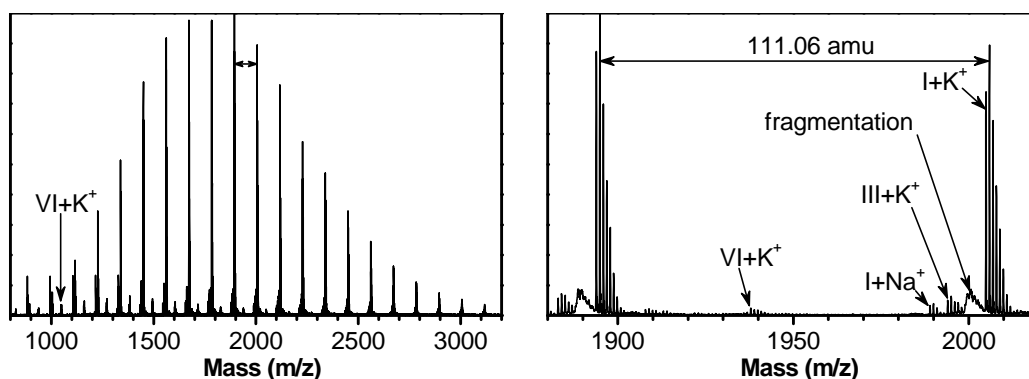
Figure 7.12: MALDI-ToF-MS spectrum of PVP prepared with *S*-(2-cyano-2-propyl) *O*-ethyl xanthate (X6) ($M_{n, SEC}$ = 2640 g·mol^{-1} (PMMA equivalents in HFIP), PDI = 1.21). Right: enlargement in the region 1880 – 2020 a.m.u.

Initiation
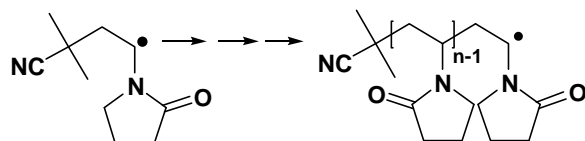
I• or R •

Propagation

Chain-transfer to CTA

(I)

Termination

Disproportionation

(II) **(III)**

Combination

(IV)

Chain-transfer via proton abstraction

(II)

Chain-branching

(V)

Xanthate elimination

Formation of NVP-xanthate

Hydrolysis

Fragmentation at the xanthate chain-end (during analysis)
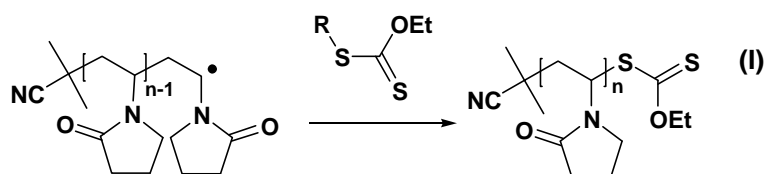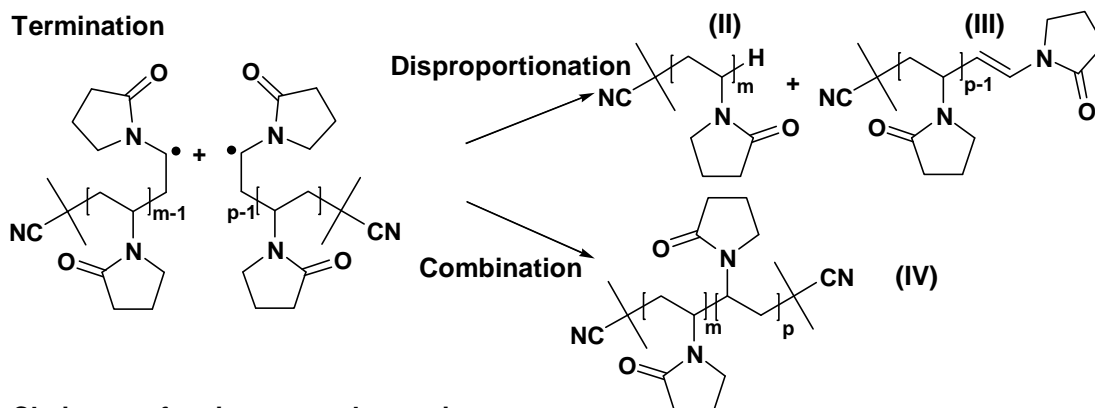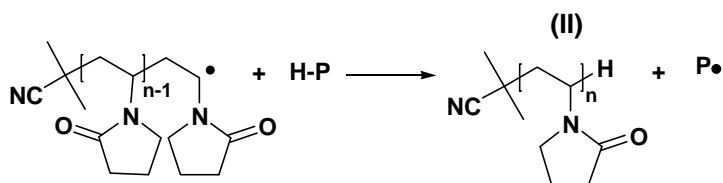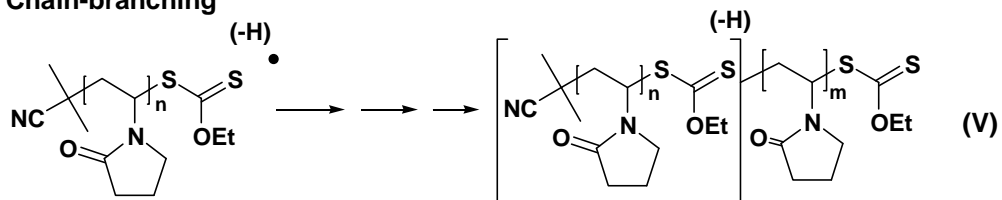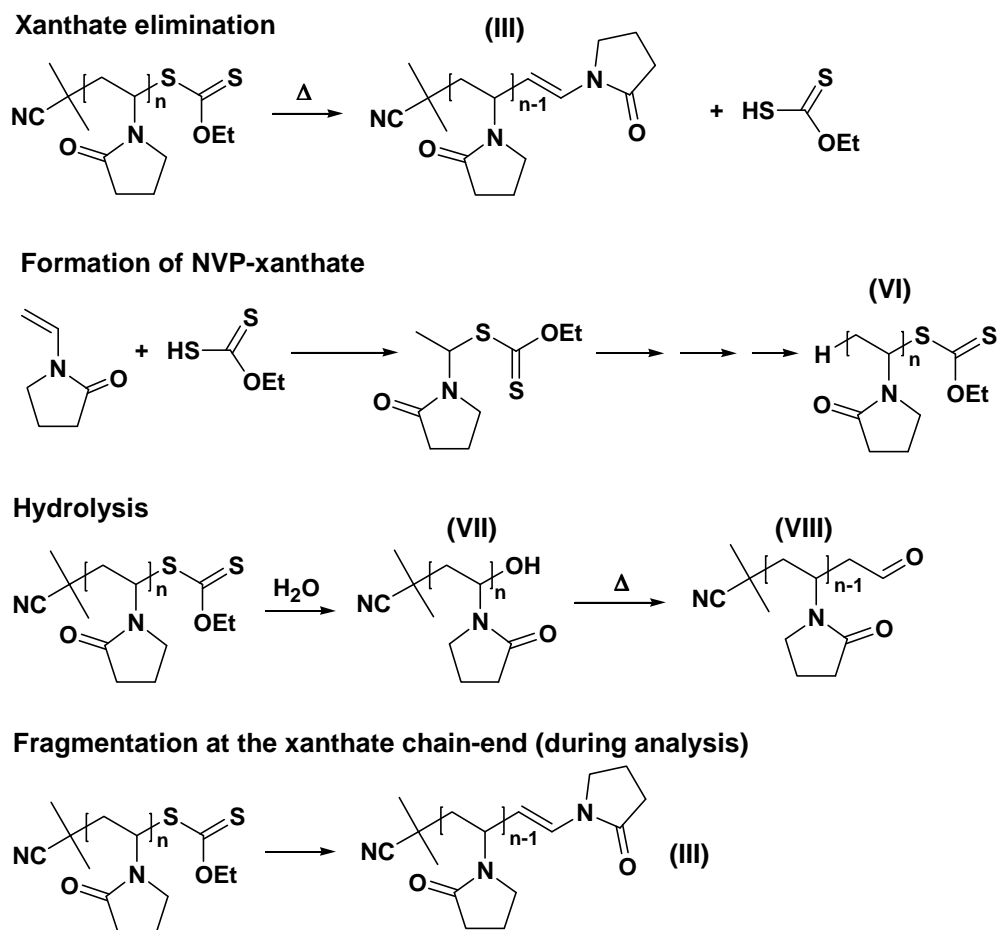
Scheme 7.4: possible end-groups expected from the polymerization of NVP in the presence of *S*-(2-cyano-2-propyl) *O*-ethyl xanthate (X6).

HPLC of PVP with variable end-groups

HPLC at critical conditions (HPLC-CC) can be particularly useful to determine the chemical composition homogeneity of polymers.[29] It is often used to determine the comonomer distribution and separate block copolymer from homopolymer in mixtures thereof.[30] In the present study, where homopolymers were prepared, the aim was to determine the homogeneity in terms of chain-end functionalization. The challenge was to find the critical eluent composition, where the eluent is good enough a solvent to enable elution of the polymer but still allows for enthalpic interactions between the column and the polymer; then under these conditions to determine whether the presence of variable end-groups would modify the interactions between the polymer and the eluent and/or the

column sufficiently to separate the chains on the basis of the end-group structure. The procedure for determining critical conditions for a given polymer generally involves preparing narrowly distributed polymer standards (PDI < 1.1) with the same end-groups in a range of molar masses and identifying the eluent composition (at a given temperature with a given column) where the polymers elute at the same volume regardless of the M_n value. PVP standards were not available in our labs to perform this routine procedure and therefore our attempt to determine critical conditions was carried out with polymer samples, which chain endfunctionalities were to be confirmed by the same method. Consequently conditions determined here may not be strictly critical conditions but "close to critical conditions". The figures below illustrate the difficulty to determine critical conditions with samples which structures are not genuinely well-defined in terms of polydispersity index and end-groups.

The elugrams (Figure 7.13 C and D) indicate a difference between the polymer before (C) and after (D) thermal treatment but they are multimodal. The bimodality is not consistent with ^{1}H-NMR results, which indicated homogeneous end-groups. At eluent composition 74 : 26 (v/v, water : acetonitrile) the peak maximum value (for the peak with the lowest elution volume) still increased slightly with decreasing M_n values, indicating that the critical conditions for the most hydrophilic species in the samples had not been reached yet but were most likely between 74 and 75 % water. Moreover the higher the M_n value, the bigger the first peak compared to the second. This suggests that the bimodality is rather due to heterogeneity in molar masses (the PDI of these polymers was comprised between 1.2 and 1.4) rather than successful separation according to the end-groups. Unfortunately increasing the water content to 75 % resulted in outspread peaks and part of the polymer not eluting within 40 min (elution volume = 20 mL). A gradient eluent with higher acetonitrile content had to be applied to desorb the polymer from the column. Nonetheless the transition between the exclusion and the adsorption mode was consistent between the 2 sets of samples and consequently a rough estimation of the critical conditions in the range 73 – 75 % (water content) was established from this experiment.
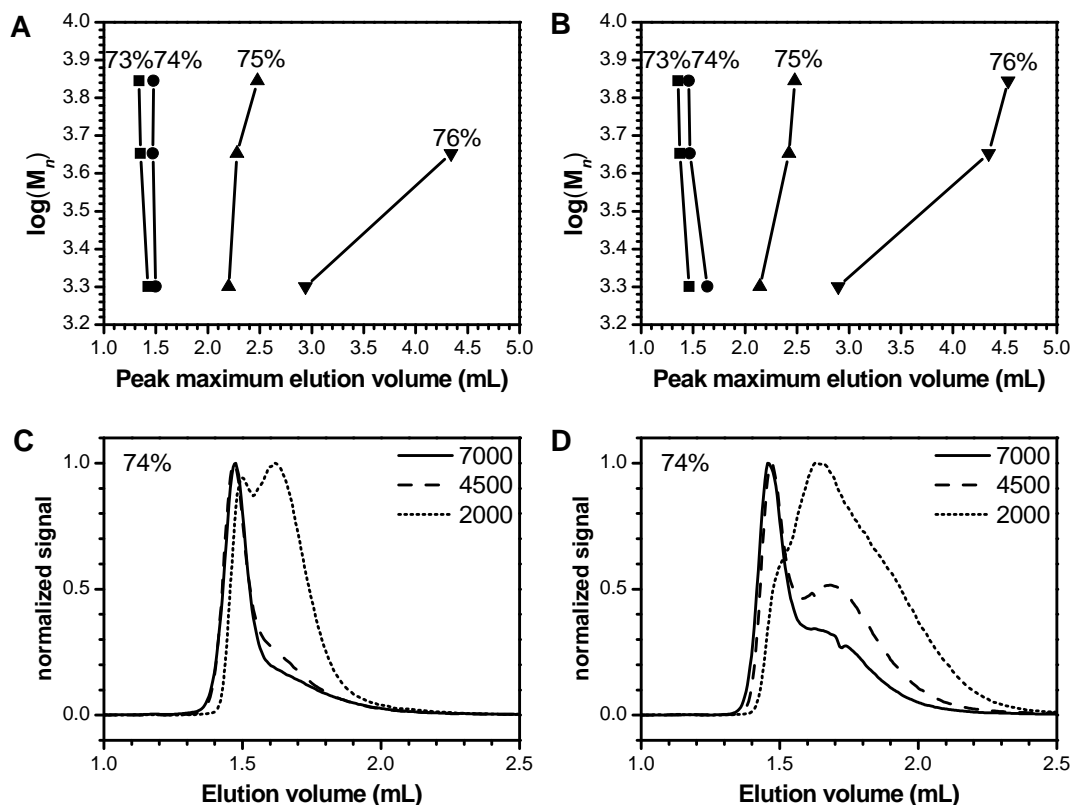
Figure 7.13 A, B, C and D: HPLC evaluation of critical conditions for PVP

Each point represents the elution volume corresponding to the elution peak maximum. 3 polymer samples were eluted under isocratic conditions with an eluent composition ranging from 71:29 to 76:24 (v/v) water (0.01 % formic acid) : acetonitrile. The polymer samples ($M_{n,SEC}$ = 2000; 4500; 7000 g·mol-[1], PDI = 1.2-1.4) were dialyzed at room temperature for graphs A and C, and were heated at 130 ºC for 22 h for graphs B and D. The elugrams, which were used to compile graphs A and B are presented in graphs C and D respectively, for the eluent composed of 74 % water.

Further experiments focused on the separation of PVPs according to the end-groups with the use of gradient polymer elution chromatography (GPEC). The initial eluent composition was chosen close to the critical composition so as to avoid precipitation of the polymer on the column, limit eluent composition changes and reduce the length of the experiment and yet assure successful separation. The detector used (ELSD) does not give information on the structure of the end-groups. The use of GPEC for end-group analysis is therefore limited, but has some advantage over ^{1}H-NMR, *e.g.* lower mass of sample, higher sensitivity and lower costs when used for routine analyses. As illustrated by the figure below, the same polymer eluted at different times depending on the post polymerization treatment. The elugrams (Figure 7.14) confirmed that the xanthate end-group was successfully removed by thermolysis (b), hydrolysis (c) or

aminolysis (e). Thermal treatment performed on the precipitated polymer resulted in unsaturated end-groups (peak 2), whereas thermolysis of the hydrolyzed compound produced the aldehyde end-group (peak 1). Therefore we can conclude that the low amount of hydrolyzed end-groups (peak 1) present in the precipitated sample (a) must have formed during the sample preparation, storage and/or analysis due to the water content of the eluent. The elugrams are similar whether aminolysis was applied or thermolysis and thus the analyses were insufficient for the determination of unsaturated chain ends in aminolyzed samples and vice versa. The MALDI-ToF-MS and SEC data indicated that the aminolyzed sample was mostly in the form of disulfides. Therefore it may be possible to obtain a separation between unsaturated and thiol end-groups by performing GPEC under reducing conditions.
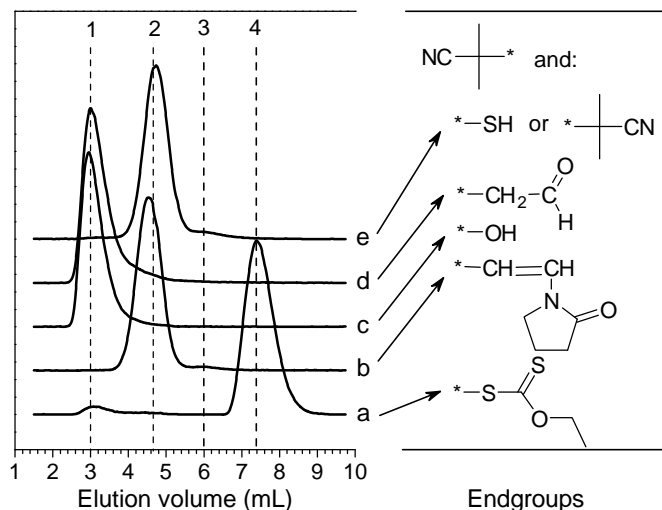
Figure 7.14: Gradient polymer elution chromatograms of poly(*N*-vinylpyrrolidone)s with various end-groups. The end-group structures correspond to a minimum of 80 % of the chain-ends as determined via ^{1}H NMR spectroscopy.

The samples were prepared by dissolving the polymer ($M_{n,SEC}$ = 2900 g·mol^{-1}, PDI = 1.24) in the eluent at a concentration of 3 mg·mL^{-1}. The acetonitrile content in the eluent was initially 25 % and increased to 35 % within 12 min to ensure desorption of all polymeric species.

GPEC may not be used on its own to determine the end-group composition of chain-end functionalized PVPs but it can be useful in a comparative manner. The conditions determined here enable the separation of PVP with xanthate end-groups from their products of thermolysis, aminolysis and hydrolysis.

Thermal stability of PVP with variable end-groups

The stability of PVP was investigated via thermogravimetric analysis. The thermograms in Figure 7.15, obtained at a heating rate of 10 ℃ / min under nitrogen atmosphere, show a mass loss from the lowest temperature of the analysis to approximately 60 – 80 ℃, regardless of the polymer end-group (*i.e.* regardless of the post-polymerization treatment), which is most likely due to evaporation of water and residual solvents from the sample. A significant mass loss occurs on xanthate endfunctional polymers from 120 ℃, which most likely corresponds to the loss of end-groups. The onset for xanthate elimination seems to be lower than 120 ℃, however, which is consistent with NMR spectroscopy results where a significant fraction of xanthate end-groups were lost at temperatures lower than 80 ℃. The chains with aldehyde endfunctionality appear to be stable up to approximately 260 ℃. The main mass-loss occurs at temperatures higher than 360 ℃, which is consistent with degradation of the polymer backbone as reported in the literature.[31] None of the end-groups studied here seemed to entail particular sensitivity of the chains towards thermal degradation.
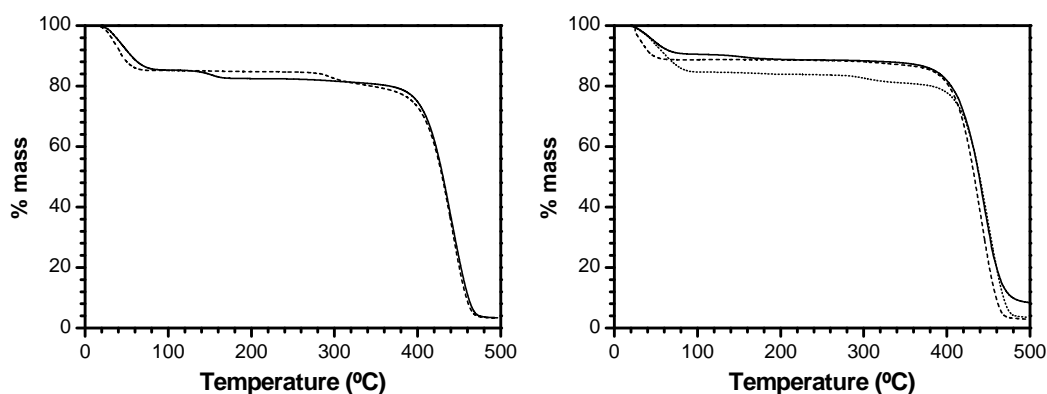
Figure 7.15: thermograms of poly(*N*-vinyl pyrrolidone)s with different end-groups. The end-groups were identified via ^{1}H NMR spectroscopy as *O*-ethyl xanthate (solid line); aldehyde (dashed line) and thiol end-groups (dotted line). The molecular weight data of the precursor polymers were $M_{n,SEC}$ = 2640, PDI = 1.21 (left) and $M_{n,SEC}$ = 17000, PDI = 1.24 (right).

Synthesis of polymer-protein conjugates

Polymer-protein conjugates for therapeutic applications have traditionally been prepared with poly(ethylene glycol) (PEG).[32] The PEGylation chemistry consists of

coupling a functional PEG precursor to the amino group of lysine residues or via disulfide bond formation to cysteine residues of proteins.[33] The conjugates generally display increased stability and solubility in body fluids and increased bioavailability compared to the unmodified protein. There is currently a concerted effort between medical and polymer scientists to provide alternatives to the PEGylation chemistry.[34,35] The behavior of PVP in solution, its low cytotoxicity, its ability to form hydrogen bonds and solubilize hydrophobes and also preliminary pharmacokinetic studies suggest that it may be a good candidate. Kaneda et al. compared PVP with PEG bioconjugates with Tumor Necrosis Factor-α (TNF-α).[36] They found longer plasma half-life with PVP compared to PEG and restricted tissue distribution, which suggests that PVP is a good modifier for localizing the conjugate in the blood. Previously they demonstrated higher anti-tumor effect for PVP- compared to PEG-conjugates and reduced toxicity compared to the native TNF-α.[37] PVP-IL-6 conjugates showed 50-fold greater thrombopoietic potency in vivo than native IL-6.[38] So far the molecular weight of the polymers for such applications and chain-end functionalities were limited due to the polymerization technique. Typically low M_n PVPs ($M_n < 6000$ g·mol^{-1}) with carboxylic acid chain end functionality were prepared via free-radical polymerization using a functional initiator and 3-mercaptopropionic acid transfer agent. With the recent advances in xanthate-mediated polymerization of NVP it is now possible to prepare narrowly distributed PVP in the M_n range 1000 – 50 000 g·mol^{-1} and control the end-groups. As shown in the previous sections, aldehyde and thiol end-groups can be obtained with this method and therefore the polymers could potentially be conjugated to either lysine or cysteine residues. Conjugation of PVP with thiol end-groups to a peptide and an oligonucleotide was recently published.[5] In this section, conjugation of the model protein lysozyme to aldehyde endfunctional PVP via reductive amination (Scheme 7.5) is presented.
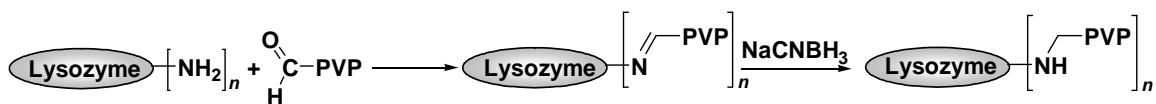
Scheme 7.5: Synthesis of lysozyme-PVP bioconjugates via reductive amination

Lysozyme was dissolved in phosphate buffer at pH = 5.4 and reacted with an excess of aldehyde endfunctional PVP ($M_{n,GPC} = 7000$ g·mol^{-1}, PDI = 1.38) at room temperature. After one hour sodium cyanoborohydride was added to the solution to

reduce the intermediate imino compound. Samples were withdrawn after 17 h, 90 h and 140 h, immediately freeze-dried and analyzed with SDS-PAGE (Figure 7.16). After 17 h already no free lysozyme remained. Its apparent molecular weight significantly increased in the polymer-conjugate. Lanes A and B were identical, indicating that under these conditions PVP was not bound to the protein via hydrogen bonding nor hydrophobic interactions. Therefore the protein in lanes C, D and E was covalently bound to the polymer. There was a slight difference among the samples taken at different times. It seemed that less low molecular weight species were present in the sample reacted for 90 h than 17 h, which could indicate that the number of polymer chains per protein increased with time, in other words the reaction was not complete after 17 h and more than one polymer chains per protein was covalently bound. This result was expected as lysozyme possesses 7 lysine residues, *i.e.* a total of 8 amino groups including the terminal one, and 4 times excess aldehyde functionalities were introduced in the reaction mixture.

Aldehyde chain-end functional PVPs with different M_n in the range 2640 - 17000 g·mol^{-1} (PMMA equivalents in HFIP) were tested. As expected, the lower the M_n of the polymer, the further the migration of the conjugate in SDS-PAGE analysis, *i.e.* the smaller the size of the conjugate (Figure 7.16, lanes L to O). A series of blank experiments were carried out where PVPs with xanthate, thiol or hydroxyl end-groups were incubated with lysozyme under the same conditions as the polymer with aldehyde end-groups.
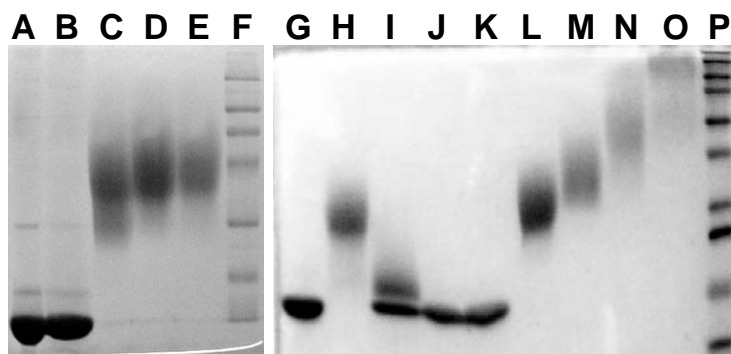
Figure 7.16: SDS-PAGE of lysozyme-PVP conjugates

Lane A: free lysozyme mixed with xanthate endfunctional PVP; B and G: free lysozyme; C, D and E: lysozyme-PVP conjugates samples at time 17 h, 90 h, and 140 h respectively; F and P: protein markers (10 – 250 kDa); H, I, J and K: lysozyme reacted with PVP with unsaturated, hydroxyl, thiol and xanthate end-groups, respectively; L to O: lysozyme-PVP conjugates with increasing PVP chain-length ($M_{n,SEC}$ [g·mol^{-1}](PDI) = 2640 (1.21); 7600 (1.31) and 17000 (1.24), respectively).

Polymers which did not bear aldehyde end-functionality did not produce stable conjugates with lysozyme, as indicated by the presence of free-lysozyme solely via SDS-PAGE analysis. The case of the polymer sample with unsaturated chain-ends (lane H) is peculiar, as the analysis shows the unexpected presence of conjugates. The polymer with xanthate end-group had been kept in contact with air prior to thermolysis. It is likely that hydrolysis had occurred to a significant extent, and that a significant fraction of aldehyde end-groups were present, which lead to conjugation of the polymer to the protein. The conjugation reaction was also carried out in the absence of reducing agent, in which case even the aldehyde chain-end functional PVP was not bound to the protein during the analysis.

Conclusions

PVP with well-defined end-groups was prepared via xanthate-mediated polymerization. The xanthate chain-ends were modified to yield aldehyde, thiol or unsaturated chain-ends under the conditions summarized in Scheme 7.6.
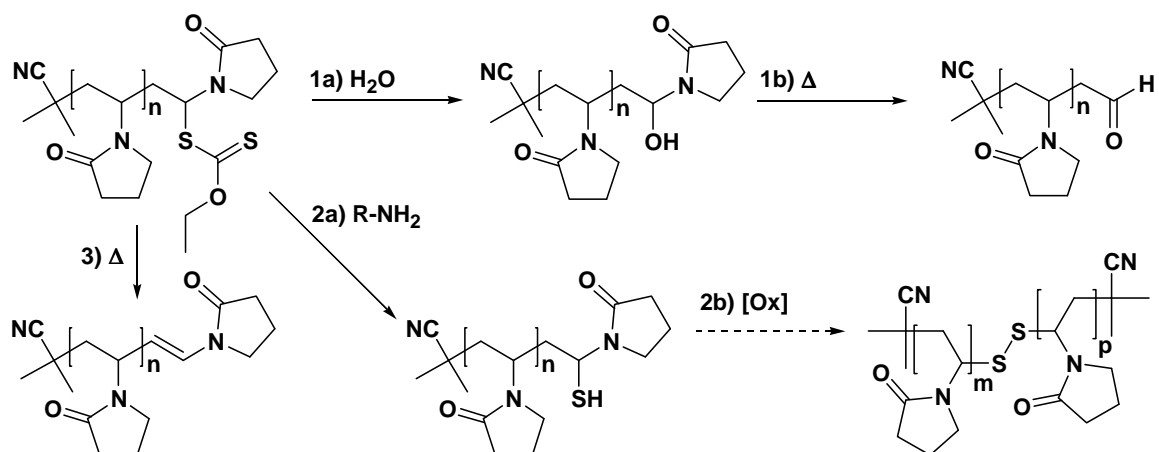
Scheme 7.6: Modification of poly(*N*-vinylpyrrolidone) xanthate chain-end into aldehyde, thiol and unsaturated end-groups. Reagents and conditions: 1a) distilled water, 40 ºC, 16 h. 1b) 120 ºC, 1 mbar, 20 h. 2a) cyclohexylamine in degassed tetrahydrofuran or dichloromethane, 25 ºC, 16 h. 2b) *e.g.* in dimethylsulfoxide. 3) 120 ºC, 1 mbar, 20 h or in chlorobenzene, reflux, 16 h.

Thermolysis at relatively low temperature (120-130 ºC) in the dry state or in water-free (non-polar) solvents produced stable unsaturated chain-ends. For the preparation of functional polymers aminolysis and hydrolysis were applied. Aminolysis

resulted in thiol endfunctional PVP. Conversion of the end-groups was confirmed via UV-Vis spectroscopy. The absorption of the xanthate chain-ends was observed at 280 nm in aqueous solution and the thiol end-groups were derivatized with Ellman's reagent, which produced the characteristic absorption at 412 nm. Hydrolysis of the xanthate end-groups was quantitative under particularly mild conditions of pH (4-10) and temperature (40 ℃). The product of hydrolysis, most likely hydroxyl endfunctional PVP, was quantitatively converted to an aldehyde endfunctional PVP upon heating at 120 ℃ under reduced pressure. PVP oligomers ($M_{n,\text{SEC}}$ = 2900 g·mol^{-1}, PDI = 1.24 for the xanthate endfunctional precursor) were separated according to the endgroup structure via gradient polymer elution chromatography. Identification of the endgroup structure was carried out qualitatively and quantitatively via NMR spectroscopy. The structures were confirmed in most cases via MALDI-ToF-MS. Fragmentation of the end-groups during analysis, in particular xanthate and hydroxyl end-groups was significant and therefore MALDI-ToF-MS under our conditions is not sufficient to study PVP end-groups. Thermogravimetric analysis indicated that PVP thermal decomposition was not significantly influenced by the end-group structure, whether they were xanthate, thiol or aldehyde. The molecular weight characteristics of the polymers did not vary upon end-group modification, except for treatment with an amine or hydrolysis at pH > 10, where thiol end-groups were produced. In such cases the thiol endfunctional chains could couple via disulfide bond formation resulting in the average molecular weight doubling, as observed via SEC and MALDI-ToF-MS. The reactivity of aldehyde chain-end functional PVP was utilized for the preparation of polymer-protein conjugates with lysozyme via reductive amination with lysine residues. The apparent molecular weight of the protein increased significantly after incubation with the polymer and a reducing agent. The longer the polymer chain, the larger the polymer-protein conjugate, as indicated by SDS-PAGE analysis.

The present yet unexpected findings that xanthate endfunctional PVP may be converted to aldehyde endfunctional lysine-reactive polymer substantiates Zard's enlightened recommendation to follow "the trail of xanthates".[39]

Reference List

(1)	Chan, M.F.; Garst, M.E. *J. Chem. Soc., Chem. Commun.* **1991**, *7*, 540-541.
(2)	Lima, V.; Jiang, X.; Brokken-Zijp, J.; Schoenmakers, P.J.; Klumperman, B.; Van der Linde, R. *J. Polym. Sci., Part A: Polym. Chem.* **2005**, *43*, 959–973.
(3)	Deletre, M.; Levesque, G. *Macromolecules* **1990**, *23*, 4733-4741.
(4)	Sumerlin, B.S.; Lowe, A.B.; Stroud, P.A.; Zhang, P.; Urban, M.W.; McCormick, C.L. *Langmuir* **2003**, *19*, 5559-5562.
(5)	Zelikin, A.N.; Such, G.K.; Postma, A.; Caruso, F. *Biomacromolecules* **2007**, *8*, 2950-2953.
(6)	Chong, B.; Moad, G.; Rizzardo, E.; Skidmore, M.; Thang, S.H. *Aust. J. Chem.* **2006**, *59*, 755-762.
(7)	Perrier, S.; Takolpuckdee, P.; Mars, C.A. *Macromolecules* **2005**, *38*, 2033-2036.
(8)	Destarac, M.; Kalai, C.; Petit, L.; Wilczewska, A.Z.; Mignani, G.; Zard, S.Z. *Polym. Prepr. (Am. Chem. Soc., Div. Polym. Chem.)* **2005**, *46*, 372-373.
(9)	Liard, A.; Quiclet-Sire, B.; Zard, S.Z. *Tetr. Lett.* **1996**, *37*, 5877-5880.
(10)	Chong, Y.K.; Moad, G.; Rizzardo, E.; Thang, S.H. *Macromolecules* **2007**, *40*, 4446-4455.
(11)	Legge, T.M.; Slark, A.T.; Perrier, S. *J. Polym. Sci., Part A: Polym. Chem.* **2006**, *44*, 6980-6987.
(12)	Moad, G.; Chong, Y.K.; Postma, A.; Rizzardo, E.; Thang, S.H. *Polymer* **2005**, *46*, 8458-8468.
(13)	Xu, J.; He, J.; Fan, D.; Tang, W.; Yang, Y. *Macromolecules* **2006**, *39*, 3753-3759.
(14)	Postma, A.; Davis, T.P.; Li, G.; Moad, G.; O'Shea, M.S. *Macromolecules* **2006**, *39*, 5307-5318.
(15)	Pound, G.; McLeary, J.B.; McKenzie, J.M.; Lange, R.F.M.; Klumperman, B. *Macromolecules* **2006**, *39*, 7796 - 7797.
(16)	Brandrup, J.; Immergut, E.H.; Grulke, E.A. *Polymer Handbook*; John Wiley and Sons, Inc, **1999**.
(17)	Thomas, D.B.; Convertine, A.J.; Hester, R.D.; Lowe, A.B.; McCormick, C.L. *Macromolecules* **2004**, *37*, 1735-1741.
(18)	Marten, F.L. In *Encyclopedia of Polymer Science and Engineering*, 2nd ed.; John Wiley and Sons, Inc., **1989**; Vol. 17, p 202.
(19)	Castro, E.A. *Chem. Rev.* **1999**, *99*, 3505-3524.
(20)	Whittaker, M.R.; Goh, Y.-K.; Gemici, H.; Legge, T.M.; Perrier, S.; Monteiro, M.J. *Macromolecules* **2006**, *39*, 9028-9034.
(21)	Patton, D.L.; Mullings, M.; Fulghum, T.; Advincula, R.C. *Macromolecules* **2005**, *38*, 8597-8602.
(22)	Qiu, X.-P.; Winnik, F.M. *Macromol. Rapid Commun.* **2006**, *27*, 1348-1653.
(23)	Favier, A.; Ladavière, C.; Charreyre, M.-T.; Pichot, C. *Macromolecules* **2004**, *37*, 2026-2034.
(24)	Cleland, W.W. *Biochemistry* **1964**, *3*, 480-482.
(25)	Xu, J.; He, J.; Fan, D.; Wang, X.; Yang, Y. *Macromolecules* **2006**, *39*, 8616-8624.
(26)	You, Y.-Z.; Manickam, D.S.; Zhou, Q.-H.; Oupicky, D. *Biomacromolecules* **2007**, *8*, 2038-2044.

(27) Ellman, G.L. *Arch. Biochem. Biophys.* **1958**, *74*, 443-450.

(28) Staal, B.B.P. *Characterization of (co)polymers by MALDI-TOF-MS; Chapter 4: The relationship between the MMD from MALDI and from SEC*; Technische Universiteit Eindhoven, **2004**.

(29) Philipsen, H.J.A. *J. Chromatogr. A* **2004**, *1037*, 329-350.

(30) Pasch, H. *Adv. Polym. Sci.* **2000**, *150*, 1-66.

(31) Peniche, C.; Zaldivar, D.; Pazos, M.; Paz, S.; Bulay, A.; San Roman, J. *J. Appl. Polym. Sci.* **1993**, *50*, 485-493.

(32) Zalipsky, S. *Bioconjugate Chem.* **1995**, *6*, 150-165.

(33) Woghiren, C.; Sharma, B.; Stein, S. *Bioconjugate Chem.* **1993**, *4*, 314-318.

(34) Schilli, C.; Muller, A.H.E.; Rizzardo, E.; Thang, S.; Chong, Y.K.B. *ACS Symposium Series* **2003**, *854*, 603.

(35) Heredia, K.L.; Maynard, H.D. *Org. Biolmol. Chem.* **2007**, *5*, 45-53.

(36) Kaneda, Y.; Tsutsumi, Y.; Yoshioka, Y.; Kamada, H.; Yamamoto, Y.; Kodaira, H.; Tsunoda, S.-i.; Okamoto, T.; Mukai, Y.; Shibata, H.; Nakagawa, S.; Mayumi, T. *Biomaterials* **2004**, *25*, 3259-3266.

(37) Kamada, H.; Tsutsumi, Y.; Yamamoto, Y.; Kihira, T.; Kaneda, Y.; Mu, Y.; Kodaira, H.; Tsunoda, S.-i.; Nakagawa, S.; Mayumi, T. *Cancer Res.* **2000**, *60*, 6416-6420.

(38) Tsunoda, S.; Kamada, H.; Yamamoto, Y.; Ishikawa, T.; Matsui, J.; Koizumi, K.; Kaneda, Y.; Tsutsumi, Y.; Ohsugi, Y.; Hirano, T.; Mayumi, T. *J. Control. Rel.* **2000**, *68*, 335-341.

(39) "Our peregrinations were hardly planned from the outset; we simply went where the chemistry took us" Zard, S.Z. *Angew. Chem. Int. Ed. Engl.* **1997**, *36*, 672-685.

Chapter 8 : Epilogue

A detailed study on the living xanthate-mediated polymerization of *N*-vinylpyrrolidone, as was presented in this thesis, gives valuable insight into practical considerations. The main findings, recommendations and perspectives, with particular attention to applications, are discussed in this chapter.

Technological assessment

Living free-radical polymerization of *N*-vinylpyrrolidone was achieved. In the presence of selected xanthates, poly(*N*-vinylpyrrolidone) was obtained with PDIs as low as 1.21 in the molecular weight range 2000 – 25000 g·mol^{-1} (PMMA equivalents in HFIP). The level of control depends on the nature of the xanthate R group and experimental conditions. The most successful polymerizations were carried out in bulk at 60 ℃ (with AIBN as an initiator). The lowest values of PDI were obtained by stopping the polymerization at 40-60 % conversion. The most suitable R groups among those tested were 2-cyano-2-propyl, 1-cyanoethyl and 2-ethylpropionate. The polymerization product is xanthate ω-end-functional. The xanthate end-group can be modified to yield unsaturated chain-ends via thermolysis, thiol end-groups via aminolysis or aldehyde end-groups via hydrolysis. The aldehyde endfunctional PVP is reactive to primary amines, which enables its conjugation to protein lysine residues via reductive amination in buffered solution. Side-reactions have been identified during the polymerization of NVP, which may occur whether a xanthate is used or not. These include hydration in apolar medium in the presence of trace amounts of water and dimerization in the presence of a proton-donor catalyst. Side-reactions affecting the xanthate at the chain-end include xanthate elimination and hydrolysis in aqueous solution. These points are further discussed in the following paragraphs with respect to macromolecular design.

On the enhancement of the control over the molecular weight distribution

In chapter 4, the effect of a systematic variation of the xanthate R group on the xanthate-mediated polymerization of NVP was presented. The study revealed that ^{1}H-NMR spectroscopy is a valuable technique to investigate the behavior of RAFT agent-monomer systems. It enabled us to classify the R groups according to their overall reactivity towards fragmentation / cross-propagation with respect to the monomers NVP and VAc. In particular the technique enabled us to distinguish between systems where selective initialization takes place as opposed to hybrid or poorly controlled systems. Another accessible and valuable parameter is how the rate of monomer consumption during initialization compares with the rate of polymerization, *i.e.* whether initialization is fast compared to polymerization, or not. *In situ* ^{1}H-NMR spectroscopy initialization studies are fast, straightforward and can be applied to any monomer-controlling agent combination. It enabled us to identify suitable R groups for NVP, among which 2-cyano-2-propyl and 2-cyanoethyl, but also ethyl propionate, whereas the analyses pointed at the long initialization period where the phenylethyl R group was used and a hybrid system with the *tert*butyl R group. It was confirmed experimentally that fast and selective initialization guarantees a good control over the molecular weight distribution of the polymer.

On the control over the chain-ends

The monomer NVP can undergo a number of side-reactions, as presented in chapter 5, and reactions affecting the polymer living chain-end, as presented in chapter 7. The mechanisms of such side-reactions seem to involve ionic species rather than radicals. The side-products of these reactions may have a higher transfer constant in comparison with the monomer and polymer. Also, due to side reactions, the conversion of monomer into polymer may not reach 100 %. One research strategy is to try and reduce the consequences of NVP reactivity, by making sure that no impurities were present, *i.e.* no traces of water or oxygen, by controlling the pH of the solution along the polymerization

and by reducing the temperature. We focused on identifying the side-reactions and taking advantage of them when applicable. Xanthate thermal elimination results in an unwanted increase in the polydispersity index when it occurs during the polymerization. On the other hand, it was used to quantitatively remove labile end-groups and thus increase the stability of the polymer (PVP with xanthate end-groups stored at room temperature develops a bad smell, most likely due to the formation of xanthic acid derivatives, whereas no smell was noticed from samples which xanthate end-groups were removed). Xanthate hydrolysis prevents control over the polymerization in aqueous medium. On the other hand, post-polymerization hydrolysis of xanthate end-groups enabled us to produce aldehyde endfunctional PVP.

On transfer and termination reactions

The propensity of NVP-derived radicals to abstract labile protons is most likely a cause for the increase in polydispersity index observed when a solvent was used. Transfer reactions may be responsible for the not-so-low polydispersity index (generally 1.2-1.4 depending on initial concentration ratios and conversion) obtained in spite of the use of seemingly suitable CTAs (chapter 3). The production of dead chains via proton abstraction could not be satisfactorily studied under our experimental conditions. Firstly, the number of dead chains due to irreversible transfer may remain low even though the impact on the polydispersity index may be significant. Secondly, dead chains are difficult to identify because they produce saturated unreactive chain-ends, *i.e.* the dead chain-ends cannot be derivatized. Finally, MALDI-ToF-MS, which could have helped us identify these structures, was not conclusive. The main reason for the inadequacy of MALDI-ToF-MS, is that fragmentation of chain-ends occurred in all samples, which produces a strong signal that would overrule the presence of low amounts of saturated chain-ends. ^{1}H-NMR spectroscopy therefore remains the most promising technique to date to investigate the end-groups. For this purpose we can suggest the use of deuterated solvents and analysis of the chain-ends via [2]D-NMR spectroscopy to investigate transfer to solvent during polymerization. The study on PVP end-groups presented in this thesis is not sufficient to decipher on the role of irreversible transfer during xanthate-mediated

polymerization of NVP. In particular, short chains were targeted, whereas the effects of irreversible transfer are more pronounced where high molecular weights are targeted (and high M_ns justify the use of solvents to ensure mobility of the chains and processability of the product). Our strategy consisted of avoiding the use of a solvent and stopping the reaction at moderate conversion (< 60 %). However, this strategy may not be applicable industrially and it would be interesting to investigate the use of a solvent. Polymerization in a solvent with a lower transfer constant than the solvents tested (other than ethanol, tetrahydrofuran or dioxane) should be studied. Dichloromethane may be a good choice although its low boiling point would require low polymerization temperatures or a pressurized reactor. *tert*-Butyl alcohol has a low transfer constant (see values for VAc)[1] and could be tested for the xanthate-mediated polymerization of NVP. A shortcoming for the use of *tert*-butyl alcohol as a solvent may be degradation of the monomer or the RAFT agent (see reaction of NVP with alcohols in chapter 5) and should be tested in preliminary experiments. Alternatively the unreacted monomer could be recycled once separated from the polymer to avoid wasting large quantities of monomer in cases where it is also used as a solvent.

Lower temperatures are often synonymous with reduction of side-reactions and as such may enhance control over the polymerization of NVP. In particular we reported that xanthate elimination for dormant species was observed even at 60 ºC (chapter 5), which increases the polymer polydispersity index and alters the chain-end functionality. Living polymerization of NVP at room temperature was recently achieved via ATRP[2] and cobalt-mediated polymerization.[3] In order to perform xanthate-mediated polymerization at low temperature it is necessary to find an alternative radical source to the use of AIBN, which decomposition rate is too low at temperatures close to room temperature. For example photo-induced initiation may be investigated.

Comparison between NVP and VAc

A rapid glance at the kinetics and mechanism of the xanthate-mediated polymerization of NVP compared to that of VAc suggests that NVP may be considered

as VAc's close relative, only less reactive radically. NVP-derived radicals are slightly more stabilized than VAc's and therefore NVP requires higher temperatures than VAc to obtain the same rate of polymerization, and the xanthate R group must be slightly more stable than for VAc for initialization to be selective (Chapters 3 and 4). In theory, the higher reactivity of VAc radicals would result in poorer selectivity of the reactions, *i.e.* a higher propensity for transfer, radical combination and head to head addition than in the polymerization of NVP and thus higher polydispersity indexes for the resulting PVAc compared to PVP. It is not the case. PVAc could easily be prepared in our labs with a suitable xanthate (*S*-(2-ethylpropionyl) *O*-ethyl xanthate) with PDI = 1.18 (M_n = 18 000 g·mol^{-1} (PS equivalents in THF)), whereas the lowest PDI for PVP with similar M_n value was 1.24 (M_n = 17100 g·mol^{-1} (PMMA equivalents in HFIP), prepared with *S*-(2-cyano-2-propyl) *O*-ethyl xanthate). Short of PVP standards for SEC calibration, we cannot strictly exclude that the PDIs determined for PVP may be higher than actual PDIs. However, evidence for significant side-reactions in the case of NVP, which were not identified in the case of VAc, suggests that there are actual differences between the two monomers, which are not simply due to electronic stabilization of the double-bond (Chapter 5 and 7). Hence, xanthate elimination from polymer dormant species and side-reactions such as hydration and dimerization were observed with NVP but not with VAc. In other words, just as electronic effects are not the only parameters that govern the reactivity of vinyl compounds towards radical addition,[4] the effect of the vinyl bond substituents may not be reduced to their electron-donating ability. With respect to non-radical reactions, NVP was found to be substantially more reactive than VAc.

Macromolecular architectures

In this thesis the preparation of block-copolymers comprising a poly(ethylene glycol) segment was presented (chapter 6). The methodology, which consists of growing a PVP chain (or PVAc) from a xanthate end-functional polymer, may be applied to produce other block copolymers with NVP and VAc. In chapter 7, we presented the preparation of PVP-protein conjugates from an aldehyde end-functional PVP. Although it is very likely that modification of the xanthate chain-end into an aldehyde requires the

presence of the NVP repeating unit adjacent to the xanthate, the methodology is potentially applicable to a broad range of polymers by incorporation of a short PVP segment at the chain-end. The range of macromolecular structures that can be obtained via the RAFT process is not limited to linear, semi-telechelic structures. For example we briefly presented the use of difunctional xanthates (comprising a poly(ethylene glycol) or ethylene-glycol-based R group), which produce telechelic (co)polymers. Chain-end modification of these polymers may lead to thiol (via aminolysis) or aldehyde (via hydrolysis) telechelics. The methodology is described in the literature to prepare high M_n polymers comprising disulfide bridges, which can be reduced to release their low M_n building blocks.[5,6] The concept is attractive to revive the application of PVP as a plasma expander. The polymer could be injected in its high M_n form, which ensures suitable isotonicity, and may be reduced in vivo to enable its necessary elimination from the body. α,ω-Hetero-telechelic PVP and copolymers of NVP may also be obtained with the use of a xanthate with a functional R group. Applications may include fluorescence labeling for medical diagnosis.[7] The ability of PVP main chains to bind selectively to the surface of nanocrystals makes it possible to coat inorganic Bi_2S_3 nanocrystals, providing the first in vivo nanomaterials suitable as probes for tomography imaging.[8] The use of PVP with functional end-groups, prepared via RAFT, may enable targeting of these long circulating nanoparticles to selected organs in the body.

Other structures accessible via RAFT include gradient, stars, graft copolymers, gels, hybrid organic-inorganic structures, surface modifications, etc. Let us note for instance that PVP, used for cosmetic applications, may be prepared with a dye-reactive end-group (or a dye-containing R group), whereas the xanthate end-group may be modified for the polymer to be reactive to hair or other proteins from the skin, teeth or nails, which contain aldehyde-reactive amines. Non-linear multifunctional polymer can be obtained from multifunctional xanthates, for instance 4-arm PVP stars were prepared from a CTA comprising 4 xanthate functionalities.[9] End-group modification of these multi-chain-end functional polymers may lead to the preparation of PVP hydrogels, which are promising for many applications in the medical field. The reactive end-groups readily accessible so far (chapter 7) are thiol and aldehyde, which yield reducible, hydrolizable or hydrolytically stable linkages depending on the reaction conditions. In

chapter 7, we also presented facile modification of PVP end-groups into unsaturated species. ^{1}H-NMR spectroscopy studies indicated that they do not seem to act as macromonomers for radical polymerization, however their use as macromonomers for thiol-ene polymerization[10] or as substrates for Michael-type additions[11] or atom transfer radical additions[12] have not been examined yet.

Finally, advances in the chemistry of NVP free-radical polymerization are supplemented with the development of post-polymerization processing techniques. Let us cite electrospinning, which appears as a valuable tool for the preparation of structured materials with a high surface and tunable morphologies, and was recently applied to PVP.[13,14]

For a broader picture

It is a generally accepted and frequently verified concept that nature holds the keys for chemists to unfold mysteries. To this respect, it was pointed out in 1938 (*i.e.* before Watson and Crick elucidated the three-dimensional structure of DNA) that "*the carbonyl-imid-methine (C(=O)NC) sequence in heterocyclic configuration similar to pyrrolidone*" is of particular significance in nature and a recurring structure in cell differentiation promoting compounds.[15] Structural similarities between PVP and proteins have guided the scientific curisosity to investigate the potential of NVP (co)polymers as active substances (*i.e.* not solely as an inert additive), *e.g.* for polymerase chain reaction (PCR) amplification[16,17] or as antimicrobial component.[13,18-20] The cyclic amide structure participates in hydrogen-bonding and weak hydrophobic interactions, which are affected by the size of the structure (chain-length when incorporated in a polymer) and the concentration. Additionally, the cyclic structure is in equilibrium with a ring-opened structure which displays an amine and a carboxylic acid moiety and as such NVP pendant group may be seen as a dynamic (reactive) structure. This characteristic reactivity of cyclic amides may be considerably annoying when "inert", "well-defined" structures are required and deceiving when prediction of reactivity is attempted. However from other perspectives this reactivity is a golden opportunity. Hence surprising outcomes were

reported regarding the properties of PVP, for instance the electrical conductivity of PVP blends with polyaniline[21,22] is "quite unusual to its (PVP) neutral nature".[21] Outstanding applications for PVP have been reported, including "*exceptional*" behavior as a phase-transfer catalyst (copolymer with styrene)[23] or as a surface modifier for fuel cell carbon nanomaterials, where it dramatically enhanced the electrocatalytic activity of the material towards oxidation of methanol[24] (note that copolymers of NVP have been proposed as an enhanced alternative to Nafion® (electron conducting, less permeable to methanol and more stable to oxidation) for the preparation of methanol fuel cell membranes[25,26]). In the context of the present thesis, the ability to produce a polymer with reactive aldehyde end-groups via hydrolysis and elimination of the ultimate monomer unit for instance (chapter 7) is at least as valuable as it was unpredicted.

The reader must have realized that only synthetic investigations were reported in this thesis, but the range of applications for PVP is broad. From the generous pool of publications on PVP (see references in the present chapter and in chapter 2) we can perceive that it is anticipated and gradually confirmed as a unique polymer for applications where colloidal properties (hydrogen-bonding and hydrophobic interactions) are crucial. An interesting feature is that the polymer is non-ionic but polar and thus water-soluble. Historically we can notice a tendency for water-soluble ionic structures to be replaced with non-ionic structures, mostly because the non-ionic ones are generally less toxic to the environment. Hence ionic surfactants are replaced with non-ionic amphiphilic compounds. Another noticeable trend is for small molecules to be replaced by long (polymeric) chains. This trend is again consistent with the strategy of nature, where small molecules are barely necessary to maintain the fluidity of living organisms (water and substances which are eliminated by the body), as fast energy sources (glucose, ATP, etc.) and for fast physiological response (neurotransmitters), whereas the vital structural compartmentalization of living organisms and storage of essential functionalities relies on polymeric structures (proteins). Therefore it is likely that an amphiphilic polymer such as PVP, which is edible and biocompatible, presents attractive mechanical and structural properties, but also electronic and optical peculiarities[27] will find more applications in the future.

In conclusion, the range of applications and consequently perspectives for future research is broad. In the present context, xanthate-mediated polymerization is a valuable tool for the preparation of narrowly distributed PVP with one or more functional end-groups and its copolymers. Suggestions for future applications were made in this chapter and many more are to be unveiled in the future. Just as the 1st steps of polymer science were severely jostled by two world wars,[28] the discipline has not yet thrown off the yoke of its (geo)political, social and economic background. As a consequence, our choices as scientists are still a reflection of the constraints of our environment. The current domination of economic considerations and the resulting global injustice are such that future investigations may focus on cosmetic applications or the treatment of 1st world country discomfort rather than applications consistent with the preservation of humanity. Yet I believe that polymer science has a lot to do with facilitating the access to food[29] and medicine for all, development of sustainable energies, restoration and preservation of the environment.[30] Therefore, I hope that these areas will be the focus of future investigations.

Reference list

(1)   Brandrup, J.; Immergut, E.H.; Grulke, E.A. *Polymer Handbook*; John Wiley and Sons, Inc, **1999**.

(2)   Lu, X.; Gong, S.; Meng, L.; Li, C.; Yang, S.; Zhang, L. *Polymer* **2007**, *48*, 2835-2842.

(3)   Debuigne, A.; Willet, N.; Jerome, R.; Detrembleur, C. *Macromolecules* **2007**.

(4)   Moad, G.; Solomon, D.H. *The chemistry of free radical polymerization*, First ed.; Elsevier Science Ltd, **1995**.

(5)   You, Y.-Z.; Manickam, D.S.; Zhou, Q.-H.; Oupicky, D. *Biomacromolecules* **2007**, *8*, 2038-2044.

(6)   Gemici, H.; Legge, T.M.; Whittaker, M.; Monteiro, M.J.; Perrier, S. *J. Polym. Sci. Part A: Polym. Chem.* **2007**, *45*, 2334-2340.

(7)   Chin, W.W.L.; Lau, W.K.O.; Bhuvaneswari, R.; Heng, P.W.S.; Olivo, M. *Cancer Lett.* **2007**, *245*, 127-133.

(8)   Rabin, O.; Perez, J.M.; Grimm, J.; Wojtkiewicz, G.; Weissleder, R. *Nature Mat.* **2006**, *5*, 118-122.

(9)   Nguyen, T.L.U.; Eagles, K.; Davis, T.P.; Barner-Kowollik, C.; Stenzel, M.H. *J. Polym. Sci. Part A: Polym. Chem.* **2006**, *44*, 4372–4383.

(10)   Hoyle, C.E.; Lee, T.Y.; Roper, T. *J. Polym. Sci. Part A: Polym. Chem.* **2004**, *42*, 5301-5338.

(11)   Mather, B.D.; Viswanathan, K.; Miller, K.M.; Long, T.E. *Prog. Polym. Sci.* **2006**, *31*, 487-531.

(12)   Curran, D.P.; Ko, S.-B. *Tetr. Lett.* **1998**, *39*, 6629-6632.

(13)   Ignatova, M.; Manolova, N.; Rashkov, I. *Eur. Polym. J.* **2007**, *43*, 1112-1122.

(14)   Sun, B.; Duan, B.; Yuan, X. *J. Appl. Polym. Sci.* **2006**, *102*, 39-45.

(15)   Hammett, F.S. *Nature* **1938**, *141*, 82-83.

(16)   Koonjul, P.; Brandt, W.; Farrant, J.; Lindsey, G. *Nucl. Acids Res.* **1999**, *27*, 915-916.

(17)   Zhang, L.; Liang, Y.; Meng, L.; Lu, X.; Liu, Y. *Chem. Biodiv.* **2007**, *4*, 163-174.

(18)   Temiz, A.; Togay, S.Ö.; Sener, A.; Güven, G.; Rzaev, Z.M.O.; Piskin, E. *J. Appl. Polym. Sci.* **2006**, *102*, 5841-5847.

(19)   Chen, K.-S.; Ku, Y.-A.; Lin, H.-R.; Yan, T.-R.; Sheu, D.-C.; Chen, T.-M. *J. Appl. Polym. Sci.* **2006**, *100*, 803-809.

(20)   Peng, Q.; Lu, S.; Chen, D.; Wu, X.; Fan, P.; Zhong, R.; Xu, Y. *Macromol. Biosci.* **2007**, *7*, 1149-1159.

(21)   Subramanian, E.; Anitha, G.; Vijayakumar, N. *J. Appl. Polym. Sci.* **2007**, *106*, 673-683.

(22)   Murugesan, R.; Anitha, G.; Subramanian, E. *Mat. Chem. Phys.* **2004**, *85*, 184-194.

(23)   Kondo, S.; Ozeki, M.; Nakashima, N.; Suzuki, K.; Tsuda, K. *Angew. Makromol. Chem.* **1988**, *163*, 139-147.

(24)   Hsin, Y.L.; Hwang, K.C.; Yeh, C.-T. *J. Am. Chem. Soc.* **2007**.

(25)   Smitha, B.; Sridhar, S.; Khan, A.A. *J. Power Sources* **2006**, *159*, 846-854.

(26)   Qiao, J.; Hamaya, T.; Okada, T. *Polymer* **2005**, *46*, 10809-10816.

(27)   Mishra, A.; Ram, S. *J. Chem. Phys.* **2007**, *126*, 084902/084901-084902/084906.

(28)   Ringsdorf, H. *Angew. Chem. Int. Ed.* **2004**, *43*, 1064-1076.

(29)   *in terms of food, I do not mean that humanity would be better off with synthetic food, but instead that polymers can be made use of for applications in sustainable agriculture.*

(30)   Reeves, H. *Mal de Terre*; Editions du Seuil, collection "Science ouverte": Paris, **2003**.

Appendix A: NMR spectroscopy peak assignment

^{1}H NMR and ^{13}C NMR one-dimensional experiments, selective TOCSY and NOESY experiments and a series of two-dimensional experiments including homonuclear H, H-COSY, TOCSY, NOESY and DOSY as well as heteronuclear-correlated HSQC and HMBC NMR spectroscopy experiments on *ex situ* samples enabled the assignment of peaks for the various species involved in the xanthate-mediated polymerizations. The structures thus identified, which are relevant to the initialization and polymerization studies presented in chapters 3 and 4, are reported in the following tables with their corresponding ^{1}H and ^{13}C chemical shifts. Note that the numbering was attributed by the application used for drawing the chemical structures and is arbitrary. Where enantiomers were present a prime (') designates the signals belonging to one of the two enantiomers. The letters A and B are used in combination with the carbon number to differentiate between protons of diastereotopic methylene groups.

Table 1 : Structures and chemical shifts of monomers, initiator and product of primary radical combination (TMSN).
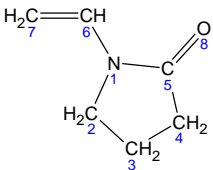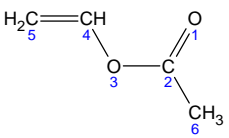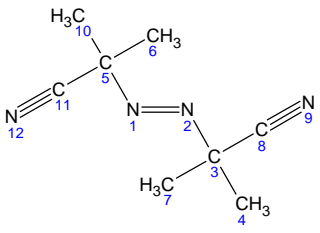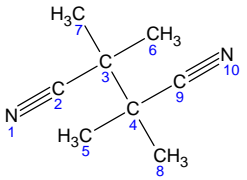
Structure	δ (ppm)
N-vinylpyrrolidone (NVP)	7.01, 1, dd, $^3J_{trans}$ = 16.1, $^3J_{cis}$ = 9.0, C$\underline{H}$=CH$_2$ (6)
	4.19, 1, d, $^3J_{trans}$ = 16.1, CH=C$\underline{H_2}$ (7A)
	4.14, 1, d, $^3J_{cis}$ = 9.0, CH=C$\underline{H_2}$ (7B)
	3.04, 2, t, ^3J = 7.2, N-C$\underline{H_2}$-CH$_2$ (2)
	2.06, 2, t, ^3J = 8.2, CH$_2$-C$\underline{H_2}$-C=O (4)
	1.56, 2, p, ^3J = 7.7, CH$_2$-C$\underline{H_2}$-CH$_2$ (3)

^{13}C NMR [ppm] 173.19 (5); 130.44 (6); 94.11 (7); 44.88 (2); 31.73 (4); 17.99 (3).

Structure	δ (ppm)
vinyl acetate (VAc)	7.11, 1, dd, $^3J_{trans}$ = 13.8, $^3J_{cis}$ = 6.2, C$\underline{H}$=CH$_2$ (4)
	4.64, 1, d, $^3J_{trans}$ = 13.8, CH=C$\underline{H_2}$ (5A)
	4.28, 1, d, $^3J_{cis}$ = 6.2, CH=C$\underline{H_2}$ (5B)
	1.73, 3, s, C$\underline{H_3}$ (6)

^{13}C NMR [ppm] 167.40 (2); 141.57 (4); 97.04 (5); 20.14 (6).

Structure	δ (ppm)
2,2-azobis(isobutyronitrile) (AIBN)	
	1.37, s, 12, C$\underline{H_3}$ (4,6,7,10)

^{13}C NMR [ppm] 120.02 (8,11); 68.86 (3,5); 25.53 (4,6,7,10).

Structure	δ (ppm)
tertramethyl succinonitrile (TMSN)	
	1.10, s, 12, C$\underline{H_3}$ (5,6,7,8)

^{13}C NMR [ppm] 121.57 (2,9); 39.37 (3,4); 22.93 (5,6,7,8).

Table 2 : Structures and chemical shifts of X6 and its derivatives.
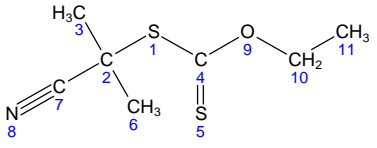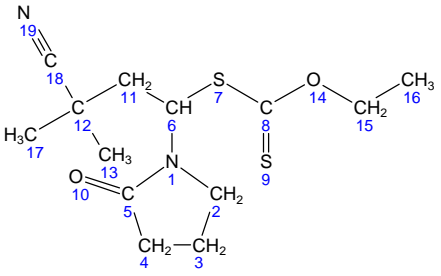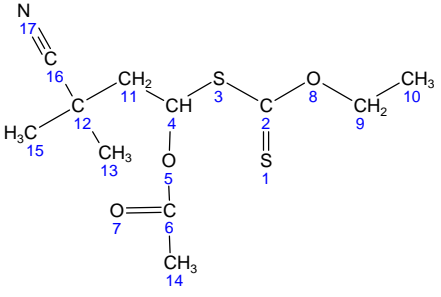
Structure	δ (ppm)

S-2-cyano-2-propyl O-ethyl xanthate (X6)

4.43, 2H, q, ^{3}J=7.1, O-$\underline{CH_2}$-CH$_3$ (10)

1.44, 6H, s, C(CN)($\underline{CH_3})_2$ (3,6)

1.19, 3H, t, ^{3}J = 7.1, CH$_2$-$\underline{CH_3}$ (11)

^{13}C NMR [ppm] 208.86 (4); 121.92 (7); 71.63 (10); 42.01 (2); 28.60 (11); 27.53 (3,6).

Single monomer adduct NVP-X6

6.22, 1H, dd, ^{3}J=3.2, 12.4, $\underline{CH}$ (6)

4.39, 2H, 2*dq (12p), O-$\underline{CH_2}$-CH$_3$ (15)

3.32, 1H, ddd, ^{3}J=4.9, 2*8.8, N-$\underline{CH_2}$-CH$_2$ (2A)

3.10, 1H, ddd, ^{3}J=6.3, 2*8.7, N-$\underline{CH_2}$-CH$_2$ (2B)

2.22, 1H, dd, ^{3}J=12.4, ^{2}J=14.6, CH-$\underline{CH_2}$-C (11A)

1.58, 1H, m, CH-$\underline{CH_2}$-C (11B)

2.13, 1H, m, CH$_2$-$\underline{CH_2}$-C=O (4A)

2.02, 1H, m, CH$_2$-$\underline{CH_2}$-C=O (4B)

1.84, 1H, m, CH$_2$-$\underline{CH_2}$-CH$_2$ (3A)

1.63, 1H, m, CH$_2$-$\underline{CH_2}$-CH$_2$ (3B)

1.25, 3H, s, C(CN)($\underline{CH_3})_2$ (13 or 17)

1.13, 3H, 2*d, ^{3}J=5.6, 7.1, $\underline{CH_3}$-CH$_2$-O (16)

1.09, 3H, s, C(CN)($\underline{CH_3})_2$ (13 or 17)

^{13}C NMR [ppm] 211.52 (8); 175.31 (5); 124.93 (18); 71.32 (15); 58.95 (6); 44.31 (2); 42.31 (11); 31.48 (4); 31.19 (12); 29.27 (13,17); 25.25 (13,17); 18.40 (3); 14.42 (16).

Single monomer adduct VAc-X6

6.74, 1H, dd, ^{3}J=3.0, 10.6, $\underline{CH}$ (4)

4.33, 2H, 12 peaks, O-$\underline{CH_2}$-CH$_3$ (9)

2.18, 1H, dd, ^{3}J=10.5, ^{2}J=14.7, CH-$\underline{CH_2}$-C (11A)

1.84, 3H, s, $\underline{CH_3}$-C(O)O (14)

1.78, 1H, m, CH-$\underline{CH_2}$-C (11B)

1.12, 3H, s, C(CN)($\underline{CH_3})_2$ (13 or 15)

1.03, 3H, s, C(CN)($\underline{CH_3})_2$ (13 or 15)

1.07, 3H, t, ^{3}J=7.2, $\underline{CH_3}$-CH$_2$-O (10)

^{13}C NMR [ppm] 209.98 (2); 169.05 (6); 123.85 (16); 76.98 (4); 70.50 (9); 44.90 (11); 30.32 (12); 28.07, 25.39 (13,15); 20.57 (14) ; 13.53 (10).

Table 3 : Structures and chemical shifts of X14 and its derivatives.

Structures derived from X14	δ (ppm)
S-2-phenylacetic acid, ethyl ester O-ethyl xanthate (X14)	

7.33, 2H, d, ^3J = 7.3, $C\underline{H}_{Ar}$ (2,6)

7.08-7.16, 3H, m, $C\underline{H}_{Ar}$ (3-5)

5.47, s, 1H, $C\underline{H}$-S (7)

4.62, 2*q, 2H, ^3J = 7.1, ^3J = 7.3, C(S)O-$C\underline{H}_2$ (14)

4.25, 2H, m, C(O)O-$C\underline{H}_2$ (17)

1.40, 3H, 2*t, ^3J = 7.1, ^3J = 7.3, $C\underline{H}_3$ (15)

1.25, 3H, 2*t, ^3J = 7.06, ^3J = 7.26, $C\underline{H}_3$ (18)

^{13}**C NMR [ppm]** 211.65 (9); 169.18 (11); 133.37 (1); 127.9-129.2 (2-6); 70.18 (14); 62.09 (17); 56.97 (7); 14.00 (18); 13.58 (15).

Single monomer adduct NVP-*X14*

7.04-7.11, 3H, m, $C\underline{H}_{Ar}$ (20-22)

6.02, 1H, dd, ^3J = 5.4; ^4J = 10.74, $C\underline{H}$-S (6);

5.85, 1H, dd, ^3J = 5.4; ^4J = 10.25, $C\underline{H}$-S (6');

4.20-4.30, 2H, m, C(S)O-$C\underline{H}_2$ (16)

3.62, 1H, t, ^3J = 7.0 (12); 3.55, 1H, t, ^3J = 7.0 (12')

2.72, (11A) 2.55, (11B); 2.16, (11').

^{13}**C NMR [ppm]** 211.29, 210.92 (8,8'); 174.27, 173.89 (5,5'); 138.62 (13); 70.34, 70.14 (16); 60.48, 59.89 (6,6'); 49.37, 49.26 (12,12'); 44.08, 43.48 (2,2'); 37.01, 36.69, 36.50 (11A,11B,11').

Table 3 : Structures and chemical shifts of X14 and its derivatives. (continued).

Structures derived from X14 (continued)	δ (ppm)

Single monomer adduct VAc-X14

7.05-7.15, 3H, CH_{Ar} (3-5)

6.65, 1H, dd, 3J = 6.0, 13.7, CH-S (9)

6.50, 1H, dd, 3J = 8.3, 13.9, CH-S (9')

4.34, 2H, 2*q, C(S)O-CH_2-CH$_3$ (19)

3.95, 2H, m, C(O)O-CH_2-CH$_3$ (22)

3.68, 1H, t, ^{3}J = 7.3, C(O)-CH (7)

2.74 ; 2.24, 1H, 12 peaks, CH-CH_2-CH(8A',8B')

2.67 ; 2.14, 1H, 12 peaks, CH-CH_2-CH(8A,8B)

1.87, 3H, s, CH_3-CO (24)

1.10-1.02, C(S)O-CH$_2$-CH_3 (20)

0.96-0.90, C(O)O-CH$_2$-CH_3 (23)

^{13}**C NMR in CDCl$_3$ [ppm]** 209.7, 209.4 (11) ; 172.6, 172.7 (13) ; 169.7, 168.9 (16) ; 137.7 (1) ; 127.9-27.8 (3,4,5) ; 78.9, 78.8 (9) ; 70.3, 70.1 (19) ; 62.5 (22) ; 48.4, 48.2 (7,7') ; 38.0, 37.3 (8,8') ; 20.8 (24) ; 14.0, 13.9 (20) ; 13.7, 1.36 (23).

Table 4 : Structures and chemical shifts of X3 and its derivatives.
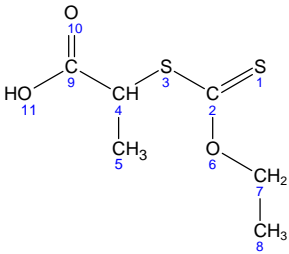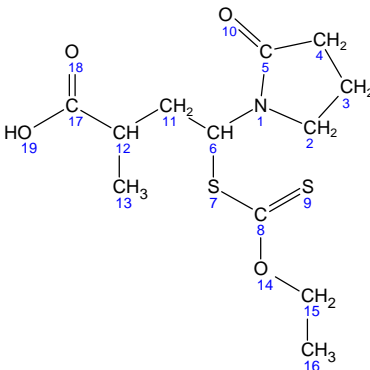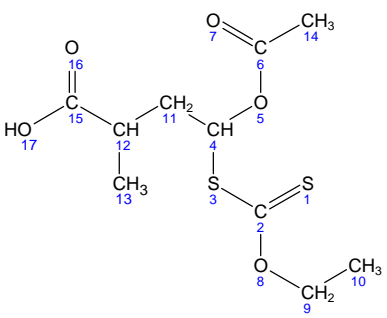
Structure	δ (ppm)

S-2-propionic acid O-ethyl xanthate (X3)

4.34, 2H, 2*q, ^{3}J=7.1, O-_CH_$_2$-CH$_3$ (7A, 7B)

4.28, 1H, q, ^{3}J=7.3, CH$_3$-_CH_ (4)

1.37, 3H, d, ^{3}J=7.3, _CH$_3$_-CH (5)

1.05, 3H, t, ^{3}J=7.1, CH$_2$-_CH$_3$_ (8)

^{13}**C NMR [ppm]** 215.5 (2); 171.9 (9); 70.5 (7); 47.4 (4); 17.2 (5); 13.5 (8)

Single monomer adduct NVP-X3

6.04;6.04 , 1H, 2*dd, ^{3}J = 5.2, 11.0; 5.8, 9.9, _CH_ (6,6')

4.37, 2H, q, ^{3}J = 7.0, _CH_$_2$ (15)

3.10, 2H, m, C_H_$_2$ (2)

2.30, 1H, 2*ddd, _CH_ (12,12')

1.86;1.72, 2H, m, _CH_$_2$ (11)

1.10, 3H, t _CH$_3$_-CH$_2$ (16)

1.05, 3H, 2*d, _CH$_3$_-CH (13)

^{13}**C NMR [ppm]** 211.26, 211.12 (8,8'); 176.40 (17); 174.58 (5); 70.52 (15); 59.62, 59.61 (6,6'); 43.41 (2); 36.87 (12);

17.5 (13); 13.5 (16).

Single monomer adduct VAc-X3   6.66, 1H, 2*dd, J (Hz) = 5.9, 7.5 ; 5.6, 8.5, _CH_ (4)

Table 5 : Structures and chemical shifts of *N*-vinylpyrrolidone derivatives.
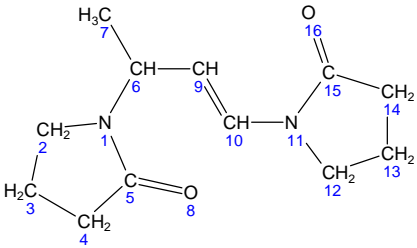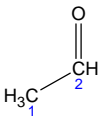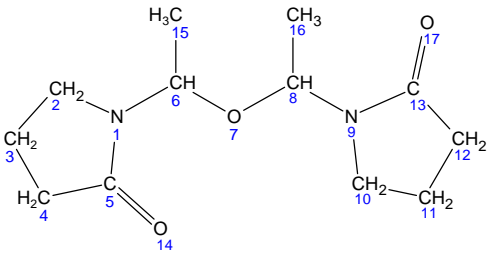
Structure	δ (ppm)

1,3-Bis(pyrrolidin-2-on-1-yl)but-1-ene (NVP dimer)

6.85, 1H, d, ^{3}J = 14.2, =C*H*-N (10)

4.73, 1H, m, CH$_3$-C*H* (6)

4.68, 1H, dd, ^{3}J = 14.2,6.4 CH-C*H*=CH (9)

3.01, 2H, m, N-C*H$_2$*-CH$_2$ (2,12)

2.07, 2H, m, CH$_2$-C*H$_2$*-C=O (4,14)

1.59, 2H, m, CH$_2$-C*H$_2$*-CH$_2$ (3,13)

1.06, 3H, d, ^{3}J = 6.4, C*H$_3$* (7)

^{13}C NMR [ppm] 173.64, 172.91 (5,15); 125.33 (10); 110.47 (9); 46.47 (6); 44.90 (2,12); 31.30-30.90 (4,14); 18.07-17.20 (3,13); 17.65 (7).

Acetaldehyde

9.42, 1H, q, C*H* (2)

1.77, 3H, d, C*H$_3$* (1)

^{13}C NMR [ppm].

Saturated NVP hydrated dimer (NVP-O-NVP)

5.37, 1H, q, ^{3}J = 6.2, C*H* (6,8); 5.30, 1H, q, ^{3}J = 6.0, C*H* (6',8')

1.09, 3H, d, ^{3}J = 6.2, C*H$_3$* (5,16); 1.07, 3H, d, ^{3}J = 6.0, C*H$_3$* (5',16').

^{13}C NMR [ppm] 175.21 (2), 174.78 (2'); 74.86 (6), 75.21 (6'); 41.71 (5), 41.52 (5'); 18.79 (7), 19.52 (7').

Table 6 : Structures and chemical shifts of NVP derivatives due to the presence of a xanthate.

Structure	**δ (ppm)**

Unsaturated elimination product from single adduct

with X14 (X_{14}-EP)

7.25, 2H, d, ^3J = 7.8, =C*H*- (13,17)

7.10-7.15, m, C*H* (14-16)

7.09, 1H, d, ^3J = 14.2, =C*H*-N (6)

5.19, 1H, dd, ^3J = 8.8, ^3J = 14.2, CH-C*H*=CH (7)

4.29, 1H, d, ^3J = 8.8, C*H*-CH=CH (8)

4,29, 2H, q, O-C*H$_2$*-CH$_3$ (19)

2.99, 2H, m, N-C*H$_2$*-CH$_2$ (2)

2.05, 2H, m, CH$_2$-C*H$_2$*-C=O (4)

1.53, 2H, m, CH$_2$-C*H$_2$*-CH$_2$ (3)

1.00, 3H, t, ^3J = 7.3, C*H$_3$* (20)

^{13}*C NMR [ppm]* 172.58 (5); 140.06 (9); 133 (12); 129.0-128.8 (14-16); 128.34, 128.29 (13,17); 126.18 (6); 109.03 (7); 62.89 (19); 52.79 (8); 44.63 (2); 35.58 (4); 18.4 (3); 13.57 (20)

Unsaturated elimination product from single adduct

with X6 (X_6-EP)

7.11, 1H, d, ^3J = 14.7 Hz, =C*H*- (6)

4.70, 1H, d, ^3J = 14.7 Hz, =C*H*- (7)

3.01, 2H, m, N-C*H$_2$*-CH$_2$ (2)

1.17, 6H, s, C(C*H$_3$*)$_2$ (9,11)

^{13}*C NMR [ppm]* 172.6 (5); 125.2 (6); 124.5 (12); 112.6 (7); 44.8 (2); 32.9 (8); 27.8 (9,11).

S-(1-pyrrolidonyl ethane) O-ethyl xanthate (NVP-xanthate) observed in the presence of X14

6.05, 1H, q, ^3J = 6.8, C*H*-S (6)

4.35, 2H, q (overlap), O-C*H$_2$*-CH$_3$ (13)

2.88, 2H, m, N-C*H$_2$*-CH$_2$ (2)

1.29, 3H, d, ^3J = 6.8, C*H$_3$*-CH-S (11)

^{13}*C NMR [ppm]* 211.84 (8); 173.21 (5); 70.41 (13); 57.30 (6); 43.13 (2); 17.5 (11); 13.5 (14).

Table 6 : Structures and chemical shifts of NVP derivatives due to the presence of a xanthate. (continued).

Structure	δ (ppm)
S-2-propionic acid, N-1-ethylpyrrolidonyl ester O-ethyl xanthate (X3,-NVPester)	6.57;6.55, 1H, 2*q, ^3J = 6.3, CH$_3$-C$\underline{H}$-O (6,6')

6.57;6.55, 1H, 2*q, ^3J = 6.3, CH$_3$-C$\underline{H}$-O (6,6')

4.36, 2H, q, ^3J = 7.0, C$\underline{H_2}$-O (18)

4.18;4.11, 1H, 2*q, ^3J = 7.3, CH$_3$-C$\underline{H}$-S (12,12')

3.10, 2H, m, N-C$\underline{H_2}$-CH$_2$ (2)

2.02, 2H, m, CH$_2$-C$\underline{H_2}$-C=O (4)

1.60, 2H, m, CH$_2$-C$\underline{H_2}$-CH$_2$ (3)

1.33;1.30, 3H, 2*d, ^3J = 7.3, C$\underline{H_3}$-CH-S (16,16')

1.19, 3H, 2*d, ^3J = 6.3, C$\underline{H_3}$-CH-O (11,11')

1.10, 3H, t, ^3J = 7.0, C$\underline{H_3}$-CH$_2$-O (19)

^{13}**C NMR [ppm]** 211.99, 211.85 (14,14'); 174.48, 174.32 (5,5'); 169.55, 169.37 (8,8'); 75.17, 75.33 (6,6'); 70.73, 70.70 (18,18'); 47.26, 47.08 (12,12'); 42.02, 41.92 (2,2'); 31.08 (4); 18.10, 18.07 (3,3'); 17.72, 17.69 (11,11'); 16.82, 16.67 (16,16'); 13.5 (19).

Comments on identification of species via NMR spectroscopy

The structure NVP-xanthate was unambiguously identified thanks to the correspondence between C8 (characteristic of the xanthate species) with the protons on both sides, *i.e.* CH (6) and CH$_2$ (13). The shape of the signal for the methine proton CH(6) (q) and its coupling to the methyl protons CH$_3$(11) (d) indicate their belonging to the moiety CH-CH$_3$ with CH being isolated from the rest of the structure by heteroatoms. The correspondence between CH (6) and C2 and C5 confirm the presence of the pyrrolidone ring. Methylene carbons belonging to the pyrrolidone ring (*e.g.* C3 and C4 in NVP-xanthate) were not specifically assigned due to peak overlap. It was always confirmed however that many peaks were present in the relevant region which could correspond to the species claimed. In this case peak overlap was a problem because these moieties are too far from the characteristic moieties (CH6) to be identified amongst other signals via HMBC experiments.

Acknowledgements

Helmut Ringsdorf paved my way to this PhD. I thank them for their encouragement and spirited discussions. I feel wonderfully lucky and grateful to have met people who make my South African days brighter. For their friendship, I thank in particular Lee-Sa, Jane, Amandine, Kora, M.C., Valérie, Aurora, Magali, Maya, Anne, Nox, Núria, Clément, Arnaud, Amanuel, Thomas, Tom, Sven, Ibo, Paul, Aman, Luc, Frédéric, Simeon, Francesco, whom I met in South Africa and my close friends from Europe: Hélène, Cécile, Aurélie, Céline, Christelle, Lucile and Jelena. Many thanks to Louis, my viola teacher, a master in turning dullness into light and Gilles for eye-opening heart-warming correspondence. The support from my parents was boundless. I thank them for sowing the seeds of freedom, confidence, curiosity and love in my life. Thank you to my sister for being (mon rayon de soleil ma venus ma mie mon églantine ma pucette ma musique ma prairie ma douce et tendre sorette). Cristiano, meu amor, agradeço o seu apoio. Ao seu lado a vida é tão bela que não quero mais ****-la. Thank you soooOOOooo much!

To the many South Africans whom I bumped into hardly long enough for them to ask me why I decided to come to South Africa, I would like to answer the following. An ad was posted on the website of the department of Polymer Science at the University of Stellenbosch for a student to come and do a PhD. I was familiar with and interested in the topic (that is, the chemistry of RAFT polymerizations). I then documented myself on South Africa. I read that, since the end of the apartheid, South Africa is the country which constitution is the most democratic in the whole world. I saw breathtaking pictures of mountains and oceans, of wildlife and of the people. Nearly four years after my arrival, I am sincerely grateful to many South Africans for allowing me and other foreigners to stay and work in their country. I still have the memory of France calling itself a welcoming country. I wish it were still open to diversity. I strongly believe that a country that loses its colors loses its essence.

Ce manuscrit fut rédigé en anglais sans autre regret que celui de n'avoir pu imprimer en ces termes : "L'expérimentation dévoila une issue dont nul manuel de chimie ne nous eût dévoilé l'existence. Selon un imaginaire extravagant nous supputâmes la transformation qui nous mit sur la voie. Le dithiocarbonate oligomérique dissimulait un aldéhyde."